

A GENERIC STABILITY AND CONTROL TOOL FOR FLIGHT VEHICLE
CONCEPTUAL DESIGN: AEROMECH SOFTWARE DEVELOPMENT

by

GARY JOHN COLEMAN JR.

Presented to the Faculty of the Graduate School of
The University of Texas at Arlington in Partial Fulfillment
of the Requirements
for the Degree of

MASTER OF SCIENCE IN AEROSPACE ENGINEERING

THE UNIVERSITY OF TEXAS AT ARLINGTON

May 2007

Copyright © by Gary John Coleman Jr. 2007

All Rights Reserved

ACKNOWLEDGEMENTS

This work could not have been possible without the support of several individuals whom I wish to acknowledge.

I would like to express my appreciation to my advisor, Dr. Bernd Chudoba, for his support, encouragement, feed-back and even his constructive criticism. The high level of academic, professional and engineering standards he sets drive and challenges his students to grow and learn throughout their education. This Thesis is the implementation and application of methodology and mathematical frame work derived by Dr. Chudoba. With out this foundation the current research could not have been conducted.

I would like to acknowledge the contribution of Kiran Pippalapalli of the AVD Lab to the present research. His initial work on the *AeroMech* software has been invaluable, and has provided an excellent starting point for my research. I would also like to thank him for his guidance, advice and friendship during my graduate studies.

Dr. Edward Lan of the University of Kansas has been instrumental during this research in aiding with the use and application of his aerodynamic prediction tool VORSTAB. His insight into both the computation and physical aspects of aerodynamics have been of great value during this research

Gerald C. Blausey (former Lockheed Martin flight dynamists) and Robert G. Hoey (former USAF flight test engineer) have contributed greatly to my understanding

of stability and control and its application to both design and flight testing. Their experience, insight, and timely response to my questions are greatly appreciated, and have directly influenced this research.

I would like acknowledge the contributions of Dr. Danielle Soban (Georgia Institute of Technology) and John Jeffery (J2 Aircraft Solutions Ltd.). Their timely feed-back and experience with the application of stability and control in design have been very helpful for this research.

I would like express my appreciation to the AVD lab team members, Xiao Huang, Andy Huizenga, Amit Oza, Bryan Mixon, Kristen Roberts, Brad Mixon, and Nauman Mhaskar. Their friendship and assistance have made my graduate studies at the University of Oklahoma and the University of Texas at Arlington an enjoyable experience.

I would like to thank my parents, for their support, direction and encouragement. I would also like to thank my younger brothers, Daniel, Dennis and Nick for their “*constructive*” criticism and feed-back during my Masters research. I hope I can return the favor someday.

Finally, I would like to thank my fiancé Jessica, without her love, understanding and support this work could not have been possible. Her friendship and laughter constantly remind me of what is truly important.

April 19, 2007

ABSTRACT

A GENERIC STABILITY AND CONTROL TOOL FOR FLIGHT VEHICLE CONCEPTUAL DESIGN: AEROMECH SOFTWARE DEVELOPMENT

Publication No. _____

Gary John Coleman Jr., M.S.

The University of Texas at Arlington, 2006

Supervising Professor: Dr. Bernd Chudoba

During the conceptual design (CD) phase, various solution concepts must, and should, be explored to select the best flight vehicle size and configuration in order to meet the mission requirements. As the aerospace industry advances novel aerospace flight vehicle configurations promising larger operational performance and overall efficiency, demanding integrated flight vehicles like the flying wing configuration (FWC) or blending wing body (BWB) are under investigation. Some of these novel configurations rely on novel control effectors (CE) and complex flight control systems in order to obtain the desired performance objectives. Clearly, stability and control plays an important roll in the design of advanced flight vehicles.

Chudoba¹ recognized that that the conceptual design of such vehicles requires a truly generic stability and control approach to enable consistent comparisons of novel aircraft configurations with conventional aircraft aircraft shapes. Consequently, *AeroMech* analyzes both symmetric and asymmetric flight vehicles in symmetric and asymmetric flight conditions. The methodology and software *AeroMech* contributes to (1) sizing primary control effectors to possess adequate physical control power throughout the flight envelope, the tool (2) provides trimmed aerodynamics for improved performance-optimal stability and control solutions, and (3) it analyses static and dynamic stability in all axes (open and closed loop) for ensure flight vehicle safety and compliance with certification regulations throughout the flight envelope.

The development of this methodology and software has been following three fundamental steps: (1) derivation of the *AeroMech* methodology and mathematic framework, (2) development of the stand-alone *AeroMech* prototype software for validation purposes, and (3) integration of *AeroMech* into the multi-disciplinary design tool AVDS-PrADO for multi-disciplinary flight vehicle synthesis. With the first step accomplished by Chudoba¹, the second step initiated by Pippalapalli⁶, the present work describes the completed development of the stand-alone *AeroMech* prototype software and its validation using the Northrop YB-49 flying wing as the primary case study demonstrating physical correctness of the algorithm but in particular the software's potential to enable true control-configured vehicle (CCV) design during the early conceptual design phase.

TABLE OF CONTENTS

ACKNOWLEDGEMENTS.....	iii
ABSTRACT	v
TABLE OF CONTENTS	vii
LIST OF ILLUSTRATIONS.....	xi
LIST OF TABLES.....	xv
NOTATION.....	xviii
Chapter	
1. INTRODUCTION AND OBJECTIVES.....	1
1.1 Introduction.....	1
1.2 Background, Research Approach and Objectives	8
1.2.1 Research Objectives.....	10
2. STABILITY AND CONTROL IN CONCEPTUAL DESIGN.....	12
2.1 Review of Stability and Control Techniques in Conceptual Design.....	12
2.1.1 Assessment of the Classical Approach.....	15
2.1.2 Assessment of the State-of-the-Art.....	22
2.2 Summary of Results and Prototype System Requirements	26
3. AEROMECH METHODOLOGY AND THEORY	28
3.1 Methodology Overview.....	28
3.2 Input and Control Allocation.....	32

3.3 Aerodynamic Prediction	35
3.4 Stability and Control Analysis.....	40
3.4.1 Steady State 6-DOF Trim Equations of Motion.....	41
3.4.1.1 Steady-State Straight-Line Flight (SSLF)	45
3.4.1.2 Steady-State Pull-Up/Push-Over (SSPUPO).....	48
3.4.1.3 Steady-State Roll Performance (SSRP).....	49
3.4.1.4 Steady-State Turning Flight (SSTF).....	52
3.4.1.5 Quasi-Steady-State Take-Off Rotation (QSTORM)	54
3.4.2 Trimmed Aerodynamics	57
3.4.3 Dynamic Stability and Control Analysis	60
3.4.3.1 Small Perturbation Equations of Motion	60
3.4.3.2 Dynamic Open and Closed Loop Analysis	65
3.5 Output Definition.....	70
4. AEROMECH PROTOTYPE SYSTEM DEVELOPMENT	71
4.1 AeroMech Development Background and Process	71
4.1.1 AeroMech Background.....	71
4.1.2 AeroMech Prototype Software Development Process	74
4.2 Evolution of the AeroMech Prototype Stand-alone Software	79
4.3 Future Work and Recommendations	104
5. APPLICATION OF AEROMECH IN CONCEPTUAL DESIGN	106
5.1 Stability and Control ‘Road Map’ to Conceptual Design.....	106
5.2 Validation Case Study: Northrop YB-49 Flying Wing	126

5.2.1 Northrop YB-49 Flying Wing Development History	126
5.2.2. Baseline Configuration	128
5.2.3. Design Constraining Flight Conditions (DCFC)	129
5.2.4. Analysis of the YB-49 Using AeroMech.....	131
5.2.4.1. Aircraft and DCFC Input for AeroMech	131
5.2.4.2. Control Allocation	133
5.2.4.3. Creation of the Untrimmed Aerodynamic Database	134
5.2.4.4. Control Power Analysis for CE Sizing.....	135
5.2.4.5. Trimmed Aerodynamic Analysis	157
5.2.4.6. Static and Dynamic Stability	159
5.2.5. Summary of Results.....	171
6. CONTRIBUTIONS SUMMARY AND RECOMMENDATIONS	176
6.1 Contributions Summary.....	176
6.2 Recommendations for Future Work	178
Appendix	
AEROMECH USER’S GUIDE.....	181
DIGITAL DATCOM USER’S GUIDE.....	193
VORSTAB USER’S GUIDE	210
AEROMECH INPUT FILE DESCRIPTION.....	225
DERIVATION OF STEADY-STATE EQUATIONS OF MOTION	231
STABILITY AND CONTROL MAP BIBLIOGRAPHY	248
REFERENCES	255

BIOGRAPHICAL INFORMATION.....260

LIST OF ILLUSTRATIONS

Figure	Page
1.1 Range of aircraft configurations explored in aerospace ¹	1
1.2 The aircraft development process ²	2
1.3 Conceptual design compares various solution-concepts for a specific mission	3
2.1 AeroMech Overall Methodology	24
3.1 AeroMech Detailed Overall Methodology.....	30
3.2 Three-View of the Northrop YB-49 Flying Wing	31
3.3 <i>AeroMech</i> Input and Preprocessing.....	32
3.4 Three-Surface Configuration, Piaggio Avanti.	33
3.5 Longitudinal control allocation for the YB-49 flying wing	34
3.6 <i>AeroMech</i> Overall Methodology: Aerodynamic Analysis.....	38
3.7 <i>AeroMech</i> Overall Methodology Stability and Control Analysis	40
3.8 Axis Definition for Symmetric and Systemic aircraft for <i>AeroMech</i> ¹	44
3.9 SSLF Asymmetric Scenarios of CE Sizing1	46
3.10 Control deflections for the YB-49 during approach	47
3.11 Longitudinal and lateral/directional control deflections for the YB-49 during a Pull-up maneuver	49
3.12 YB-49 lateral/directional roll control deflections required.	51
3.13 Control deflections for the YB-49 during SSTF for two bank angles.	53

3.14 Quasi-Steady State Take-Off Rotation Diagram ¹	54
3.15 Rotation Velocity for the YB-49	56
3.16 Trimmed aerodynamic data at 21% MAC	58
3.17 Trimmed aerodynamic efficiency for the YB-49 as a function of the longitudinal static margin.....	59
3.18 Continuous Controller and Airframe Model, Longitudinal Motion ²³	64
3.19 Dynamic Stability and Control Analysis Methodology ¹	66
3.20 Open-loop root locus for the YB-49 with decreasing static longitudinal margin	68
3.21 YB-49 Open-Loop Short Period ω_n and ζ with Decreasing Static Margin	69
3.22 YB-49 Closed-Loop gains and additional control power required for longitudinal stability augmentation.	69
3.23 <i>AeroMech</i> Overall Methodology Output.....	70
4.1 First <i>AeroMech</i> Stand-alone Prototype Software Overview ⁶	72
4.2 Partial <i>AeroMech</i> stand-alone prototype software N/S structogram ⁶	77
4.3 Initial <i>AeroMech</i> stand-alone prototype software N/S structogram.....	81
4.4 Modification of the VORSTAB input file.....	86
4.5 Nonlinear Newton-Raphson function algorithm.....	89
4.6 ILOCUS.f90 Source Code Breakdown	92
4.7 Longitudinal stability augmentation system ²³	94
4.8 Lateral/directional stability augmentation system ²³	94
4.9 Angle-of-attack feedback effect of a statically unstable vehicle.....	95

4.10 Control gain selection logic for longitudinal motion	96
4.11 Control gain selection logic for the lateral/directional motion.	97
4.12 <i>AeroMech</i> aerodynamic look-up table Screen Shot	99
4.13 Final AeroMech Driver N/S Structogram	103
5.1 Generic mission profile demonstrating various mission segments, with the DCFC's, failure conditions and configuration settings detailed for Take-off, Initial Climb and Cruise.....	110
5.2 Layout of the primary and secondary controls of the YB-49 flying wing.	129
5.3 Longitudinal control allocation for the YB-49 during cruising flight.	134
5.4 YB-49 VORSTAB Model Visualization	135
5.5 Comparison of YB-49 AeroMech 1-g Trim results with flight test report data ¹⁹ for the cruise and low-Speed Flight Segments	136
5.6 YB-49 wing slot anti-stall device is deployed with the landing gear.....	137
5.7 Effects of relaxed longitudinal static stability on the required LoCE (trim flap) trim deflection during cruise, low-speed flight and approach	138
5.8 Effects of Relaxed longitudinal Static Stability during the take-off rotation maneuver for the YB-49	139
5.9 Comparison of YB-49 Pull-Up / Push-Over <i>AeroMech</i> results with flight test report data ¹⁹ for the low-speed flight segment.....	141
5.10 Effects of relaxed longitudinal static stability on the required LoCE (trim flap) trim deflection during Cruise, Low-speed Flight and Approach....	142
5.11 Required DiCE (drag rudder) trim deflection during Cruise, Low-speed Flight and Approach.....	145
5.12 Required DiCE (drag rudder) turn Coordination deflections during cruise, low-speed flight and approach.....	147

5.13 Required DiCE (drag rudder) deflections to maintain coordinated during Cruise, Low-speed Flight and Approach.....	149
5.14 Required LaCE (elevon) deflections for 1-g trim with side-slip during Cruise, Low-speed Flight and Approach.....	151
5.15 Maximum roll rate capability of the YB-49' LaCE (elevon) compared to flight test results ¹⁹ during Low-speed flight.....	152
5.16 Maximum Roll rate Capability of the YB-49' LaCE (elevon) during Cruise, Low-speed Flight and Approach.....	153
5.17 Required DiCE (drag rudder) turn Coordination deflections during Cruise, Low-speed Flight and Approach.....	155
5.18 Effects of relaxed longitudinal static stability on L/DTrim for Cruise, Low-speed Flight and Approach.....	157
5.19 Longitudinal Static Stability as a function of angle of attack for Cruise, Low-speed Flight and Approach.....	160
5.20 Lateral Directional Static Stability as a function of angle of attack for Cruise, Low-speed Flight and Approach.....	162
5.21 Mil-Spec short-period frequency requirements for Category B and C flight Phases ³²	164
5.22 Longitudinal Short Period Mode with stability augmentation for Cruise, Low-speed Flight and Approach.....	165
5.23 Longitudinal Short Period Mode with stability augmentation for Cruise, Low-speed Flight and Approach.....	166
5.24 Longitudinal Phugoid Mode with stability augmentation for Cruise, Low-speed Flight and Approach.....	167
5.25 Lateral / Directional dynamic stability mode with and without SAS for Cruise, Low-speed Flight and Approach.....	170

LIST OF TABLES

Table	Page
2.1 Design-Oriented Approaches to Stability and Control Analysis ¹	13
2.2 Classic DCFC's for Control Effector Sizing ¹³	16
2.3 Longitudinal Trim and Maneuvering Models from Nicolai ⁷⁰ and Roskam ⁸	18
2.4 Static Stability Requirements, Nicolai ¹³	19
2.5 Short Period Open and Closed Loop Reduced Order Models, Roskam ¹⁰	20
2.6 Guidelines for Control Effector Sizing ¹³	21
2.7 Summary of Modern Stability and Control Methods for Conceptual Design	22
3.1 Modeling Capabilities of VORSTAB ⁵ , Digital DATCOM ⁷ , and VORLAX ¹⁸	37
3.2 <i>AeroMech</i> Aerodynamic Input File Organization	39
3.3 Steady-State Equations of Motion Assumptions	42
3.4 Steady-State Maneuvers Summary ¹	45
3.5 Flight Condition for the YB-49 During Approach	47
3.6 Flight Condition for the YB-49 during a Pull-up Maneuver	48
3.7 Flight Condition for the YB-49 during a Steady-State Roll Maneuver	51
3.8 Flight Condition for the YB-49 during Steady-State Turning Flight	52
3.9 Typical Instantaneous Pitch Acceleration ¹⁰	55

3.10 Flight Condition for the YB-49 during Take-off Rotation.....	56
3.11 Flight Condition Description for the YB-49 during Cruising Flight	57
3.12 Summery of Available Small-Perturbation Analysis Tools	62
4.1 Nassi-Schneiderman (N/S) structogram basic structures ²⁵	76
4.2 Summery of Current Prototype System Evolution.....	83
4.3 Summary of Major <i>AeroMech</i> Subroutines	102
5.1 DCFC's for Control Effector Sizing ¹	112
5.2 DCFC's for Trimmed Aerodynamics, Static Stability and Dynamic Stability.....	113
5.3 Trim Deliverables Map	115
5.4 Maneuvering Deliverables Map.....	116
5.5 Trimmed Aerodynamics Map	118
5.6 Static Stability Analysis Map.....	120
5.7 Longitudinal Dynamic Stability and Control Deliverables Map	123
5.8 Lateral/Directional Dynamic Stability and Control Deliverables Map.....	124
5.9 YB-49 Specifications and Three-View Drawing	128
5.10 YB-49 DCFC Summary	130
5.11 Flight Condition Input for the YB-49 for the Required Mission Segments	131
5.12 Weight and Balance Input for the YB-49 for the Required Mission Segments	132
5.13 Configuration Input for the YB-49 for the Required Mission Segments	133
5.14 Mil-Spec Time to Bank Requirements for Class III Aircraft ³²	154

5.15 Mil-Spec Longitudinal Dynamic Stability Requirements ³²	163
5.16 Mil-Spec Minimum and Maximum Lateral / Directional Dynamic Stability Requirements ³²	169
5.17 YB-49 DCFC Summary of Results.....	172

NOTATION

Abbreviations

AVDS	=	Aerospace Vehicle design Synthesis
BD	=	Baseline Design
CE	=	Control Effector
CD	=	Conceptual Design
CCV	=	Controls Configured Vehicle
CS	=	Configuration Setting
DCFC	=	Design Constraining Flight Condition
DD	=	Detail Design
DiCE	=	Directional Control Effector
DOF	=	Degrees of Freedom
FC	=	Failure Condition
FCS	=	Flight Control System
FD	=	Feasibility Design
FWC	=	Flying Wing Configuration
GUI	=	Graphical User Interface
LaCE	=	Lateral Control Effector
LoCE	=	Longitudinal Control Effector
LOTS	=	Linear-Optimum Trim Solution

OFWC	=	Oblique Flying Wing Configuration
OWC	=	Oblique Wing Configuration
QSTORM	=	Quasi-Steady-State Take-off Rotation
PD	=	Preliminary Design
PrADO	=	Preliminary Aerospace Design and Optimization
SAS	=	Stability Augmentation System
SM	=	Static Margin
SSLF	=	Steady-State Strait line Flight
SSPUPO	=	Steady-State Pull-up / Push-over
SSRP	=	Steady-State Roll Performance
SSTF	=	Steady-State Turning Flight
TAC	=	Tail Aft Configuration
TFC	=	Tail First Configuration
TSC	=	Three Surface Configuration
VLM	=	Vortex Lattice Method

Symbols

b	=	Span
\bar{c}	=	Mean Aerodynamic Chord
C_L	=	Coefficient of lift
C_D	=	Coefficient of Drag
C_m	=	Coefficient of pitching moment

C_Y	=	Coefficient of side force
C_l	=	Coefficient of rolling moment
C_n	=	Coefficient of yawing moment
C_T	=	Thrust Coefficient, one for each direction
C_{ref}	=	Reference chord
g	=	Gravitational Constant
h	=	Altitude
h'_x	=	Rotational inertia of spinning rotors along the x axis
h'_y	=	Rotational inertia of spinning rotors along the y axis
h'_z	=	Rotational inertia of spinning rotors along the z axis
I_x	=	Moment of inertia about the x axis
I_y	=	Moment of inertia about the y axis
I_z	=	Moment of inertia about the z axis
I_{xz}	=	Product Moment of inertia
I_{xy}	=	Product Moment of inertia
I_{yz}	=	Product Moment of inertia
K_q	=	Pitch rate gain
K_p	=	Roll rate gain
K_r	=	Yaw rate gain
K_α	=	Angle of attack gain

L/D	=	Lift to Drag Ratio
L/D_{Trim}	=	Trimmed Lift to Drag Ratio
M	=	Mach number
m	=	Mass
n	=	Load factor
\bar{q}	=	Dynamic pressure
S_{ref}	=	Reference Area
T_i	=	Thrust available per engine
V	=	Relative Velocity
V_{rot}	=	Take-off Rotation Velocity
W	=	Weight
X_{cg}	=	X Location of the Center of Gravity
X_T	=	X Location of the thrust vector
Y_T	=	Y Location of the thrust vector
Z_T	=	Z Location of the thrust vector
δ_{DiCE}	=	Directional Control Effector Deflection
δ_{LoCE}	=	Longitudinal Control Effector Deflection
δ_{LaCE}	=	Lateral Control Effector Deflection
δ_{TF}	=	Trim flap deflection
α	=	Angle of attack
β	=	Side-slip angle

γ	=	Flight path angle
$\Delta\alpha$	=	Angle of attack disturbance
Δp	=	Roll rate disturbance
Δq	=	Pitch rate disturbance
Δr	=	Yaw rate disturbance
$\Delta C_{L\delta}$	=	Lift coefficient increment due to control surface deflection
$\Delta C_{D\delta}$	=	Drag coefficient increment due to control surface deflection
$\Delta C_{m\delta}$	=	Pitching moment coefficient increment due to control surface deflection
$\Delta C_{Y\delta}$	=	Side force coefficient increment due to control surface deflection
$\Delta C_{l\delta}$	=	Rolling moment coefficient increment due to control surface deflection
$\Delta C_{n\delta}$	=	Yawing moment coefficient increment due to control surface deflection
$\Delta\delta_{LaCE}$	=	additional control surface deflection required due to SAS
$\ddot{\theta}$	=	Instantaneous pitch acceleration for take-off rotation
τ	=	Percent of available thrust
$\omega_{s,p}$	=	Short Period Natural Frequency
$\zeta_{s,p}$	=	Short Period Damping Ratio
ψ_{Ti}	=	lateral angle of the thrust vector, measured in the horizontal plane
ϕ_{Ti}	=	longitudinal angle of the thrust vector, measured in the vertical plane
ϕ	=	Bank angle

CHAPTER 1

INTRODUCTION AND OBJECTIVES

1.1 Introduction

Competition and profitability are the two primary drivers of the aerospace industry. These forces have lead design environments to explore a variety of different aircraft configurations in the pursuit of greater performance and efficiency, as shown in Figure 1.1.

TAC	T ail- A ft C onfiguration	sym metric
TFC	T ail- F irst C onfiguration	sym metric
TSC	T hree- S urface C onfiguration	sym metric
FWC	F lying- W ing C onfiguration	sym metric
OWC	O blique- W ing C onfiguration	asym metric
OFWC	O blique F lying- W ing C onfiguration	asym metric

Tail-Aft Configuration



Tail-First Configuration



Three-Surface Configuration



Flying-Wing Configuration



Oblique-Wing Configuration



Oblique-Flying-Wing Configuration



Figure 1.1: Range of aircraft configurations explored in aerospace¹

To enable steady progress, today's high-technology aerospace industry requires designers to balance both the technical and market risks with the need to produce innovative concepts which possess a competitive edge.

The development of aerospace vehicles can be broken into the following design phases defined below (Figure 1.2).

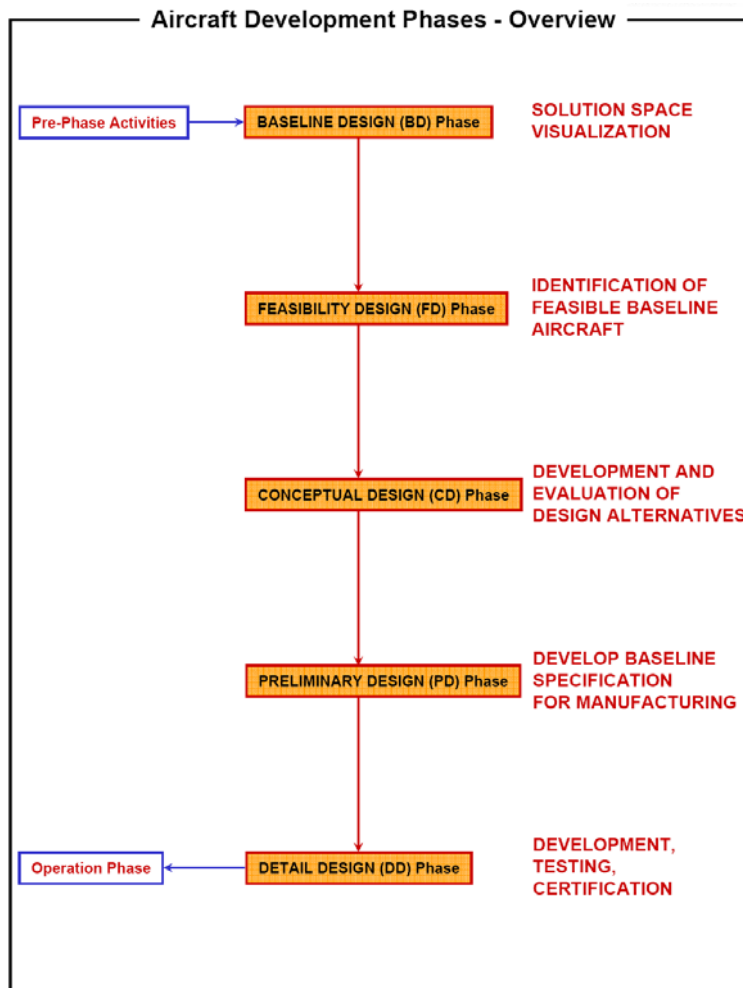


Figure 1.2: The aircraft development process²

In this organization scheme the first three steps (BD, FD, and CD) are decomposed from the classical definition of conceptual design, “*Conceptual design extends from the development of requirements to the determination of a vehicle concept and a size estimate*”,². As a rule of thumb, it can be assumed that 80% of the vehicle configuration is determined during the conceptual design phase. Thus, the execution of a well-orchestrated CD phase is vital for future success of the product.

By this definition, the purpose of the CD phase is to *identify and size various design concepts for both technical and economic feasibility and select the concept that shows the most potential*, as illustrated in Figure 1.3.

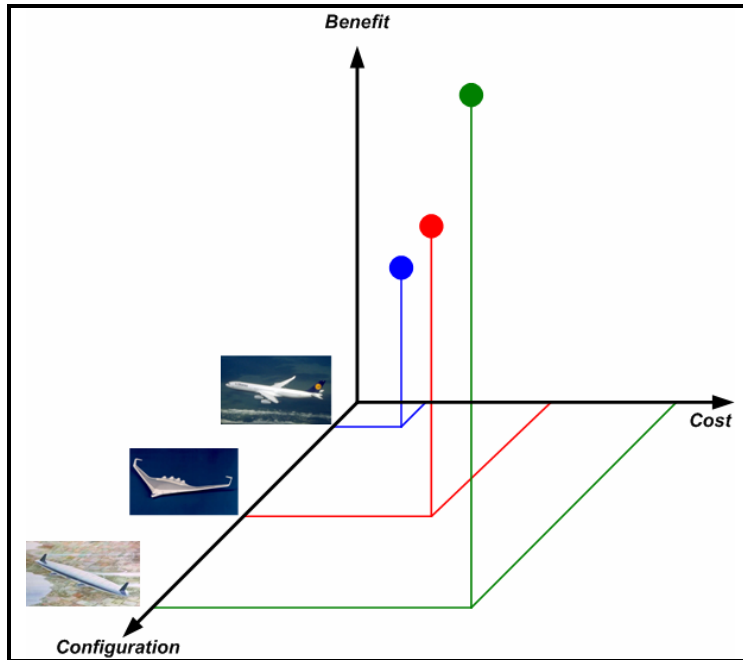


Figure 1.3: Conceptual design compares various solution-concepts for a specific mission

From this standpoint, the conceptual designer must adequately size and then describe the costs and benefits of these solution concepts to provide the necessary information to management for a configuration selection. Some of the novel configurations shown in Figure 1-1 (TFC, TSC, FWC, OWC and OWFC) place a great deal of importance on stability and control analysis at the conceptual design level due to novel control effectors, novel control allocation methods, and inherent instabilities which may require an advanced flight control system (FCS) to provide flight safety.

Flight control systems can have a significant impact on both the cost and performance of the aircraft and thus must be considered during configuration selection.

The classical roll of stability and control during vehicle sizing is described below by Mr. Gerald Blausey, former Lockheed Martin Skunk Works Flight Dynamists³.

“... The first steps in conceptual design are fuselage and wing sizing. ... Little or no thought is given to the empennage while this portion of the design process takes place.

After the wing and fuselage are initially sized, the empennage is sized and added through a separate design effort. Stability and control requirements are considered one-at-a-time and the smallest empennage which meets all of the requirements is determined. Wing position on the fuselage and landing gear position are sometimes shifted during the empennage design process.

At some point in the design process, and usually before the engineers are ready, management dictates a configuration freeze. After this time design changes are very difficult to make. However, small changes are possible.

This is when wing strakes are reshaped, dorsal fins and ventral fins are added, wing and horizontal tail dihedral angles change, and wing fences, vortex generators, body strakes, fuselage plugs and wingtip extensions are added.

These features usually appear when design deficiencies become evident after configuration freeze. Every last bit of control effectiveness is also squeezed out through leading and trailing edge flap deflection optimization. ... In the final stages of the design, stability and control takes on the dominant role in the aircraft development process.³”

Essentially, during the early design stages the stability and control analysis is classically left incomplete which leads to corrections later in the design process when stability and control takes on a more dominate roll. While this approach is not ideal, it is acceptable for traditional TAC where the primary lifting surface (wing), primary volume supply (fuselage) and primary control surfaces (empennage) are relatively decoupled. This tolerates for small but late corrections later in the design process as described above.

The style of conceptual design described above creates problems for aircraft when the primary volume supply, lifting surface, and control surfaces are integrated in some fashion. For example, the flying wing integrates the primary lifting surface, volume supply, and control surfaces into a single component, the wing. With the wing serving all three functions, any change later in the design process for stability and control purposes can adversely affect the aerodynamic efficiency of the wing or reduce the internal payload capacity.

Furthermore, with the constant improvements in flight control system technology, aircraft can obtain significant performance improvements through relaxed static stability. This involves rebalancing the vehicle in order to reduce the aircraft's static stability, to reduce trim drag, while relying on a flight control system (FCS) to provide adequate flying and handling qualities. This can result in reduced overall flight vehicle size, translating into reduced fuel burn and/or improved range performance. Aircraft considering such technology during the initial design phase are termed control configured vehicles (CCV). Clearly, the conceptual design of CCVs requires an advanced stability and control analysis logic to be executed during the BD and CD design phases to quantify performance-optimal stability and control design solutions.

Mason⁴ depicts the problem of utilizing stability and control during the conceptual design as;

“The flight control guys (if they’re even there ...): ‘We need a complete 6-DOF, with an aero math model from -90⁰ to +90⁰ or else forget it.’ The Conceptual designers: ‘Just use the usual volume coefficient⁴”

Neither of these two extremes are acceptable at the conceptual design level. Volume coefficients may be adequate for an initial estimate of control surface sizes, but restrict the designer to a statistical data base which is not applicable for most novel vehicle configurations. On the other extreme, full 6-DOF flight simulation is time consuming and requires a detailed aircraft model which usually is not available during the conceptual design phase. Clearly, there is a need for a middle ground between these two approaches, which is applicable to a wide variety of configurations and yields the proper level of fidelity to meet the capability expectation of the conceptual design phase.

This presents an interesting problem. In order for the aerospace industry to progress and innovate it must explore beyond the traditional aircraft configurations, but a lack of stability and control analysis capability at the conceptual design level leaves issues such as inherent stability (flight safety), control power, trimmed aerodynamics, etc., left unexamined resulting in uncertainties related to an aircraft performance, safety, and cost. This increases the risk of pursuing novel vehicle configurations which already possess greater risks, inherent to their unconventional nature. This leads to the dilemma for the designers and management, having to investigate novel flight vehicle configurations with an apparent high level of risk and uncertainty compared to the conventional class of flight vehicles where the overall risk level is far lower. Clearly, to better compare flight vehicle configurations, it is required to improve stability and control modeling in order to arrive at a more realistic representation of the product while exploring potential to improvement to the vehicle, yielding better performance

and sizing estimates. The difficulty in comparing such notably different configurations at the conceptual design phase is that the stability and control team typically does not have the tool capability to consistently compare such novel configuration to traditional ones in a reasonable amount of time.

This problem was recognized by Chudoba in reference 1. In this work, Chudoba presents the solution, *AeroMech*, a generic (flight vehicle configuration independent) stability and control tool for conceptual design, which is capable of analyzing a wide variety of flight vehicle configurations across all applicable design constraining flight conditions (DCFC), where DCFC's are defined as “... *flight conditions with an overall governing effect on aircraft hardware sizing...*”¹

AeroMech analyzes a proposed configuration for the assessment of

1. control power leading to the sizing of the primary control effectors;
2. static and dynamic stability (open and closed loop) for flight safety;
3. 6-DOF trimmed aerodynamics for aircraft performance estimates.

The primary control effectors are defined as

- ***Longitudinal Control Effector (LoCE)*** -The control surface responsible for controlling pitching motion about the y-axis, typically the elevator.
- ***Lateral Control Effector (LaCE)*** - The control surface responsible for controlling rolling motion about the x-axis, typically the aileron.
- ***Directional Control Effector (DiCE)*** - The control surface responsible for controlling yawing motion about the z-axis, typically the rudder.

This thesis presents this unique stability and control methodology as an executable software prototype module for alpha testing (validation, calibration, design case study). This is accomplished through a description of the tool's theory, the methodology devised, the implementation of this process into an executable source code prototype which is validated and calibrated via design case studies of conventional and unconventional flight vehicles.

1.2 Background, Research Approach and Objectives

This research is the implementation of Dr. Bernd Chudoba Ph.D. dissertation "*Stability and Control of Conventional and Unconventional Vehicles, a Generic Approach¹*". The primary objective of the current research investigation is to develop the remaining building blocks required to arrive at an executable software.

Overall, the development of this system consists of 3 steps: (1) development of the mathematical framework and methodology concept, (2) development of a prototype, stand-alone software module *AeroMech* for validation and demonstration purposes of the tool, (3) integration of *AeroMech* into AVDS PrADO, a unique multidisciplinary design synthesis tool enabling utilization of *AeroMech* in a completely multi-disciplinary design framework.

Dr. Chudoba's work contributed to the first step towards the development of *AeroMech*, showing the feasibility and contribution of this generic tool to conceptual design:

1. development of the underlying methodology and overall process logic of *AeroMech*;

2. selection of the non-linear vortex lattice method VORSTAB⁵ as the most appropriate generic aerodynamic prediction tool;
3. derivation of the coupled 6-DOF steady-state equations of motion for key flight maneuvers: trim, pull-up/push-over maneuver, turn performance, rolling performance, and take-off rotation;
4. derivation of the coupled 6-DOF small perturbation equations of motion for open and closed loop dynamic mode analysis of both symmetric and asymmetric flight vehicle configurations;
5. demonstrating the feasibility and contribution of *AeroMech* to conceptual design

Former graduate student Kiran Pippalapalli took the critical next step in implementing this methodology into an executable source code⁶. While this work did not complete the prototype system, it laid the ground work for the current research undertaking. The major contributions by Pippalapalli to *AeroMech* were:

1. re-derivation of the coupled 6-DOF steady-state equations of motion as well as the coupled 6-DOF small perturbation equations of motion as manual check to the original derivation;
2. initial *AeroMech* pseudo code and structogram;
3. software integration of VORSTAB into *AeroMech*;
4. development of a partial prototype system programmed in Fortran, complete through the steady-state equations of motion analysis.

Pippalapalli⁶ documents the first version of the *AeroMech* prototype system, which contained certain deficiencies aside from being incomplete. These deficiencies in

the implementation of the *AeroMech* methodology are explained in Chapter 4 and are primarily related with the solution method to the non-linear trim equations of motion. This solution method effected the integration of the aerodynamic prediction tool VORSTAB and detracted from the generic nature of the tool. Thus, his version of *AeroMech* was limited in both, the stability and control analysis and aerodynamic analysis. These limitations aside, the source code structure and input file organization worked well for the prototype system and have been retained in the current system.

1.2.1 Research Objectives

The current prototype system is based on the valuable foundation developed by Pippalapalli. The primary objective of this research investigation is to complete the prototype stand-alone *AeroMech* software requiring the following steps:

1. revisiting the aerodynamic integration and steady state trim solution method developed in reference 6;
2. advance the aerodynamic prediction method integration to include other aerodynamic prediction tools (e.g., Digital DATCOM⁷ to compensate for deficiencies in VORSTAB;
3. research, select and integrate a pre-existing aircraft dynamics stability analysis package capable of both open and closed loop dynamic behavior analysis; time constraints prohibited implementing the dynamic stability method proposed in reference 1;
4. research and develop the output file organization and visualization;

5. validate *AeroMech* through historic aircraft case studies, thereby exemplifying the contribution of *AeroMech* related to the need for advanced stability and control analysis capability during the conceptual design phase;
6. continue to research and develop a clear approach to stability and control in conceptual design through the development of a 'Road Map' to stability and control during conceptual design and utilize *AeroMech* according to this guide.

CHAPTER 2

STABILITY AND CONTROL IN CONCEPTUAL DESIGN

2.1 Review of Stability and Control Techniques in Conceptual Design

Stability and control in conceptual design classically consists of empennage sizing through the use of statistical volume coefficients and reduced order models, assumptions limiting the approach naturally to conventional TAC aircraft only. As discussed in Chapter 1, this style of analysis is not sufficient for the conceptual design of future aerospace vehicles.

In Reference 1, Chudoba outlines the critical works in *design-oriented* stability and control techniques from 1935 to 2000. Design-oriented stability and control techniques are defined as procedures and tools which use stability and control analysis compatible with the conceptual design phase. This omits certain stability and control texts which focus on higher-fidelity controls theory. Table 2.1 presents an updated version of the original review of techniques based on Reference 1 (the updated techniques are in bold and italicized).

Table 2.1 Design-Oriented Approaches to Stability and Control Analysis¹

Implementation	Reference, Year	Comments
Stand-Alone Methods		
Root	1935	Design contribution to LoCE, based on Gates's dynamic longitudinal stability theory by the use of stability diagrams. Consideration of TAC only.
Silverstein	1939	Design of LoCE with emphasis on the evaluation of those design variables that affect the performance of the CE's, The discussion applies, in part, to the design of DiCE. Consideration of TAC only
Root	1939	Design contribution to LoCE and DiCE base on aerodynamic efficiencies of the CEs supported by analysis of empirical data. Consideration of TAC only
Morgan, <i>et al</i>	1945	Design of LoCE, DiCE, and LaCE based primarily on the analysis of empirical data compared to the theoretical approach. Consideration of TAC only
Wimpenny	1954	Design of LoCE, DiCE, and LaCE based on volume coefficients, empirical data, and stability and control requirements. Consideration of TAC and FWC
Lee	1961	Design of LoCE, DiCE, and LaCE win non-aerodynamic stability methods by fully integrating power control systems, auto-stabilization, and fly by-wire as contrasted by the classical (aerodynamic means of airframe design
Wood	1963	Design of LoCE, DiCE, and LaCE based on empirical and analysis of stability and controllability. Discussion of design parameters. Consideration of TAC only.
Burns	1972	Design of LoCE, DiCE, and LaCE based on static and dynamic stability and control design criteria for satisfactory handling characteristics. Detailed discussion of design parameters. Aircraft configuration independent discussion
Torenbeek	1990	Design of LoCE, DiCE, and LaCE based on static and dynamic stability and control design criteria, empirical data, volume coefficients, and design-critical flight conditions. Detailed discussion of design parameters. Consideration of TAC only.
Nicolai	1984	Design of LoCE, DiCE, and LaCE based on static only stability and control design criteria, empirical data, volume coefficients, and design-critical flight conditions. Detailed discussion of design parameters. Consideration of TAC, TFC, and FWC.
Hunecke	1987	Design of LoCE, DiCE, and LaCE based static and dynamic stability and control design criteria, empirical data, volume coefficients, and design critical flight conditions. Detailed discussion of design parameters. Consideration of TAC only.
Whitford	1987	Design of LoCE, DiCE, and LaCE based on static and dynamic stability and control design criteria, empirical data, volume coefficients, and design-critical flight conditions, Detailed discussion of design parameters. Consideration of TAC, TFC, and FWC.
Stinton	1991	Design of LoCE, DiCE, and LaCE based on static and dynamic stability and control design criteria, empirical data, volume coefficients, and design-critical flight conditions, Detailed discussion of design parameters. Consideration of TAC and FWC.
Raymer	1992	Design of LoCE, DiCE, and LaCE based on static and dynamic stability and control design criteria, empirical data, volume coefficients, and design-critical flight conditions, Detailed discussion of design parameters. Consideration of TAC and FWC.
Heinermann	1997	Design of LoCE, DiCE, and LaCE based on static and dynamic stability and control design criteria, volume coefficients, and design-critical flight conditions, Detailed discussion of design parameters. Consideration of TAC only.
Hunecke	1998	Design of LoCE, DiCE, and LaCE based on static and dynamic stability and control design criteria, empirical data, volume coefficients, and design-critical flight conditions, Detailed discussion of design parameters. Consideration of TAC only
Stinton	1998	Design of LoCE, DiCE, and LaCE based on static and dynamic stability and control design criteria, empirical data, volume coefficients, and design-critical flight conditions, Detailed discussion of design parameters. Consideration of TAC and FWC.
Anderson	1999	Design of LoCE, DiCE, and LaCE based on empirical data and volume coefficients. Consideration of TAC only. Descriptive character.
Jenkinson, <i>et al</i>	1999	Design of LoCE, DiCE, and LaCE based on empirical data and volume coefficients. Consideration of TAC only. Descriptive character.
Scholz	1999	Design of LoCE, DiCE, and LaCE based on static and dynamic stability and control design criteria, empirical data, volume coefficients, and design-critical flight conditions, Detailed discussion of design parameters. Consideration of TAC only.
Howe	2000	Design of LoCE, DiCE, and LaCE based on static and dynamic stability and control design criteria, empirical data, volume coefficients, and design-critical flight conditions, Detailed discussion of deisn parameters. Consideration of TAC, TFC, and FWC.
Integrated into a Synthesis Environment		
Oman	1977	Design of LoCE and DiCE with tail volume coefficients and computed tail arms. Consideration of TAC only.
Thorbeck	1984	Design of LoCE via evaluation of controllability and stability criteria. Statistical data for the design of DiCE and LaCE, Consideration of TAC only.
Alsina	1987	Design of LoCE and DiCE for design-critical flight conditions and with the use of statistical data
Bil	1988	Design of LoCE, DiCE and LaCE with statistical data and volume coefficients. Follow-on design sequence designing the LoCE and DiCE via evaluation of controllability and stability criteria. Consideration of TAC only.
Kay ⁸	1993	Design of LoCE, DiCE and LaCE based on static and dynamic stability and control design criteria and design-critical flight conditions. Detailed discussion of design parameters. Consideration of TAC, TFC, TSC, FWC.
Heinze ⁹	1994	Design of LoCE, DiCE and LaCE with tail volume coefficients and design-critical flight conditions. Consideration of TAC and FWC.
Roskam ¹⁰	1995	Design of LoCE, DiCE, and LaCE based on static and dynamic stability and control design criteria, volume coefficients, and design-critical flight conditions, Detailed discussion of design parameters. Consideration of TAC only.
Nunes	1995	Design of LoCE for design-critical flight conditions. Consideration of TAC, TFC, and TSC
MacMillin	1996	Design of LoCE, DiCE and LaCE based on static and dynamic stability and control design criteria and design-critical flight conditions. Detailed discussion of design parameters. Consideration of TAC only.
Soban¹⁰	1996	Design of LoCE based linear Vortex lattice method VORLAX and flying qualities (CAP parameter) analysis. Integrated into ACSYNT, Applicable for TAC, TFC, TSC, FWC, OFWC, OWC
Pohl ¹¹	1997	Design of LoCE, DiCE, and LaCE based on static and dynamic stability and control design criteria, empirical data, volume coefficients, and design-critical flight conditions, Detailed discussion of design parameters. Consideration of TAC only
Lee, <i>et al</i> ¹²	1998	Design of LoCE, DiCE and LaCE based on static and dynamic stability and control design criteria taking a FCS and design-critical flight conditions. Detailed discussion of design parameters. Consideration of FWC (X-33) only.
Nicolai ¹³	1999	Design of LoCE, DiCE and LaCE with a generic VLM (VORLAX) and 2d PM (QUADPAN. Consideration of a range of conventional and unconventional aircraft configurations.
Chudoba¹	2000	Design of LoCE, DiCE, and LaCE with a non-linear VLM (VORSTAB) and a generic set of coupled 6 DOF equations of motion. Applicable to TAC, TFC, TSC, FWC, OFWC, and OWC
Jeffery¹⁴	2006	Design of LoCE, DiCE and LaCE with multiple aerodynamic prediction methods of 6-DOF modeling and simulation. Integrated into the J2 Universe System. Applicable for TAC, TFC, TSC, FWC, OFWC, OWC
Takahashi¹⁵	2007	Design of LoCE, DiCE and LaCE with linear vortex lattice methods and ROM from Lee¹² and Kay^{7b}. In addition linear control system model is used to size the FCS. Integrated into an MDO. Applicable for TAC, TFC, FWC

Of all of these methods, five have been identified to adequately represent the diversity of stability and control techniques in conceptual design (1) Nicolai¹³ and Roskam¹⁰ (classical approach), (2) Pohl¹¹ (3) Kay⁸, (4) Lee¹², (5) Chudoba¹. The approaches proposed by Pohl, Kay, Lee and Chudoba can be considered improvements or adaptations to the classical methodology outlined by Nicolai¹³ and Roskam¹⁰. All of these methods can be said to follow the following basic steps. While each method does not necessarily follow these steps in this particular order, they do address these issues.

1. ***Initial control effector sizing*** - Typically done through the use of volume coefficients and previous aircraft design and operational experience.
2. ***Identification of DCFC's*** - Before any analysis can be performed during the CD phase, the designer must first define which flight conditions are considered critical with respect to performance and optimal sizing of control effectors.
3. ***Aerodynamic prediction of stability and control derivatives*** - During the CD phase, the aerodynamic team concentrates on predicting lift, drag and pitching moment. The stability and control team must predict control derivatives, static stability derivatives and dynamic stability derivatives for the flight vehicle configuration under investigation.
4. ***Trim and maneuver analysis*** - The objective is to predict the control surface size and/or deflections required for steady state trimmed and maneuvering flight. This is typically done through 1-DOF or 3-DOF reduced order models.
5. ***Static stability analysis*** - comparing the static stability of the airframe to design requirements.

6. ***Dynamic stability analysis*** – Prediction of the dynamic behavior of the flight vehicle in all axes for comparison to design and safety requirements. This may include both open and closed loop analysis.
7. ***Assessment of Control Power*** - From the above analysis the designer must decide if the controls configuration selected for the flight vehicle is adequate over the range of DCFC tested, thus the critical corners of the flight envelope. If not, either the vehicle must be rebalanced (shift center of gravity), the control effector size must be changed, or the control effectors must be relocated (increase the lever arm).

The classical approach to stability and control is explained in the following section.

2.1.1 Assessment of the Classical Approach

The classical approach to stability and control during the conceptual design phase can be seen through the methods proposed by Nicolai¹³ and Roskam¹⁰. These approaches apply stability and control to the sizing and analysis of symmetric flight vehicles such as the TAC, TFC and FWC.

Initial Sizing

The LoCE, LaCE, and DiCE are initially sized using statistical volume coefficients (Equation 1) from vehicles of similar size and mission.

$$C_{ce} = \frac{S_{ce} I_{ce}}{S_{ref} c_{ref}} \quad \text{Eq. 1.1}$$

Where, S_{CE} and l_{CE} are the area and distance from the control effector to the c.g.

Once an appropriate volume coefficient is selected from a statistical data base, the location and size of the control effector can be estimated.

Identification of DCFC's

The DCFC's are organized into flight conditions which size the LoCE, LaCE, DiCE. These design-critical flight conditions are summarized in Table 2.2.

Table 2.2 Classic DCFC's for Control Effector Sizing¹³

DCFC	Description
LoCE	
Trimmed Cruise	Estimation of trim drag from the LoCE.
High g Maneuvering	LoCE's ability to perform pull-up/push-over maneuvers at maximum g loading.
Take-off Rotation	LoCE's ability to lift the nose of the ground at rotation speed.
High α , Low speed	LoCE's ability to maintain trim at forward c.g. during low-speed landing approach with flaps-down, engines at idle, and high angle of attack.
DiCE	
Crosswind Landing	DiCE's ability to maintain straight ground path during take-off and landing
Anti-symmetric Power	DiCE's ability to maintain straight flight path with most outboard engine inoperable
Adverse Yaw	DiCE's ability to compensate for yawing moments produced by the aileron during rolls or high a, low speed, steep coordinated turns.
LaCE	
Roll Performance	LaCE's ability to bank the aircraft to a required bank angle in the required time.

The remaining analysis steps of aerodynamic prediction, steady state analysis, static stability and dynamic stability are then repeated for each DCFC's and the control effectors are sized to meet the condition that imposes the greatest demands.

Aerodynamic Prediction of Stability and Control Derivatives

The stability and control derivatives are calculated using a component build up method, similar to the methods presented in the USAF Stability and Control DATCOM⁶¹. These methods combine the influence of each distinct hardware components of the aircraft (wing, fuselage, horizontal tail, etc.) to predict the total flight vehicle derivatives. The effects of each component are calculated individually and

finally summed using semi-empirical methods which combine experimental data with theoretical equations. These methods are very useful for conceptual design of conventional vehicles but limit the designer to conventional configurations which have previously been produced.

Trim and Maneuvering Analysis

Trim and maneuvering analysis utilizes steady-state 1-DOF or 3-DOF models to evaluate control power available in the longitudinal and lateral/directional planes. Flight vehicle geometric symmetry is assumed to decouple these planes of motion. Consequently, these equations of motion are not applicable to asymmetric configurations such as the OWFC nor the asymmetric flight conditions of symmetric flight vehicles. As an example, the longitudinal trim and maneuvering equations of motion utilized by these methods are presented in Table 2.3.

Table 2.3 Longitudinal Trim and Maneuvering Models from Nicolai⁷⁰ and Roskam⁸

Equations	Description
Longitudinal Trim (1-DOF, Nicolai⁷³)	
$\delta_{LoCE} = \frac{-C_{m_0} + (SM)C_L}{C_{m\delta_{LoCE}}}$	1-DOF approximation for trim. The LoCE deflection to trim is calculated to balance the pitching moment equation. The lift required to trim is calculated separately, thus this derivation neglects the effect of the LoCE on the total lift of the aircraft.
Longitudinal Trim (3-DOF, Roskam¹⁰)	
$W \sin \gamma = (C_D) \bar{q} S + T \cos(\phi_T + \alpha)$	The LoCE deflection to trim can be found through numerically solving the system of equations or through the graphical solution presented in Reference 8.
$W \cos \gamma = \left(C_{L_0} + C_{L_\alpha} \alpha + \sum C_{L_{\delta_{LoCE}}} \delta_{LoCE} \right) \bar{q} S + T \sin(\phi_T + \alpha)$	
$0 = \left(C_{m_0} + C_{m_\alpha} \alpha + \sum C_{m_{\delta_{LoCE}}} \delta_{LoCE} \right) \bar{q} S \bar{c} + T d_T$	
Pull-Up/Push-Over (1-DOF, Nicolai¹³)	
$\delta_{LoCE} = (\delta_{LoCE})_{Trim} + \Delta \delta_{LoCE}$ $\Delta \delta_{LoCE} = \frac{\left(-SM + \frac{\rho S \bar{c}}{4m} C_{m_q} \right) (n-1) C_{L_{n-1}}}{C_{m\delta_{LoCE}}}$	The additional LoCE deflection to sustain a load factor n is calculated. This deflection is then added to the trimmed deflection. The LoCE must have enough control power to achieve the maximum load factor required.
Pull-Up/Push-Over (1-DOF, Roskam¹⁰)	
$\delta_{LoCE} = (\delta_{LoCE})_{Trim} + (\partial \delta_{LoCE} / \partial n) n_{req}$ $(\partial \delta_{LoCE} / \partial n) = \frac{-C_{L_\alpha} C_{m_q} \frac{\bar{c} g}{2U^2} n - C_{m_\alpha} C_{L_1}}{C_{L_\alpha} C_{m\delta_{LoCE}} - C_{L_{\delta_{LoCE}}} C_{m\delta_\alpha}}$	The additional LoCE deflection to sustain a load factor n is calculated. This deflection is then added to the trimmed deflection. The LoCE must have enough control power to achieve the maximum load factor required. C_{L_1} is the lift required for trim.

These reduced order models generate physical insight, enabling the visualization of the interaction of certain design variables for sizing of the LoCE. However, those models are limited to symmetric aircraft in symmetric flight conditions.

Static Stability Analysis

Static stability requirements for aircraft provide important information for the sizing of control effectors and stabilizing surfaces (i.e. vertical tails, horizontal tails, canards, etc.). The requirements typically state that the aircraft be statically stable throughout the flight envelope in the longitudinal, directional and lateral planes. The exception to this is with CCV's which can be designed to fly statically unstable to

improve maneuverability or reduce trim drag. These requirements are outlined in Table 2.4.

Table 2.4 Static Stability Requirements, Nicolai¹³

Criterion	Description
Longitudinal	
$C_{m_\alpha} = -(SM)C_{l_\alpha} < 0$	When satisfied, any disturbance in pitch will result in a restoring pitching moment. This requirement may be relaxed to improve performance or maneuverability.
Directional	
$C_{n_\beta} > 0$	When satisfied, any disturbance in side-slip will result in a restoring yawing moment. Primarily effected by the vertical lifting surface.
$C_{l_\beta} < 0$	When satisfied, any disturbance in side-slip will result in a restoring rolling moment. Primarily effected by the dihedral effect.
Lateral (spin resistance and roll reversal)	
$C_{n_{\beta_{dyn}}} = C_{n_\beta} - C_{l_\beta} \frac{I_{zz}}{I_{xx}} \tan \alpha > 0$	Provides an approximation for aircraft spin resistance during non-rolling maneuvers, no control inputs. Usually important for fighter and high-speed aircraft.
$LCSP = C_{n_\beta} - C_{l_\beta} \frac{C_{n_\delta}}{C_{l_\delta} \frac{LaCE}{LaCE}} > 0$	Lateral Control Spin Parameter provides an approximation for roll reversal. Adverse yaw induced by the aileron combined with low directional stability can produce a natural roll reversal. Usually important for fighter and high-speed aircraft.

These requirements are not restricted by symmetry assumptions but are depended upon the capability of the aerodynamic tool set to predict the stability derivatives for the configuration and flight condition of interest. Overall, the degree to which these requirements must be met depends upon the mission and design requirements for the vehicle.

Dynamic Stability Analysis

With the trim point defined for the flight condition considered, the dynamic stability of the aircraft for this flight condition can be calculated. In Nicolai¹³ this is addressed by placing requirements on the dynamic derivatives ($C_{mq} < 0$, $C_{lp} < 0$) and in Roskam¹⁰ the dynamic stability modes are calculated through reduced order models for the open loop longitudinal (short period mode, phugoid mode) and lateral/directional modes (Dutch roll mode, spiral mode, roll mode). Roskam¹⁰ also presents a procedure

for estimating the fight control system FCS gains for stability augmentation of a closed loop aircraft. For example, the short period open and closed loop reduced order models are shown in Table 2.5

Table 2.5 Short Period Open and Closed Loop Reduced Order Models, Roskam¹⁰

Model	Description
Open Loop	
$\omega_{n_{SP}} = \sqrt{\frac{Z_\alpha M_q}{U} - M_\alpha}$ $\xi_p = \frac{-M_q + (Z_\alpha/U) + M_{\dot{\alpha}}}{2\omega_{n_{SP}}}$	An approximation of the short period natural frequency and damping ratio. These must meet minimum requirements throughout the fight envelope. The natural frequency can never be negative and thus the configuration must be statically stable. The configuration must also be symmetric to decouple the longitudinal from the lateral/directional modes.
Closed Loop	
Stiffness Restoration	
$(C_{m_\alpha})_{req} = \left[(Z_\alpha M_q / U) - (\omega_{n_{SP}}^2)_{req} \right] \frac{I_{yy}}{qS\bar{c}}$ $k_\alpha = \frac{(C_{m_\alpha})_{req} - C_{m_\alpha}}{C_{m_{\delta_{LoCE}}}}$	To restore stiffness through a closed loop stability augmentation system, the gain, K_α , is predicted by estimating the required C_{m_α} from the required natural frequency.
Damping Restoration	
$(C_{m_q})_{req} = \left[(-2\omega_{n_{SP}} \xi_{sp})_{req} - (Z_\alpha / U_\alpha) - M_\alpha \right] \frac{2I_{yy}U}{qS\bar{c}^2}$ $k_q = \frac{\left((C_{m_q})_{req} - C_{m_q} \right) \left(\frac{\bar{c}}{2U} \right)}{C_{m_{\delta_{LoCE}}}}$	To restore the short period damping ratio through a closed loop stability augmentation system the gain, K_q , is estimated the required C_{m_q} from the natural frequency and damping requirements

As shown, the usefulness of these models is restricted to statically stable symmetric vehicle configurations in symmetric flight conditions. However, these reduced order models provide physical insight into the relationship between design parameters and dynamic stability.

Roskam¹⁰ also treats several special considerations such as aeroelasticity and inertia coupling, which can have a significant effect of the control surface sizing of some vehicles.

Assessment of Control Power

The following guidelines are provided with Nicolai's¹³ methodology for sizing the control effectors (CE) (Table 2.6).

Table 2.6 Guidelines for Control Effector Sizing¹³

Configuration	LoCE	DiCE	LaCE
Tail-Aft Configuration (TAC)	The horizontal surface area is chosen to maintain the static stability requirements. The LoCE is sized by examining the control surface deflections required for trim and maneuvering across the DCFC's.	The vertical stabilizer is sized to meet the static directional stability requirement. The DiCE is sized to meet the DCFC trim and maneuvering.	LaCE is sized to meet roll rate requirements for the design.
Tail-First Configuration (TFC)	Same procedure as outlined for TAC.	Same procedure as outlined for TAC.	Same procedure as outlined for TAC.
Flying Wing Configuration (FWC)	No guidelines provided. FWC requires several multi-disciplinary iterations to size CE.	Same procedure as outline by the TAC	Same procedure as outline by the TAC

In summary, these methods provide physical insight into sizing CEs for stability and control requirements but are deficient in the following ways.

1. The difficulty to predict aerodynamic stability derivatives for asymmetric flight conditions and flight vehicle shapes limits the designer to traditional symmetric aircraft and the linear symmetric flight conditions.
2. The reduced-order trim, maneuver and dynamic equations of motion are only applicable to the design of symmetric vehicles in mostly symmetric flight conditions.

2.1.2 Assessment of the State-of-the-Art

The methods produced by Pohl¹¹, Kay⁸, Lee¹², and Chudoba¹ build on the classical approach to improve the designer's ability to accomplish the stability and control goals demanded during the conceptual design phase. These methods represent the state-of-the-art in stability and control analysis during the CD phase and their contributions to the major process-categories are summarized in Table 2.7.

Table 2.7 Summary of Modern Stability and Control Methods for Conceptual Design

	Pohl ¹¹	Kay ⁸	Lee ¹²	AeroMech, Chudoba ¹
Initial Control Effector Sizing	Volume Coefficients	No method presented	No method presented	Use of an Engineering Knowledge based system (KBS) to initial size CE based on past experience and Knowledge
Identification of DCFC's	Same as Classical	Same as Classical	DCFC for the X-33 space access vehicle	Additional failure conditions and cross-coupling conditions applicable to symmetric and asymmetric configurations and flight conditions
Aerodynamic Prediction of Stability and Control Derivatives	Multiple Methods: Panel Code, ESDU Sheets, Existing Data, etc.	Linear vortex lattice method	Non-linear vortex lattice method	Non-linear vortex lattice method, VORSTAB
Trim and Maneuvering Analysis	Same as Classical	Classical reduced order models with control allocation (LOTS) ¹⁶	Numerical solution to trim equations, nature of equations unknown	Numerical solution to a generic set 6-DOF coupled steady-state equations of motion. Control allocation with (LOTS) ¹⁶
Static Stability Analysis	Same as Classical	Same as Classical	Same as Classical	Same as Classical
Dynamic Stability Analysis	No Method	Reduced order models for stability modes and inertia coupling	Root locus method for decoupled longitudinal and lateral/directional motion	Root locus method for a coupled 6-DOF linear system of equations. Applicable to symmetric and asymmetric configurations and flight conditions
Assessment of Control Power	Same as Classical	No iteration or resizing method presented	No iteration or resizing method presented	No iteration or resizing method presented

The method developed by Kay⁸ possesses the following advancements.

1. Utilization of a linear vortex lattice method. Vortex lattice methods (VLM) are applicable to a large array of both systemic and asymmetric vehicle configurations and flight conditions.
2. Incorporation of the control allocation logic, LOTS¹⁶. Control allocation is utilized when a vehicle has more than one primary control effector, leading to an over determined system for trim and maneuvering. To trim these vehicles, LOTS solves for a minimum trim drag solution for three surface configurations (TSC) and two surface configurations (TFC) incorporation thrust vectoring, when applicable. LOTS is explained in further detail in Chapter 3.

The key advancements included in Lee's method are;

1. The use of a non-linear vortex lattice method for aerodynamic prediction. Control effectors are typically sized at the non-linear corners of the flight envelope (i.e. stall) and thus a linear method can not adequately predict control power.
2. The numerical solution for steady-state trim and maneuvering includes control cross-coupling effects, thrust vectoring, and reaction control system (RCS) thrusters. This represents an improvement to the classical 1-DOF and 3-DOF models.
3. Dynamic stability is analyzed utilizing a root locus method for predicting the dynamic modes for both open and closed loop stability augmentation. The control power from this stability augmentation is also calculated.

4. This method shows potential for integration into a multidisciplinary design environment, see Nicolai¹⁷. The integration of the method into a multidisciplinary design environment gives the designer the ability to explore the effects of stability and control truly multi-disciplinary (such as the effects on performance, cost, weight, structure, etc.).

Chudoba¹ incorporated and significantly advanced the above improvements to the classical approach via the derivation of a generic 6-DOF trim and dynamic stability mathematical model, thereby taking both inertia and aerodynamic cross-coupling effects of asymmetric flight vehicle configurations and flight conditions into account. The top-level *AeroMech* methodology is summarized in Figure 2.1.

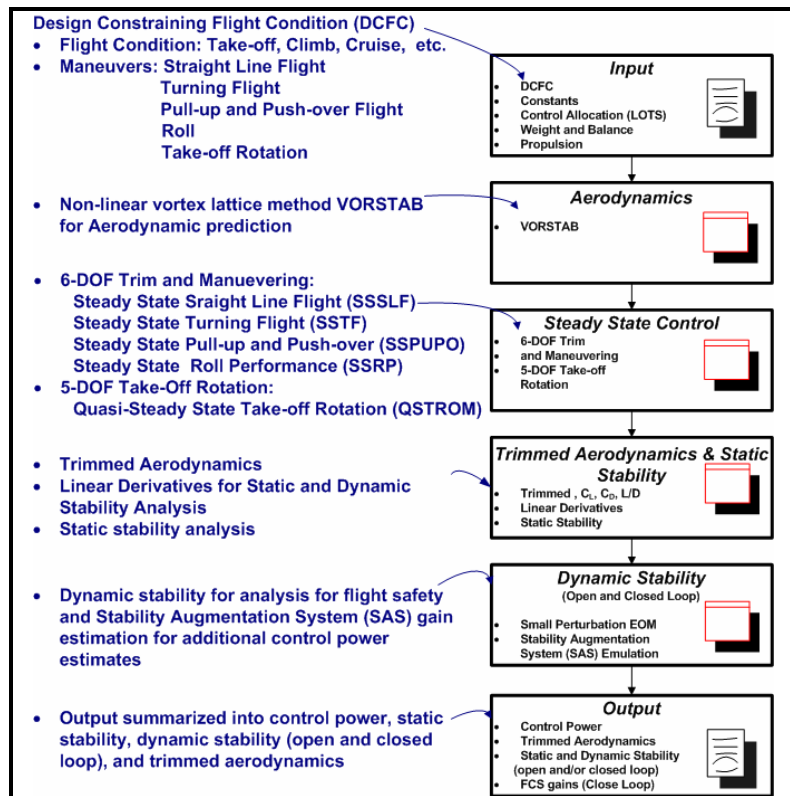


Figure 2.1: AeroMech Overall Methodology

This methodology enables the designer to explore both symmetric and asymmetric aircraft configurations and flight conditions using a consistent tool set, thus gives the designer the ability to truly explore the design space from either the disciplinary flight mechanics perspective or multi-disciplinary design perspective.

Reference 1 proposes to integrate *AeroMech* into PrADO⁸⁷ (Preliminary Aerospace Design and Optimization), a multidisciplinary design synthesis environment. PrADO has the ability iterate, converge, and optimize aircraft concepts through all major aerospace disciplines, as opposed to the two or three disciplines usually considered with current Multi-disciplinary Design Optimization MDO tools. For each discipline, PrADO contains a method library where the user selects the most appropriate method for the application at hand. *AeroMech* will be integrated as one method into the flight mechanics methods library, enabling the design engineers to arrive at conservative CE sizing, or the exploration of performance-optimal control-configured vehicles (CCV) design solutions.

While *AeroMech* presents a unique capability to advanced stability and control problems during the CD phase, its generic capability enables the engineer to utilize the tool for simple, thus non-complicated design problems. For example, the coupled 6-DOF small perturbation equations can create complications in distinguishing roots such as the short period and Dutch roll motion and require computation of certain cross coupling derivatives that may be beyond the ability of the aerodynamic prediction tools available. Additionally, utilizing a variety of aerodynamic prediction methods, similar to the approach seen with Pohl¹¹, would be preferable for the conceptual designer rather

than relying solely on a single aerodynamic prediction tool like the non-linear VLM VOSTAB. While VORSTAB is a power vortex lattice method it does not predict unsteady aerodynamic derivatives and has difficulties with completely asymmetric vehicle configurations such as the OWC, other VLM's are cable of calculating. For classical configurations such as the TAC a semi-empirical handbook method, such as Digital DATCOM, may be more appropriate and less time consuming to build the aircraft model.

2.2 Summary of Results and Prototype System Requirements

From this review it is clear that the method proposed by Chudoba¹ incorporates the most generic trim, maneuvering and dynamic stability capability of the 5 methods presented. Once the *AeroMech* module is implemented into PrADO, the designer will be able to truly explore and compare traditional with radically different configurations in a truly multi-disciplinary context.

As stated in Chapter 1 the present work is to complete the second stage of the development of *AeroMech*, which is to develop an executable software prototype, operated stand-alone for validation and demonstration purposes. To complete this prototype system, the following modifications have been made to the initial methodology of the prototype system.

1. The aerodynamic prediction tool VORSTAB has been complemented with the semi-empirical tool Digital DATCOM, and the linear vortex lattice method VORLAX. The combination of these tools will give the prototype system the ability to analyze a wider variety of configurations for validation purposes.

2. The inclusion of classical decoupled root locus method (separate linear systems for longitudinal and lateral/directional motion) to allow for a more straight forward assessment of the dynamic stability of symmetric vehicles in symmetric and asymmetric flight conditions and to compare the decoupled and coupled results for the asymmetric vehicles and flight cases.

These modifications aside, the original methodology and mathematical framework from Chudoba¹ has been implemented into the stand-alone prototype system *AeroMech* which is further explained in the following chapter.

CHAPTER 3

AEROMECH METHODOLOGY AND THEORY

3.1 Methodology Overview

AeroMech's methodology and mathematical frame work are the result of Dr. Bernd Chudoba's PhD. research¹, "*Stability and Control of Conventional and Unconventional Aircraft Configurations – A Generic Approach*". This robust methodology enables designers to quickly analyze and assess a wide range of flight vehicle configurations for stability and control issues relevant to conceptual, design such as;

- control power assessment for the purpose of sizing the primary control effectors;
- trimmed aerodynamics in all axes for symmetric and asymmetric flight conditions and flight vehicles enabling vehicle sizing and performance assessment;
- static and dynamic stability assessment in all axes to enable true control configured vehicle (CCV) design;

To accomplish this *AeroMech* utilizes the following methodology originally developed in Reference 1 and slightly modified here (Figure 3.1). The methodology consists of four main components;

1. **Input** - Defining the Design Constraining Flight Conditions (DCFC's), the critical flight conditions and maneuvers that impose the greatest demand on a

flight vehicle which size its major components¹. This section also defines flight vehicle constants, constraints and the control allocation schedule.

2. **Aerodynamic Analysis** - Consisting of the non-linear vortex lattice method (VLM) VORSTAB⁵, the semi-empirical tool Digital DATCOM⁷, the linear vortex lattice method VORLAX¹⁸ and the option to manually input aerodynamic data. These tools are utilized to develop the initially un-trimmed aerodynamic data set.
3. **Stability and Control Analysis** – Produces control power, trimmed aerodynamics, static and dynamic stability analysis for statically stable, indifferent, and unstable flight vehicles in any axis.
4. **Output** - Consisting of control power information, trimmed aerodynamics and stability information for each DCFC. In addition, summary output files are created to presentation results covering all DCFCs considered.

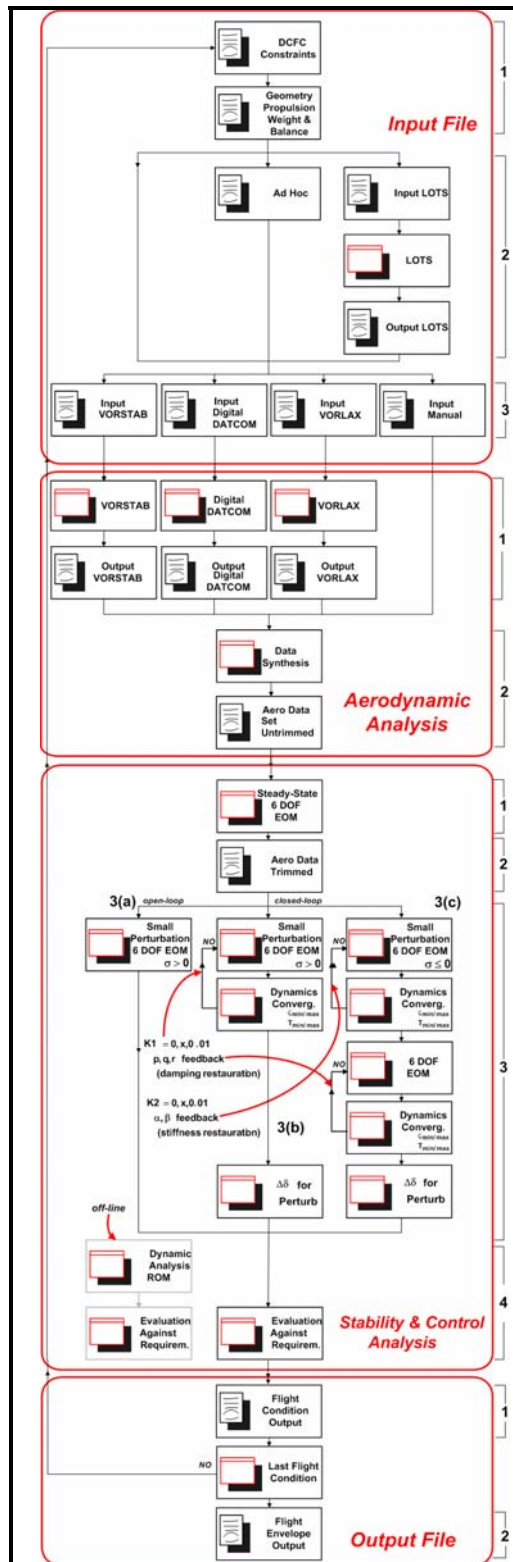


Figure 3.1: AeroMech Detailed Overall Methodology

To aid in the description of the stability and control algorithm, the example of the Northrop YB-49 Flying Wing will be utilized as a validation case study (Figure 3.2).

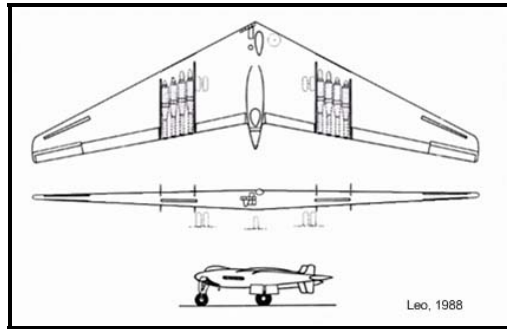


Figure 3.2: Three-View of the Northrop YB-49 Flying Wing

The flying wing configuration (FWC) has been selected as the primary case study to demonstrate *AeroMech* because

1. the FWC tends to be a more demanding configuration arrangement compared to the TAC, enabling to demonstrate *AeroMech*'s generic (configuration-independent) analysis capability;
2. of the availability of performance and stability and control flight test data (References 19 and 20) for validation purposes;
3. the flying wing debate has centered historically on the aerodynamic efficiency only; however, such a vehicle can only be superior compared to the classical tail-aft configuration (TAC) when flown with relaxed static stability in the pitch axes, ultimately reducing flight vehicle size and trim drag; this ultimately requires the flying wing to be a controlled configured vehicle (CCV), thus demonstrating the advanced capability of *AeroMech*.

This vehicle will be discussed in more detail in Chapter 4 and is used here merely for demonstration purposes of the individual stability and control features.

3.2 Input and Control Allocation

Input for AeroMech consists of three parts: (1) aircraft and design constraining flight condition (DCFC) input, (2) control allocation scheduling, and (3) aerodynamic input, see Figure 3.3.

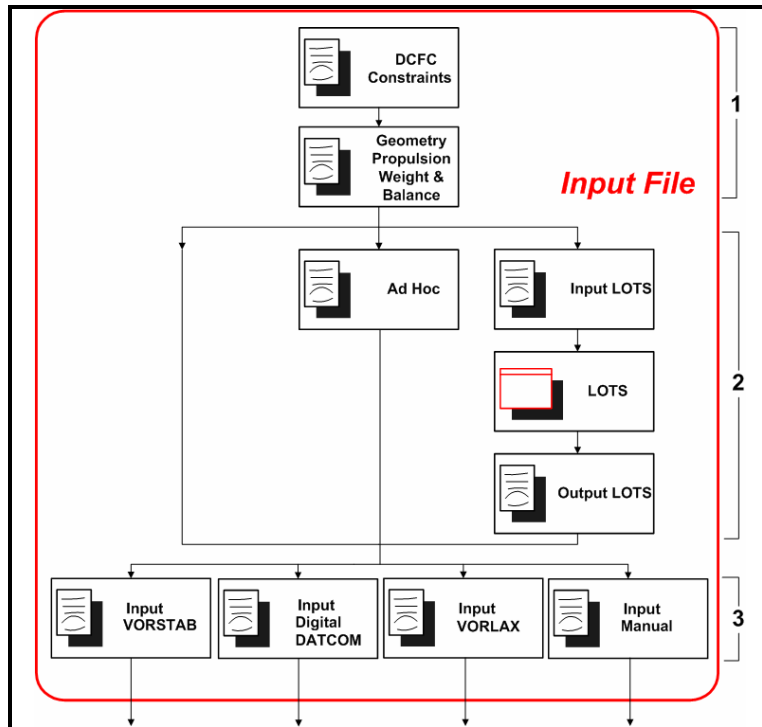


Figure 3.3: *AeroMech* Input and Preprocessing

(1) *DCFC and Aircraft Input:* These input files define the flight conditions, vehicle constants and constraints for each DCFC. The DCFC input file consists of

- flight condition variables (h , M , etc.);
 - type of maneuvers tested (straight-line flight, pull-up, take-off rotation, etc.);
- multiple maneuvers can be examined in a single run;

- vehicle design requirements and certification constraints ($\omega_{s.p.}$, $\zeta_{s.p.}$, δ_{LoCE} , δ_{LaCE} , δ_{DiCE} , etc.).

The geometry, propulsion, and weight and balance input file consists of

- geometry input (b_{ref} , c_{ref} , S_{ref} , landing gear location, etc.);
- weight and balance input (W , $X_{c.g.}$, I_x , I_y , I_z , I_{xz} , I_{xy} , I_{yz});
- propulsion input, where the thrust vector is defined by T_i , ψ_{Ti} , ϕ_{Ti} , X_T , Y_T , Z_T ;

(2) *Control Allocation*: Some aircraft configurations utilize redundant control effecters (CE) to improve performance. A three surface aircraft (TSC), such as the Piaggio Avanti (Figure 3.4), can utilize both a canard and tail plane to trim to a range of angles-of-attack and center-of-gravity locations at constant velocity and altitude by varying the longitudinal load distribution between the canard, wing, and horizontal tail. In contrast, traditional tail aft aircraft (TAC) must trim to a single angle-of-attack and center-of-gravity location at constant velocity and altitude because of the availability of only a single control effector for the pitch axis.

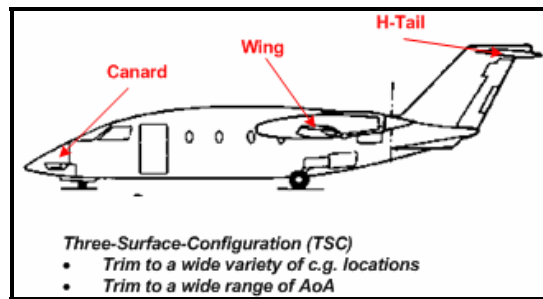


Figure 3.4: Three-Surface Configuration, Piaggio Avanti.

Thus, the three-surface configuration (TSC) presents an over-determined system (due to the extra control effector in the longitudinal axis) for longitudinal stability, control, and trim, giving the designer the freedom to schedule the over determined

LoCE's to either minimize trim drag, minimize control surface deflections, etc. The logic chosen to schedule the longitudinal control effectors is referred to as control allocation.

To address the control allocation issue, *AeroMech* utilizes two methods. First, the designer can manually schedule the longitudinal, directional and lateral CEs based on experience. In *AeroMech* this is referred to as the 'ad hoc' method. Second, the Linear Optimum Trim Solution (LOTS)¹⁶ methodology can be used to solve for a minimum longitudinal trim drag solution for three-surface configurations and two-surface configurations with thrust vectoring. This code uses a Lagrange's formulation to obtain a longitudinal load distribution that will minimize a quadratic trim drag model¹⁶.

For the YB-49 flying wing case study, longitudinal control allocation is required due to the availability of two independent longitudinal CEs located on the trailing edge of the wing, being the elevon and trim flap on the outer wing panel (Figure 3.5).

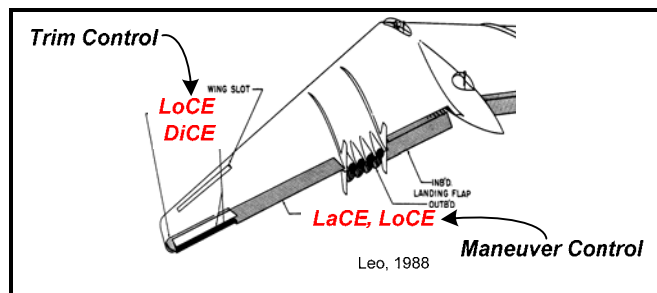


Figure 3.5: Longitudinal control allocation for the YB-49 flying wing

The YB-49 uses the trim flap to trim the vehicle for straight-line flight, whereby the elevons are used for maneuvering control. This manual allocation of the longitudinal CEs represents the 'ad-hoc' approach in scheduling the CEs in *AeroMech*.

(3) *Aerodynamic Input*: In *AeroMech* the designers can opt for four methods providing aerodynamic input:

- VORSTAB⁵, a non-linear vortex lattice method;
- Digital DATCOM⁷, a digital semi-empirical handbook method;
- VORLAX¹⁸, a linear vortex lattice method;
- manual data input (aerodynamic look-up tables);
- or any combination of the above.

The input files for VORSTAB, Digital DATCOM and VORLAX are constructed based upon the geometry of the aircraft. The input files for these individual methods are described in more detail in Appendices B and C. A brief description of the methods themselves is provided in the next chapter.

3.3 Aerodynamic Prediction

AeroMech utilizes the non-linear vortex lattice method VORSTAB, the semi-empirical code Digital DATCOM and the linear vortex lattice method VORLAX for the prediction of aerodynamic coefficients and derivatives. As detailed in Reference 1, *VORSTAB* was chosen as the primary aerodynamic tool for *AeroMech* due to its ability to handle a wide variety of flight vehicle configurations and its superior non-linear aerodynamic modeling capability. This ability is key since control effectors are typically sized to meet stability and control requirements in the non-linear corners of the flight envelope, such as an aircraft during its final approach at low dynamic pressure and high angles of attack (AoA). For this reason, VORSTAB's ability to model non-linear aerodynamics is critical for correct control effector sizing.

However, VORSTAB contains limitations as every aerodynamic estimation code. The primary draw back of VORSTAB is its inability to model unsteady aerodynamics, which is inherent to any vortex lattice method. Thus, critical derivatives for dynamic analysis such as $C_{m\dot{\alpha}}$ and $C_{L\dot{\alpha}}$ are not computed. These derivatives have a significant effect on longitudinal damping of certain aircraft configurations, such as the tail-aft configuration, thus must be estimated before dynamic stability can be addressed. VORSTAB also is limited in modeling asymmetric flight vehicle configurations since the code has not been initially written for those applications. Although VORSTAB is capable of modeling an oblique flying wing (OFWC) alone, the code is currently not able to model vertical surfaces or a fuselage in combination with the asymmetric wing.

To overcome some of the deficiencies of VORSTAB, Digital DATCOM and VORLAX are utilized in support. Digital DATCOM is used to generate the unsteady aerodynamic derivatives and other control effector types that are not easily modeled in VORSTAB. VORLAX is used to model asymmetric vehicle configurations such as the oblique wing configuration (OWC). The individual modeling capabilities of VORSTAB, Digital DATCOM and VORLAX are summarized in Table 3.1.

Table 3.1 Modeling Capabilities of VORSTAB⁵, Digital DATCOM⁷, and VORLAX¹⁸

	VORSTAB	Digital DATCOM	VORLAX
<i>Mathematical Model</i>	non-linear vortex lattice	semi-empirical methods	linear vortex lattice
<i>Flight Conditions</i>	subsonic and supersonic	subsonic, supersonic, hypersonic, transonic with experimental data	subsonic and supersonic
<i>Static Derivatives</i>	yes	yes	yes
<i>Dynamic Derivatives</i>	yes, no unsteady aerodynamic derivatives	yes	yes, no unsteady aerodynamic derivatives
<i>Control Derivatives</i>	yes	yes	yes
<i>Configurations</i>	up to 5 surfaces and 1 fuselage. asymmetric wing alone, no fuselage or vertical fins	Symmetric fuselage, wing, horizontal tail, vertical tail, ventral Fin. twin vertical tail for subsonic speeds only	symmetric and asymmetric configurations
<i>Longitudinal Control Surfaces and High Lift System Types</i>	plain flaps and leading edge slats	plain, single slotted, double slotted, Fowler slotted, split, leading edge and Krueger flaps, pure jet flaps, jet flap & mech., IBF*, EBF**	Any flap that can be modeled with flat plate sections
<i>Lateral Control Surfaces</i>	antisymmetric deflected Ailerons	plug, flap, slotted spoilers, differential horizontal tails, and ailerons	any flap that can be modeled with flat plate sections
<i>Directional Control Surfaces</i>	rudder	no	yes
<i>Non-linear Aerodynamic Prediction</i>	yes	yes	No
<i>Ground Effect</i>	yes	yes	No

*Externally blown flap

**Internally blown flap

In addition to these methods, *AeroMech* allows for manual input of aerodynamic data in a generic data file, enabling users to utilize numerical aerodynamic information

from miscellaneous sources. The use of such generic data file will enable us to integrate *AeroMech* easily into the synthesis system, AVDS PrADO.

The organization of these four options providing aerodynamic input is detailed in Figure 3.6.

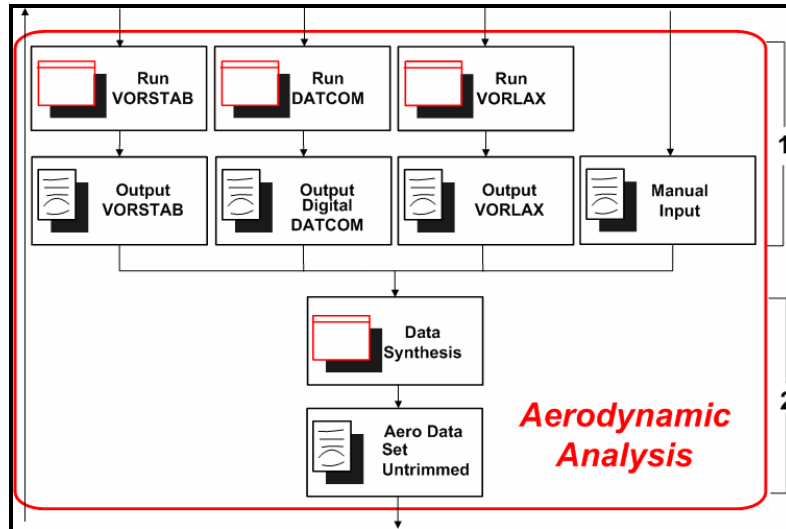


Figure 3.6: *AeroMech* Overall Methodology: Aerodynamic Analysis

(1) *Aerodynamic Analysis*: These three codes are operated in different ways and thus require their own unique integration schemes which are represented by RunVORSTAB, RunDATCOM, and RunVORLAX. These are stand-alone executables, built for *AeroMech*, programmed to execute in stand-alone mode while formatting the output and automating several executions of the tools as required. These codes are described in further detail in Chapter 4.

(2) *Data Synthesis*: Once the appropriate aerodynamic data has been generated, the data contained in the separate output files for each method are combined into a consistent untrimmed aerodynamic input file. In the current prototype system this is done manually by the designer. This process will be automated in future versions.

The aerodynamic input file contains the untrimmed aerodynamic data in the form of aerodynamic lookup tables. At a set Mach number, coefficients and derivatives are tabulated as a function of angle of attack, side-slip angle and control surface deflection angles as shown in Table 3.2.

Table 3.2 *AeroMech* Aerodynamic Input File Organization

<i>Static Derivatives</i>	<i>Dynamic Derivatives</i>	<i>LoCE Increments</i>	<i>LaCE Increments</i>	<i>DiCE Increments</i>
$C_L = f(\alpha, \beta)$	$C_{L_{\dot{\alpha}}} = f(\alpha, \beta)$	$\Delta C_L = f(\alpha, \delta)$	$\Delta C_L = f(\alpha, \delta)$	$\Delta C_L = f(\alpha, \delta)$
$C_D = f(\alpha, \beta)$	$C_{m_{\dot{\alpha}}} = f(\alpha, \beta)$	$\Delta C_D = f(\alpha, \delta)$	$\Delta C_D = f(\alpha, \delta)$	$\Delta C_D = f(\alpha, \delta)$
$C_m = f(\alpha, \beta)$	$C_{L_q} = f(\alpha, \beta)$	$\Delta C_m = f(\alpha, \delta)$	$\Delta C_m = f(\alpha, \delta)$	$\Delta C_m = f(\alpha, \delta)$
$C_{Y_p} = f(\alpha, \beta)$	$C_{m_q} = f(\alpha, \beta)$	$\Delta C_Y = f(\alpha, \delta)$	$\Delta C_Y = f(\alpha, \delta)$	$\Delta C_Y = f(\alpha, \delta)$
$C_{l_p} = f(\alpha, \beta)$	$C_{Y_{\dot{\alpha}}} = f(\alpha, \beta)$	$\Delta C_l = f(\alpha, \delta)$	$\Delta C_l = f(\alpha, \delta)$	$\Delta C_l = f(\alpha, \delta)$
$C_{n_\beta} = f(\alpha, \beta)$	$C_{l_p} = f(\alpha, \beta)$	$\Delta C_n = f(\alpha, \delta)$	$\Delta C_n = f(\alpha, \delta)$	$\Delta C_n = f(\alpha, \delta)$
	$C_{n_p} = f(\alpha, \beta)$			
	$C_{n_r} = f(\alpha, \beta)$			
	$C_{l_r} = f(\alpha, \beta)$			
	$C_{n_r} = f(\alpha, \beta)$			

This organization includes all the typical aerodynamic effects as well as the aerodynamic cross coupling effects that become significant for asymmetric vehicles and asymmetric flight conditions.

3.4 Stability and Control Analysis

At the heart of the *AeroMech* methodology is the generic stability and control analysis module. This module is based upon a generic mathematical framework consisting of steady state and dynamic analysis¹. The stability and control analysis methodology is shown in Figure 3.7 and contains 4 basic steps. (1) Solve trim equations of motion to determine control power available, (2) produce trimmed aerodynamics, (3) solve the small perturbation equations of motion, and (4) compare results to requirements.

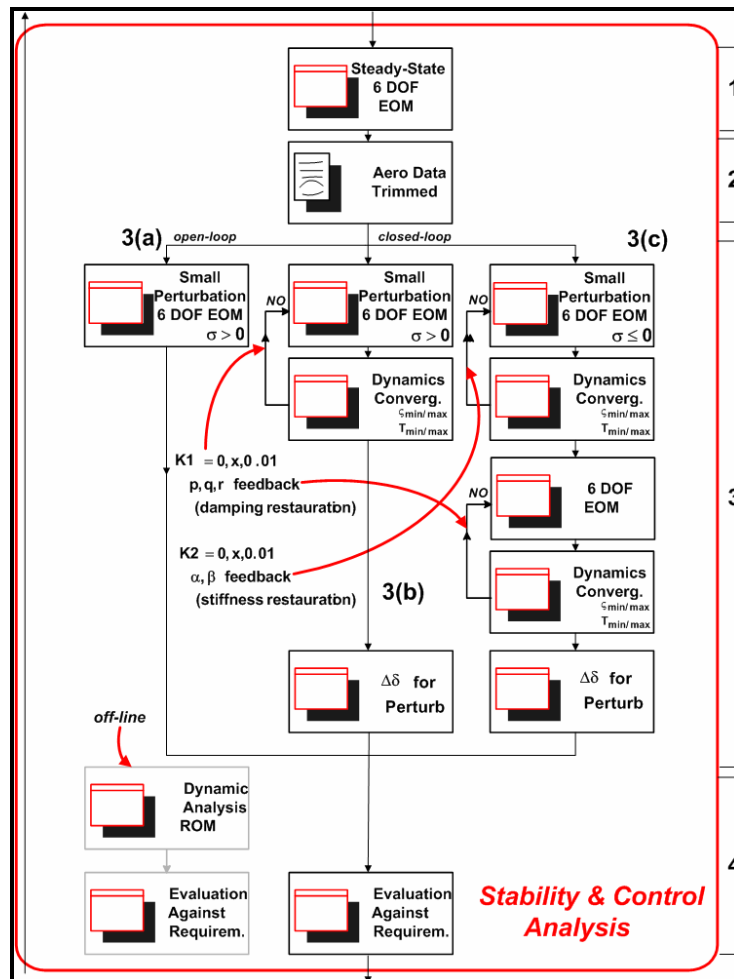


Figure 3.7: *AeroMech* Overall Methodology Stability and Control Analysis

3.4.1 Steady State 6-DOF Trim Equations of Motion

Assessing a vehicle's control power requires examining the critical flight conditions and maneuvers that impose the greatest demand on the control effectors; these have been termed Design Constraining Flight Conditions (DCFC)¹. These flight conditions tend to consist of 5 basic maneuvers which occur during controlled flight.

- **Straight-Line Flight:** Sustained flight at a constant heading and glide path angle (i.e. cruise, climb, descent).
- **Pull-up/Push-Over Maneuver:** longitudinal motion pitching motion in the nose-up or nose-down direction (i.e. speed recover, load factor maneuvering capability).
- **Roll Performance:** rolling motion about the body or stability axis primarily induced by the LaCE (i.e. aileron rolls).
- **Turning Flight:** inducing and maintaining a turning motion characterized by a change of heading. (i.e. turn coordination, steady state turning flight).
- **Take-off Rotation:** a pitching motion initiated by the LoCE during the take-off run to lift the nose wheel off the ground.

In *AeroMech* these maneuvers are modeled through solving the coupled (both aerodynamic and inertial) steady-state 6-DOF equations of motion. These equations are based upon the *General Euler Equations of Motion with Spinner Rotors*¹ (Equations 3.1 through 3.16), with the following assumptions Table 3.3.

Table 3.3 Steady-State Equations of Motion Assumptions

Assumptions	
1	The Earth is treated as flat and stationary in inertia space.
2	Equations are valid for any orthogonal axis system fixed at the c.g. of the aircraft.
3	Aircraft is a rigid body having any number of rigid spinning rotors.
4	Spinning rotors have a constant angular velocity relative to the body axis.
5	Wind velocity is zero.
6	Steady state flight, no acceleration.
7	No plane of symmetry, i.e. full moment of inertia matrix. I_{xy} and I_{zy} are included.
8	Aerodynamic cross coupling included.

$$X_A + X_T - mg \sin \theta = m(qw - rv) \quad \text{Eq. 3.1}$$

$$Y_A + Y_T + mg \cos \theta \sin \phi = m(ru - pw) \quad \text{Eq. 3.2}$$

$$Z_A + Z_T + mg \cos \theta \cos \phi = m(pv - qu) \quad \text{Eq. 3.3}$$

$$L_A + L_T = I_x \dot{p} - I_{yz} (q^2 - r^2) - I_{zx} pq - I_{xy} rp - (I_y - I_z) qr + qh'_z - rh'_y \quad \text{Eq. 3.4}$$

$$M_A + M_T = I_y \dot{q} - I_{zx} (r^2 - p^2) - I_{xy} qr - I_{yz} pq - (I_z - I_x) rp + rh'_x - ph'_z \quad \text{Eq. 3.5}$$

$$N_A + N_T = I_z \dot{r} - I_{zx} (p^2 - q^2) - I_{yz} rp - I_{xy} qr - (I_x - I_y) pq + ph'_y - qh'_x \quad \text{Eq. 3.6}$$

$$p = \dot{\phi} - \dot{\psi} \sin \theta \quad \text{Eq. 3.7}$$

$$q = \dot{\theta} \cos \phi + \dot{\psi} \sin \phi \cos \theta \quad \text{Eq. 3.8}$$

$$r = -\dot{\theta} \sin \phi + \dot{\psi} \cos \phi \cos \theta \quad \text{Eq. 3.9}$$

$$\dot{\phi} = p + (q \sin \phi + r \cos \phi) \tan \theta \quad \text{Eq. 3.10}$$

$$\dot{\theta} = q \cos \phi - r \sin \phi \quad \text{Eq. 3.11}$$

$$\dot{\psi} = (q \sin \phi + r \cos \phi) \sec \theta \quad \text{Eq. 3.12}$$

$$\dot{x}^E = u^E \cos \theta \cos \psi + v^E (\sin \phi \sin \theta \cos \psi - \cos \phi \sin \psi) + w^E (\cos \phi \sin \theta \cos \psi + \sin \phi \sin \psi) \quad \text{Eq. 3.14}$$

$$\dot{y}^E = u^E \cos \theta \sin \psi + v^E (\sin \phi \sin \theta \sin \psi + \cos \phi \cos \psi) + w^E (\cos \phi \sin \theta \sin \psi - \sin \phi \cos \psi) \quad \text{Eq. 3.15}$$

$$\dot{z}^E = -u^E \sin \theta + v^E \sin \phi \cos \theta + w^E \cos \phi \cos \theta \quad \text{Eq. 3.13}$$

Including the aerodynamic and thrust components in the force and moment Equations 2 – 7 yields the following generic trim equations written in stability axis as provided in Equations 17 to 22. The thrust coefficients (C_T) are defined in Appendix C.

$$\left(-C_{T_D} \tau + C_D(\alpha, \beta) + C_{D_q}(\alpha, \beta) \frac{q\bar{c}}{2V} + \Delta C_{D_{LoCE}}(\alpha, \delta_{LoCE}) + \Delta C_{D_{LaCE}}(\alpha, \delta_{LaCE}) + \Delta C_{D_{DiCE}}(\alpha, \delta_{DiCE}) \right) \bar{q} S_{ref} - \text{Eq. 3.17}$$

$$- mg \sin \gamma - mrV \sin \beta = 0$$

$$\left(C_{T_Y} \tau + C_Y(\alpha, \beta) + C_{Y_r}(\alpha, \beta) \frac{rb}{2V} + C_{Y_p}(\alpha, \beta) \frac{pb}{2V} + \Delta C_{Y_{LoCE}}(\alpha, \delta_{LoCE}) + \Delta C_{Y_{LaCE}}(\alpha, \delta_{LaCE}) + \Delta C_{Y_{DiCE}}(\alpha, \delta_{DiCE}) \right) \bar{q} S_{ref} -$$

$$- mg \cos \gamma \sin \phi - mrV = 0$$

Eq. 3.18

$$- \left(-C_{T_L} \tau + C_L(\alpha, \beta) + C_{L_q}(\alpha, \beta) \frac{q\bar{c}}{2V} + \Delta C_{L_{LoCE}}(\alpha, \delta_{LoCE}) + \Delta C_{L_{LaCE}}(\alpha, \delta_{LaCE}) + \Delta C_{L_{DiCE}}(\alpha, \delta_{DiCE}) \right) \bar{q} S_{ref} - \text{Eq. 3.19}$$

$$- mg \cos \gamma \cos \phi + mqV - mpV \sin \beta = 0$$

$$\left(C_{T_l} \tau + C_l(\alpha, \beta) + C_{l_r}(\alpha, \beta) \frac{rb}{2V} + C_{l_p}(\alpha, \beta) \frac{pb}{2V} + \Delta C_{l_{LoCE}}(\alpha, \delta_{LoCE}) + \Delta C_{l_{LaCE}}(\alpha, \delta_{LaCE}) + \Delta C_{l_{DiCE}}(\alpha, \delta_{DiCE}) \right) \bar{q} S_{ref} b +$$

$$+ I_{yz}(q^2 - r^2) + I_{zx}pq - I_{xy}rp + (I_y - I_z)qr - qh'_z + rh'_y = 0$$

Eq. 3.20

$$\left(C_{T_m} \tau + C_m(\alpha, \beta) + C_{m_q}(\alpha, \beta) \frac{q\bar{c}}{2V} + \Delta C_{m_{LoCE}}(\alpha, \delta_{LoCE}) + \Delta C_{m_{LaCE}}(\alpha, \delta_{LaCE}) + \Delta C_{m_{DiCE}}(\alpha, \delta_{DiCE}) \right) \bar{q} S_{ref} \bar{c} +$$

$$+ I_{zx}(r^2 - p^2) + I_{xy}qr - I_{yz}pq + (I_z - I_x)rp - rh'_x + ph'_z = 0$$

Eq. 3.21

$$\left(C_{T_n} \tau + C_n(\alpha, \beta) + C_{n_r}(\alpha, \beta) \frac{rb}{2V} + C_{n_p}(\alpha, \beta) \frac{pb}{2V} + \Delta C_{n_{LoCE}}(\alpha, \delta_{LoCE}) + \Delta C_{n_{LaCE}}(\alpha, \delta_{LaCE}) + \Delta C_{n_{DiCE}}(\alpha, \delta_{DiCE}) \right) \bar{q} S_{ref} b +$$

$$+ I_{zx}(p^2 - q^2) + I_{yz}rp - I_{xy}qr + (I_x - I_y)pq - ph'_y + qh'_x = 0$$

Eq. 3.22

These equations are unique in that they account for (1) aerodynamic cross-coupling, (2) inertial cross-coupling and (3) spinning rotor cross-coupling. These effects are typically neglected during the conceptual design phase due to the small effect on traditional symmetric vehicles, such as the tail-aft configuration (TAC). However, these effects are significant when analyzing asymmetric configurations such as the oblique

flying wing (OFW) or asymmetric flight conditions such as maximum side-slip. These equations re-written in the stability axis as defined below for a symmetric and asymmetric aircraft configuration (Figure 3.8).

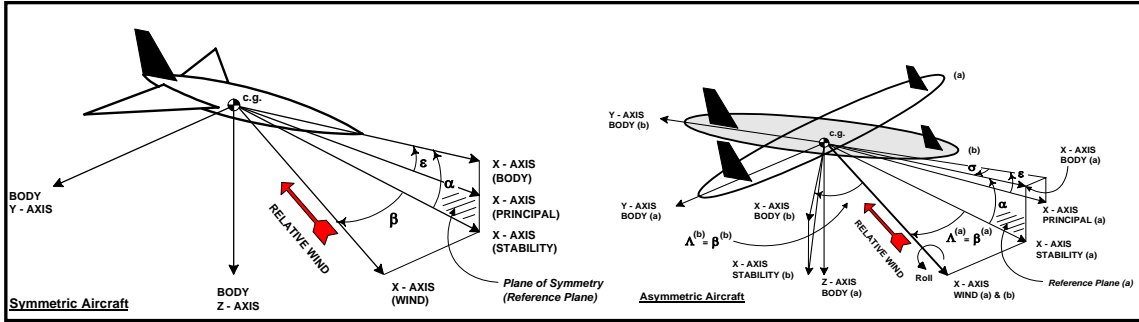


Figure 3.8: Axis Definition for Symmetric and Systemic aircraft for *AeroMech*¹

Therefore, these equations can be considered generic trim equations of motion because they can be applied to both symmetric and asymmetric vehicles and symmetric and asymmetric flight conditions, allowing the designer to explore configurations at flight conditions not mastered by conventional stability and control tools.

To solve these equations for the 5 steady-state maneuvers described previously, the following steps are taken.

1. The steady-state pitch (q), roll (p) and yaw (r) rates are specified for each maneuver. These are defined from the kinematics equations. For example, during steady-state straight line flight $q = p = r = 0$.
2. The appropriate attitude (α , β , ϕ , etc.) and control surface deflections (δ_{LoCE} , δ_{LaCE} , δ_{DiCE}) are solved iteratively for the prescribed angular velocities.

The five steady-state maneuvers are described in Table 3.4. These represent the basic maneuvers that a vehicle performs during flight; however there are multiple

perturbations of these maneuvers that must be considered for proper sizing of the primary control effectors.

Table 3.4 Steady-State Maneuvers Summary¹

Maneuver	Description	Diagram
SSLF	Steady-state Straight-Line Flight	
SSTF	Steady-State Turning Flight	
SSPUPO	Steady-State Pull-Up/Push-Over Flight	
SSRP	Steady-State Roll Performance	
QSTORM	Quasi-Steady State Take-Off Rotation	

3.4.1.1 Steady-State Straight-Line Flight (SSLF)

SSLF represents constant forward velocity flight with no angular velocities ($p = q = r = 0$) and can be applied to cruise, shallow climbs, and descents. During the conceptual design phase the control effectors (CE) must be sized to meet requirements for SSLF conditions such as maximum sustained side-slip, forward and aft c.g. clearances, single engine inoperable conditions, etc., all dependent upon design and regulation requirements.

This type maneuver can be broken into four basic scenarios of engine failures and maximum side-slip angles throughout the flight envelope, as demonstrated in Figure 3.9.

- a) zero side-slip, all engines operable;
- b) maximum side-slip, all engines operable;
- c) zero side-slip, one engine inoperable (OEI);
- d) maximum side-slip, one engine inoperable (OEI).

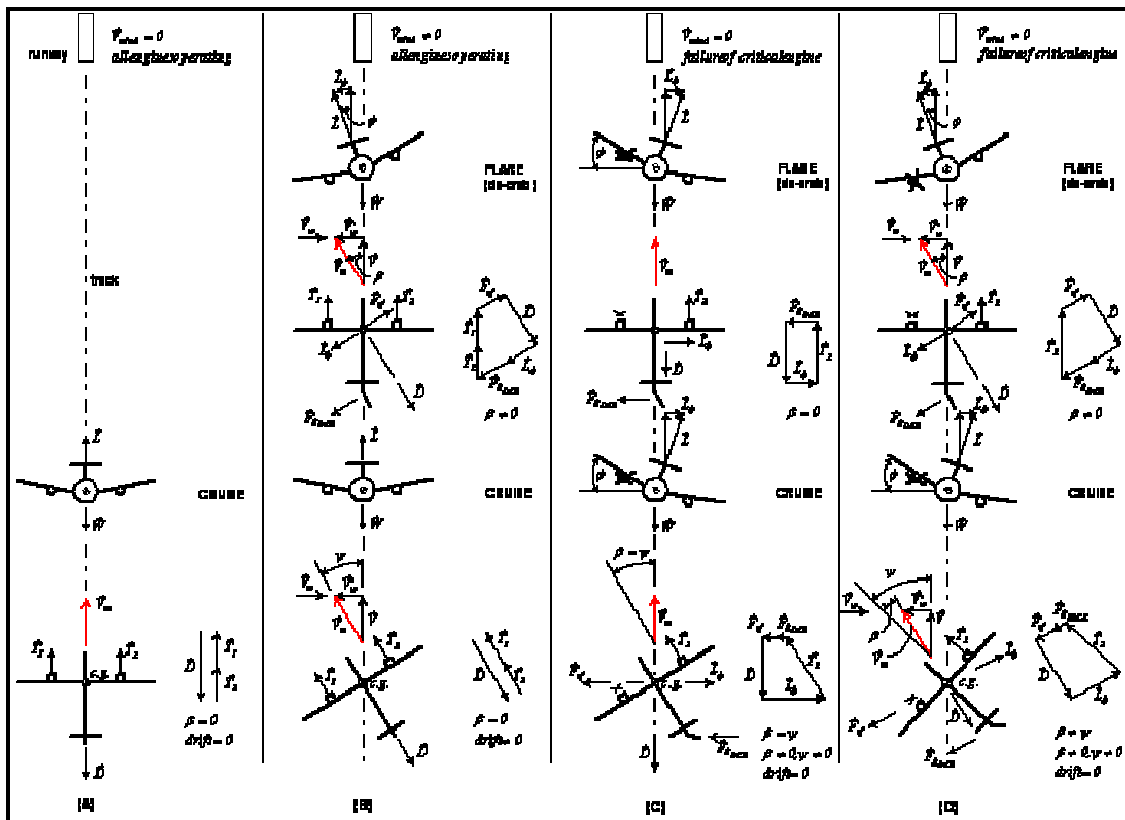


Figure 3.9: SSLF Asymmetric Scenarios of CE Sizing1

For example, the YB-49 flying wing must have adequate control power in all three axes during approach to trim the forward c.g. at maximum side-slip angle, see scenario (b). A description of this flight condition can be found in Table 3.5.

Table 3.5 Flight Condition for the YB-49 During Approach

DCFC	Test	Flight Condition					
		N	Air Speed		Altitude	Flight Path Angle	Side-Slip angle
			(ft/s)	(M)	(ft)	(deg)	(deg)
Approach	Longitudinal, Lateral and Directional Trim	1	140 (86 kts)	0.18	Sea-Level	-3.00	-20.0 to 20.0

The results generated by *AeroMech* are presented with Figure 3.10.

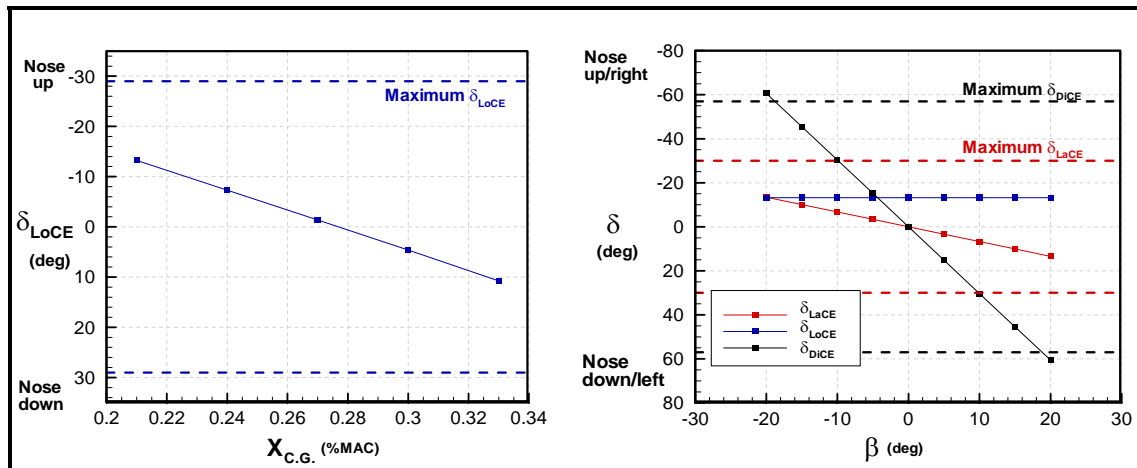


Figure 3.10: Control deflections for the YB-49 during approach

During approach, the YB-49's trim flaps are utilized for pitch trim (LoCE) and the elevens (LaCE) are used for roll control. As shown in Figure 3.8, the YB-49's LoCE and LaCE do not reach their respective saturation limits and the DiCE reaches its deflection limit at 20° side-slip angle.

3.4.1.2 Steady-State Pull-Up/Push-Over (SSPUPO)

The SSPUPO maneuver models a vehicle during a constant pitch rate maneuver defined in terms of load factor and bank angle (Equations 23 to 26, derived in Appendix E).

$$q = \frac{g}{u}(n-1)\cos\phi \quad \text{Eq. 3.22}$$

$$p = 0 \quad \text{Eq. 3.23}$$

$$r = -\frac{g}{u}(n-1)\sin\phi \quad \text{Eq. 3.24}$$

This maneuver's primary purpose is to size the primary LoCE to maintain a required load factor range. This can represent a pull-up and/or push-over maneuver anywhere in the flight envelope with any combination of engine failure or side-slip condition. For example, the YB-49 is shown below in an approach configuration at zero side-slip angle (Table 3.6).

Table 3.6 Flight Condition for the YB-49 during a Pull-up Maneuver

DCFC	Test	Flight Condition					
		N	Air Speed	Altitude	Flight Path Angle	Side-Slip angle	
			(ft/s)	(M)	(ft)	(deg)	(deg)
Approach	SSLF	1.0	239.0 (140 kts)	0.2	10,000	0.0	0.0
	SSPUPO	1.0 to 2.0	239.0 (140 kts)	0.2	10,000	0.0	0.0

The results generated by *AeroMech* are shown in Figure 3.11

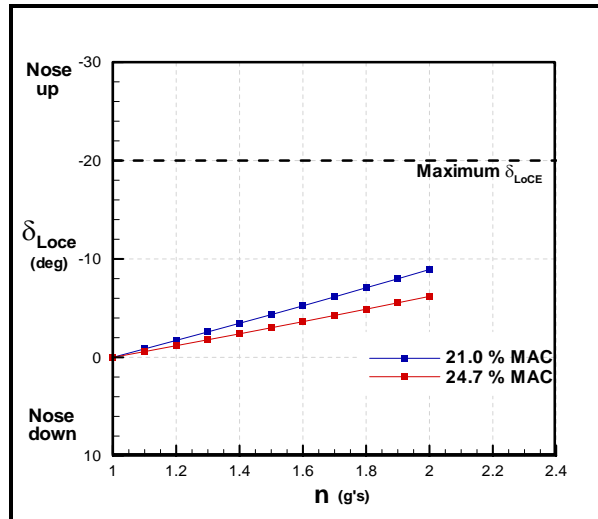


Figure 3.11: Longitudinal and lateral/directional control deflections for the YB-49 during a Pull-up maneuver

As shown, the LoCE has sufficient control power during this maneuver. The limiting factor during this maneuver proves to be the maximum lift coefficient. This is discussed in greater depth in Chapter 5 for the YB-49.

3.4.1.3 Steady-State Roll Performance (SSRP)

The SSRP maneuver models a flight vehicle during a constant roll rate defined in terms of load factor and bank angle. The purpose of this maneuver is to size the primary LaCE to induce and hold the required roll rates or roll helix. This analysis is organized with two complementing analysis methods:

1. 6-DOF steady-state rolling motion solution;
2. 1-DOF time to bank calculations.

The mathematical steady-state 6-DOF rolling motion formulation is similar compared to the other steady-state conditions since it solves the 6-DOF steady-state

trim equations while taking the following pitch, roll and yaw conditions into account (Equations 26 to 28):

$$q = 0 \quad \text{Eq. 3.26}$$

$$p = \dot{\phi} \quad \text{Eq. 3.27}$$

$$r = 0 \quad \text{Eq. 3.28}$$

The estimation of time to bank is a complex dynamic problem for both symmetric and asymmetric vehicles and flight conditions, since this maneuver is influenced by aeroelastic effects, flight control system rate limits, and aerodynamic and inertial cross-coupling effects¹. For this reason, a 1-DOF formulation has been selected to estimate time to bank. The formulation is rederived in Appendix C and is presented here in Equation 29.

$$\int p dt = \phi(t) = -\frac{2V}{b} \frac{C_{l_{\delta_{LaCE}}} \delta_{LaCE}}{C_{l_p}} \left[t + \frac{1}{L_p} (1 - e^{L_p t}) \right] \quad \text{Eq. 3.29}$$

Although the results obtained may be optimistic, they are known to be adequate.

Similarly to the other steady-state solutions, the steady-state 6-DOF solution can be applied to investigate asymmetric coupling of aerodynamic, inertial and control effects that are significant to the design of the control surfaces. Continuing the example of the YB-49 flying wing, a steady state rolling motion commanded with a FWC requires larger DiCE deflections compared to a traditional TAC due to the large adverse yawing motion produced by the elevons relative to the static yaw stability of the total FWC. To demonstrate this, the YB-49 has been modeled in its approach configuration with the flight condition defined in Table 3.7. The time to bank to 30 degrees will also be calculated using the 1-DOF model.

Table 3.7 Flight Condition for the YB-49 during a Steady-State Roll Maneuver

DCFC	Test	Flight Condition					
		N	Air Speed		Altitude	Flight Path Angle	Side-Slip angle
			(ft/s)	(M)	(ft)	(deg)	(deg)
Approach	SSLF	1.0	239.0 (140 kts)	0.2	10,000	0.0	0.0
	SSRP	1.0	239.0 (140 kts)	0.2	10,000	0.0	0.0

The results generated with *AeroMech* are presented in Figure 3.12.

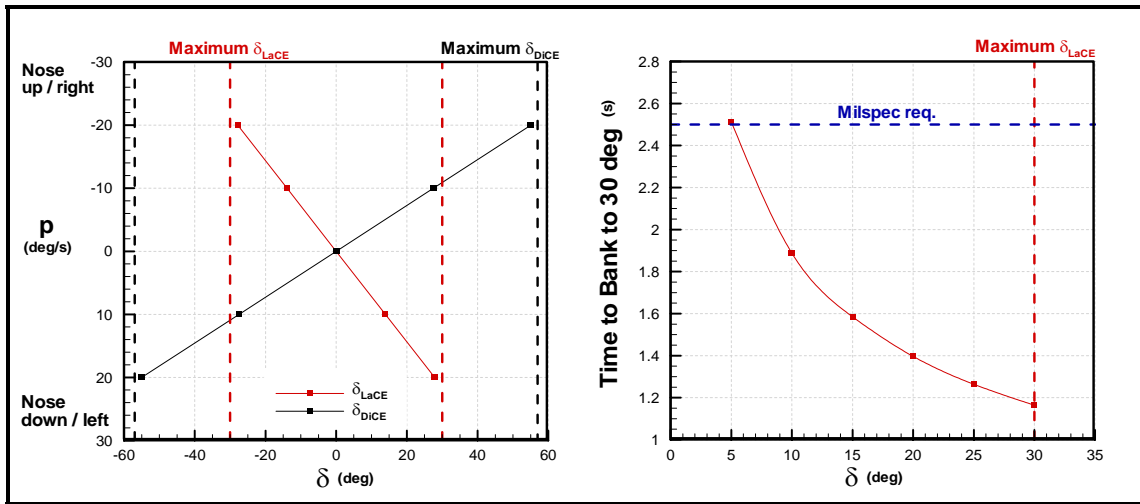


Figure 3.12: YB-49 lateral/directional roll control deflections required.

As shown in Figure 3.12, the maximum sustainable roll rate for the YB-49 is about 20 deg/s and significant rudder deflections are required to compensate the adverse yawing motion due to deflecting the elevons (LaCE). While the DiCE does not reach its saturation limit, the yaw deflection angles required are significant for this maneuver. The time to bank calculation shows that the YB-49 can meet the MIL Spec for a large transport or bomber at low speed.

3.4.1.4 Steady-State Turning Flight (SSTF)

The SSTF maneuver models a flight vehicle during turning flight as a function of load factor and bank angle. The purpose of this maneuver is to determine the control power required by the LoCE, LaCE and DiCE to do so. This analysis can be performed for any combination of load-factor, bank-angle and failure conditions that the vehicle may encounter during operation. The underlying mathematical formulation is similar compared to the other steady-state maneuvers, the main distinction being the definition of the pitch, roll and yaw rates as shown with Equations 30 to 32:

$$q = \frac{g}{u} n \sin^2 \phi \quad \text{Eq. 3.30}$$

$$p = 0 \quad \text{Eq. 3.31}$$

$$r = -\frac{g}{u} \tan \phi \frac{1}{n} \quad \text{Eq. 3.32}$$

To demonstrate the control power requirements for this maneuver, the YB-49 is analyzed for load factors ranging from 1.0 to 2.5 for bank angles of 10 deg and 30 deg. The flight condition is summarized in Table 3.8.

Table 3.8 Flight Condition for the YB-49 during Steady-State Turning Flight

DCFC	Test	Flight Condition					
		N	Air Speed		Altitude	Flight Path Angle	Side-Slip angle
			(ft/s)	(M)	(ft)	(deg)	(deg)
Approach	SSLF	1.0	239.0 (140 kts)	0.2	10,000	0.0	0.0
	SSTF	1.0 to 2.0	239.0 (140 kts)	0.2	10,000	0.0	0.0

The results generated with *AeroMech* are shown in Figure 3.13.

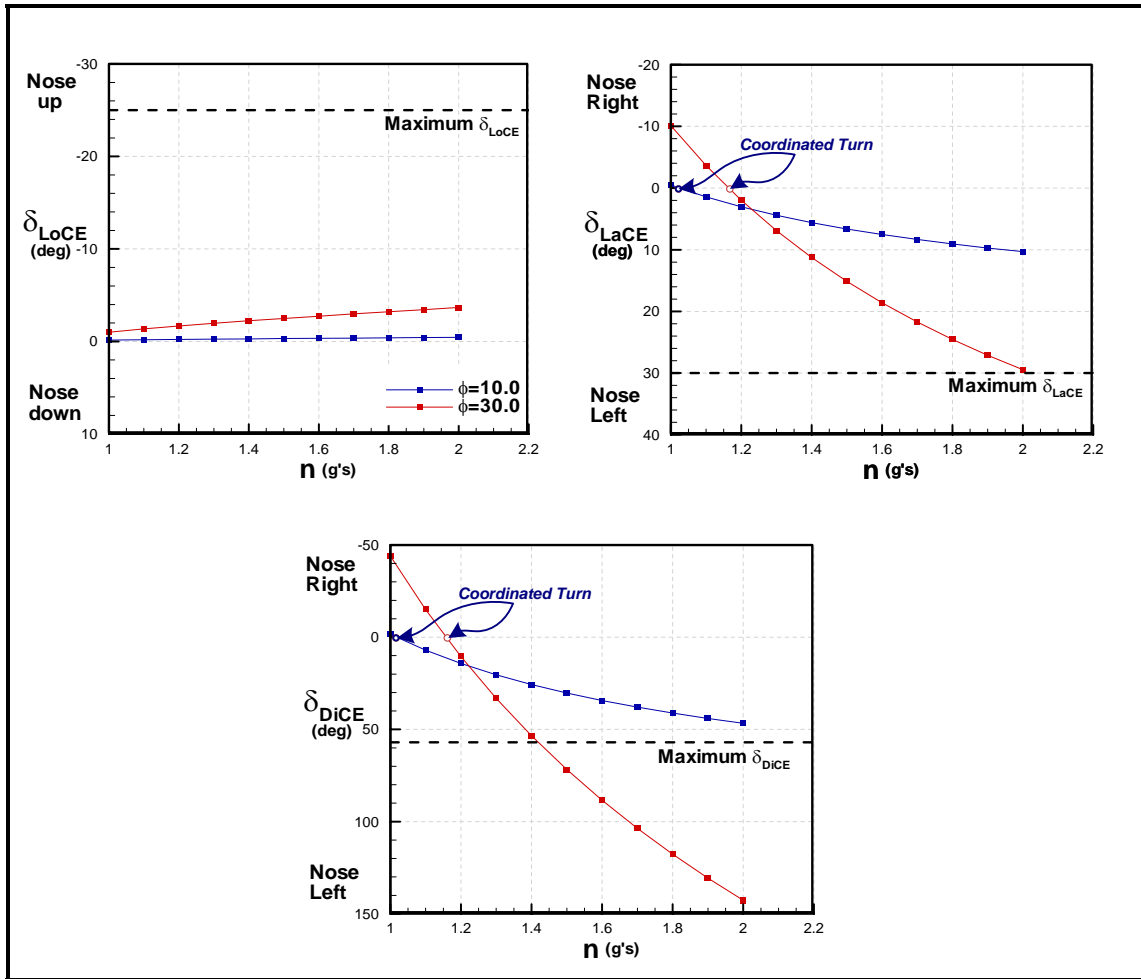


Figure 3.13: Control deflections for the YB-49 during SSTF for two bank angles.

These results show that turn coordination occurs at 1.05g and 1.15g for bank angles of 10 and 30 deg respectively. To decrease the turning radius at these bank angles, greater LoCE power is required and the LaCE and DiCE must compensate for the additional yawing and rolling moment to maintain a horizontal flight path. This leads to CE saturation as shown in Figure 3.10. This method of increasing load factor actually examines the extent of control power available. If the pilot wishes to increase the load factor the bank-angle is typically increased. However, increasing the bank-angle at the speed commanded will require an increase in angle of attack that moves the

vehicle closer to the stall point. If greater maneuverability at this speed is required, then the landing flaps must be deployed further.

3.4.1.5 Quasi-Steady-State Take-Off Rotation (QSTORM)

The QSTORM maneuver is a quasi-steady state model that predicts the ability of the LoCE to induce a take-off rotation maneuver. Take-off rotation is characterized by a pitch acceleration at rotation speed while the aircraft is accelerating horizontally down the runway as shown in the free-body diagram in Figure 3.14.

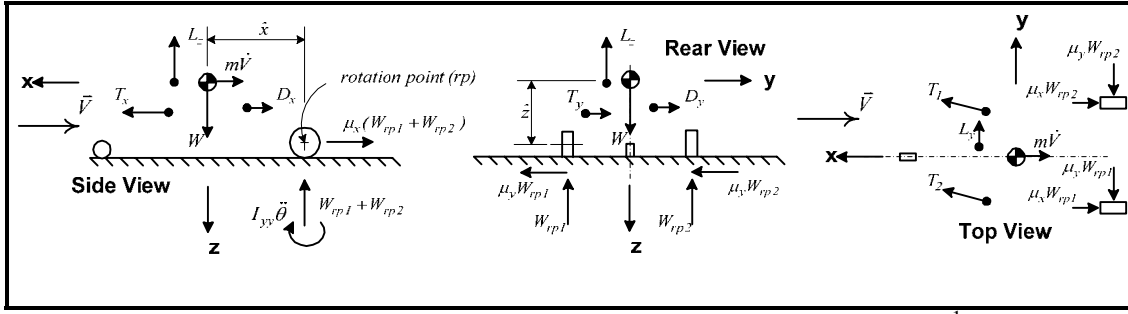


Figure 3.14: Quasi-Steady State Take-Off Rotation Diagram¹

To account for the translational and rotational accelerations, the steady-state equations are modified by including a horizontal acceleration term, \dot{V} , and a pitch acceleration term, $\ddot{\theta}$. The side-force equation is neglected in this derivation by assuming no lateral sliding of the a/c on the runway¹, which produces the following system of equations (Equations 3.33 to 3.37).

$$\left(-C_{T_D} \tau + C_D + C_{D_q} \frac{q\bar{c}}{2V} + \Delta C_{D_{LoCE}} + \Delta C_{D_{LaCE}} + \Delta C_{D_{DiCE}} \right) \bar{q} S_{ref} + W_{rp} \mu_{LG} - m \dot{V} = 0 \quad \text{Eq. 3.33}$$

$$-\left(-C_{T_L} \tau + C_L + C_{L_q} \frac{q\bar{c}}{2V} + \Delta C_{L_{LoCE}} + \Delta C_{L_{LaCE}} + \Delta C_{L_{DiCE}} \right) \bar{q} S_{ref} - W_{rp} + mg = 0 \quad \text{Eq. 3.34}$$

$$\left(C_{T_l} \tau + C_l + C_{l_r} \frac{rb}{2V} + C_{l_p} \frac{pb}{2V} + \Delta C_{l_{LoCE}} + \Delta C_{l_{LaCE}} + \Delta C_{l_{DiCE}} \right) \bar{q} S_{ref} b + I_{xy} \ddot{\theta} = 0 \quad \text{Eq. 3.35}$$

$$\left(C_{T_m} \tau + C_m + C_{m_q} \frac{q\bar{c}}{2V} + \Delta C_{m_{LoCE}} + \Delta C_{m_{LaCE}} + \Delta C_{m_{DiCE}} \right) \bar{q} S_{ref} \bar{c} - I_y \ddot{\theta} = 0 \quad \text{Eq. 3.36}$$

$$\left(C_{T_n} \tau + C_n + C_{n_r} \frac{rb}{2V} + C_{n_p} \frac{pb}{2V} + \Delta C_{n_{LoCE}} + \Delta C_{n_{LaCE}} + \Delta C_{n_{DiCE}} \right) \bar{q} S_{ref} b + I_{yz} \ddot{\theta} = 0 \quad \text{Eq. 3.37}$$

This system models the take-off rotation maneuver at the instant where the pilot commands nose wheel lift-off, thus pitch velocity (q) is still zero but pitch acceleration is at its maximum¹. The LoCEs are sized to induce instantaneous pitch acceleration. Typical values of this pitch acceleration are shown in Table 3.9.

Table 3.9 Typical Instantaneous Pitch Acceleration¹⁰

<i>Aircraft Type</i>	<i>Instantaneous Pitch Acceleration,</i>
Large Transports	6 to 8 deg/s ²
Small Transports	8 to 10 deg/s ²
Light Airplanes and Fighters	10 to 12 deg/s ²

In analogy to the other steady-state systems of equations, this mathematical model allows the designer to include aerodynamic and inertial coupling effects for a realistic assessment of the control power required for this maneuver. This mathematical model can be applied to the take-off rotation of both symmetric and asymmetric flight vehicles with any combination of side-slip angle and engine failure conditions.

For example, *AeroMech* can be used to estimate the YB-49's take-off rotation speed given maximum LoCE deflection angle for two take-off weights over a range of center of gravity locations, given the following flight conditions (Table 3.10).

Table 3.10 Flight Condition for the YB-49 during Take-off Rotation

DCFC	Test	Flight Condition					
		N	Air Speed		Altitude	Flight Path Angle	Side-Slip angle
			(ft/s)	(M)	(ft)	(deg)	(deg)
Take-Off	QSTR	-	150	0.1	Sea-Level	0.0	0.0
	OM	-	(89 kts)				
	QSTR	-	150	0.1	Sea-Level	0.0	0.0
	OM	-	(89 kts)				

The results generated by *AeroMech* are presented with Figure 3.15.

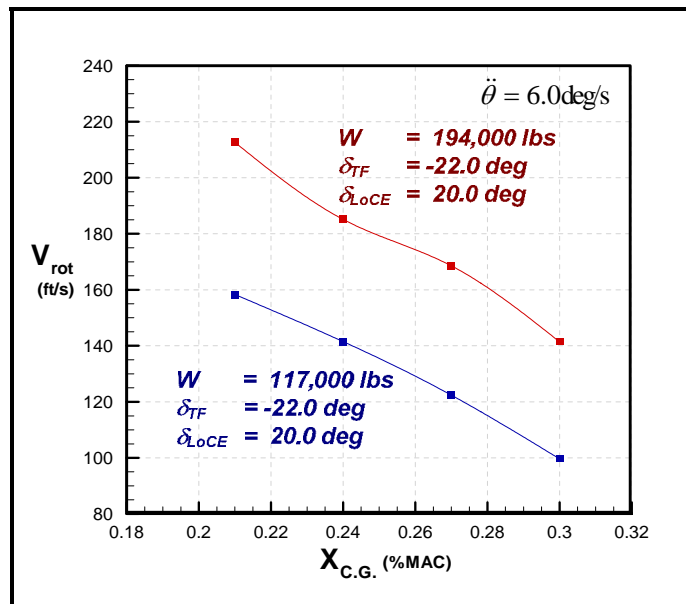


Figure 3.15: Rotation Velocity for the YB-49

The results show that as the center of gravity moves aft the rotation velocity decreases. While the aft center of gravity shift will reduce the lever arm of the LoCE it also reduces the moment created between the landing gear and the center of gravity. This reduction in the landing gear moment is dominating compared to the reduction in control power available, finally reducing the take-off rotation speed which translates into sufficient longitudinal control power available even at lower rotation speeds.

3.4.2 Trimmed Aerodynamics

The *AeroMech* methodology (1) solves the steady state trim condition, (2) produces trimmed aerodynamics, and (3) solves the dynamic behavior of the vehicle. Trimmed aerodynamics are required for correct control power assessment, dynamic stability analysis around a trim point, accurate performance calculations, and finally realistic comparisons of different flight vehicle concepts (i.e. TAC vs. FWC) based on trimmed L/D. *AeroMech* produces this data by

1. solving for the 6-DOF SSLF angle of attack, side-slip angle and control surface deflections required (control power assessment);
2. interpolating the trimmed aerodynamic data from the untrimmed aerodynamic data set at the conditions defined in the 6-DOF SSLF calculation;
3. calculating the linear derivatives about the trim point using a center difference method.

For example, *AeroMech* generates the following trimmed aerodynamic data set in all axes for the YB-49 during cruising flight. The flight condition is described in Table 3.11.

Table 3.11 Flight Condition Description for the YB-49 during Cruising Flight

DCFC	Test	Flight Condition					
		N	Air Speed (ft/s)	(M)	Altitude (ft)	Flight Path Angle (deg)	Side-Slip angle (deg)
Cruise	SSLF	1.0	472.6 (280 kts)	0.4.9	30,000	0.0	0.0

AeroMech produces trimmed aerodynamic data for all c.g. locations as shown in

Figure 3.16 for the forward c.g. position.

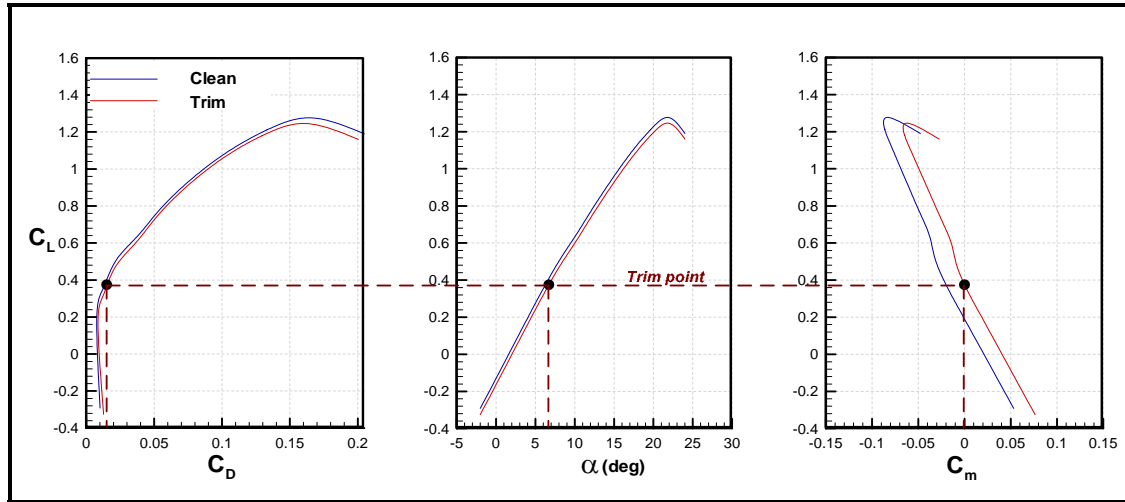


Figure 3.16: Trimmed aerodynamic data at 21% MAC

For this longitudinal statically stable configuration setting, the YB-49 requires a nose up LoCE deflection leading to a higher AoA required for trim, a condition ultimately reducing lift due to the so-called transient-lift effect. The resulting trim drag and increased angle of attack reduces the overall vehicles lift to drag ratio, thus its overall aerodynamic efficiency. One key technique for alleviating this performance penalty of the trimmed lift to drag ratio is through relaxed longitudinal static stability²¹. By varying the c.g. location of the YB-49 at this cruise condition, *AeroMech* predicts the following effects of relaxed static stability, see Figure 3.17.

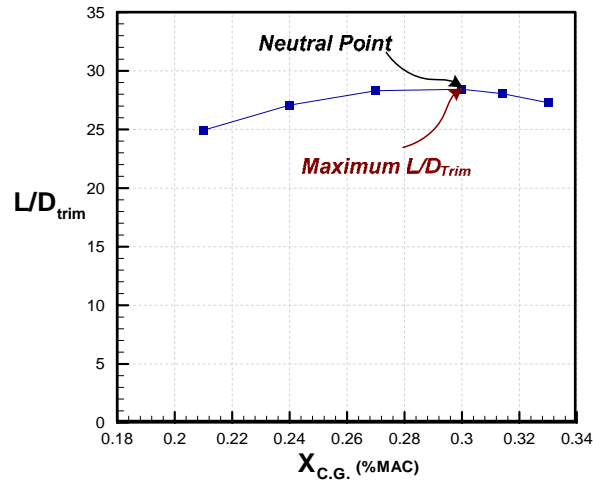


Figure 3.17: Trimmed aerodynamic efficiency for the YB-49 as a function of the longitudinal static margin.

Relaxing static longitudinal stability shows a significant increase of the trimmed lift to drag ratio from 25 to 29. In the case of the YB-49, the maximum lift to drag ratio occurs just before the longitudinal neutral point (np). This relaxation of static longitudinal stability requires a stability augmentation system to provide adequate flying and handling qualities. This is demonstrated in section 3.4.4.

The linear derivatives for the YB-49 are presented Chapter 4. These derivatives along with the neutral point and maneuver point calculation²², see Equations 38 and 39, are used for static longitudinal stability analysis as shown in the validation case study.

$$\frac{x_{NP}}{\bar{c}} = \frac{x_{cg}}{\bar{c}} - \frac{c_{m\alpha}}{c_{L\alpha} \cos(\alpha)} \quad \text{Eq. 3.38}$$

$$\frac{x_{MP}}{\bar{c}} = \frac{x_{NP}}{\bar{c}} - \frac{\rho S \bar{c}}{4m} c_{mq} \quad \text{Eq. 3.39}$$

3.4.3 Dynamic Stability and Control Analysis

Having the trim point and the linear trimmed aerodynamics defined, the designer can predict the vehicles dynamic behavior using the small perturbation equations of motion. At the conceptual design level it is of utmost importance to quantify a vehicle's dynamic stability to meet flight safety and performance requirements. Such early assessment serves to provide the designer an early design feedback. In the case of aircraft with relaxed longitudinal static it is required to emulate a stability augmentation system (SAS) to enable the prediction of additional control power requirements for such vehicles.

3.4.3.1 Small Perturbation Equations of Motion

In order to provide the designer with a tool set to analyze the dynamic behavior of symmetric and asymmetric aircraft at symmetric and/or asymmetric flight conditions, the small perturbation equations must include the aerodynamic, inertial and control cross-coupling terms. This requirement prohibits the classical decoupling of the longitudinal and lateral/directional planes of motion. The following system of equations represents the coupled, 6-DOF small perturbation equations of motion derived in Reference 1 (Equation 34). The system in Equation 3.40 for was derived by linearizing the *General Euler Equations of Motion with Spinner Rotors*¹ (Equations 2 through 16)

$$\begin{bmatrix} \Delta \dot{u} \\ \dot{v} \\ \dot{w} \\ \dot{p} \\ \dot{q} \\ \dot{r} \\ \dot{\phi} \\ \Delta \dot{\theta} \\ \dot{\psi} \end{bmatrix} = \underbrace{\begin{bmatrix} x_u & x_v & x_w & x_p & x_q & x_r & 0 & x_\theta & 0 \\ y_u & y_v & y_w & y_p & y_q & y_r & y_\phi & 0 & 0 \\ z_u & z_v & z_w & z_p & z_q & z_r & 0 & z_\theta & 0 \\ l_u & l_v & l_w & l_p & l_q & l_r & 0 & l_\theta & 0 \\ m_u & m_v & m_w & m_p & m_q & m_r & 0 & m_\theta & 0 \\ n_u & n_v & n_w & n_p & n_q & n_r & 0 & n_\theta & 0 \\ 0 & 0 & 0 & 1 & 0 & \tan \theta_0 & 0 & 0 & 0 \\ 0 & 0 & 0 & 0 & 1 & 0 & 0 & 0 & 0 \\ 0 & 0 & 0 & 0 & 0 & \sec \theta_0 & 0 & 0 & 0 \end{bmatrix}}_A \underbrace{\begin{bmatrix} \Delta u \\ v \\ w \\ p \\ q \\ r \\ \phi \\ \theta \\ \psi \end{bmatrix}}_{\tilde{x}} + \underbrace{\begin{bmatrix} x_{\delta_{LoCE}} & x_{\delta_{DiCE}} & x_{\delta_{LaCE}} & x_\tau \\ y_{\delta_{LoCE}} & y_{\delta_{DiCE}} & y_{\delta_{LaCE}} & y_\tau \\ z_{\delta_{LoCE}} & z_{\delta_{DiCE}} & z_{\delta_{LaCE}} & z_\tau \\ l_{\delta_{LoCE}} & l_{\delta_{DiCE}} & l_{\delta_{LaCE}} & l_\tau \\ m_{\delta_{LoCE}} & m_{\delta_{DiCE}} & m_{\delta_{LaCE}} & m_\tau \\ n_{\delta_{LoCE}} & n_{\delta_{DiCE}} & n_{\delta_{LaCE}} & n_\tau \\ 0 & 0 & 0 & 0 \\ 0 & 0 & 0 & 0 \\ 0 & 0 & 0 & 0 \end{bmatrix}}_B \underbrace{\begin{bmatrix} \delta_{LoCE} \\ \delta_{DiCE} \\ \delta_{LaCE} \\ \tau \\ \tilde{c} \end{bmatrix}}_{\tilde{c}}$$

Eq. 3.40

This system includes the aerodynamic and inertial cross-coupling terms (x_p , x_r , y_q , z_q , etc.) and the control coupling terms ($z_{\delta_{LaCE}}$, $z_{\delta_{DiCE}}$, etc.) which are not of significance of for symmetric aircraft at symmetric flight conditions, but represent essential cross coupling effects in asymmetric vehicles at symmetric or asymmetric flight conditions and symmetric vehicles at asymmetric flight conditions. While this system can clearly be applied to both symmetric and asymmetric vehicles and flight conditions, it challenges the prediction of the aerodynamic cross-coupling dynamic derivatives (m_p , m_r , n_q , l_r , etc.). These derivatives could be calculated with the linear vortex lattice method VORLAX, but little or no validation data currently exists to check the physical correctness of any model. If the designer judges that these particular aerodynamic derivatives are negligible for the design problem at hand, then the mathematical model can be utilized to take into account inertial and control cross-coupling of asymmetric aircraft and symmetric aircraft in asymmetric flight conditions.

It should be noted at this point that Equation 40 inherently incorporates the traditional decoupled longitudinal and lateral/directional equation of motion. The

decoupled formulation usually provides more physical visibility for classical symmetric aircraft and they serve as a datum to determine the magnitude of the cross-coupling effects found when compared with the effects estimated using the fully coupled equations of motion solution. Due to time constraints, only the decoupled small-perturbation equations of motion have been incorporated in the current *AeroMech* prototype system. It is recommended that both systems be retained in the next version of *AeroMech*.

A survey of existing decoupled small-perturbation analysis tools has been performed. The results are summarized in Table 3.12.

Table 3.12 Summary of Available Small-Perturbation Analysis Tools

<i>Author</i>	<i>Methods</i>	<i>Program Name</i>	<i>Software Available</i>	<i>Language</i>	<i>FCS Modal Available</i>	<i>Comments</i>
<i>Abzug²</i>	<i>Linear system root locus, and reduced order models</i>	<i>ILOCS</i>	<i>Yes</i>	<i>FORTRAN 77</i>	<i>Yes</i>	<i>Easy to implement, can be adapted to coupled EOM, transparent FCS sizing</i>
<i>Chudoba¹</i>	<i>Linear System Root Locus</i>	<i>AeroMech</i>	<i>No</i>	<i>NA</i>	<i>Yes</i>	<i>Can be used as the Airframe Model with a Modified Abzug style FCS</i>
Stenge ¹³	Linear Root Locus and Numerical Integration with State Transition matrix, and Reduced Order Models	FLIGHT and SURVEY	Yes	MATLAB	Yes	Code in MATLAB therefore would not be easy to implement
Stevens ¹⁴	Linear Root Locus and Non-Linear Numerical Integration of Euler 6-Dof EOM	TRIMMER and JACOB	Yes	MATLAB	Yes	Codes Primarily in MATLAB and would Require adaptation
Phillips ¹⁵	Linear System Root Locus, Closed Form and Numerical Solutions to Quaternion Formulations, and Reduced Order Models	NA	NA	NA	No	No Source Code
Etkin ¹⁶	Linear Root Locus and Reduced Order Models	NA	NA	NA	Yes	No Source Code
Nelson ¹⁷	Linear Root Locus and Reduced Order Models	NA	NA	NA	Yes	No Source Code

Of the tools surveyed, the code from Abzug (ILOCS.for) stands out due to its integrated flight controller model and the available source code in FORTRAN 77, enabling swift integration into *AeroMech*. This code combines the classic decoupled

(longitudinal and lateral/directional) small perturbation equations of motion with an analog flight controller model to compute the Eigenvalues of the total system. The analog controller model allows the conceptual designer to estimate additional control power requirements due to the stability augmentation system. Although the detailed choice of the controller architecture depends on the particular aircraft type under consideration, the purpose of the tool in the present context is not to design an advanced flight control system for the aircraft but to emulate a controller only for the estimation of control power requirements.

The longitudinal and lateral/directional airframe equations of motion used by Abzug are shown in matrix form below (equations 34 and 35)²³.

Longitudinal

$$\begin{bmatrix} \dot{u} \\ \dot{\alpha} \\ \dot{\theta} \\ \dot{q} \end{bmatrix} = \begin{bmatrix} X_u & X_\alpha & -g \cos \theta & \frac{-W_0}{(Z_q + U_0)} \\ Z_u & Z_\alpha & -g \sin \theta & \frac{1}{VZ} \\ \frac{VZ}{0} & \frac{VZ}{0} & \frac{VZ}{0} & M_q + \frac{M_\alpha(Z_q + U_0)}{VZ} \\ M_u + \frac{M_\alpha}{VZ} & M_\alpha + \frac{M_\alpha}{VZ} & \frac{-M_\alpha g \sin \theta}{VZ} & \frac{M_\alpha}{VZ} \end{bmatrix} \begin{bmatrix} u \\ \alpha \\ \theta \\ q \end{bmatrix} + \begin{bmatrix} 0 \\ \frac{Z_{\delta_e}}{VZ} \\ 0 \\ M_{\delta_e} + \frac{M_\alpha Z_{\delta_e}}{VZ} \end{bmatrix} \delta_e \quad \text{Eq. 3.41}$$

Lateral/Directional

$$\begin{bmatrix} \dot{\beta} \\ \dot{\phi} \\ \dot{p} \\ \dot{r} \end{bmatrix} = \begin{bmatrix} Y_v & \frac{g \cos \theta}{VEL} & W_0 / VEL & 0 & Y_r^* - \frac{U_0}{VEL} \\ 0 & 0 & 1 & 0 & \tan \theta \\ L'_v & 0 & L'_p & 0 & L'_r \\ 0 & 0 & 0 & 0 & 1 / \cos \theta \\ N'_v & 0 & N'_p & 0 & N'_r \end{bmatrix} \begin{bmatrix} \beta \\ \phi \\ p \\ r \end{bmatrix} + \begin{bmatrix} Y'_{\delta_a} & Y'_{\delta_r} \\ L'_{\delta_a} & L'_{\delta_r} \\ 0 & 0 \\ N'_{\delta_a} & N'_{\delta_r} \end{bmatrix} \begin{bmatrix} \delta_a \\ \delta_r \end{bmatrix} \quad \text{Eq. 3.42}$$

Abzug applies these airframe equations of motion to two subsystems, the Continuous Controller (Equation 3.43) and Airframe and Instrumentation (Equation 3.44).

Controller

$$\begin{aligned} \dot{\mathbf{x}}_1 &= \mathbf{P1}\mathbf{x}_1 + \mathbf{H1}\mathbf{u}_1 \\ \mathbf{w}_1 &= \mathbf{S1}\mathbf{x}_1 + \mathbf{R1}\mathbf{u}_1 \end{aligned} \tag{Eq. 3.43}$$

where **P1** is the plant for the controller, **H1** are the autopilot gains, **S1** are the control gains, and **R1** are the thrust gains.

Airframe and Instrumentation

$$\begin{aligned} \dot{\mathbf{x}}_2 &= \mathbf{P2}\mathbf{x}_2 + \mathbf{H2}\mathbf{u}_2 \\ \mathbf{w}_2 &= \mathbf{S2}\mathbf{x}_2 + \mathbf{R2}\mathbf{u}_2 \end{aligned} \tag{Eq. 3.44}$$

where **P2** is the airframe plant, **H2** is the control and thrust effectiveness matrix, **S2** and **R2** are the flight instrument gains. The total system is visualized in Figure 3.18.

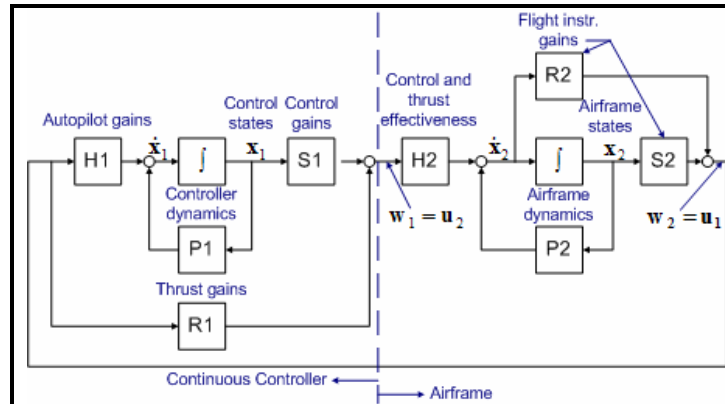


Figure 3.18: Continuous Controller and Airframe Model, Longitudinal Motion²³

As shown in Figure 3.16 the two subsystems interconnect at $\mathbf{u}_1 = \mathbf{w}_2$ and $\mathbf{u}_2 = \mathbf{w}_1$. With some algebra these two systems are combined into a single set of

equations. The Eigenvalues of the total system are then computed and thus the total airframe and flight controller stability can be calculated.

3.4.3.2 Dynamic Open and Closed Loop Analysis

When designing an aircraft, the designer needs to decide if a stability augmentation system is a requirement, and if so, what level of complexity is required. For example, modern fighter aircraft are flown statically unstable to fulfill maneuver requirements. For most fighter applications, the stability augmentation system (SAS) function artificially stabilizes the aircraft in contrast to modern commercial transports, that are usually flown statically stable but may require some stability augmentation only at certain flight conditions. Since the degree of longitudinal and lateral/directional static stability is a primary design variable, *AeroMech* provides for each axis three analysis options, *3(a)* open loop, *3(b)* closed loop damping restoration, and *3(c)* closed loop stiffness and damping restoration, see Figure 3.19.

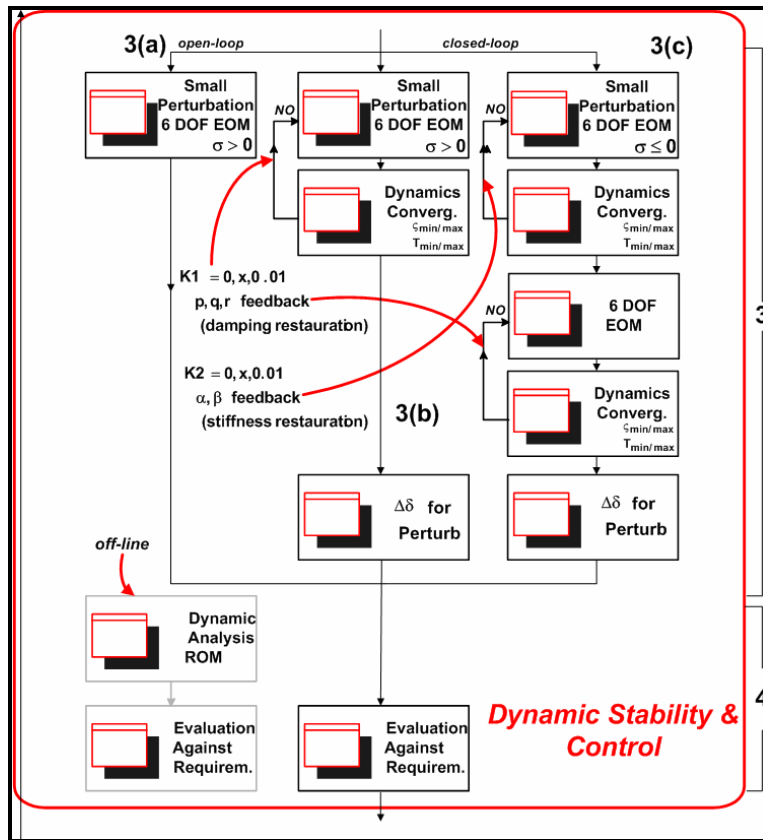


Figure 3.19: Dynamic Stability and Control Analysis Methodology¹

3(a) *Open Loop*: If no stability augmentation is desired, then only the open loop behavior of the vehicle is determined. In this case the vehicles dynamic behavior can only be altered through adjusting the airframe geometry and mass properties.

3(b) *Close Loop Damping Restoration (SAS)*: This branch represents the stability augmentation system (SAS) function for an aircraft with relaxed static stability. In this case the vehicle is still statically stability but does not meet certain dynamic stability requirements. Thus, pitch, roll and yaw feedback are used to artificially increase dynamic stability until the requirements are met. These feedback gains require additional control power as seen with Equations 39 through 40. From a predefined perturbation from trim, additional restoring control surface deflection can be estimated.

$$\Delta\delta_{LoCE} = \Delta q K_q \quad \text{Eq. 3.45}$$

$$\Delta\delta_{LaCE} = \Delta p K_p \quad \text{Eq. 3.46}$$

$$\Delta\delta_{DiCE} = \Delta r K_r \quad \text{Eq. 3.46}$$

3(c) *Close Loop Stiffness and Damping Restoration (SAS)*: This branch represents the SAS requirements for an inherently unstable aircraft in any axes. Such a vehicle requires the SAS to artificially restore stiffness and damping. This is to be accomplished by a) angle of attack and side-slip feedback to first restore stiffness and then b) pitch, roll, and yaw feedback to restore damping accordingly. Additional control power is required for this type of stability augmentation as shown with Equations 41 through 43. In practice, angle of attack and side-slip feedback should be used sparingly as angle of attack and side-slip angle sensors are prone to noise²².

$$\Delta\delta_{LoCE} = \Delta q K_q + \Delta\alpha K_\alpha \quad \text{Eq. 3.47}$$

$$\Delta\delta_{LaCE} = \Delta p K_p \quad \text{Eq. 3.48}$$

$$\Delta\delta_{DiCE} = \Delta r K_r + \Delta\beta K_\beta \quad \text{Eq. 3.49}$$

For example, in section 3.4.2 it was demonstrated that the YB-49 could achieve a significant increase in L/D through relaxed longitudinal static stability. This performance increase comes at the cost of decreased longitudinal dynamic stability, thus additional physical longitudinal control power is mandatory to enable this enhanced stability augmentation function. Figure 3.20 shows the open loop root locus for a decreasing static longitudinal margin for the YB-49.

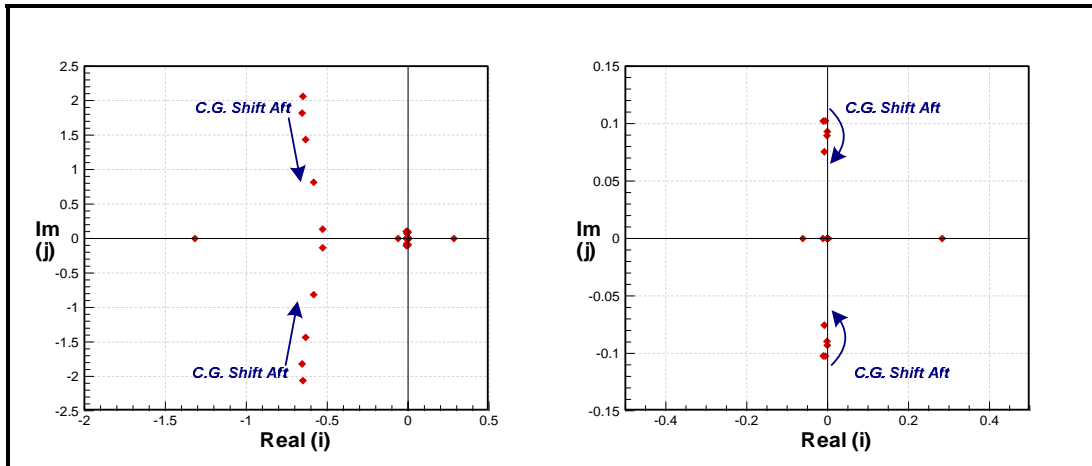


Figure 3.20: Open-loop root locus for the YB-49 with decreasing static longitudinal margin

The figure shows that the imaginary portion of the short period root is significantly affected by the decrease in the static longitudinal margin since it splits and combines with the phugoid to form the two non-oscillatory modes and the third oscillatory mode of a statically unstable configuration ($sm < 0$). These roots produce a decrease in natural frequency and an increase in the short-period damping ratio while the phugoid motion experiences a decrease in both frequency and damping ratio, see Figure 3.21.

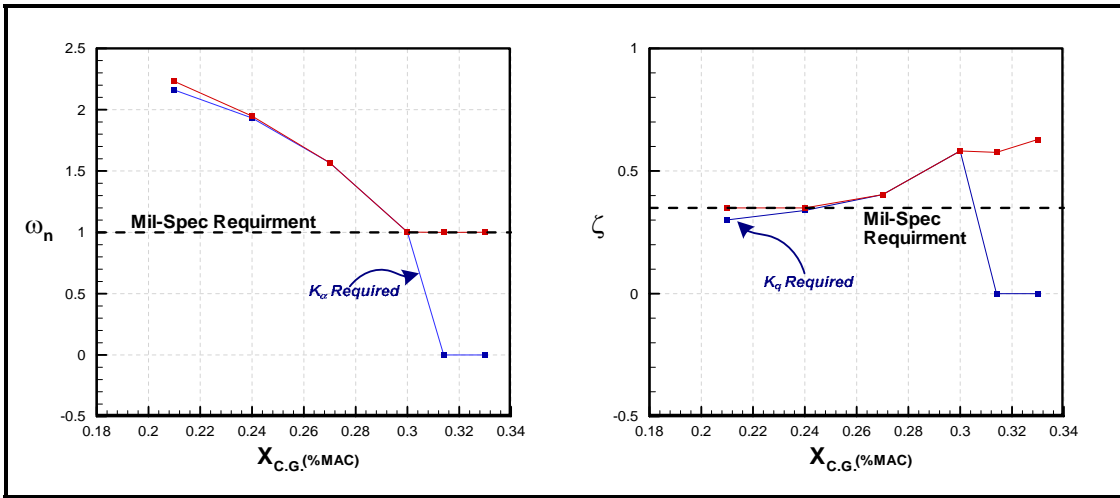


Figure 3.21: YB-49 Open-Loop Short Period ω_n and ζ with Decreasing Static Margin

When taking Mil-Spec 8785C requirements into account it is clear that stiffness restoration is required for c.g. locations aft of about 0.3% MAC and damping restoration is required for c.g. locations forward of about 0.24% MAC. Using a second order lag model for the controller ($\omega_n = 12.0$, $\zeta = 0.707$), *AeroMech* estimates the following gains and additional control power for the YB-49 as shown in Figure 3.22.

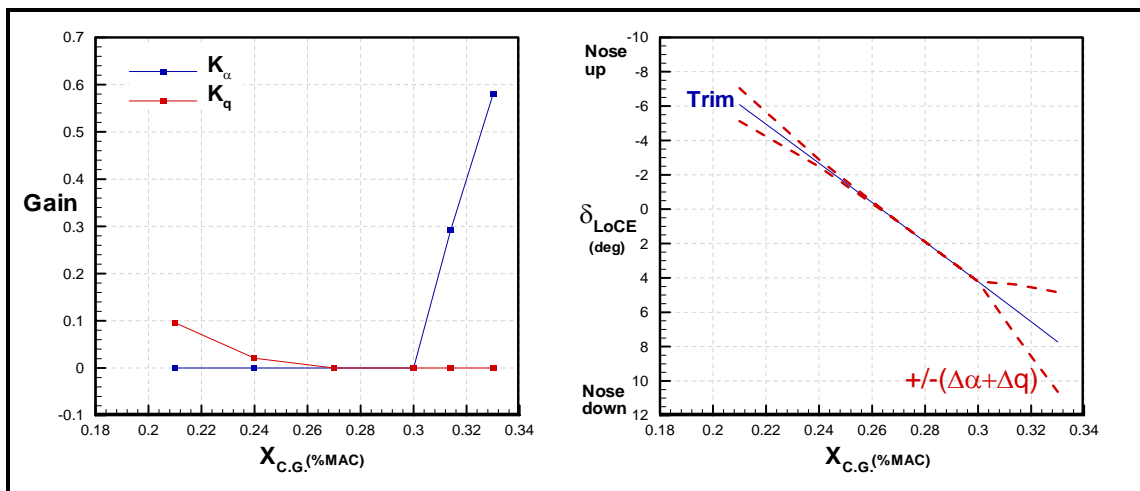


Figure 3.22: YB-49 Closed-Loop gains and additional control power required for longitudinal stability augmentation.

3.5 Output Definition

With the combination of the steady state control power, trimmed aerodynamics, static and dynamic stability modules a large and diverse data set can be produced quickly. Proper organization and visualization of this data is required to provide meaningful information to the conceptual designer. To accomplish this, *AeroMech*'s output is organized into two principal parts: a) individual flight condition output and b) summary output over the entire flight envelope (Figure 3.23).

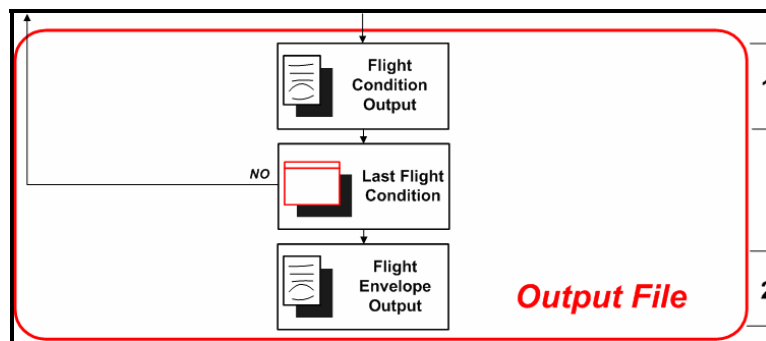


Figure 3.23: *AeroMech* Overall Methodology Output

Each DCFC analyzed by *AeroMech* has an individual detailed output file, providing information related to control power and stability characteristics. Having executed all of the design-constraining flight conditions (DCFC) over the flight envelope, a summary flight envelope output file is created detailing how control power and stability changes over the flight envelope. This enables the designer to identify the design critical corners in the flight envelope, where either control power is lacking or marginal, where poor flying and handling qualities can be expected. Having generated such information, *AeroMech* enables the designer to define design modifications in the form of trade studies or point designs.

CHAPTER 4

AEROMECH PROTOTYPE SYSTEM DEVELOPMENT

4.1 *AeroMech* Development Background and Process

4.1.1 AeroMech Background

The development of *AeroMech* follows the 3 basic steps described in Chapter 1: (1) initial concept development (2) prototype stand-alone *AeroMech* software development, and (3) integration of *AeroMech* into PrADO. As discussed in Chapter 1, the initial concept of *AeroMech* was developed by Chudoba¹ and the first version of the prototype stand-alone software was developed by Pippallapalli⁶. This first version of the alpha prototype software consists of five fundamental steps, see also Figure 4.1:

1. Read input files.
2. If control allocation is required, then run LOTS and modify VORSTAB input file accordingly.
3. Run VORSTAB to calculate aerodynamic and control coefficients and derivatives.
4. Run VORSTAB three additional times to with different wing, horizontal tail and vertical tail incidences to calculate the effects of a variable incidence wing, horizontal tail, and vertical tail.
5. Dependent on the maneuvers specified (SSLF, SSPUPU, SSRP, SSTF, or QSTORM) a separate subroutine is called which solves for the control surface

and incidence deflections required. This data is output into a separate file for each maneuver.

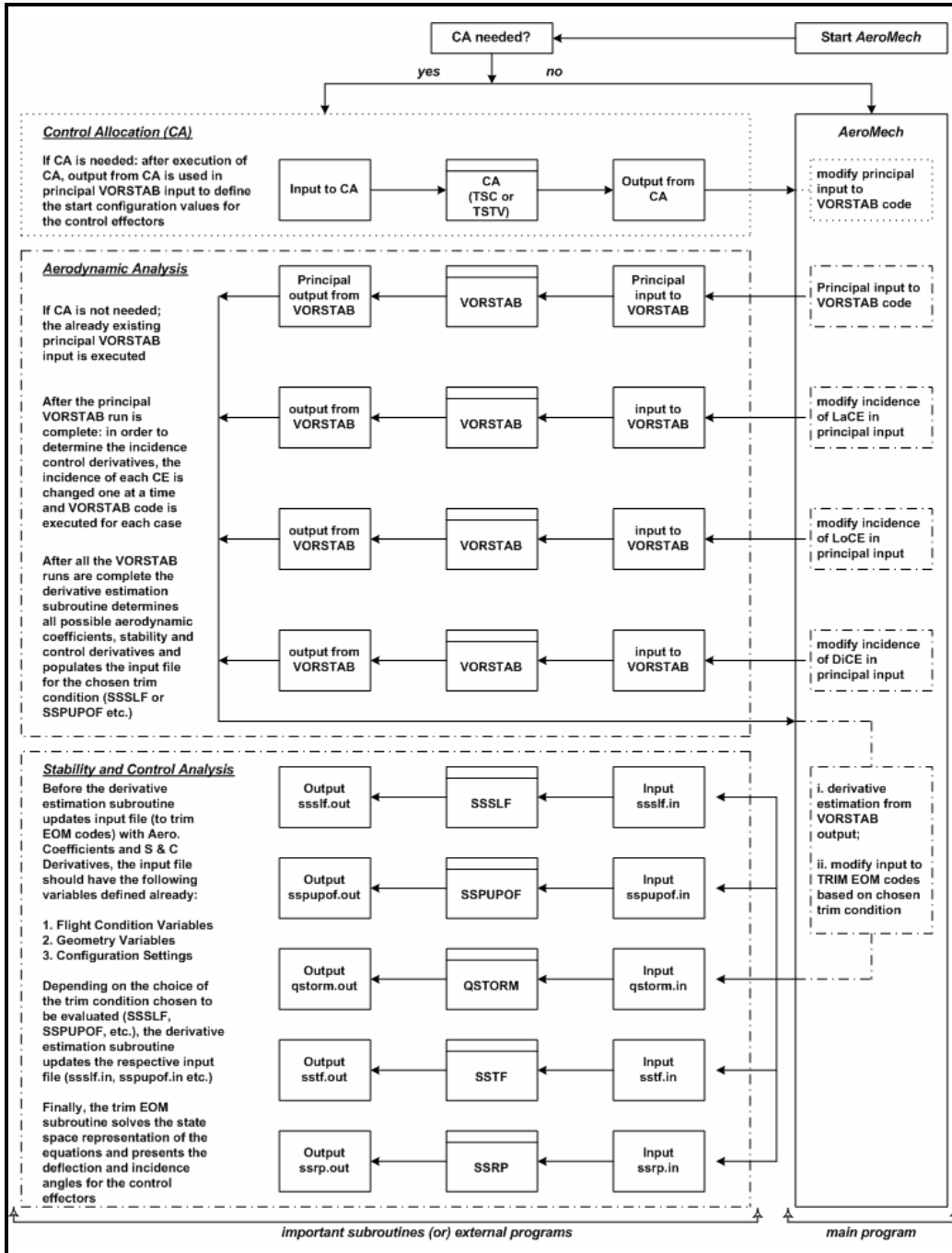


Figure 4.1: First AeroMech Stand-alone Prototype Software Overview⁶

This code attempted to solve the coupled 6-DOF non-linear trim equations (, Chapter 3, Equations 3.17-3.22) of motion through utilizing a linear system solution method. This required the equations to be arranged such that all the non-linear terms be located on the right-hand side of the equation and the linear terms on the left to produce the linear system, $\mathbf{Ax} = \mathbf{B}$. In this version of *AeroMech*, a separate set of equations was derived for each maneuver where the thrust coefficients are explicitly stated. For example, the system for steady-state straight line flight is shown below (Equation 4.1).

$$\begin{bmatrix} C_{D_{\delta_{LoCE}}} & C_{D_{\delta_{DiCE}}} & C_{D_{\delta_{LaCE}}} & C_{D_{\delta_{\alpha}}} & C_{D_{\delta_{\beta}}} & C_{D_{\delta_{\gamma}}} \\ C_{Y_{\delta_{LoCE}}} & C_{Y_{\delta_{DiCE}}} & C_{Y_{\delta_{LaCE}}} & C_{Y_{\delta_{\alpha}}} & C_{Y_{\delta_{\beta}}} & C_{Y_{\delta_{\gamma}}} \\ C_{L_{\delta_{LoCE}}} & C_{L_{\delta_{DiCE}}} & C_{L_{\delta_{LaCE}}} & C_{L_{\delta_{\alpha}}} & C_{L_{\delta_{\beta}}} & C_{L_{\delta_{\gamma}}} \\ C_{l_{\delta_{LoCE}}} b & C_{l_{\delta_{DiCE}}} b & C_{l_{\delta_{LaCE}}} b & C_{l_{\delta_{\alpha}}} b & C_{l_{\delta_{\beta}}} b & C_{l_{\delta_{\gamma}}} b \\ C_{m_{\delta_{LoCE}}} \bar{c} & C_{m_{\delta_{DiCE}}} \bar{c} & C_{m_{\delta_{LaCE}}} \bar{c} & C_{m_{\delta_{\alpha}}} \bar{c} & C_{m_{\delta_{\beta}}} \bar{c} & C_{m_{\delta_{\gamma}}} \bar{c} \\ C_{n_{\delta_{LoCE}}} b & C_{n_{\delta_{DiCE}}} b & C_{n_{\delta_{LaCE}}} b & C_{n_{\delta_{\alpha}}} b & C_{n_{\delta_{\beta}}} b & C_{n_{\delta_{\gamma}}} b \end{bmatrix} \bar{q} S^* \begin{bmatrix} \delta_{LoCE} \\ \delta_{DiCE} \\ \delta_{LaCE} \\ i_{LoCE} \\ i_{LaCE} \\ i_{DiCE} \end{bmatrix} = \begin{bmatrix} -[C_{D_{\alpha}} + C_{D_{\beta}}] \bar{q} S - mg \sin \gamma + \sum_{i=1}^k T_i (\cos \phi_i \cos \psi_i \cos \alpha + \sin \phi_i \sin \alpha) - \sum_{i=1}^{n_E} \Delta X_{D_i} \\ -[C_{Y_{\alpha}} + C_{Y_{\beta}}] \bar{q} S - mg \sin \phi \cos \gamma - \sum_{i=1}^k T_i \cos \phi_i \sin \psi_i \\ -[C_{L_{\alpha}} + C_{L_{\beta}}] \bar{q} S + mg \cos \gamma \cos \phi + \sum_{i=1}^k T_i (-\cos \phi_i \cos \psi_i \sin \alpha + \sin \phi_i \cos \alpha) \\ -[C_{l_{\alpha}} + C_{l_{\beta}}] \bar{q} S b - \sum_{i=1}^k T_i \cos \alpha (-\cos \phi_i \sin \psi_i z_i + \sin \phi_i y_i) - \sum_{i=1}^k T_i \sin \alpha (\cos \phi_i \sin \psi_i x_i - \cos \phi_i \cos \psi_i y_i) \\ -[C_{m_{\alpha}} + C_{m_{\beta}}] \bar{q} S \bar{c} - \sum_{i=1}^k T_i (\cos \phi_i \cos \psi_i z_i - \sin \phi_i x_i) \mp \sum_{i=1}^{n_E} \Delta M_{D_i} \\ -[C_{n_{\alpha}} + C_{n_{\beta}}] \bar{q} S b - \sum_{i=1}^k T_i \sin \alpha (\cos \phi_i \sin \psi_i z_i - \sin \phi_i y_i) - \sum_{i=1}^k T_i \cos \alpha (\cos \phi_i \sin \psi_i x_i - \cos \phi_i \cos \psi_i y_i) \mp \sum_{i=1}^{n_E} \Delta N_{D_i} \end{bmatrix}$$

Eq. 4.1

The \mathbf{x} vector in this equation contains 3 primary control effector deflections:(a) longitudinal control effector deflection (δ_{LoCE}), (b) lateral control effector deflection (δ_{LaCE}), and (c) directional control effector deflection (δ_{DiCE}), along with 3 incidence deflections i_{LoCE} , i_{LaCE} , and, i_{DiCE} , which represent the incidence of the stabilizer surface of the horizontal tail, the incidence setting of the wing, and the incidence of the stabilizer surface of the vertical tail. These incidence controls were added to this system in order to produce 6 unknowns for 6 equations. While incidence controls are utilized on aircraft it is rare to have an aircraft with both three all-movable surfaces with an additional control device on each surface. Clearly, this system of equations detracts

from the generic nature of *AeroMech* due to the need for three surfaces to vary incidences. The Northrop YB-49 or Boeing BWB flying wings) do not possess variable incidence stabilizer surfaces. In addition, typical TAC aircraft typically do not have control of the wing or vertical tail incidence.

Conceptually, when trimming an aircraft in 6-DOF the LoCE, LaCE and DiCE are used to trim the moments about the center of gravity and thrust, angle of attack and bank-angle are used to trim drag, lift and side forces respectively. The above system of equations has replaced the thrust, angle of attack and bank angle with variable wing incidence, horizontal stabilizer incidence, and vertical tail incidence. A more generic formulation would allow the designer to specify the LoCE, LaCE and DiCE as either an all-moveable surface, flap surface, spoiler, etc. and use the aircrafts attitude (angle of attack and bank angles) trim lift and side-force equations while thrust balances drag. Any additional control surfaces would require control allocation which is specified earlier in the *AeroMech* methodology.

This approach required modification of the VORSTAB input file to change to incidences of each surface and rerun to the code in order to obtain the required derivatives for the **A** matrix in Equation 1. Both the solution method to the steady-state equations of motion and the integration of VORSTAB where revisited in the development of the current prototype system.

4.1.2 AeroMech Prototype Software Development Process

There are two main approaches to software development, Top-down and Bottom-up²⁴. The Top-down approach requires planning of the codes logic and sub-

functions before any coding begins. This allows for greater understanding of the problem and structures the remaining coding effort, while delaying testing and experimentation. Conversely, the Bottom-up approach requires the individual sub-functions be written, tested and then linked together. This allows for immediate testing and experimentation but can lead to unorganized software which is difficult to modify and maintain. In modern software development a mixture of these two schools of thought are typically used²⁴.

For the development of the initial prototype *AeroMech* software, a Top-down approach was initially utilized by Pippalapalli⁶, utilizing the structured programming approach from Nassi and Schneiderman²⁵. The conceptual logic for *AeroMech* from Chudoba¹ was (1) transferred into detailed Nassi-Schneiderman (N/S) structograms and (2) the source code was written according to these N/S diagrams. Due to time constraints the source code not be sufficiently completed...

N/S structograms are a beneficial tool to develop the logic of a code in detail, allowing the designer to think critically about the interfaces of subroutines, etc. The basic structures of N/S structograms are explained below in Table 4.1, which is summarized from Pippalapalli⁶ and Nassi and Schneiderman²⁵.

Table 4.1 Nassi-Schneiderman (N/S) structogram basic structures²⁵

Structure	Traditional Flow Diagram	N/S Structure	Comments
Sequence			Represents a series of commands and procedures
Selection			If the condition is true then process x is executed, if false, process y is executed
While Loop			While the condition is true process x is repeated until the condition is no longer true
Until Loop			Similar to a while loop. Typically used for a set iteration such as a do loop. Example, do for l=1 to l=10
Switch			A second method of visualizing simple a selection in N/S diagrams

An example of a N/S structogram detailing AeroMech from Pippalapalli⁶ is shown in Figure 4.2.

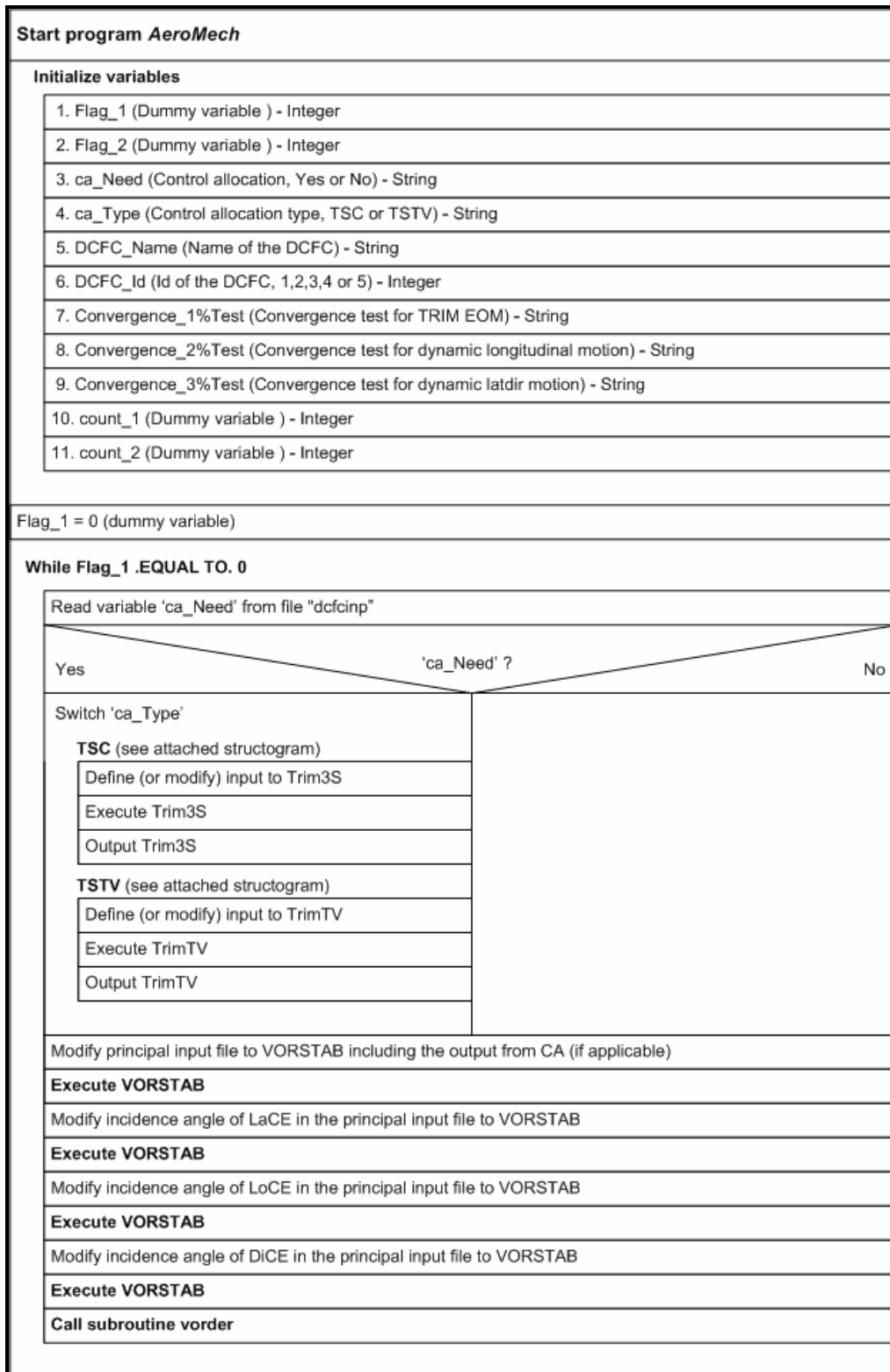


Figure 4.2: Partial *AeroMech* stand-alone prototype software N/S structogram⁶

While structured programming can be an efficient means of source code development, it is difficult for inexperienced programmers to detail source code in a N/S flow chart due to their limited knowledge of programming techniques. It is necessary for novice programmers to experiment with different coding techniques to gain an understanding of how to implement methods and theories into executable source code. This lack of experience can make structured programming overwhelming.

In order to gain programming experience while retaining the obvious benefits of structured programming it was decided to include some bottom-up techniques to enable more experimentation early. The development processes for the current effort was (1) retain the basic structure developed by Pippalapalli⁶, (2) to strip down the original system and flow diagrams to a basic level and incrementally build the system components, using a bottom-up approach. Essentially, a Top-down approach is utilized for the overall-system development and a Bottom-up approach for individual algorithm development. This allows for sufficient structure for the source code while allowing for experimentation and functionality earlier in the design process.

During the development of the AeroMech software, the following guidelines were followed to enable a systematic and transparent software development process.

1. **Keep the tool as generic.** This required considering both symmetric and asymmetric flight vehicle configurations during the development effort.
2. **Document variables in a single location.** This involved keeping track of all variables created during coding for future reference.

3. **Keep the flow charts and structograms simple to visualizing the code.** The structograms developed by Pippalapalli⁶ were very detailed and resembled both the look and length of the actual source code. The purpose of structograms is to complement the source code to aid in planning, understanding and interpreting the logic.

4.2 Evolution of the *AeroMech* Prototype Stand-alone Software

The first step in developing the source code has been to step back and redevelop the foundation of the system. This involved understanding the original source code from Pippalapalli⁶ and reducing it to its basic functions. The method of solving the steady-state equations of motion for trim and maneuvering analysis (described in Section 4.4.1.1) led to coding issues which detracted from the generic application of *AeroMech*. To accomplish this *AeroMech* was first stripped down to the components required to solve the steady-state equations of motion and then experiment with different solution methods,

The level of detail in the *AeroMech* N/S diagrams, which resemble well commented source code, led to adopting a different strategy of developing the overall *AeroMech* logic, modifying and reducing the main *AeroMech* drive program to resemble an executable N/S structogram with switches to call the major *AeroMech* Modules. It was not understood at the time by the author that N/S were not intended to be as detailed as produced by Pippalapalli⁶. Nassi²⁵ states that one of the important advantages of N/S diagrams over traditional flow charts is that “complete though structures can and should fit on no more than one page,” requiring the diagram to self

contained. The N/S diagrams from Pippalapalli⁶ take several pages to describe the overall logic of the tool. Furthermore, during the planning stages of the code the need to visualize the initialization of each individual variable is not necessary. This tends to lengthen and clutter the structogram and detracts from the visualization of the structure. To demonstrate this style of N/S diagrams, the initial *AeroMech* main driver program developed for the current research is visualized in the following N/S flow chart (Figure 4.3).

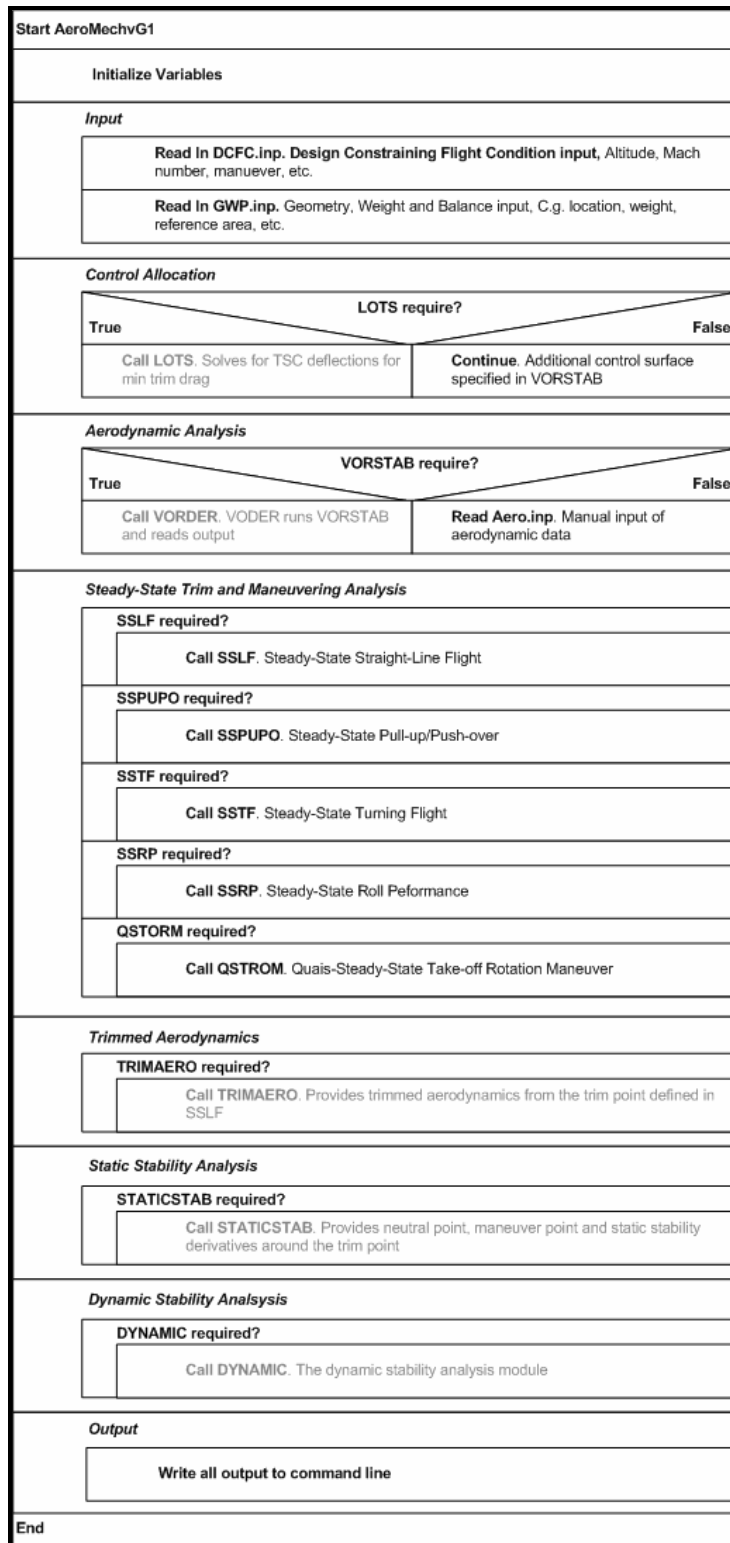


Figure 4.3: Initial *AeroMech* stand-alone prototype software N/S structogram.

As demonstrated, for planning purposes only the major components are define to visualize the input-analysis-out structure of the code. In Figure 4.3 the subroutines LOTS, VODER, TRIMAERO, and DYNAMIC are grayed out to indicate that those modules are not included in this initial version.

From this foundation, the additional components of *AeroMech* were assembled and adapted as summarized in Table 4.2. Each module was planned, implemented and tested before moving on the remaining modules. This gave room to experiment with the code, build programming experience, and give AeroMech functionality thought the development phase. In Table 4.2 Version 1 represents the version of *AeroMech* from Pippalapalli⁶, and versions 2 through 7 represent the various perturbations of *AeroMech* during this research.

Table 4.2 Summary of Current Prototype System Evolution

Version	1	2	3	4	5	6	7
Components							
Input	<i>DCFC and aircraft constants for, several DCFC's in a single run</i>	<i>Basic files from reference 59, one DCFC's at a time</i>	<i>Improved Input file structure, several DCFC's in a single run</i>	Improved Input file structure, several DCFC's in a single run	Improved Input file structure, several DCFC's in a single run	Improved Input file structure, several DCFC's in a single run	Improved Input file structure, several DCFC's in a single run
Control Allocation	<i>'Ad hoc' and LOTS used off-line</i>	-	-	-	-	-	<i>'Ad hoc' and LOTS used off-line</i>
Aerodynamics	<i>VORSTAB for Linear Derivatives</i>	<i>Manual Input of linear derivatives</i>	<i>Manual input and VORSTAB for Linear Derivatives</i>	Manual input and VORSTAB for Linear Derivatives	Manual input and VORSTAB for Linear Derivatives	<i>Manual input, VORSTAB, and Digital DATCOM to build Aerodynamic Look-up tables</i>	<i>Manual input, VORSTAB, and Digital DATCOM to build Aerodynamic Look-up tables</i>
Steady-State Trim and Control	<i>Linear System Solution</i>	<i>Mod. Linear System Solution</i>	<i>Mod. Linear System Solution</i>	<i>Non-linear Solution Method</i>	Non-linear Solution Method	Non-linear Solution Method	Non-linear Solution Method
Trimmed Aerodynamics	-	-	Computed internally for dynamics stability	Computed internally for dynamics stability	<i>Computed for dynamics, linear derivatives around trim point</i>	<i>Computed for dynamics, linear derivatives around trim point</i>	<i>Computed for dynamics, linear derivatives around trim point, output for visualization</i>
Static Stability	-	-	-	-	-	-	<i>Derivatives and neutral point, calculated and output for visualization</i>
Dynamic Stability	-	-	ROM and Decoupled open loop EOM from Etkins ¹⁶	ROM and Decoupled open loop EOM from Etkins ¹⁶	<i>Open and Closed loop analysis from Abzug</i>	Open and Closed loop analysis from Abzug	Open and Closed loop analysis from Abzug
Output File Organization	<i>Separate output files for each steady-state condition</i>	<i>Command line</i>	<i>Command line</i>	<i>Command line</i>	<i>Separate output files for each module</i>	<i>Separate output files for each module</i>	<i>Separate Files for each analysis module and summary files across all DCFC, Output formatted for Excel and TECPLOT visualization</i>

The first generation of the *AeroMech* software was developed by Pippalapalli⁶ as discussed previously, and it was this system that was the starting point for the current research investigation leading to the fully functional AeroMech software as documented

in this report.. The major modifications of each version, from from version two to generation seven are described below.

Version 2

This version of *AeroMech* focused on improving the integration of the steady-state trim and maneuver algorithms, to make them readily applicable to a wider variety of aircraft configurations, relative to the algorithm developed in Pippalapalli⁶. This step required decomposing the code, i.e. the removal of the control allocation module, the output file generation module, and the aerodynamic modules. This required programming an interim aerodynamic input file where the linear derivatives are input manually. Although the decomposition was done to simplify *AeroMech* for code development purposes, it became apparent that this functional modularization is highly useful for the incorporation of a wide variety of aerodynamic prediction tools. This feature has been retained as an option in later versions.

The linear system solution from Reference 6 was modified by first removing the incidence control derivatives in favor of attitude variables (angle of attack, bank angle, etc). The idea was to use one variable that primarily trimmed each equation of motion (e.g., α to increase lift to balance weight, δ_{LoCE} to balance the pitching moment equation, etc). A separate mathematical model was developed for each maneuver. For example, this produced the following mathematical model for the SSLF maneuver.

$$\begin{bmatrix}
-C_{T_D} & 0 & C_{D_\alpha} & C_{D_{LoCE}} & C_{D_{DiCE}} & C_{D_{DiCE}} \\
C_{T_Y} & \frac{mg \cos \gamma}{qS} & 0 & C_{Y_{LoCE}} & C_{Y_{LoCE}} & C_{Y_{DiCE}} \\
-C_{T_L} & 0 & C_{L_\alpha} & C_{L_{LoCE}} & C_{L_{LoCE}} & C_{L_{DiCE}} \\
C_{T_i} & 0 & 0 & C_{l_{LoCE}} b & C_{l_{LoCE}} b & C_{l_{DiCE}} b \\
C_{T_m} & 0 & C_{m_\alpha} \bar{c} & C_{m_{LoCE}} \bar{c} & C_{m_{LoCE}} \bar{c} & C_{m_{DiCE}} \bar{c} \\
C_{T_n} & 0 & 0 & C_{n_{LoCE}} b & C_{n_{LoCE}} b & C_{n_{DiCE}} b
\end{bmatrix}
\bar{qS}
\begin{Bmatrix}
\%Ta \\
\phi \\
\alpha \\
\delta_{LaCE} \\
\delta_{LoCE} \\
\delta_{DiCE}
\end{Bmatrix}
=
\begin{bmatrix}
-(C_{D_0}) \bar{qS} - mg \sin \gamma - \sum_{i=1}^{nfe} \Delta X_{D_i} \\
-(C_{Y_0} + C_{Y_\beta} \beta) \bar{qS} \\
-(C_{L_0}) \bar{qS} + mg \cos \gamma \\
-(C_{l_0} + C_{l_\beta} \beta) \bar{qS} b \\
-(C_{m_0}) \bar{qS} \bar{c} \pm \sum_{i=1}^{nfe} \Delta M_{D_i} \\
-(C_{n_0} + C_{n_\beta} \beta) \bar{qS} b \pm \sum_{i=1}^{nfe} \Delta N_{D_i}
\end{bmatrix}
\quad \text{Eq. 4.2}$$

Notice, in this system the drag equation is trimmed with percent thrust, the side-force equation is trimmed with bank angle, and lift equation is trimmed with the angle of attack. This is in contrast to the wing incidence, horizontal stabilizer incidence and vertical tail incidence of the method used by Pippalapalli⁶. This system worked well but made small angle assumption for the bank angle and relied on linear derivatives to solve this system. This, however, presents a problem at the stall angle of attack because of the non-linear nature of the aerodynamic data. This versions of AeroMech is visualized in Figure 4.3

Version 3

This version re-integrated the VLM VORSTAB into the source code to actively predict the linear derivatives in question. This required to a modification of the *AeroMech* input file structure to enable the analysis of multiple DCFC in a single computer run. The integration of VORSTAB was accomplished using the same input file subroutines from the first version of the prototype system⁶. The process logic of version 2 is described below:

1. Read input files.
2. Run VORSTAB.

3. Read aerodynamic data generated by VORSTAB.
4. Compute linear derivatives.
5. Solve linear steady-state equations of motion.
6. Compare the trim angle of attack to the angle of attack input into VORSTAB.
7. If new trim angle of attack and the VORSTAB angle of attack do not sufficiently match, modify VORSTAB input file with new angle of attack and control surface deflections and repeat steps 1 through 6, otherwise continue.

To automatically modify (rewrite) the VORSTAB input file with the new angle of attack and control surface deflection information, a subroutine provided by Dr. Heinze, University of Braunschweig, was utilized⁶. This subroutine reads an input file line-by-line until it finds a characteristic line specified, then reads and modifies the values below this line. This is visualized in Figure 4.4, showing the VORSTAB input file as an example.

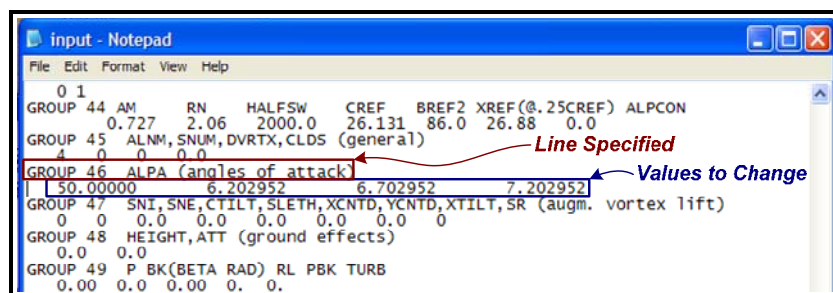


Figure 4.4: Modification of the VORSTAB input file

Although this version of *AeroMech* worked well for low angles of attack, it had convergence problems at higher angles of attack due to the non-linear character of the aerodynamic data near the stall point.

Version 4

This version of *AeroMech* represents a fundamental shift in the approach to solving steady-state non-linear equations of motion. During a meeting with Dr. Dogan it was suggested not to solve a non-linear problem with a linear system, but instead to reformulate the equations of motion into a format that could be solved with a numerical non-linear solver²⁶.

The solver selected is a Newton-Raphson Method for nonlinear systems of equations provided by Reference 27. This solver uses a Newton-Raphson (NR) multi-dimensional root finding method to compute the control vector, \mathbf{X} , for any system of equations, \mathbf{F} . This method provides a very efficient means of converging to a root if the initial guess is near the solution, but can fail to converge if the initial guess is not close to the solution²⁷. For solving the system of trim equations outlined before, the solutions are sufficiently close to an initial guess of zero for all variables; thus, the NR solver is sufficiently robust for this application.

Newton-Raphson solves a system of N equations with N unknowns. Denoting the functions as \mathbf{F} and the unknown variables (or control variables) as \mathbf{x} , the system can be expanded into the following Taylor series in the neighborhood of \mathbf{x} (Equation 4.3)²⁷,

$$F_i(\mathbf{x} + \delta\mathbf{x}) = F_i(\mathbf{x}) + \sum_{j=1}^N \frac{\partial F_i}{\partial x_j} \delta x_j + O(\delta\mathbf{x}^2) \quad \text{Eq. 4.3}$$

where,

$$\mathbf{F} = [F_1(x_1, x_2, x_3, \dots, x_N), F_2(x_1, x_2, x_3, \dots, x_N), \dots, F_N(x_1, x_2, x_3, \dots, x_N)] \quad \text{Eq. 4.4}$$

The Jacobin matrix, \mathbf{J} , is defined as,

$$J_{ij} \equiv \frac{\partial F_i}{\partial x_j} \quad \text{Eq. 4.5}$$

In matrix notation,

$$\mathbf{F}(\mathbf{x} + \delta\mathbf{x}) = \mathbf{F}(\mathbf{x}) + \mathbf{J} \cdot \delta\mathbf{x} + O(\delta\mathbf{x}^2) \quad \text{Eq. 4.6}$$

Neglecting the higher order terms and setting $\mathbf{F}(\mathbf{x} + \delta\mathbf{x}) = 0$, a linear set of equations for the corrections can be produced, $\delta\mathbf{x}$, that move each function closer to zero simultaneously (Equation 4.7).

$$\mathbf{J} \cdot \delta\mathbf{x} = -\mathbf{F} \quad \text{Eq. 4.7}$$

This matrix equation is then solved using LU decomposition and the corrections are then added to the solution vector (Equation 4.8).

$$\mathbf{x} = \mathbf{x}_{old} + \mathbf{x}_{new} \quad \text{Eq. 4.8}$$

This process is then iterated until the solution converges²⁷.

This process is available as subroutine *mnewt* in Reference 27 and is implemented into *AeroMech* as subroutines *NONLINEAR* and *NONLINEAR2* to solve the 6-DOF steady state systems (SSLF, SSPUPO, etc.) and the 5-DOF steady state system (QSTROM) respectively. The functions \mathbf{F} , which are driven to zero, are defined in *funcv* and *funcv2*. The *funcv* subroutine for the 6-DOF formulation is defined in Figure 4.5 *Funcv2* follows a similar structure for the 5-DOF system.

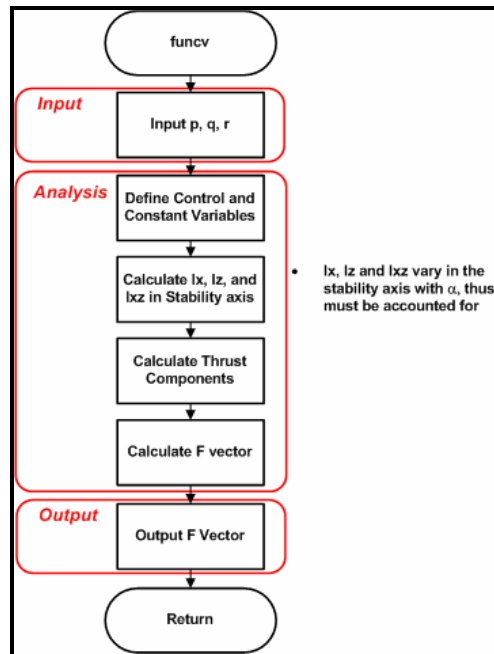


Figure 4.5: Nonlinear Newton-Raphson function algorithm.

Having implemented this major modification into version G5 of *AeroMech* allowed the removal of the small angle assumptions made during the derivation. However, the system still had run-time convergence problems near the stall angle-of-attack due to the linear derivatives used.

Version 5

Version G5 of *AeroMech* incorporated the open and closed loop root locus methods provided by the code *ILOCUS* from Abzug²³. There are several options available to emulate a stability augmentation system (SAS). These options can be subdivided into classical techniques and modern techniques. Classical techniques close feedback loops one at a time, starting with the innermost feedback loop and working outward until the dynamic requirements are met²². Typically, this technique first analyzes the effect of a single feedback loop onto the system, and then selects the gain

which provides the required dynamic response. For a MIMO (Multi-Input/Multi-Output) controller, the outer control loops can have an effect on the dynamic behavior corrected with the inner control loop. Thus, much trial and error is required to design the total system.

Modern techniques select the appropriate gains from MIMO systems simultaneously through Eigenstructure Assignment (full state feedback and output feedback), LQR (Linear Quadratic Regulator with output feedback), etc.²² The modern methods are more robust compared to the classical design techniques due to their procedural nature. For version 5 of the prototype *AeroMech* software it was decided to implement a classical design procedure for the following reasons:

1. Classical techniques are thought to implement well with the software provided by Abzug due to its ability to close inner control loops while varying the control loop of interest.
2. Classical techniques provide a higher degree of physical insight into the effects of a single feedback loop onto the total flight vehicle dynamics.
3. Classical techniques work well for SISO (single input/single output) systems such as pitch, roll, and yaw rate feedback systems.

The task of integrating Abzug's code with a classical gain iteration scheme requires: (a) a method and source code understanding, enabling the decomposition of the code into its functional components, (b) devising a scheme to efficiently transfer data between *AeroMech* and *ILOCUS*, and (c) the implementation of an iteration scheme to arrive at the closed-loop gains.

(a) *Familiarization with ILOCUS*: The code *ILOCUS* is capable of varying one gain loop while holding other feedback loops gain values constant. The basic task has been to imbed *ILOCUS* into *AeroMech* to calculate the Eigenvalues for a given gain setting. An iteration scheme around *ILOCUS* then enables the calculation of the gains required to meet the stability requirements. To accomplish this, the aerodynamic, weight and balance, and propulsion data must be transferred to *ILOCUS*. Finally, the Eigenvalues for a specific gain setting are a result transferred back to *AeroMech*.

ILOCUS has been decomposed in order to understand the logic of the program and to identify how to transfer data in and out of this code. The source code familiarization activity is presented in Figure 4.6. This figure labels the locations where data enters and exits the code.

(b) *Data transfer between AeroMech and ILOCUS*: The code *ILOCUS* utilizes common blocks to store and pass data. In order to take advantage of this, the subroutine which operates *ILOCUS* renames the variables specified by *AeroMech* to the *ILOCUS* definitions, and then stores these values in the common blocks that *ILOCUS* utilizes.

Once the data was transferring correctly to *ILOCUS* an additional common block was created to store the Eigenvalues for passage back to *AeroMech*. To handle these operations, the subroutine *RUNILOCUS* was developed.

(c) *Implementation of iteration scheme to set closed-loop gains*: Fundamentally, *AeroMech* defines an initial gain setting, uses *RUNILOCUS* to compute the Eigenvalues of the system, compares the dynamic response to the requirements, and then iterates the procedure until the requirements are satisfied. Having estimated these gains, the additional control power required is then estimated for a predefined disturbance, see Chapter 3. This requires a specific logic to iterate *ILOCUS* such, that the correct gains are selected.

Having adopted the aircraft and control system model from Abzug²³ the classical feedback logic from Stevens²² has been implemented for the longitudinal and lateral/directional planes, see Figure 4.7 and 4.8. These two systems are used in combination to provide stiffness restoration and pitch damping in the longitudinal plane, stiffness restoration in the directional plane, and roll and yaw damping in the lateral/directional planes.

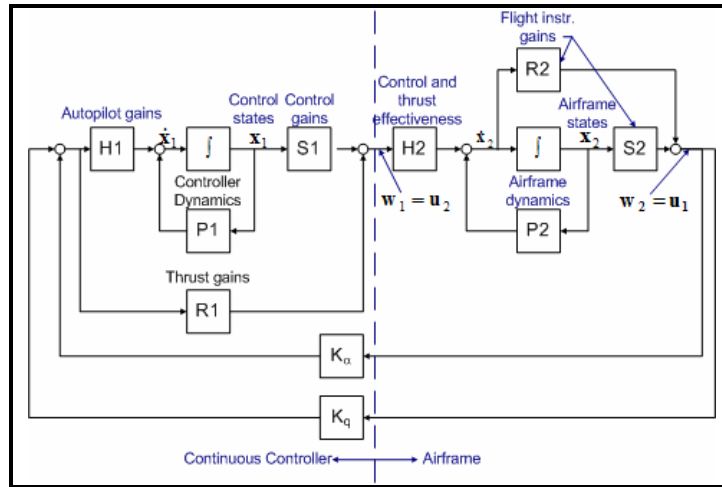


Figure 4.7: Longitudinal stability augmentation system²³

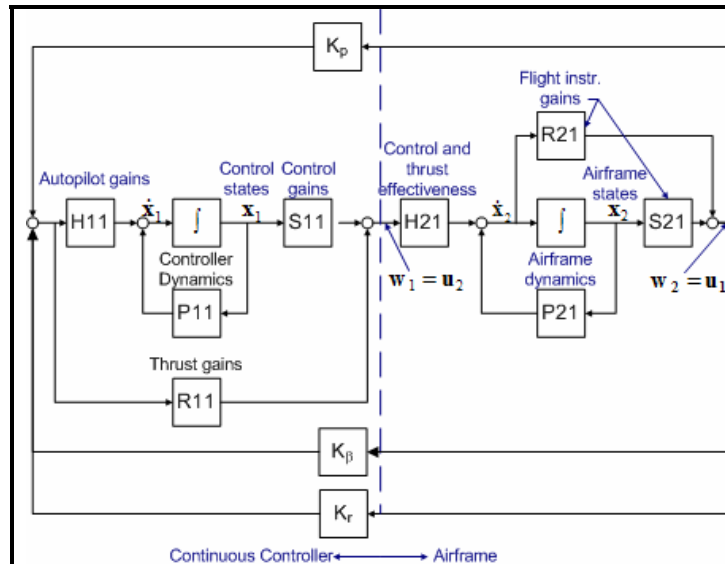


Figure 4.8: Lateral/directional stability augmentation system²³

As mentioned above, the logic for the longitudinal stability augmentation system (SAS) has been adopted from Stevens²². For a statically stable vehicle with poor flying qualities, the SAS produces a lightly damped phugoid and lightly damped short-period mode. This short-period motion can be augmented through the use of a pitch rate feedback, K_q , until the short-period damping motion meets the requirements. Pitch rate feedback has little effect on the phugoid motion. In contrast, a longitudinal statically

unstable vehicle will not exhibit the typical phugoid and short period mode behavior. Instead, the vehicle will exhibit one stable and one unstable exponential pole and a so called ‘third oscillatory mode’, which possesses a phugoid-like period with a short-period damping ratio, see Figure 4.9.

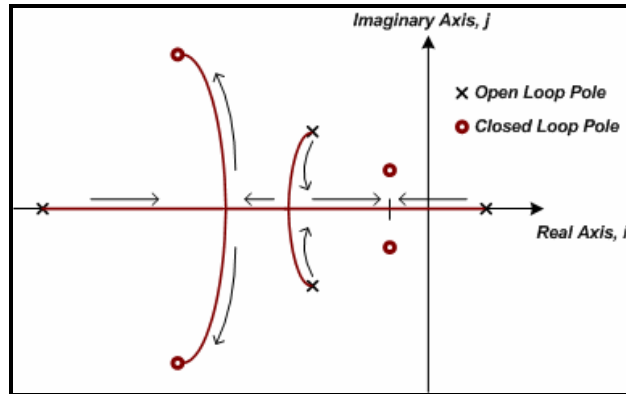


Figure 4.9: Angle-of-attack feedback effect of a statically unstable vehicle.

To correct for this flying quality deficiency, an angle-of-attack feedback, K_α , is implemented to shift the unstable pole into the left hand plane. This results in a conventional phugoid and short-period motion, see Figure 4.8. From here, pitch rate feedback, K , is used to tune the short-period mode to meet the requirements. The overall logic is shown via the subroutine DYNAMICLO, see Figure 4.10, which operates the longitudinal dynamic response calculations.

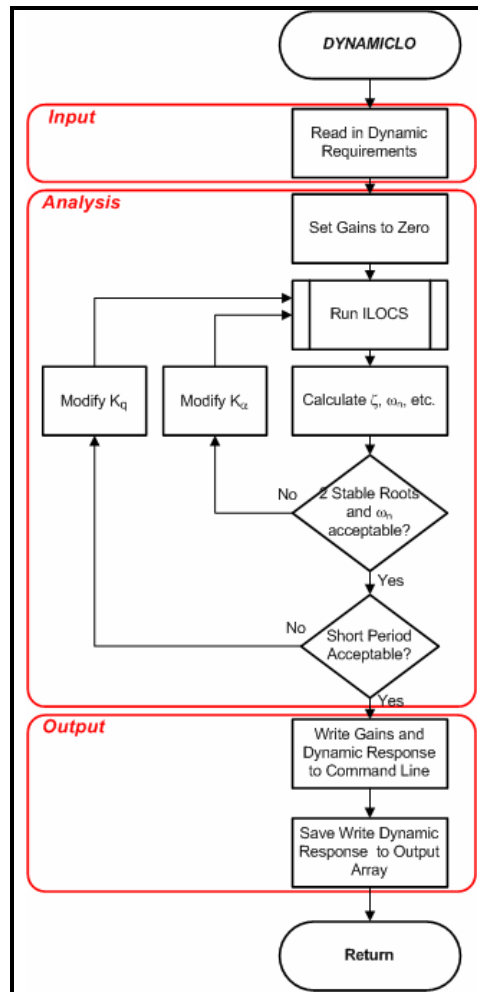


Figure 4.10: Control gain selection logic for longitudinal motion

For the lateral-directional motions, the SAS logic from Stevens²² has been implemented. First, the roll mode characteristics are compared to the requirements and, if necessary, roll-rate feedback is applied. Due to the aerodynamic coupling between roll and yaw via the use of the ailerons, roll feedback first and then yaw-rate feedback are applied to correct the Dutch roll response. The schematic of the DYNAMICCLA subroutine is shown in Figure 4.11. The DYNAMICCLA subroutine operates the lateral-directional response calculations.

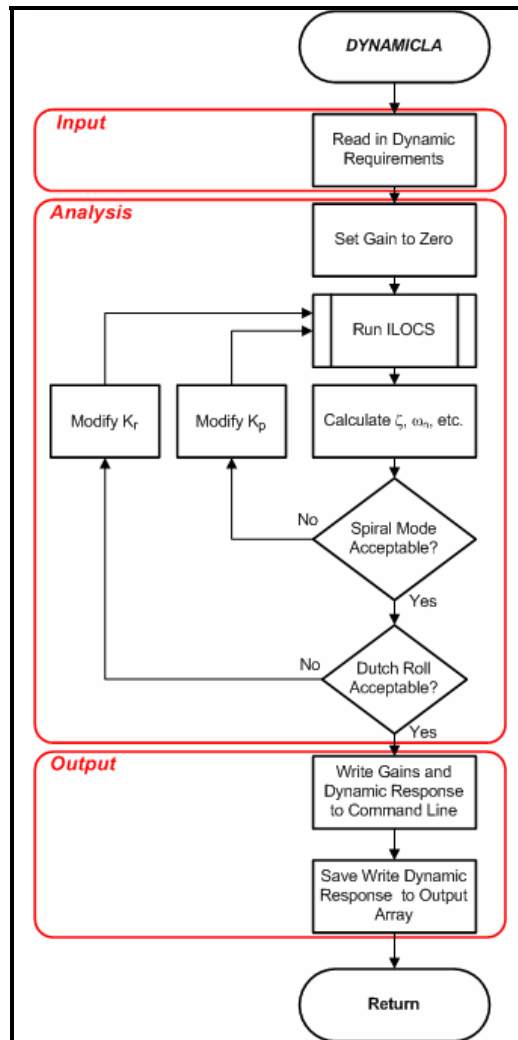


Figure 4.11: Control gain selection logic for the lateral/directional motion.

Generation 5 of *AeroMech* integrated the basic stability and control analysis modules and represents the first fully functional *AeroMech* software. Still, major deficiencies remained in this version due to the using of linear derivatives for the trim algorithm.

Version 6

The convergence problems with the trim algorithm were addressed with version 6 of *AeroMech*. The concept of solving the trim equations with linear aerodynamic

derivatives, then iterating VORSTAB until the solution converges either required excessive run times until convergence or it resulted in failed convergence dependent on the initial angle of attack and control surface deflection guess used in VORSTAB

To solve this problem it was decided to arrange the aerodynamic data in a look-up table. During the internal iterations, the Newton-Rhapson solver calls the aerodynamic look-up table when new coefficients are required. Look-up tables require an interpolation routine which must be appropriate to the physical model. A linear interpolation model would present the same problems as seen with the linear derivatives, requiring many data points to accurately model the stall region. A cubic-spline interpolation routine is, in contrast, more appropriate because it builds a cubic function using the three nearest points to the value desired. This allows to accurately retrieve both, the linear and non-linear coefficients of the aerodynamic data. Note, Earlier version of AeroMech used a center difference method to calculate the linear derivatives from the VORSTAB output.

The aerodynamic look-up table is organized such as to comply with the format used within the synthesis system AVDS PrADO for storing aerodynamic data. An example of this data file is shown with Figure 4.12.

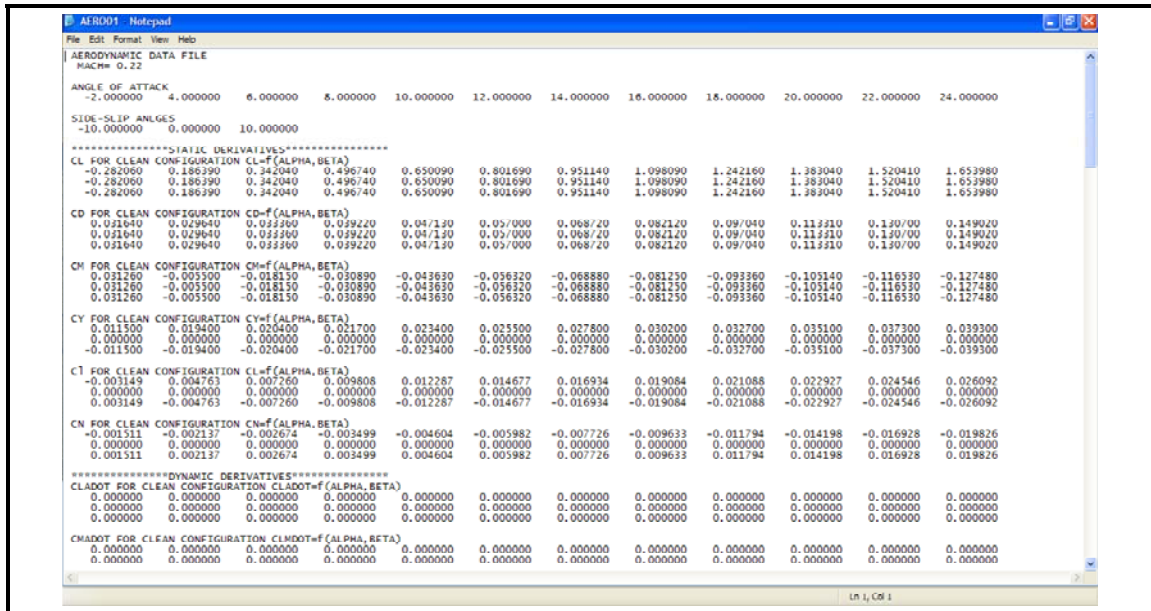


Figure 4.12: *AeroMech* aerodynamic look-up table Screen Shot

At this point during the development of *AeroMech*, the official validation and calibration process has been initiated using the Northrop YB-49 and the Lockheed F-104 as representative case studies. It was decided to incorporate digital DATCOM as a complementing aerodynamic tool to (1) allow for more efficient modeling of conventional aircraft (i.e. TAC), to (2) incorporate certain control effectors beyond plain flaps, and (3) to calculate unsteady aerodynamic derivatives. For practical purposes of building the aerodynamic representation in VORSTAB and Digital DATCOM, it was decided to program an interface to automate the VORSTAB (RUNVORSTAB.f90) and Digital DATCOM (RUNDATCOM.f90) runs. These codes provide the output in the *AeroMech* aerodynamic look-up table. Both of these executables are explained in Appendices B and C.

Version G6 of *AeroMech* has been a) working well for both the linear and non-linear corners of the flight envelope and b) this version enabled the population of the

aerodynamic prediction tool library in *AeroMech*. In general, the integration of a new aerodynamic prediction code requires formatting its output according to the format specified by the aerodynamic lookup table. The clear definition of such interfaces will also enable an easier integration of *AeroMech* into AVDS PrADO, which stores all aircraft data in a data base management system (DBS) consisting of text based files.

Version 7

With the major analysis components of *AeroMech* operational, the software underwent several refinements to increase its overall functionality. These refinements include:

1. introduction of a static stability module for neutral point and maneuver point calculations;
2. output of the linear derivatives and trimmed aerodynamics;
3. develop summary output files for each DCFC;
4. formatting of all output files such to open in MS Excel;
5. building a TECPLOT data file structure of the most commonly used figures;
6. re-introduction of LOTS as a stand-alone mode for control allocation.
7. incorporate a specific control allocation scheme for the YB-49 Example

The static stability module calculates the neutral point (np), maneuver point and static margin (sm) from the linear data, collected from the trim algorithm, and outputs the static stability derivatives as a function of angle of attack. The trimmed aerodynamic output takes the trim point defined, calculates the lift to drag ratio (L/D), and outputs

lift, drag and pitching moment curves. The output files for this system are explained in the users guide, see Appendix A.

The new control allocation scheme for the YB-49 utilizes one LoCE for trim and the second LoCE for maneuvering. Like most aircraft, the YB-49 has a trimming surface which is operated by a trim wheel in the cockpit and a primary control effector operated by the yoke. To adapt AeroMech to utilize one surface to trim and another to maneuver,

1. a secondary LoCE must be defined. This is handled in RUNVORSTAB to calculate the force and moment increments of a primary and secondary LoCE.
2. The aerodynamic look-up was modified to incorporate two LoCE's.
3. A separate subroutine SSLFCA was developed which utilizes the secondary LoCE trim to 1-g flight using the Newton-Rhapson solver.
4. This deflection is carried through the remainder of the analysis as a constant and the primary LoCE is used for the steady-state maneuvering analysis.

This system represents the latest evolution of *AeroMech*, containing the major components of (1) control allocation, (2) aerodynamic prediction (3) trim and maneuvering analysis, (3) trimmed aerodynamics, (4) static stability analysis, (5) dynamic stability analysis, and (6) output file organization. The overall organization of these components is visualized in Figure 4.13, showing *AeroMech*'s main driver program. The subroutines are defined in Table 4.2.

Table 4.3 Summary of Major *AeroMech* Subroutines

<i>Subroutine</i>	<i>Description</i>
<i>RUNVORSTAB</i>	iterates Digital DATCOM to produce the untrimmed aerodynamic lookup table; stand alone executable
<i>RUNDATCOM</i>	iterates VORSTAB to produce the untrimmed aerodynamic lookup table; stand alone executable
<i>SSLF</i>	calculates attitude and control variables to trim to 1-g flight
<i>SSLFCA</i>	calculates the secondary control effector deflection require for 1-g trim control allocation
<i>SSPUPO</i>	calculates attitude and control variables to perform a pull-up or push-over maneuver
<i>SSTF</i>	calculates attitude and control variables to perform a horizontal turn
<i>SSRP</i>	calculates attitude and control variables to perform a rolling maneuver
<i>TTB</i>	calculates the time to bank to a predefined bank angle
<i>QSTORM</i>	calculates the rotational pitch velocity given a predefined pitch acceleration and LoCE deflection
<i>SSLF2</i>	calculates attitude and control variables to define the trim point for later calculations
<i>LINAERO</i>	calculates the linear aerodynamic derivatives around the trim point from the aerodynamic lookup table
<i>TRIMAERO</i>	calculates the trimmed aerodynamic properties around the trim point
<i>STATSTAB</i>	calculates the static stability properties around the trim point
<i>DYNAMIC</i>	calculates the open and closed loop dynamic stability around the trim point for both the longitudinal and lateral/directional planes; additional control power required for the SAS function is also calculated

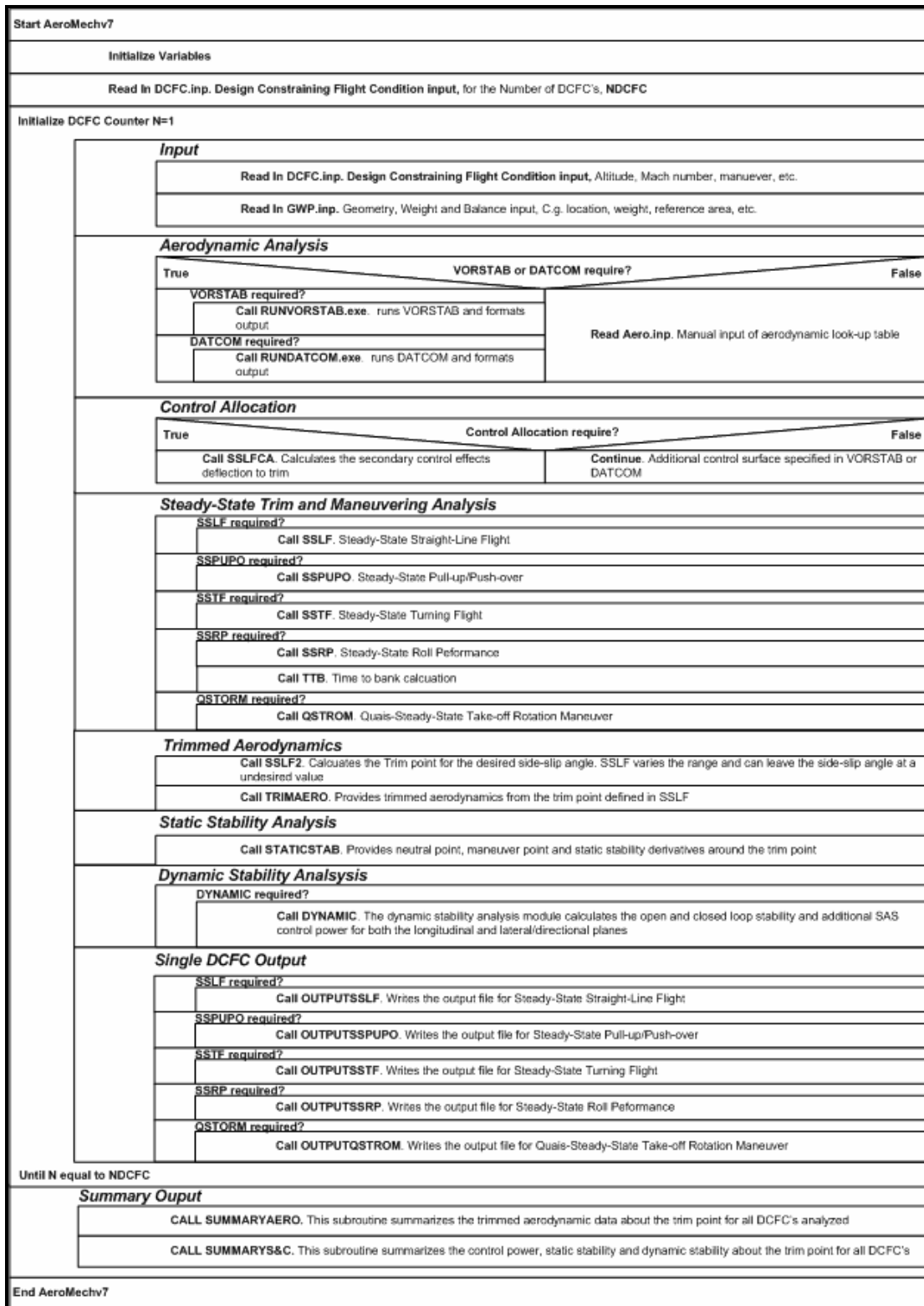


Figure 4.13: Final AeroMech Driver N/S Structogram

4.3 Future Work and Recommendations

The next step in the development of *AeroMech* is its integration into the synthesis system AVDS PrADO. This enables us to fully utilize the potential of this tool in a multi-disciplinary context. Once the current AeroMech version is integrated into AVDS PrADO, the following advancements to the individual modules are proposed:

1. Integration of the coupled 6DOF small perturbation equations of motion (derivation see Reference 1) into the dynamic stability and control module. This enables unrestricted dynamic stability analysis of asymmetric aircraft and/or symmetric aircraft in asymmetric flight conditions. This modification targets the *ILOUCS* subroutine initially provided by Abuzg²³.
2. Expand the steady-state analysis to allow the user to specify the control variables freely. This could include thrust vectoring and other significant variables contained in the mathematical models; overall, this would enable the designer to freely define six unknowns to solve for trim.
3. Include the VLM VORLAX into the aerodynamic method library to enable component analysis of asymmetric flight vehicles configurations and symmetric flight vehicles in asymmetric flight conditions, a capability VORSTAB can not handle to this point. In addition, the aerodynamic codes provided by AVDS PrADO need to be explored in the context of *AeroMech*.
4. Expand upon the coupled 6-DOF trim equations of motion by including additional conditions related to minimum trim drag, minimum CE deflections, etc., to arrive at an efficient control allocation scheme for the redundant control

surfaces. This could be accomplished by modifying the LOTS methodology to work directly with the *AeroMech* trim algorithm. Currently LOTS is limited to subsonic aircraft.

CHAPTER 5

APPLICATION OF *AEROMECH* IN CONCEPTUAL DESIGN

5.1 Stability and Control ‘Road Map’ to Conceptual Design

As explained in Chapter 1, Stability and Control is applied differently through the conceptual design (CD), preliminary design (PD) and detail design (DD) phases. It is important to ask the following question: What are the deliverables of the stability and control discipline during the conceptual design (CD) phase, during the preliminary design (PD) phase, and during the detail design (DD) phase? To effectively and efficiently enable stability and control to contribute during the conceptual design phase, a clear strategy must first be defined along with what must be delivered. As history teaches, the contribution of stability and control, particularly during the CD phase, does vary greatly between reduced order models to complete 6DOF models. In order to effectively apply stability and control to the sizing and initial (CD) evaluation of flight vehicle alternatives, it is required to arrive at a

1. **clear strategy leading to a transparent procedure.** Enabling an efficient integration of the stability and control discipline into the CD phase;
2. **generic mathematical framework** to consistently analyze and compare different flight vehicle alternatives;
3. **standardized results** to provide designers with complete and consistent information to base design decisions upon.

To meet these goals, a stability and control ‘deliverables road map’ has been developed to define a standardized set of stability and control deliverables during the CD phase. This standardization of stability and control deliverables clearly complements *AeroMech*’s generic mathematical frame. To develop such a set of standardized stability and control CD-level deliverables, an extensive literature review encompassing stability and control activities spanning conceptual design, preliminary design, detail design and flight testing was conducted. A bibliography of this review is presented in Appendix F.

Stability and control at the conceptual design level can be organized in several ways. From the literature review of stability and control techniques and having surveyed stability and control deliverables, the categorization below emerged which is the same organization used to classify the various approaches to stability and control in Chapter 2. Qualitative example figures systematically depict the stability and control deliverables required during the CD phase. The stability and control map takes into account the classification documented below:

1. **Initial control effector sizing** - Typically done through the use of volume coefficients and previous aircraft knowledge and experience.
2. **Identification of DCFC’s** - Before any analysis can be performed the designer must define which flight conditions are critical for performance and control effector sizing for the conceptual design.
3. **Aerodynamic prediction of stability and control derivatives** - The aerodynamic team concentrates on predicting lift, drag and pitching moment.

The stability and control team must predict control derivatives, static stability derivatives and dynamic stability derivatives.

4. **Trim and maneuver analysis** - Predicting the control surface size and/or deflections required for steady state trimmed and maneuvering flight in all axes.
5. **Trimmed Aerodynamics** - From the trim angle of attack and control surface deflections the trimmed aerodynamic data set is calculated taking into account the lift and drag effects of trim. This is passed forward to the static stability and dynamic stability analysis as well as to later performance calculations
6. **Static stability analysis** - comparing the static stability of the airframe to design requirements in all axes.
7. **Dynamic stability analysis** - Predicting the dynamic behavior of the vehicle for comparison to design and safety requirements in all axes. This includes both open and closed loop analysis, if required.
8. **Assessment of Control Power** - From the above analysis, the designer must decide if the controls configuration is adequate over the range of DCFC tested. If not, either the vehicle must be rebalanced (shift center of gravity), the control effectors must be enlarged or relocated (increase the lever arm). This sequence enables true control-configured vehicle (CCV) design capability.

Initial Sizing

As with the classical approaches described earlier, the LoCE, LaCE, and DiCE are initially sized using statistical volume coefficients obtained from a database of representative vehicles:

$$C_{ce} = \frac{S_{ce} l_{ce}}{S_{ref} c_{ref}} \quad \text{Eq. 5.1}$$

where, S_{ce} and l_{ce} are the area and distance from the control effector to the c.g. Once an appropriate volume coefficient has been selected as a start value from a data base, the location and size of the control effector is estimated. Examples of these statistical databases have been assembled in references like Roskam¹⁰, Torenbeek²⁸, Loftin²⁹, and Nicolai¹³.

Identification of DCFC's

“DCFC's are flight conditions with an overall governing effect on aircraft hardware sizing¹.” Recall from Chapter 1 that the goal of stability and control in the CD phase is to assess a configuration for (1) adequate control power, leading to CE sizing, (2) Trimmed Aerodynamics, leading to improved performance calculations and (3) Static and Dynamic Stability, leading to improved configuration sizing or FCS sizing. Given the typical short time frame of the CD phase, the DCFC's analyzed must be strategically selected to capture the most demanding conditions to meet the three goals of stability and control in conceptual design.

A distinction should be made between mission segments, DCFC's, and configuration settings (CS) / failure conditions (FC). A mission segment is simply a particular segment of the flight envelope such as Take-Off, Cruise, Approach, etc, where a DCFC is the specific maneuver within that mission segment. Within the DCFC's several configuration settings and failure conditions can be analyzed to check

for adequate control power, stability or proved trimmed aerodynamics. This is visualized below in Figure 5.1

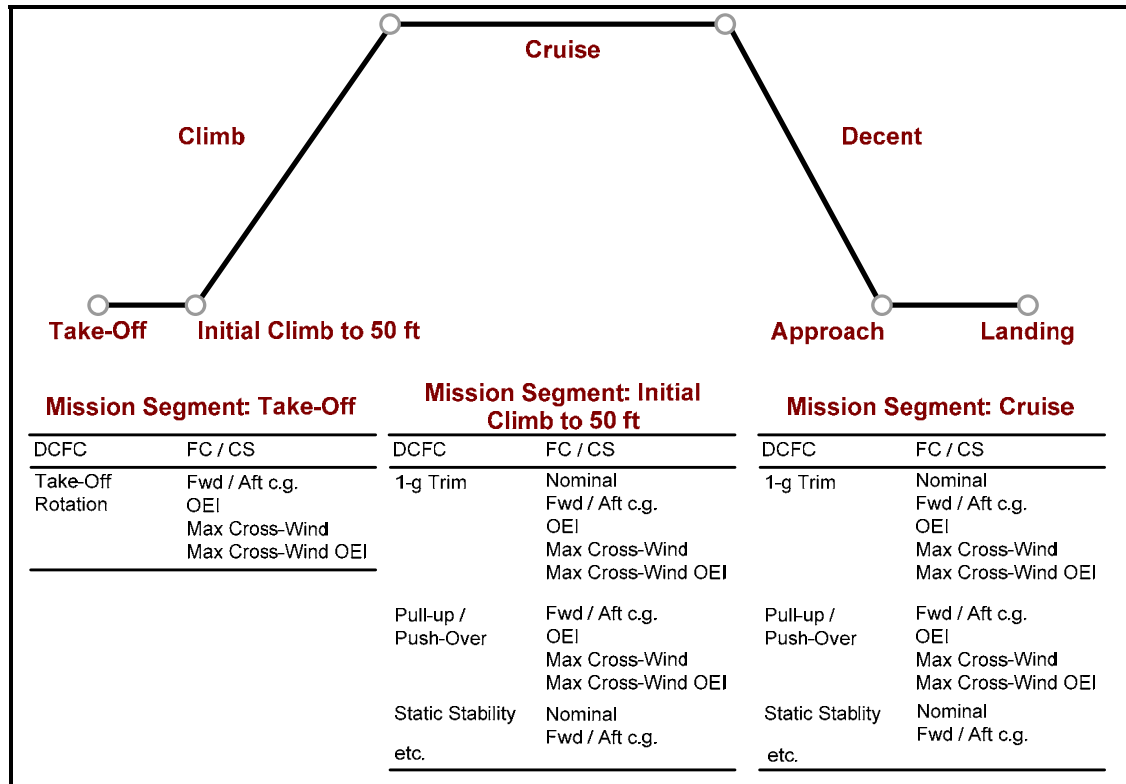


Figure 5.1: Generic mission profile demonstrating various mission segments, with the DCFC’s, failure conditions and configuration settings detailed for Take-off, Initial Climb and Cruise.

Chudoba¹ derives a set of generic DCFC’s for conceptual design which size the Longitudinal Control Effectors (LoCE), Lateral Control Effectors (LaCE) and Directional Control Effectors (DiCE). These flight conditions include conditions which are of importance for symmetric and asymmetric flight vehicle configurations and flight conditions. This organization has been modified here by DCFC’s for static stability, dynamic stability and trimmed aerodynamics. Each condition is designated as a 1st or 2nd level DCFC based on the relative importance to sizing the CE in question. The

DCFC's are summarized in Table 5.1 through 5.3 for control effector sizing (LoCE, DiCE and LaCE), static and dynamic stability and trimmed aerodynamics.

Table 5.1 DCFC's for Control Effector Sizing¹

DCFC	Failure Condition / Configuration setting / Mission Segment	Level
LOCE DCFC's		
1-g Trimmed Flight	No FC / Nominal c.g. locations / All applicable	1
	No FC / Fwd. and Aft C.G Clearance / All applicable	1
	No FC / Take-off configuration / high incidence, Minimum Control Speed, Initial Climb	1
	No FC / Landing configuration / high incidence, Minimum Control Speed, Approach	1
	Double hydraulic failure / Cruise configuration / All applicable	2
	No FC / Go-Around on 4 Engines Without Ground Effect / Take-off and Landing	2
	Trim Jam / Cruise configuration / All applicable	2
	Trim Tank Failures / Cruise and landing configuration / All applicable	2
	No FC / FCS for stability augmentation / All applicable	2
Rotation Capability	No FC / Nominal c.g. locations / Take-off	1
	No FC / Fwd. and Aft C.G Clearance / Take-off	1
	OEI / Fwd. and Aft C.G Clearance / Take-off	1
Pull-up / Push-over Load Factor Capability	No FC / Nominal c.g. locations / All applicable	1
	No FC / Fwd. and Aft c.g. locations / All applicable	1
	Double hydraulic failure / cruise configuration / All applicable	2
	Trim Jam / Cruise configuration / All applicable	2
	Trim Tank Failures / Cruise and landing configuration / All applicable	2
DiCE DCFC's		
1-g Trimmed side-slip	No FC / Nominal c.g. locations / All applicable	1
	2 Engines out / Landing and Take-Off configuration / Take-off, Landing	1
	2 Engines out / Landing and Take-Off configuration / MCS Initial Climb and Approach	1
	1 Engines out / Landing and Take-Off configuration / Max cross-wind, Landing and Take-off	1
	Double Hydraulic Failure / Landing and Take-Off configuration / Max cross-wind, Landing and Take-off	2
Turn Coordination (Adverse Yaw)	No FC / Cruise configuration / MCS Initial Climb and Approach	1
	1 Engine out / Cruise configuration / MCS Initial Climb and Approach	2
	Double Hydraulic Failure / Cruise configuration / MCS Low-speed flight	2
Horizontal Turn Load Factor Capability	No FC / Nominal c.g. locations / All applicable	1
	No FC / Fwd. and Aft c.g. locations / All applicable Approach	1
Inertial Coupling	No FC / Cruise configuration / High-speed Flight	2
LaCE DCFC's		
1-g Trimmed side-slip	No FC / Nominal c.g. locations / All applicable	1
	2 Engines out / Landing and Take-Off configuration / Take-off, Landing	1
	2 Engines out / Landing and Take-Off configuration / MCS Initial Climb and Approach	1
	1 Engines out / Landing and Take-Off configuration / Max cross-wind, Landing and Take-off	1
	Double Hydraulic Failure / Landing and Take-Off configuration / Max cross-wind, Landing and Take-off	2
Maximum Roll Rate	No FC / Cruise configuration / All applicable	1
	1 Engine out / Cruise configuration / MCS Initial Climb and Approach	2
	Double Hydraulic Failure / Cruise configuration / MCS Low-speed flight	2
Time to Bank	No FC / Cruise configuration / All applicable	1
	1 Engine out / Cruise configuration / MCS Initial Climb and Approach	2
	Double Hydraulic Failure / Cruise configuration / MCS Low-speed flight	2

Table 5.1 continued

Horizontal Turn Load Factor Capability	No FC / Nominal c.g. locations / All applicable	1
	No FC / Fwd. and Aft c.g. locations / All applicable Approach	1
Inertial Coupling	No FC / Cruise configuration / High-speed Flight	2

Table 5.2 DCFC's for Trimmed Aerodynamics, Static Stability and Dynamic Stability

DCFC	Failure Condition / Configuration setting / Mission Segment	Level
<i>Trimmed Aerodynamics</i>		
1-g Trimmed Flight	No FC / Nominal c.g. locations / All applicable	1
	No FC / Fwd. and Aft C.G Clearance / All applicable	1
	Trim Jam / Cruise configuration / All applicable	2
	Trim Tank Failures / Cruise and landing configuration / All applicable	2
	Double Hydraulic Failure / Landing and Take-Off configuration / Max cross-wind, Landing and Take-off	2
	1 Engine out / Cruise configuration / MCS Initial Climb and Approach	2
	Double Hydraulic Failure / Cruise configuration / MCS Low-speed flight	2
<i>Longitudinal Static and Dynamic Stability</i>		
1-g Trimmed side-slip	No FC / Nominal c.g. locations / All applicable	1
	No FC / Fwd. and Aft C.G Clearance / All applicable	1
	No FC / FCS for stability augmentation / All applicable	1
	Double Hydraulic Failure / Landing and Take-Off configuration / Max cross-wind, Landing and Take-off	2
	1 Engine out / Cruise configuration / MCS Initial Climb and Approach	2
	Double Hydraulic Failure / Cruise configuration / MCS Low-speed flight	2
<i>Lateral / Directional Static and Dynamic Stability</i>		
1-g Trimmed side-slip	No FC / Nominal c.g. locations / All applicable	1
	No FC / Fwd. and Aft C.G Clearance / All applicable	1
	No FC / FCS for stability augmentation / All applicable	1
	Double Hydraulic Failure / Landing and Take-Off configuration / Max cross-wind, Landing and Take-off	2
	1 Engine out / Cruise configuration / MCS Initial Climb and Approach	2
	Double Hydraulic Failure / Cruise configuration / MCS Low-speed flight	2

The following analysis is applied for the appropriate DCFC. The particular CE is sized dependent on the DCFC which demanded the largest control power. These design-critical DCFC's are said to size the control effectors.

Aerodynamic Prediction of Stability and Control Derivatives

The purpose of this step is to estimate the overall aerodynamic characteristics of the aircraft including the effects of faired and deflected control surfaces enabling the analysis of the a/c's overall stability and control properties. Aerodynamic prediction

techniques can range from hand-book component build-up methods to full Navier-Stokes CFD analysis. In the context of *AeroMech* and our current focus on the CD phase, the estimation techniques selected are the non-linear vortex lattice method (VLM) VORSTAB⁵, the semi-empirical code Digital DATCOM⁷ and the linear vortex lattice method VORLAX¹⁸. These CD-compatible codes are utilized to build the initially untrimmed aerodynamic database.

Trim and Maneuver Analysis

The trim and maneuver analysis determines the amount of control power required to stabilize and control the aircraft and compares this to the amount available with the current flight vehicle arrangement. In particular, this task is accomplished by comparing the CE deflections required to the CE deflection range available. Based on the 5 basic maneuvers described in Chapter 3, the following analysis needs to be performed for all applicable DCFC's to explore the aircrafts control power (Table 5.3 and Table 5.4)

Table 5.3 Trim Deliverables Map

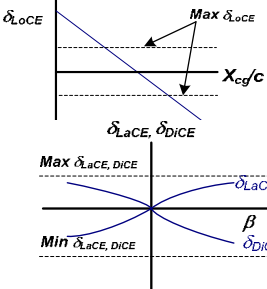
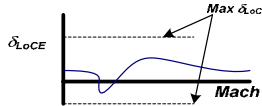
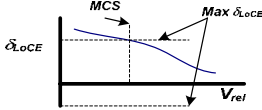
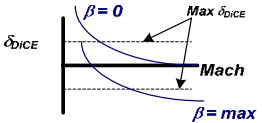
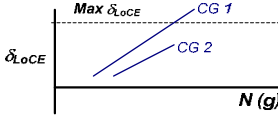
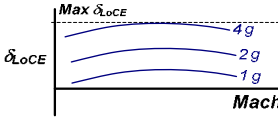
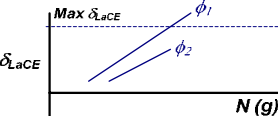
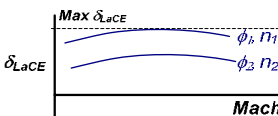
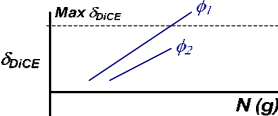
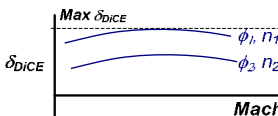
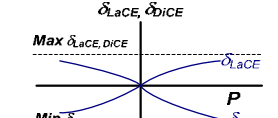
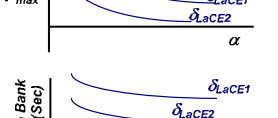
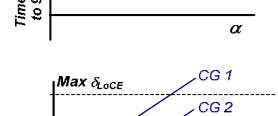
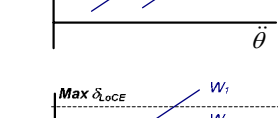
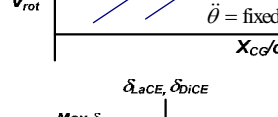
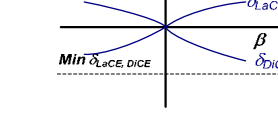
Stability and Control Analysis	Recommended Output Visualization		Comments		
Single Flight Condition Figure	Ref	Flight Envelope Figure	Ref		
Steady-State Strait-Line Flight	 <p>Graph showing δ_{LoCE} vs X_{cg}/c. The curve starts at $Max \delta_{LoCE}$ and decreases. Below the graph, curves for δ_{LaCE} and δ_{DiCE} are shown, with $Max \delta_{LaCE, DiCE}$ and $Min \delta_{LaCE, DiCE}$ indicated. A β curve is also shown.</p>	34	 <p>Graph showing δ_{LoCE} vs $Mach$. The curve starts at $Max \delta_{LoCE}$ and decreases.</p>	34	Used for both control power and defining the trim point for later stability analysis
Minimum control Speed	 <p>Graph showing δ_{LoCE} vs V_{rel}. The curve starts at $Max \delta_{LoCE}$ and decreases. A vertical dashed line indicates MCS.</p>	34	 <p>Graph showing δ_{DiCE} vs $Mach$. The curve starts at $Max \delta_{DiCE}$ and decreases. Two curves are shown for $\beta = 0$ and $\beta = max$.</p>	35	The minimum control speed may be lower than stall. Ground min control speed may be a constraint, detailed landing gear data required

Table 5.4 Maneuvering Deliverables Map

Stability and Control Analysis	Recommended Output Visualization		Comments	
	Single Flight Condition Figure	Ref		Flight Envelope Figure
Steady State Pull-up / Push Over		34		34
	Steady State Turn Performance		34	
Steady State Roll Performance and Turn Coordination			34	
	Max Roll Rate		34	
Time To Bank			34	
	Take-off Rotation		34	In this case the V_rot desired is fixed and the rotational acceleration is varied
		34		
Take-off Rotation		34	In this case the LoCE and pitch acceleration is fix and the V_rot is solved for. Both approaches are acceptable.	
		34		
Take-off Rotation		34	Could be used to approximate the ground min control speed.	
		34		

As these figures qualitatively show, the control effectors are sized by examining the available control power required to perform the maneuvers required. If the control power required exceeds the maximum control power available, then the CE must be altered such as to physically increase the control forces and subsequently moments.

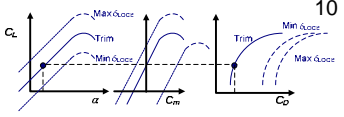
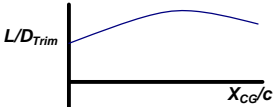
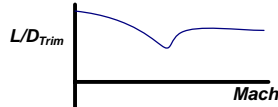
Important issues to note include:

1. The steady-state straight-line flight analysis both demonstrates control power and defines the trim point for trimmed aerodynamics, static stability, and dynamic stability.
2. Coordinated turn entry can size the DiCE during low speed, high angle-of-attack flight³⁰. This is a highly dynamic maneuver and is approximated through examining the control power available by the DiCE to overcome adverse yaw during a steady-state roll maneuver. Advanced simulation at a later stage is required to accurately capture this maneuver.
3. Ground minimum control speed requires detailed landing gear dynamics which may or may not be available during the conceptual design phase. This is approximated through examining the take-off run with side-slip.
4. If a SAS is utilized for generating artificial dynamic stability, increased physical control power is required by the CEs. This is addressed in the dynamic stability and control section.
5. A control allocation logic is required during the CD phase (e.g., ‘ad hoc’ method, minimum longitudinal trim drag solution logic LOTS). No graphical visualization of such scheduling has been developed at this time.

Trimmed Aerodynamics

The trimmed aerodynamic dataset presents the only acceptable representation of the true characteristics of an aircraft by taking the lift reduction and drag increases typically associated with trimming the aircraft into account. These effects can be visualized as shown qualitatively in Table 5.5.

Table 5.5 Trimmed Aerodynamics Map

Stability and Control Analysis	Recommended Output Visualization		Comments
	Single Flight Condition Figure ref	Flight Envelope Figure ref	
Trimmed vs. Clean, Lift, drag and Pitching moment		10	Used to demonstrate the effects of trim on lift, angle of attack, and drag
Trimmed L/D			21 Used to demonstrate the effects of trimmed L/D which relaxed static stability and over the range of operational mach number

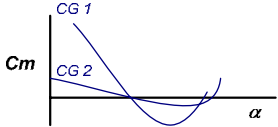
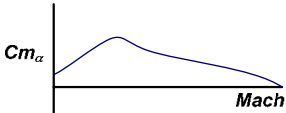
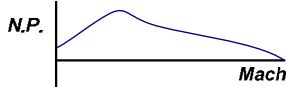
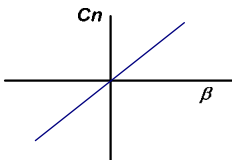
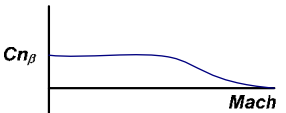
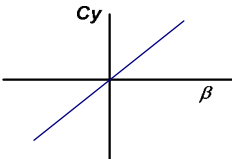
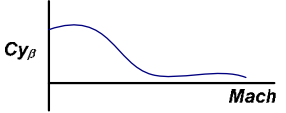
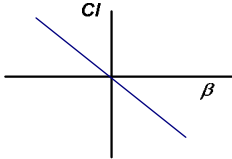
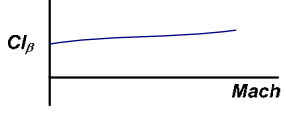
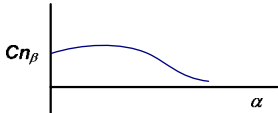
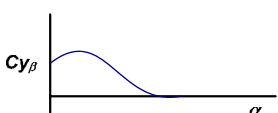
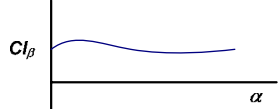
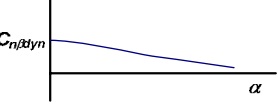
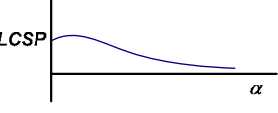
The above deliverables define the aerodynamic dataset required which is trimmed around the pitch, yaw and roll axes. This trimmed dataset represents the input data required for all successive static stability, dynamic stability, and performance calculations.

Static Stability Analysis

Static stability characterizes the vehicles tendencies to return to a pre-defined equilibrium state after being perturbed from the initial trim state. For example, if the vehicle is perturbed in pitch, the aircraft is required to produce a restoring moment opposing the motion due to the perturbation; alternatively, the a/c may not generate any opposing moment, or it may even generate a diverging moment in the same direction of

the perturbation. These three options generally represent the three states being statically stable, neutrally stable, and statically unstable, respectively. The flight vehicle static stability requirements do not necessarily require that the vehicle be inherently statically stable. The vehicle could be designed to have even neutral to unstable inherent stability level for either flight performance or maneuverability reasons as long as a flight control system (FCS) is generating an overall statically stable behavior. The typical static stability requirements have been defined in Chapter 2, Table 2.2. A qualitative visualization of these parameters is presented in Table 5.6.

Table 5.6 Static Stability Analysis Map

Stability and Control Analysis	Recommended Output Visualization		Comments	
	Single Flight Condition Figure	Ref		Flight Envelope Figure
Longitudinal Static Stability				For sizing of the stabilizing surfaces (i.e. horizontal tail)
				
Lateral Static Stability				For sizing vertical surface (i.e. vertical tail)
				
				
		10		Fight aircraft typically have reduced lateral static stability at high angles of attack
		10		
		10		
		13		shows aircraft tendency not motion
		13		shows aircraft tendency not motion

Static stability analysis typically sizes the combined CE surfaces (stability and control surfaces)³¹. For example, if on a TAC the longitudinal or directional static stability level available is unsatisfactory, then it is possible to increase the tail volume by either moving the surface aft or by enlarging the surface itself while keeping the moment arm constant. For a FWC the problem is slightly more complicated. To increase static longitudinal stability, wing sweep can be increased and/or wing twist can be increased. Both design variables have the effect of creating a longer lever arm from the tip of the wing, where the down force for static longitudinal stability is typically produced. However, these modifications will adversely influence the aerodynamic performance of the aircraft.

It is important to note that the descriptors $LCSP$ and $C_{n\beta dyn}$ are considered reduced order model approximations for the dynamic behavior of the flight vehicle. Still, these parameters are of utmost importance during the CD phase in order to demonstrate the tendency of the aircraft to diverge in roll or yaw. Clearly, those parameters are not meant to replace the flight dynamicist's accurate dynamic models during the later PD and DD phases. For these reasons they are considered static stability parameters.

Dynamic Stability and Control Analysis

Dynamic stability defines the motion of the aircraft after being perturbed from the trim point. Static stability alone cannot define the stability of an aircraft. An aircraft can be statically stable but dynamic unstable if the restoring moment continues to grow

after each oscillation. Dependent upon the mission and the DCFC considered, varying levels of dynamic stability are required. These levels are usually defined by the MIL-Spec requirements³² which give limits to the behavior of the typical dynamic modes of an aircraft, and they are finally evaluated in flight using the Cooper-Harper rating scale³³.

Dynamic stability and control analysis techniques can take on various forms, from reduced order models, root locus methods, to non-linear flight simulation. During the CD phase, there is a chronic shortage of data and time available, both facts usually preventing the utilization of more elaborate dynamic methods. Therefore, the CD phase usually utilizes reduced order models which are able to correctly characterize the dynamic behavior of the flight vehicle, thus enabling the early comparison of the flight vehicle dynamic characteristic with design and certification requirements. Clearly, the modeling of the dynamic behavior of more complex flight maneuvers requires more advanced flight simulations during the PD phase. Table 5.7 and Table 5.8 present the output visualization of the classical stability modes, for both open and closed loop aircraft, as well as additional control power requirements for a stability augmented aircraft.

Table 5.7 Longitudinal Dynamic Stability and Control Deliverables Map

Stability and Control Analysis	Recommended Output Visualization		Comments
	Single Flight Condition Figure	Flight Envelope Figure	
<i>Longitudinal Open Loop</i>			
Phugoid			34
<i>Longitudinal Close Loop (SAS)</i>			
Short Period			34
		5	
Additional Control Power			34

Table 5.8 Lateral/Directional Dynamic Stability and Control Deliverables Map

Stability and Control Analysis	Recommended Output Visualization		Comments
	Single Flight Condition Figure	Flight Envelope Figure	
Lateral Open Loop			
Roll			34
Spiral			34
Dutch Roll			
Lateral Closed Loop (SAS)			
Roll			34
Spiral			34
Dutch Roll			34
Additional Control Power			35
			36

The dynamic stability and control analysis focuses on the vehicle motion-behavior and is used to size the stabilizing surfaces to increase aerodynamic damping and stiffness or size a stability augmentation system (SAS) to artificially increase damping and stiffness. Clearly, the SAS function places additional control power demands on the control surfaces themselves.

Assessment of Control Power

The final portion of the analysis is to draw conclusions from the previous analysis to resize the control effectors and/or stabilizing surfaces, or the total vehicle to better meet the design requirements. Nicolai¹³ presents guidelines (Table 2.3) of how to iterate the design based on stability and control analysis to arrive at a feasible aircraft. These guidelines are for systematic aircraft and are centered on the tail-aft configuration (TAC).

This road map presents a standard visualization to aid the designer in both the use of *AeroMech* and the application of stability and control in conceptual design. The stability and control map is demonstrated, along with *AeroMech*, through the Northrop YB-49 flying wing validation example throughout the following chapter.

5.2 Validation Case Study: Northrop YB-49 Flying Wing

The Northrop YB-49 flying wing configuration (FWC) validation case study has been selected to demonstrate the application, overall correctness and accuracy of the data generated with *AeroMech*. This is accomplished by (a) utilizing *AeroMech* such as to generate stability and control deliverables according to the stability and control deliverables guideline, and (b) by validating *AeroMech* results with available YB-49 engineering and flight test data. The analysis here is organized such to provide useful feed-back to conceptual designers for the 3 main purposes of stability and control in conceptual design, (1) control effector sizing, (2) trimmed aerodynamics, (3) static and dynamic stability. These three components are demonstrated through the YB-49 and design feed-back is presented in the context of future flying wing aircraft.

5.2.1 Northrop YB-49 Flying Wing Development History

The Northrop YB-49 flying wing is an intriguing but in particular demanding design case study for *AeroMech*. This fact is particularly true since the stability and control discipline plays a particularly important role when assessing the overall flight performance and safety of the flying wing configuration (FWC) compared to the highly evolved tail-aft configuration (TAC). FWC-related design complications like control allocation, relaxed static stability in the pitch and yaw axes, the merging of all primary control surfaces into the wing, these and other design challenges result in the clear demand for advanced stability and control sizing techniques.

A great deal of controversy surrounds the FWC, publicly known as the 'Foa-Sears debate'. This debate centers around the question which configuration is superior -

the tail-aft configuration (TAC) or the flying wing configuration (FWC). The opinion prevails that the FWC is aerodynamically and structurally superior when compared with the TAC due to the overall ‘cleanness’ of the FWC. For the FWC, the absence of the fuselage and empennage tends to reduce certain drag terms. In addition, the distribution of the payload along the lifting line reduces primarily wing bending moments, resulting in a lighter airframe compared to concentrating the payload at the center of the bending beam (wing) as seen with all TACs. However, the design challenges seen with the flying wing are not aerodynamic or structural in nature, but are stability and control issues.

In order to trim a naturally stable flying wing in pitch, an upward elevon control surface deflection is required, thereby directly decreasing wing lift while increasing trim drag due to the short coupled LoCEs. Trim drag is as well seen with TAC, but the shorter lever arm for the LoCEs to the center of gravity creates a much larger reduction in lift and increased trim drag on the FWC relative to the TAC. The initiation of aircraft pitch stability and control on the wing itself disrupts both the chord wise and span wise lift distribution, thereby reducing the overall aerodynamic efficiency of the FWC. Askhenas²¹ contends that the key to unlocking the aerodynamic efficiency of the FWC is to operate the aircraft longitudinally static neutral to static unstable, in order to reduce the LoCE deflections required for trim, thereby retaining the performance-optimal spanwise and chordwise lift distributions. This increased aerodynamic efficiency comes at the price of reduced static and dynamic stability; thus, the aircraft must rely on a stability augmentation system (SAS).

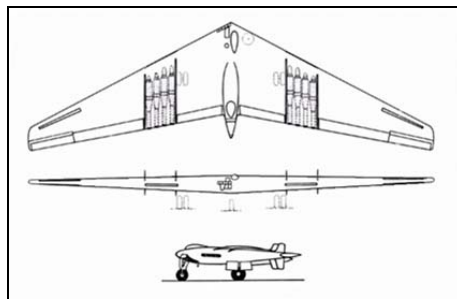
For the purposes of this study, the YB-49 is a design case study for two reasons. First, the YB-49 will be examined for software validation purposes, by comparing the simulated results generated by AeroMech to original Northrop YB-49 engineering and flight test results. Second, the YB-49 is an ideal research case study for exploring the effects of relaxed longitudinal static stability on overall a/c take-off performance, cruise performance, low-speed flight and approach performance, maneuver performance, and static and dynamic stability. The YB-49 mission profile and the maximum control surface deflections are extracted from References 19, 20, 21, 37 and 38. The dynamic stability requirements are provided by MIL-F-8785C³².

5.2.2. Baseline Configuration

The baseline configuration for this study is taken from References 19, 20, 21, 37 and 38. A three view of the YB-49 along with a brief description of the vehicle is shown in Table 5.9.

Table 5.9 YB-49 Specifications and Three-View Drawing

<i>Specification</i> ²¹	<i>Three-View Drawing</i> ³⁷
Span	172 ft
Wing Area	4,000 ft ²
MAC	25.24 ft
Airfoil Section	NACA 64A019 (root) NACA 64A018 (tip)
Max T-O Weight	196,000 lb
Max speed	430 kt
Range	3,000 to 4000 nm
Propulsion	8 Allison J-35-A-15 turbojets
Thrust	4,000 lbs each (SL)



The controls of the YB-49 consist of a trim flaps, elevons, landing flaps, and wing slots. The purpose and locations of these surfaces are shown in Figure 5.2.

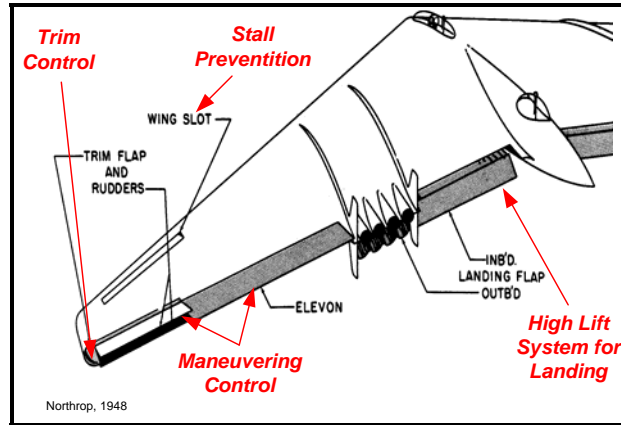


Figure 5.2: Layout of the primary and secondary controls of the YB-49 flying wing.

5.2.3. Design Constraining Flight Conditions (DCFC)

The DCFCs chosen represent design-critical corner points in the basic mission profile of the flight vehicle. The mission profile consists of the take-off, cruise, low-speed flight and the approach phase. Table 5.10 outlines the DCFC's typically analyzed at the particular mission segment along with a description conditions.

Table 5.10 YB-49 DCFC Summary

DCFC	Mission Segment	Configuration Setting	Failure Condition	Level
Control Effector Sizing				
<i>LOCE Sizing</i>				
1-g Trimmed Flight (SAS on and off)	Low-speed flight, Approach	Various c.g. locations, Flaps and gear down.	No Failures	1
	Cruise	Various c.g. Locations, Flaps and gear up.	No Failures	1
Rotation Capability	Take-off	Various c.g. locations, Flaps and gear down.	No Failures	1
Pull-up / Push-over Load Factor Capability	Low-speed flight, Approach	Various c.g. locations, Flaps and gear down.	No Failures	1
	Cruise	Various c.g. Locations, Flaps and gear up.	No Failures	1
<i>DiCE Sizing</i>				
1-g Trimmed side-slip (SAS on and off)	Low-speed flight, Approach	Various c.g. locations, Flaps and gear down.	No Failures	1
	Cruise	Various c.g. Locations, Flaps and gear up.	No Failures	1
Turn Coordination (Adverse Yaw)	Low-speed flight, Approach	Various c.g. locations, Flaps and gear down.	No Failures	1
Horizontal Turn Load Factor Capability	Low-speed flight, Approach	Various c.g. locations, Flaps and gear down.	No Failures	1
	Cruise	Various c.g. Locations, Flaps and gear up.	No Failures	1
<i>LaCE Sizing</i>				
1-g Trimmed side-slip (SAS on and off)	Low-speed flight, Approach	Various c.g. locations, Flaps and gear down.	No Failures	1
	Cruise	Various c.g. Locations, Flaps and gear up.	No Failures	1
Maximum Roll Rate	Low-speed flight, Approach	Various c.g. locations, Flaps and gear down.	No Failures	1
	Cruise	Various c.g. Locations, Flaps and gear up.	No Failures	1
Time to Bank	Low-speed flight, Approach	Various c.g. locations, Flaps and gear down.	No Failures	1
	Cruise	Various c.g. Locations, Flaps and gear up.	No Failures	1
Trimmed Aerodynamics				
1-g Trimmed Flight	Low-speed flight, Approach	Various c.g. locations, Flaps and gear down.	No Failures	1
	Cruise	Various c.g. Locations, Flaps and gear up.	No Failures	1
Static and Dynamic Stability				
<i>Longitudinal</i>				
1-g Trimmed side-slip (SAS on and off)	Low-speed flight, Approach	Various c.g. locations, Flaps and gear down. SAS on and off	No Failures	1
	Cruise	Various c.g. locations, Flaps and gear down. SAS on and off	No Failures	1
<i>Lateral / Directional</i>				
1-g Trimmed side-slip (SAS on and off)	Low-speed flight, Approach	Various c.g. locations, Flaps and gear down. SAS on and off	No Failures	1
	Cruise	Various c.g. locations, Flaps and gear down. SAS on and off	No Failures	1

5.2.4. Analysis of the YB-49 Using AeroMech

5.2.4.1. Aircraft and DCFC Input for AeroMech

For the DCFCs tested each mission segment, the *AeroMech* input variables are summarized in Table 5.11. This input is used for each DCFC according to the specified mission segment.

Table 5.11 Flight Condition Input for the YB-49 for the Required Mission Segments

Mission Segment	Flight Condition Variables						
	Load Factors	Air Speed		Altitude	Flight Path Angle	Side-Slip angle	Instantaneous Pitch acceleration
	(g's)	(ft/s)	(M)	(ft)	(deg)	(deg)	(deg/s ²)
Take-Off	-	150 (89 kts)	0.13	Sea-Level	0.0	0.0	6.0
Initial Climb	1.0	288 (170 kts)	0.13	Sea-Level	3.0	-20.0 to 20.0	-
Cruise	0.6 to 2.05	472 (280 kts)	0.48	30,000	0.0	-20 to 20.0	-
Low-Speed Flight	0.6 to 2.05	192 (114 kts)	0.18	10,000	0.0	-20 to 20.0	-
Approach	0.6 to 2.05	145 (86 kts)	0.13	Sea-Level	-3.0	-20 to 20.0	-

The weight and balance data is taken from References 21 and 37. Since the YB-49 moments of inertia are only available for a single aircraft weight, it is required to estimate the variation of the moments of inertia with weight using the radius of gyration concept. In general, this assumes that every aircraft has a single radius of gyration which relates the weight of the aircraft to the moments of inertia through the following relationships¹⁰.

$$I_x = b^2 W (\bar{R}_x)^2 / 4g \quad \text{Eq. 5.1}$$

$$I_y = L^2 W (\bar{R}_y)^2 / 4g \quad \text{Eq. 5.2}$$

$$I_z = e^2 W (\bar{R}_z)^2 / 4g \quad \text{Eq. 5.3}$$

where L is the length of the aircraft and e is defined as

$$e = \frac{b + L}{2} \quad \text{Eq. 5.1}$$

Utilizing the moments of inertia and weights provided by Reference 21, the radius of gyration has been estimated for the calculation of the moments of inertia at a specified weight. This technique cannot be used to calculate the product moment of inertia I_{xz} , since it depends on the vertical mass distribution. However, since the mass is predominantly evenly distributed along the center line of the YB-49, this fact justifies neglecting this term. Due to the aircraft symmetry the I_{xy} , and I_{yz} product moments of inertias have also been neglected.

The weight and balance input for this analysis is presented in Table 5.9 and is organized by mission segment. Each DCFC in these mission segments utilize this input data

Table 5.12 Weight and Balance Input for the YB-49 for the Required Mission Segments

Mission Segment	Weight and Balance					
	Weight	CG	lx	ly	lz	lxz
	(lbs)	(%MAC)	(slug/ft ³) x10 ⁵			
Take-Off	115,000	21.0 to 30.0	3.350	0.717	3.710	0.00
	176,000	21.0 to 30.0	5.580	1.190	6.156	0.00
Initial Climb	176,000	21.0 to 30.0	5.580	1.190	6.156	0.00
	Cruise	150,000	21.0 to 30.0	4.310	0.920	4.760
Low-Speed Flight	125,000	21.0 to 30.0	3.590	0.760	3.960	0.00
Approach	120,000	21.0 to 30.0	3.440	0.740	3.810	0.00

The configuration settings were taken from both flight test reports²¹ and the YB-49 pilots hand book³⁸ for these mission segments. This data is summarized in Table

5.10 organized by mission segment. Each DCFC within these mission segments utilize this input data.

Table 5.13 Configuration Input for the YB-49 for the Required Mission Segments

Mission Segment	Aircraft Configuration and Thrust Available					
	Landing Flap	Trim Flap	L.G	L.G. Distance from 21.0% MAC		Thrust Available
	(-)	(-)	(-)	X (ft)	Z (ft)	(lbs)
Take-Off	0.0	0.0	Yes	3.51	7.59	4000 (x8)
	0.0	0.0	Yes	3.51	7.59	4000 (x8)
Initial Climb	0.0	0.0	No	-	-	4000 (x8)
Cruise	0.0	See control allocation	No	-	-	4000 (x8)
Low-Speed Flight	16.0	See control allocation	Yes	-	-	4000 (x8)
Approach	16.0	See control allocation	Yes	-	-	4000 (x8)

5.2.4.2. Control Allocation

The basic control configuration for the flying wing consists of an elevon for pitch and roll control (LoCE and LaCE), a drag rudder for directional control (DiCE), and a trim flap for both trim in pitch and roll (LoCE and LaCE). Control allocation exists during flight between the trim and the elevon as described below. However, during the take-off ground run the trim flap is set to between 0.0 to 3.0 degs nose up³⁸.

LONGITUDINAL CONTROL ALLOCATION DURING FLIGHT

The YB-49 has two control effectors for pitch being the elevon and trim flap on the outer wing panel. According to the YB-49's Pilots Manual³⁸, the basic control allocation concept is that the trim flap (the outer surface) is used for trim control and the elevon (the inner surface) is used for maneuver control (Figure 5.3). This links the trim flaps to the trim wheel and the elevons to the control yoke in the cockpit.

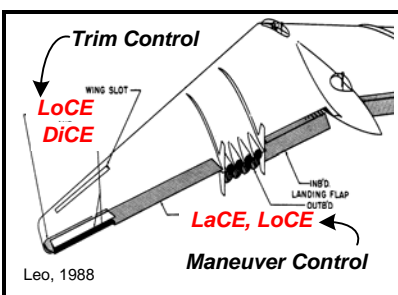


Figure 5.3: Longitudinal control allocation for the YB-49 during cruising flight.

LATERAL CONTROL ALLOCATION DURING FIGHT

As noted in the YB-49's Pilot Manual³⁸, the trim flap can also be deflected differentially for the trim in the lateral plane. However, to simplify the present analysis this function has been omitted and the elevon is used as both the trimming and maneuvering LaCE.

5.2.4.3. Creation of the Untrimmed Aerodynamic Database

For the DCFC's and Mission segments outlined, the non-linear VLM VORSTAB was utilized along with manual input to construct the untrimmed aerodynamic look-up table for *AeroMech*. The executable RUNVORSTAB.exe was utilized to incorporate the following aerodynamic effects.

1. Clean aerodynamics, zero control surface deflections
2. All control force and moment increments (CE deflections)
3. Inclusion of L.G. effects taken from Reference 21

For more information about the methods of VORSTAB automation in RUNVORSTAB.exe see Appendix C.

The effects of the drag rudders cannot be currently analyzed by VORSTAB and thus the control force and moment increment data was input manually into the

Aerodynamic look-up table from wind-tunnel results summarized in Reference 21. While novel DiCE aerodynamic data was readily available for this analysis, the aerodynamic information required could be calculate from handbook methods provided by Roskam³⁶.

The VORSTAB YB-49 wire frame model is visualized with *Tecplot*, see Figure 5.4.

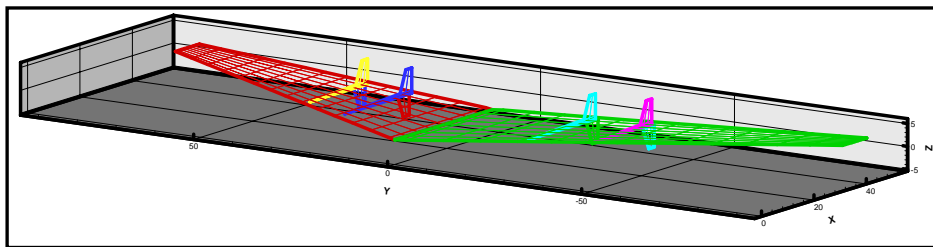


Figure 5.4: YB-49 VORSTAB Model Visualization

For each Mach number and c.g. location examined in this analysis a separate untrimmed aerodynamic look-up table was required.

5.2.4.4. Control Power Analysis for CE Sizing

The primary control effectors of an aircraft must be sized to provide trim, maneuver and stability augmentation (if a SAS is required) throughout the flight envelope. For the YB-49 the DCFC's defined previously are analyzed here to (1) examine the effects of relaxed static stability on LoCE, LaCE and DiCE sizing and (2) to validate the AeroMech steady-state trim and maneuver algorithms.

LONGITUDINAL CONTROL EFFECTOR SIZING

To analyze the effects of relaxed static stability on the LoCE the DCFC's of 1-g trim (with and with out SAS), Take-Off rotation, Pull-up / Push-over, and horizontal

turn are analyzed across the basic mission segments of Take-Off, Initial Climb, Cruise, Low-speed flight and Approach.

DCFC: 1-g Trim (SAS on and Off)

The YB-49 utilizes the trim flaps to maintain trimmed flight and thus have been defined as the primary LoCE during the Cruise, Low-Speed Flight, and Approach mission segments for this DCFC.

To validate AeroMech, the results for this DCFC are compared to flight test results¹⁹ during the cruise and low-speed flight mission segments. These are compared in Figure 5.5.

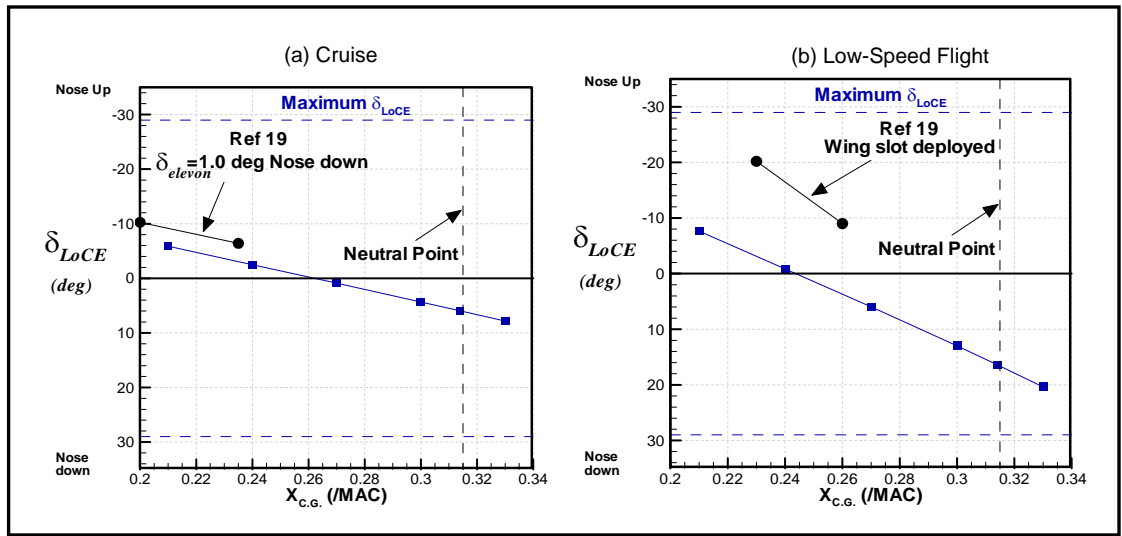


Figure 5.5: Comparison of YB-49 AeroMech 1-g Trim results with flight test report data¹⁹ for the cruise and low-Speed Flight Segments

As the c.g. shifts aft both the *AeroMech* and flight results show a similar change in LoCE deflection, however, a discrepancy exists in the total LoCE deflection. During the cruise flight test¹⁹ the trim flap was set too high for the flight condition and thus the elevon was deflected downward to trim to this condition. Hence, the AeroMech trim

flap deflections are slightly lower relative to the flight test results. For Low-Speed flight, AeroMech does not model the wing slot (Figure 5.6).

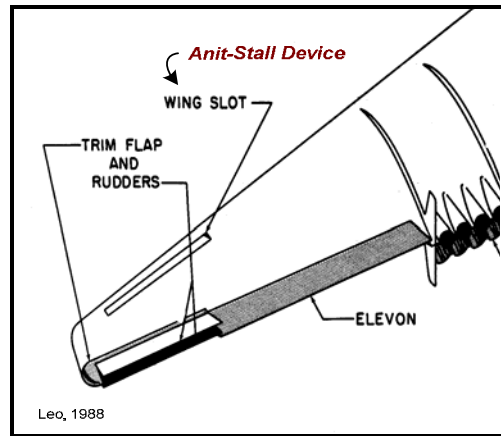


Figure 5.6: YB-49 wing slot anti-stall device is deployed with the landing gear

The wing slot is an anti-stall device which would produce an increase noise down moment. Thus, a larger trim flap deflection would be required to trim. These discrepancies aside the AeroMech results demonstrate physical correctness for this DCFC.

To explore the effects of relaxed static stability the c.g. location was varied from 21% to 33% MAC for all of the mission segments. The cruise, low-speed flight and approach mission segments utilize the trim flap as the primary LoCE to trim and the required deflections are shown in Figure 5.7. The additional control power required from a SAS is shown for standard maximum disturbances of $\Delta\alpha = \pm 5$ deg and $\Delta q = \pm 10$ deg/s, taken from Roskam¹⁰. The gain settings were selected to meet Mil-Spec³² level 1 longitudinal dynamic stability requirements. A discussion of the dynamic stability of the YB-49 is presented in Section 5.2.4.7.

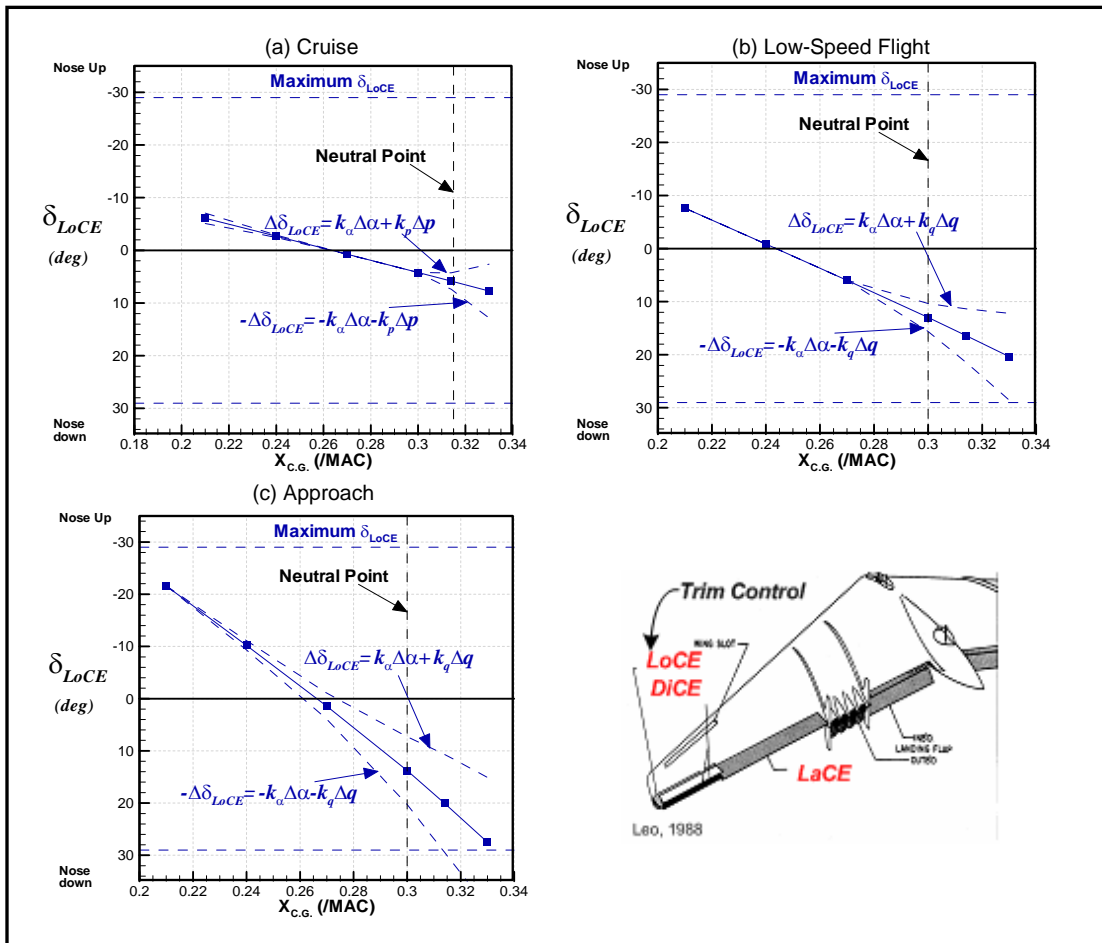


Figure 5.7: Effects of relaxed longitudinal static stability on the required LoCE (trim flap) trim deflection during cruise, low-speed flight and approach

As shown in Figure 5.7 the YB-49 possesses adequate longitudinal control power for these three mission segments while the aircraft is flown statically stable in the longitudinal plane (i.e. the c.g. is ahead of the neutral point). When the aircraft is flown statically unstable in the longitudinal plane the control saturation can occur due to additional control power required for stability augmentation during the approach segment.

From the validation and analysis of this DCFC the AeroMech results prove to be a valid representation and demonstrate no need for additional control power as the

longitudinal static stability is relaxed for all of the mission segments, with the exception of a c.g. of 33% MAC during the Approach mission segment.

DCFC: Take-Off Rotation Maneuver

The Take-Off rotation DCFC was analyzed to calculate the take-off rotation speed with the elevons deflected upward at 20 deg (maximum deflection) to command an instantaneous pitching acceleration of 6 deg/s. This DCFC was also analyzed with two gross take-off weights of 115,000 lbs and 175,000 lbs with the c.g. location ranging from 21% to 33% MAC. The results from the take-off rotation maneuver are presented in Figure 5.8.

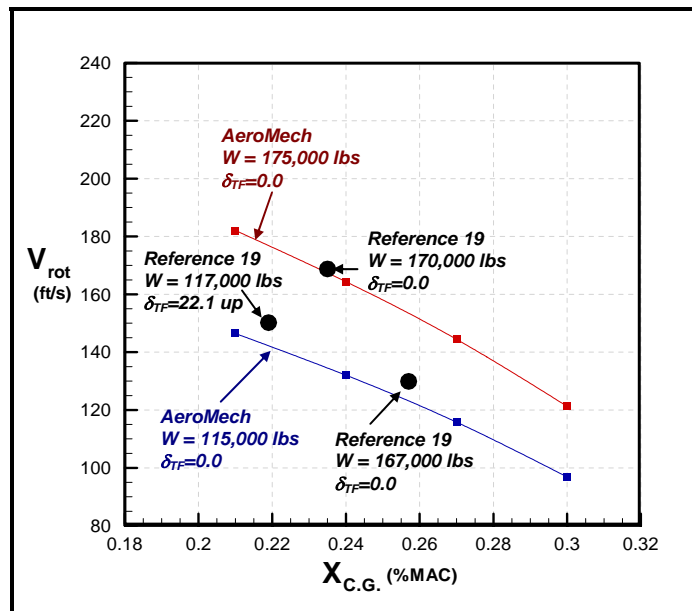


Figure 5.8: Effects of Relaxed longitudinal Static Stability during the take-off rotation maneuver for the YB-49

This maneuver is analyzed for the maximum and minimum take-off gross weights tested in Reference 19 with zero trim flap deflection ($\delta_{TF} = 0.0$ deg) to show the extremes of the YB-49's take-off rotation capability. The reference data available is

rather scattered due to the variation of trim flap settings selected during flight testing for different gross weights and c.g. locations. These inconsistencies aside, the *AeroMech* results agree well with flight test data.

AeroMech shows a reduction of the take-off rotation velocity as the center of gravity position is shifted aft. Moving the c.g. longitudinally initiates two primary effects, where the first effect is dominating. First, the aft c.g. shift reduces the load on the nose gear (this reduces the opposing moment produced by the main landing gear), but secondly shortens at the same time the moment arm between the aerodynamic center (ac) of the LoCE to the c.g. The overall effect is that an aft c.g. shift reduces the rotation velocity required. Relaxed static longitudinal stability reduces the rotation velocity while decreasing the dynamic stability once airborne; however, adequate control power exists to artificially stabilize the aircraft once airborne as shown in the 1-g trim DCFC for the initial climb. Relaxed static stability may not be necessary for this flight condition as no problems with excess rotation speeds were discovered with *AeroMech* or flight test.

DCFC: Pull-Up / Push-Over Maneuver

The YB-49 utilizes the elevons exclusively to perform the longitudinal pull-up / push over maneuver, therefore the elevon is specified as the primary LoCE.

To validate the *AeroMech* results for this DCFC the results from the Low-Speed Flight mission segment is compared to flight test results. These are compared in Figure 5.9.

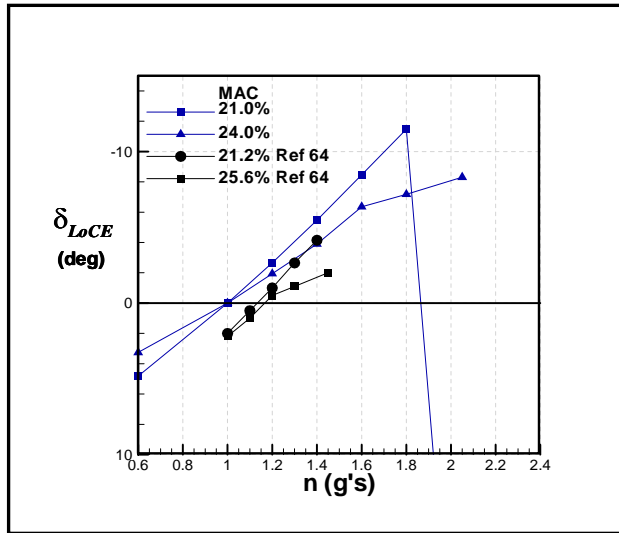


Figure 5.9: Comparison of YB-49 Pull-Up / Push-Over *AeroMech* results with flight test report data¹⁹ for the low-speed flight segment

The *AeroMech* results show the same trend for the LoCE deflection as the load factor is increased, including some of the non-linear effects. The magnitude of these deflections differ slightly between the flight test and *AeroMech* results but this can be contributed to the slightly different c.g. locations used in the *AeroMech* and flight test analysis.

To explore the effects of relaxed static stability the c.g. location was varied from 21% to 33% MAC for all of the Cruise, Low-speed flight and Approach mission segments. The required deflections are shown in Figure 5.10. This analysis was performed over a load factor range from 0.6 to 2.05, which are load factor limits provided from the pilots hand-book³⁸.

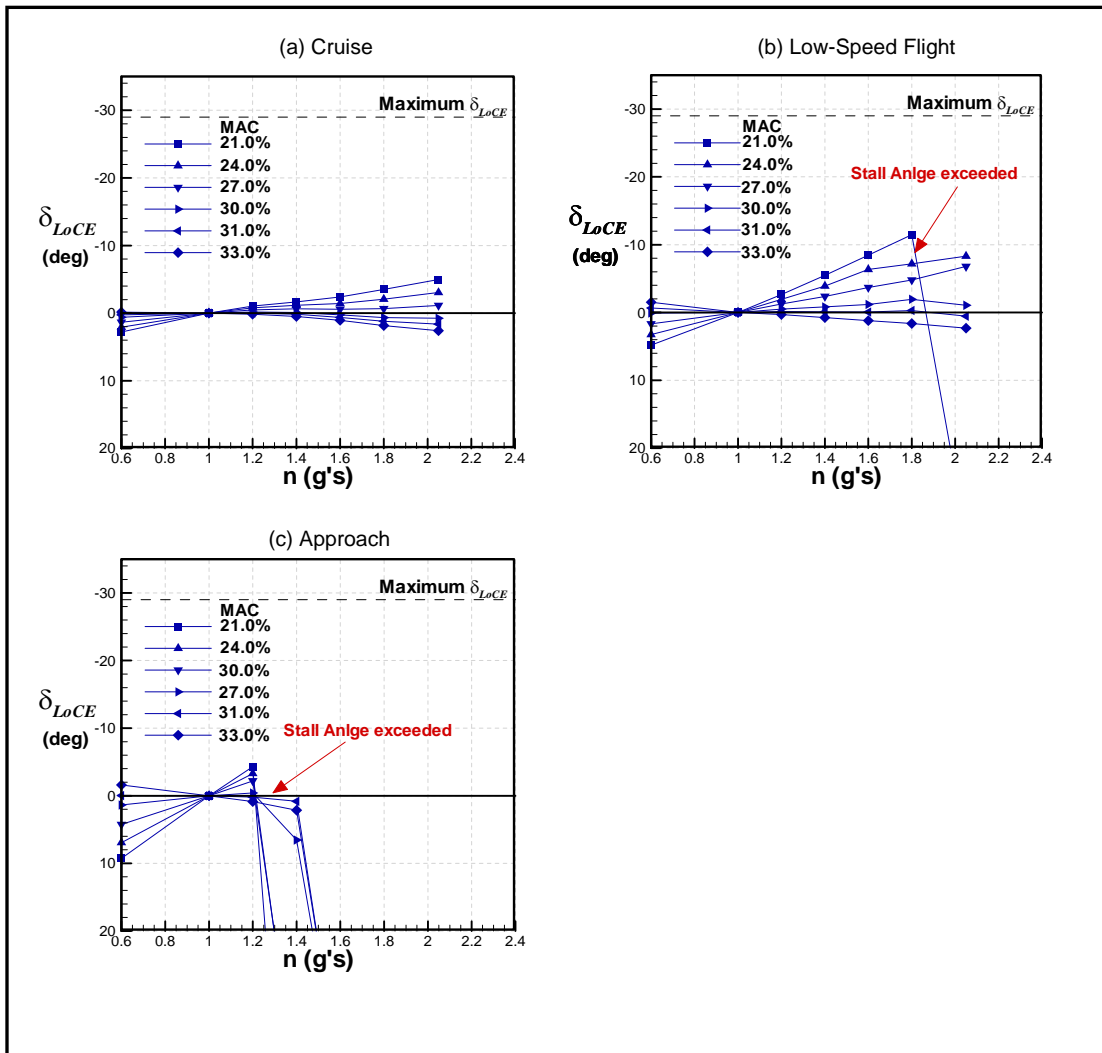


Figure 5.10: Effects of relaxed longitudinal static stability on the required LoCE (trim flap) trim deflection during Cruise, Low-speed Flight and Approach

As shown in Figure 5.10 the YB-49 possesses adequate longitudinal control power for these three mission segments, but does not possess an adequate C_{Lmax} to perform high “g” maneuvers during low-speed flight and approach. During low-speed flight and approach, however, the ability to perform the push-over maneuver for speed-recover is of more importance than the pull-up maneuver and the YB-49 has adequate

control power for speed recovery, while the aircraft is flown statically stable in the longitudinal plane (i.e. the c.g. is ahead of the neutral point).

As to be expected, smaller elevon control surface deflections are required as the c.g. moves aft to maintain the required load factor. Up to approximately 1.2g, the aircraft does demonstrate normal control characteristics for all c.g. locations investigated. However, for c.g. locations aft of 27% MAC Figure 5.13 indicates that the control surface deflections required to maintain load factors larger or equal +1.2g reverses from nose-up deflections to nose-down deflections. This indicates control instability, since the maneuver point (m.p.) moves forward of the c.g. location. This would require a flight control system (FCS) logic for safe flight operation, enabling the pilot to command nose up while in reality the elevons deflect nose down. Currently, the static and dynamic stability modules in *AeroMech* only calculate the stability of an aircraft during 1-g flight. Future version of *AeroMech* will be adapted to analyze the Pull-Up / Push-Over maneuvering stability.

Summary of LoCE DCFC's

Overall, the YB-49 possess adequate control power for DCFC's of 1-g Trim, Take-Off Rotation maneuver, and Pull-Up / Push-Over maneuver over the take-off, cruise, low-speed flight and approach Mission Segments. Some maneuvering instabilities were discovered for the cruise segment with aft c.g. locations and thus a FCS logic would be required to provide flight safety during such maneuvers. The low load factor capability during Low-Speed Flight and Approach are the result of

insufficient lift and thus greater flap deflections would be required if such maneuverability is required.

DIRECTIONAL CONTROL EFFECTOR SIZING

The drag rudder is the primary DiCE for the YB-49. This control surface is located on the outer wing panel and opens like a “clam-shell” to increase the drag on the outer portion of the wing and thus creating a yawing moment.

To explore the control power of this surface the DCFC’s 1-g Trim during side-slip, Turn coordination, which is approximated as adverse yaw, and horizontal turn performance.

DCFC: 1-g Trimmed Side-Slip

1-g Trim during side-slip requires the DiCE to balance the yawing moment produced by the side-slip angle in order to maintain a heading. The AeroMech results for a the Cruise, Low-Speed Flight and Approach mission segments are shown in Figure 5.11. The additional control power requirements from the SAS to provide the Mil-Spec level 1 dynamics stability requirements are shown for typical maximum disturbance values of $\Delta\beta = \pm 5$ deg and $\Delta r = \pm 10$ deg/s, taken from Roskam¹⁰. The effects of relaxed static stability are small for the required DiCE deflections for trim, thus only the forward c.g. of 21% MAC is presented.

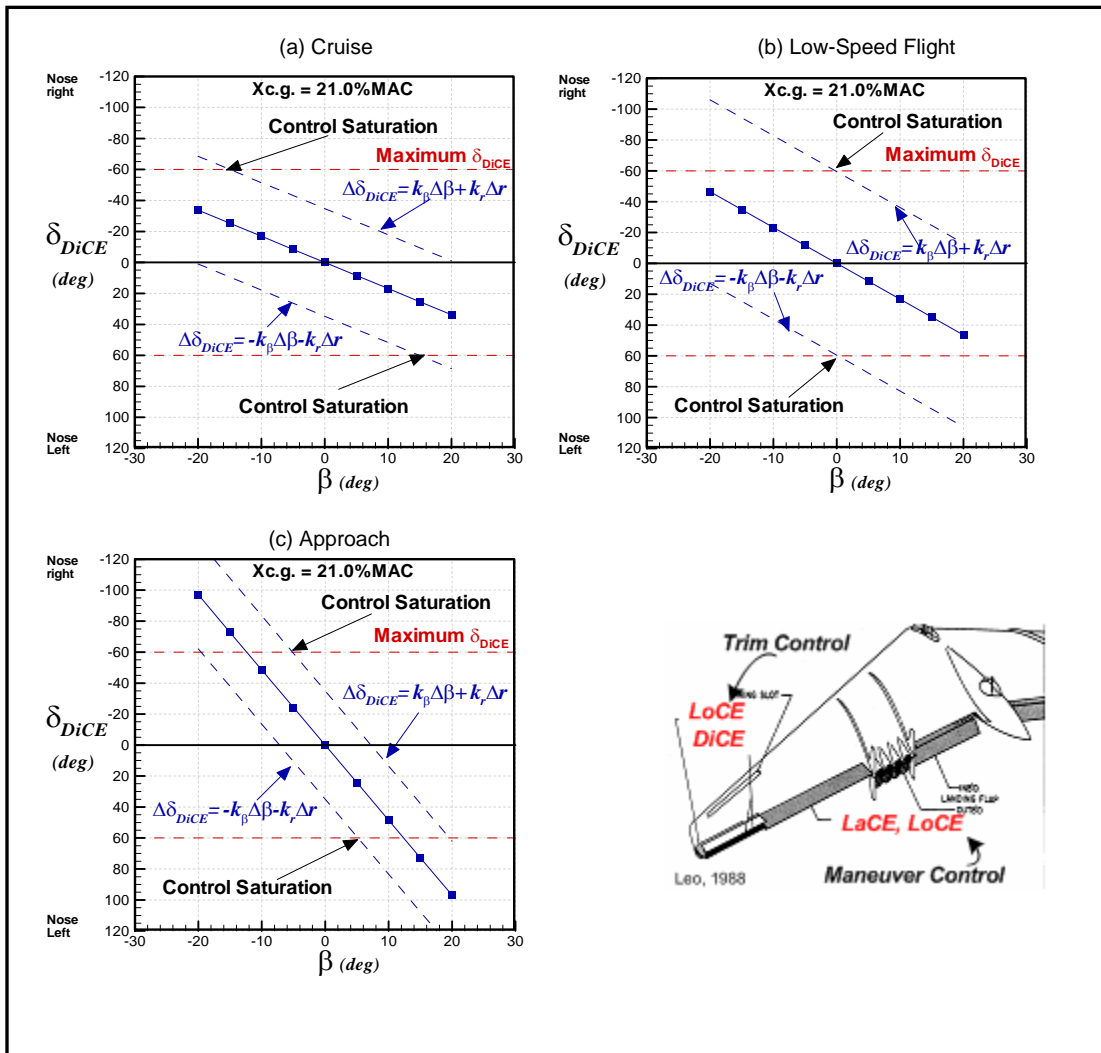


Figure 5.11: Required DiCE (drag rudder) trim deflection during Cruise, Low-speed Flight and Approach

The drag rudder has sufficient control power to tolerate side-slip divergences during cruise but is limited during Low-Speed Flight and Approach. During Low-Speed Flight the SAS could not satisfy the level 1 Dutch roll requirements for zero side-slip due to inadequate control power. Thus the DiCE saturates for any side-slip angle and cannot provide adequate artificial dynamic stability at this flight condition. During approach the level 1 requirement could be satisfied by the SAS for zero side-slip,

however, the DiCE saturates at a side-slip angle of 5 deg. Therefore the DiCE can provide both trim and stability augmentation during approach in moderate cross-winds.

The reason that the DiCE appears to have more control power during Approach than Low-Speed Flight is because the Mil-Spec requirements are slightly lower for Dutch roll during the approach phase, thus less stability augmentation is required.

In summary, the DiCE has adequate control power to trim and stabilize the YB-49 for 1-g Trimmed flight during Cruise, but cannot provide adequate stability augmentation for Low-Speed Flight and Approach.

DCFC: Turn Coordination (Adverse Yaw)

For some large transport aircraft initially coordinating a turn during low-speed flight can be a demanding flight condition for the DiCE due to the adverse yaw produced by the LaCE while rolling the aircraft and the reduced effectiveness of the DiCE due to the high angle of attack required for low-speed flight. While this is a highly dynamic maneuver, it is approximated with AeroMech by examining DiCE deflections required to maintain a steady-state roll maneuver. The steady-state roll maneuver captures the adverse yaw and high angle of attack effects but does not account for inducing the yaw and roll accelerations. Full 6-DOF flight simulation may be required to completely capture these effects.

The AeroMech results for the steady-state approximation of initial turn coordination and adverse yaw are shown in Figure 5.12.

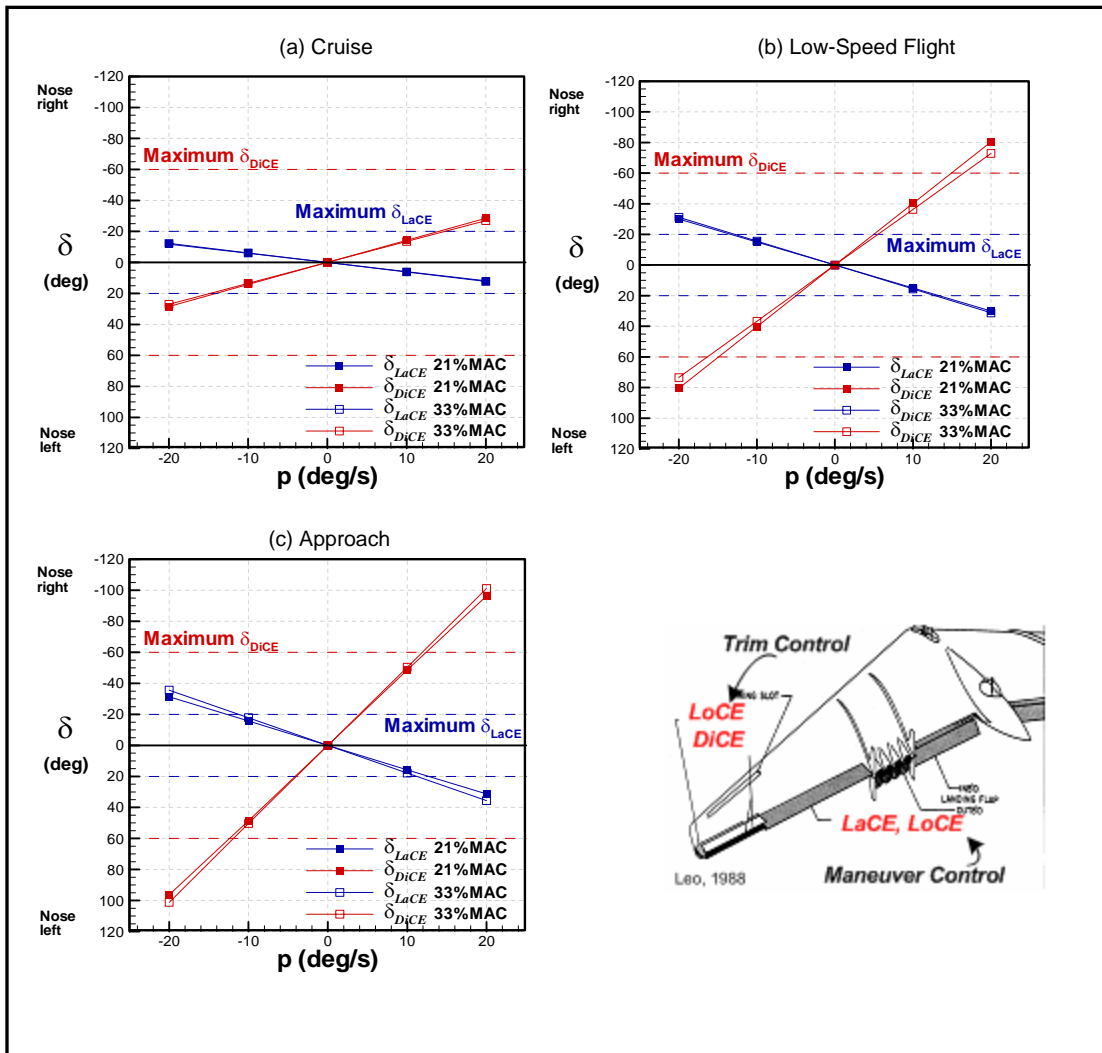


Figure 5.12: Required DiCE (drag rudder) turn Coordination deflections during cruise, low-speed flight and approach

The DiCE possess adequate control power to counter the adverse yaw produced by the LaCE during the steady-state roll maneuver during the mission segments shown in Figure 5.12. However, the DiCE saturates at the same roll rate as the LaCE during approach and thus high roll rate maneuvers should be avoided during initial turn coordination. If greater maneuverability is required during approach the DiCE must be enlarged to counter the adverse yaw from the LaCE.

DCFC: Horizontal Turn Load Factor Capability

Once the turn has been initially coordinated the DiCE deflections required should be zero due to the zero side-slip during coordinated turns. However, as noted during flight test the YB-49 could not maintain a coordinated turn during low-speed flight because of low directional stability. This can be seen through the AeroMech results for the DiCE deflections required for steady-state coordinated turns as shown in Figure 5.13.

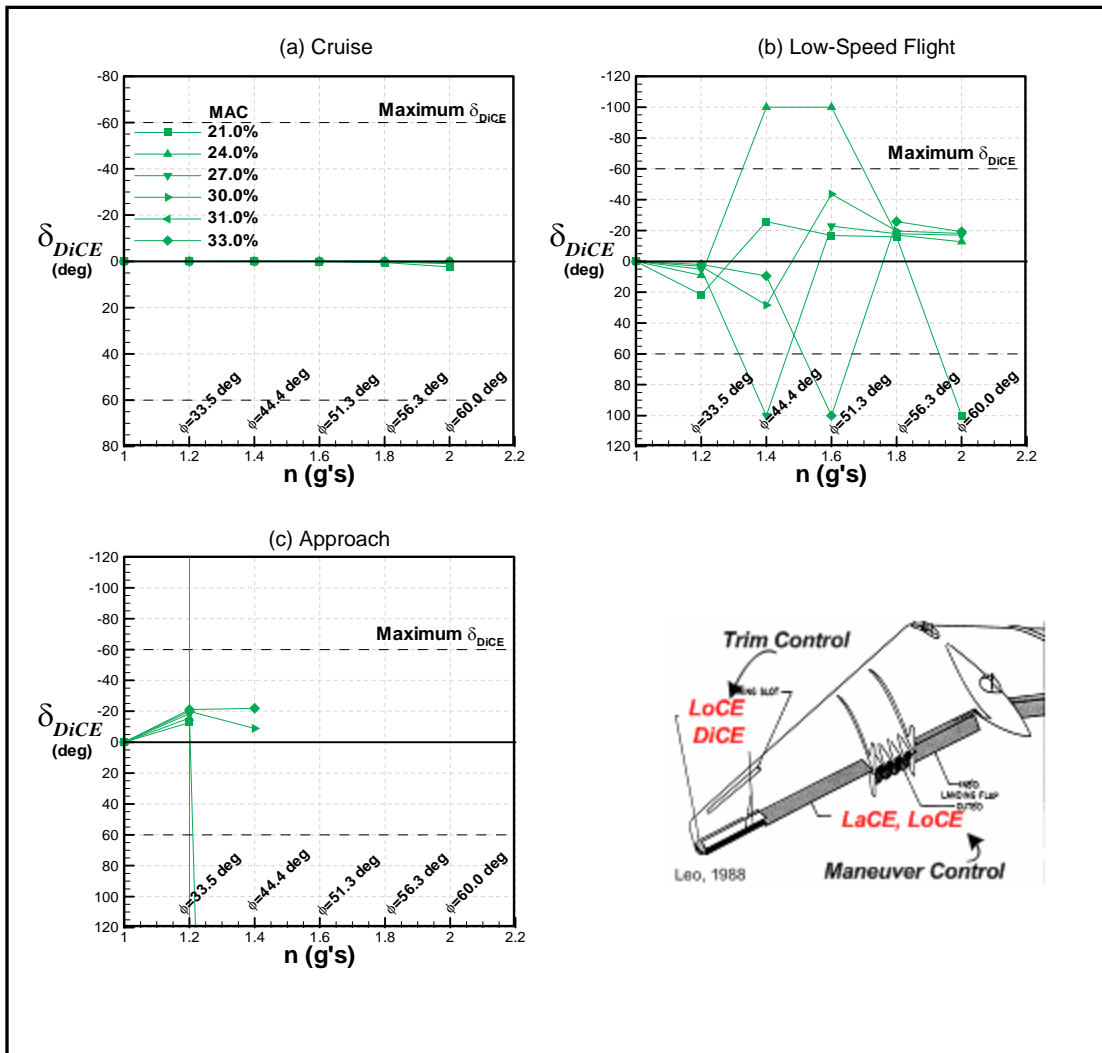


Figure 5.13: Required DiCE (drag rudder) deflections to maintain coordinated during Cruise, Low-speed Flight and Approach

As seen from Figure 5.27, numerical instabilities are a characteristic of the *AeroMech* calculations for this mission segment. These numerical instabilities directly reflect the physical control problems found with the original YB-49. These types of instabilities occur in *AeroMech* when a solution cannot be found within the aerodynamic look-up tables provided and the algorithm needs to extrapolate beyond the dataset provided to find a solution. Since maintaining a coordinated turn should require

no LaCE and DiCE deflections, the results calculated show the sensitivity of the YB-49 to small deviations from a properly coordinated turn above a load factor of 1.2 and bank angle of 33.5 deg. These results agree very well with information obtained from flight test reports reporting that the YB-49 could not maintain a coordinated turn long enough to obtain sufficient test data at this flight condition^{19,20}. In the case of Approach, no data was obtained beyond a load factor of 1.2 from AeroMech due to wing stall which prevents a pure horizontal turn.

Summary of DiCE DCFC's

The DiCE is not adequate for the mission segments and DCFC's analyzed. While the DiCE appears to be adequate for trim, stability augmentation and maneuvering during Cruise, the DiCE is not adequate for stability augmentation and maneuvering for Low-Speed Flight and Approach. Greater control power is required for Low-Speed Flight and Approach or greater directional stability is required to reduce the need for a SAS and to provide more stability during coordinated turns. The issues of insufficient DiCE control power discovered here are similar to the deficiencies found during flight test¹⁹, thus showing *AeroMech's* unique capability.

LATERAL CONTROL EFFECTOR SIZING

The elevon on the YB-49 is specified as the primary LaCE for the YB-4 and is also used the primary maneuvering LoCE.

DCFC: 1-g Trimmed Side-Slip

During 1-g Trimmed flight with side-slip the aircraft is banked to use a component of the lift force to balance the side-slip and the LaCE must be able to

maintain this bank angle. Due to the lack of a fuselage and vertical tail the side-forces for a flying wing are relatively low compared to TAC's and thus the LaCE deflections are typically not severe. The results from AeroMech for this DCFC are shown in Figure 5.14.

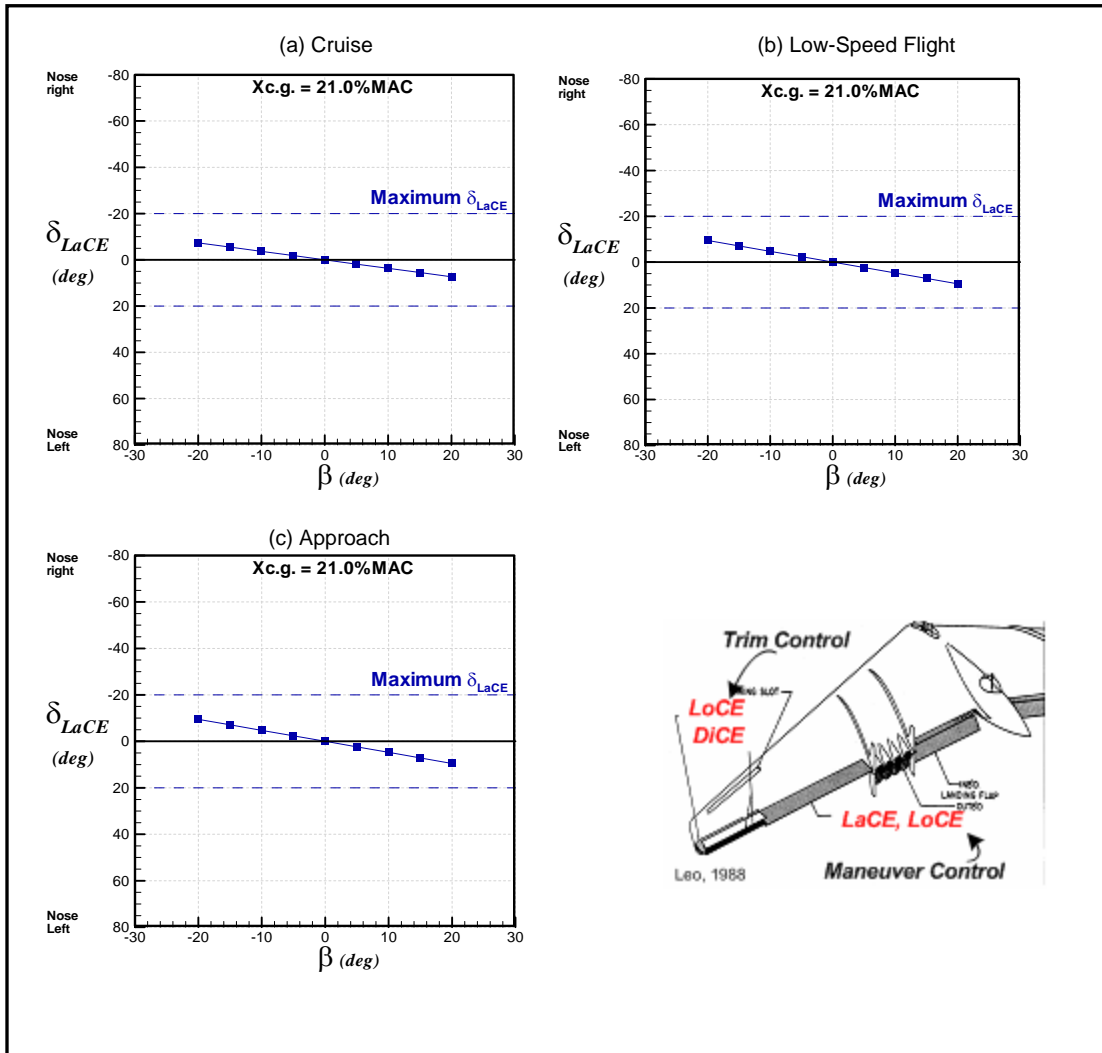


Figure 5.14: Required LaCE (elevon) deflections for 1-g trim with side-slip during Cruise, Low-speed Flight and Approach

The LaCE possesses adequate control power for all three mission segments analyzed. No additional LaCE deflections were required for stability augmentation.

DCFC: Maximum Roll Rate Capability

The YB-49 utilizes the elevons as the primary LaCE. To validate the *AeroMech*'s steady-state roll performance algorithm the *AeroMech* results are compared to flight test results¹⁹ during the Approach mission segment (Figure 5.15)

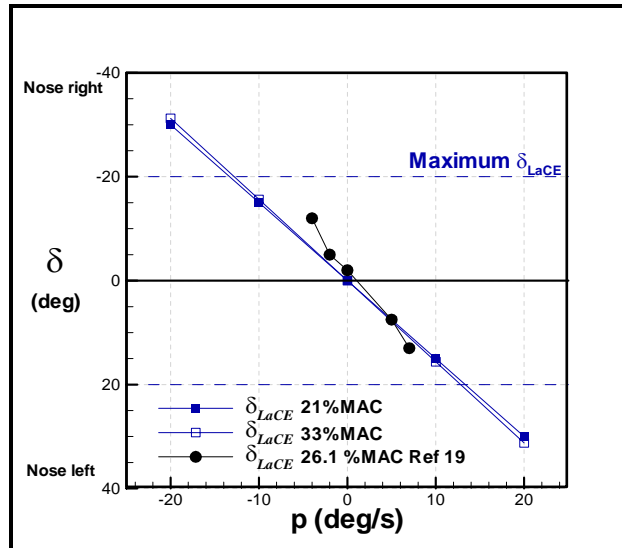


Figure 5.15: Maximum roll rate capability of the YB-49' LaCE (elevon) compared to flight test results¹⁹ during Low-speed flight

As shown in Figure 5.15, AeroMech accurately predicts the ability of the LaCE to maintain the required roll rates. The LaCE's ability to maintain roll rates up to 20 degrees for Cruise, Low-Speed Flight and Approach are shown in Figure 5.16.

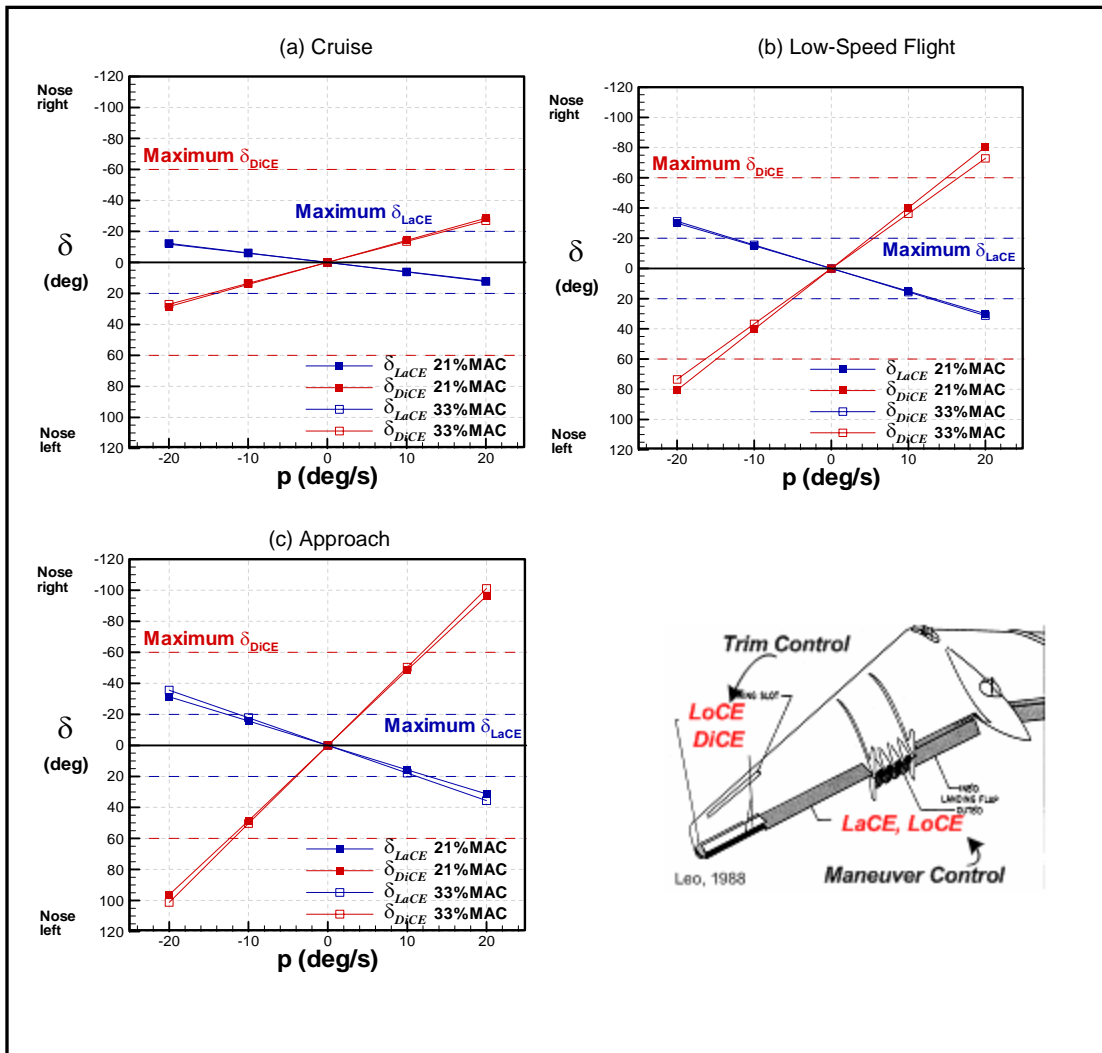


Figure 5.16: Maximum Roll rate Capability of the YB-49' LaCE (elevon) during Cruise, Low-speed Flight and Approach

The LaCE has the ability to maintain the specified roll rates for Cruise, but can only maintain roll rates of 10 deg/s for Low-Speed Flight and Approach. During Low-Speed Flight and Approach however, such maneuverability is not typically required for this type of aircraft. Thus, the LaCE is adequate for this flight condition.

DCFC: Time to Bank Roll Performance

The time to bank to 30 deg. for this type of aircraft is specified in the Mil-Specs⁷⁶ according to Table 5.14.

Table 5.14 Mil-Spec Time to Bank Requirements for Class III Aircraft³²

Speed Range	Level 1		Level 2		Level 3	
Category	B	C	B	C	B	C
<i>L</i> ($V_{min}+20 \text{ knts} < V < 1.4V_{min}$)	2.3	2.5	3.9	4.0	5.0	6.0
<i>M</i> ($1.4V_{min} < V < 0.7V_{max}$)	2.0	2.5	3.3	4.0	5.0	6.0
<i>H</i> ($0.7V_{max} < V < V_{max}$)	2.3	2.5	3.9	4.0	5.0	6.0

For the mission segments analyzed here the Cruise, Low-Speed Flight, and Approach speed ranges are *M*, *L* and *L* respectively. The AeroMech results for the YB-49's time to bank for Cruise, Low-speed flight and Approach are shown in Figure 5.17.

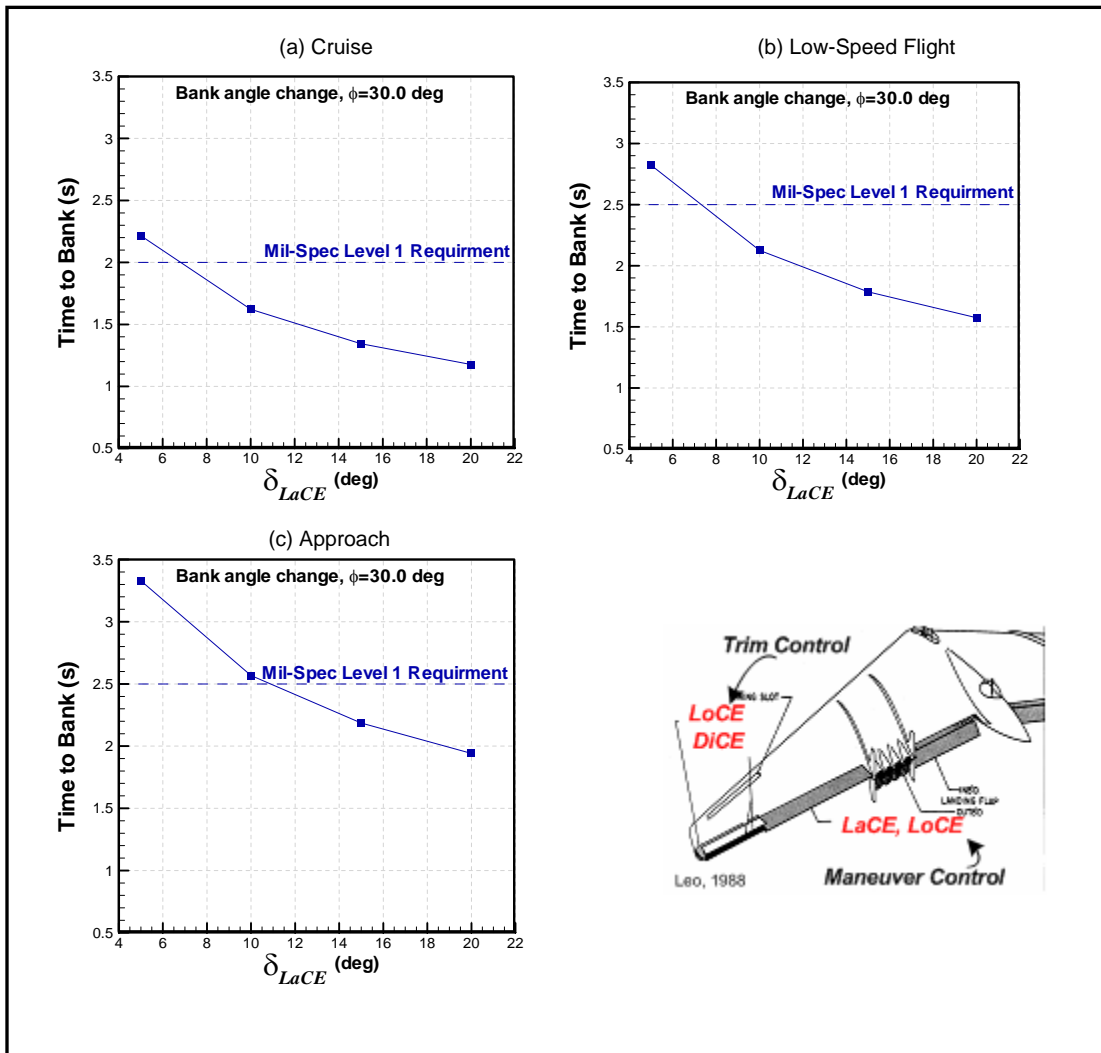


Figure 5.17: Required DiCE (drag rudder) turn Coordination deflections during Cruise, Low-speed Flight and Approach

The LaCE shows sufficient control power to meet the level 1 time to bank requirement from the Mil-Specs during the three mission segments analyzed. Thus the LaCE is of sufficient size for this DCFC.

Summary of LaCE DCFC's

LaCE has demonstrated adequate control power for trim during side-slip, sustained roll rates and time to bank during the Cruise, Low-speed flight and Approach

mission segments. *AeroMech* has also demonstrated its ability to accurately predict the steady-state roll rate capability of the YB-49.

SUMMARY OF LOCE, DICE AND LACE RESULTS

For the DCFC's analyzed here, the LoCE, and LaCE have shown sufficient control power for Cruise, Low-speed flight and Approach. The DiCE demonstrated adequate control power for cruise but lacked control power during Low-speed flight and Approach. A larger drag rudder is required to allow for greater maneuver control and stability augmentation.

Maneuvering instabilities were found for the pull-up maneuver with aft c.g. locations and for maintaining coordinated turns. The pull-up maneuver instabilities with aft c.g. would require FCS logic to handle the reversible control effects, due to the maneuvering point shifting ahead of the c.g. Maintaining of coordinated turns for this vehicle would require a FCS to artificially increase the directional stability of aircraft during this maneuver.

For all three control effector, LoCE, LaCE and DiCe, *AeroMech* has shown sufficient physical accuracy through direct comparison of the *AeroMech* results to flight test results as well as uncovering maneuvering problems which were also encountered during flight test.

5.2.4.5. Trimmed Aerodynamic Analysis

The trimmed aerodynamics for the YB-49 are calculated from the untrimmed aerodynamic look-up table using the trimmed angle of attack and control surface deflections calculated for 1-g Trimmed flight for the various mission segments. The resulting trimmed lift to drag ratio's are presented in Figure 5.18.

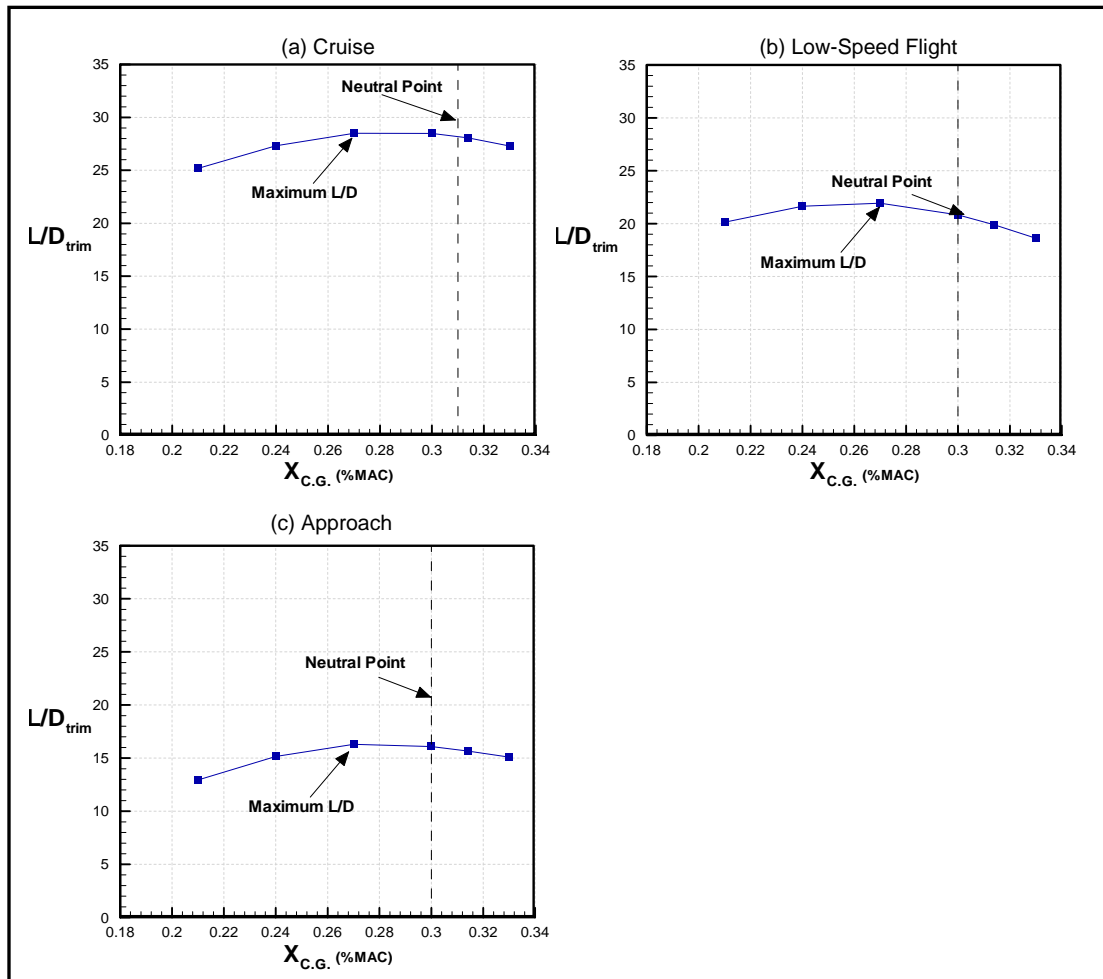


Figure 5.18: Effects of relaxed longitudinal static stability on L/D_{Trim} for Cruise, Low-speed Flight and Approach

As shown with Figure 5.17, the maximum L/D ratio occurs forward of the neutral, around 27% MAC for the three mission segments shown. Recall, during the

LoCE 1-g trim analysis the control surface deflection required was near zero at 27% MAC. Forward and aft of this position trim drag associated with the larger control surface deflections reduce the overall trimmed L/D. The YB-49 incorporates a -4.0 deg wing twist at the tip which is analogous to a downward deflected horizontal stabilizer on a traditional TAC. This twist naturally trims the YB-49 with a c.g. location of around 27% MAC.

It is important to note that the YB-49 was designed to be a statically stable aircraft and thus the built in trimming surface (negative outer wing twist) was designed accordingly. If this aircraft were design as a true control configured vehicle (CCV) the wing twist or airfoil sections could be used to tune the lift distribution (as is with traditional TAC) to increase the aerodynamic performance. Then the aircraft could be balanced to allow for small LoCE deflection for trim while relying on a FCS to artificially stabilize the aircraft. The ability to incorporate such design trades represents a unique design capability seen with *AeroMech*.

5.2.4.6. Static and Dynamic Stability

The YB-49's longitudinal and lateral / directional static stability and dynamic stability are discussed in this section for the Initial Climb, Cruise, Low-Speed Flight and Approach mission segments. In addition, the effects of relaxed longitudinal static stability on longitudinal and lateral / directional dynamic stability are also considered.

LONGITUDINAL STATIC STABILITY

The YB-49 was designed to be statically stable in pitch and thus the vehicle is statically stable for moderate angles of attack. The YB-49's static stability as a function of angle of attack is shown in Figure 5.19 through the pitching moment curve and the static and maneuvering margins.

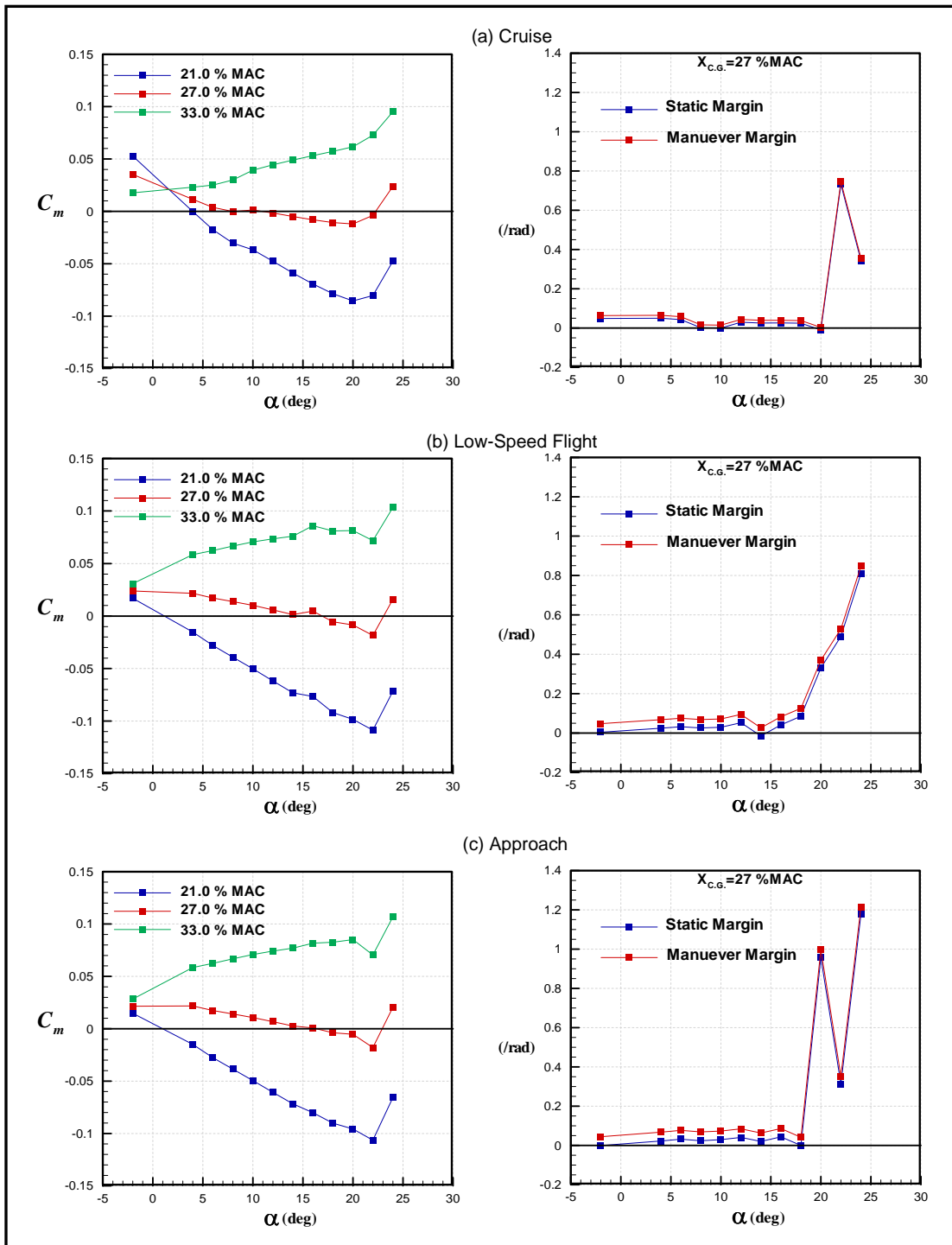


Figure 5.19: Longitudinal Static Stability as a function of angle of attack for Cruise, Low-speed Flight and Approach

For each mission segment analyzed the YB-49 has a negative pitch break at high angles of attack, which is associated with tailless aircraft, but the static and maneuver. margins stay positive. The static and maneuvering margins remain positive because they are depended on the variation of lift with pitching moment and not angle of attack. Thus the pitch break is occurring aft of the stall point. The YB-49 was flown in a statically stable configuration and thus if the aircraft entered a stall the pilot may have time to correct before the pitch break occurs but if the aircraft enters the stall too quickly, and reaches the pitch break, the aircraft would be uncontrollable as demonstrated previously by the LoCE Pull-up / Push-Over DCFC.

LATERAL / DIRECTIONAL STATIC STABILITY

The lateral directional static stability of the FWC is relatively low due to the absence of a large vertical surface. The results from AeroMech are shown in Figure 5.20 through the Directional stability Derivatives ($C_{Y\beta}$, $C_{n\beta}$, $C_{l\beta}$) and the spin resistance $C_{n\beta dyn}$ and roll reversal ($LCSP$) parameters for the Cruise, Low-Speed Flight and Approach mission segments. Figure 5.18 shows the results for a single c.g. location. The lateral / directional were not greatly influenced by the shift in c.g. The remaining c.g. location show the same effects

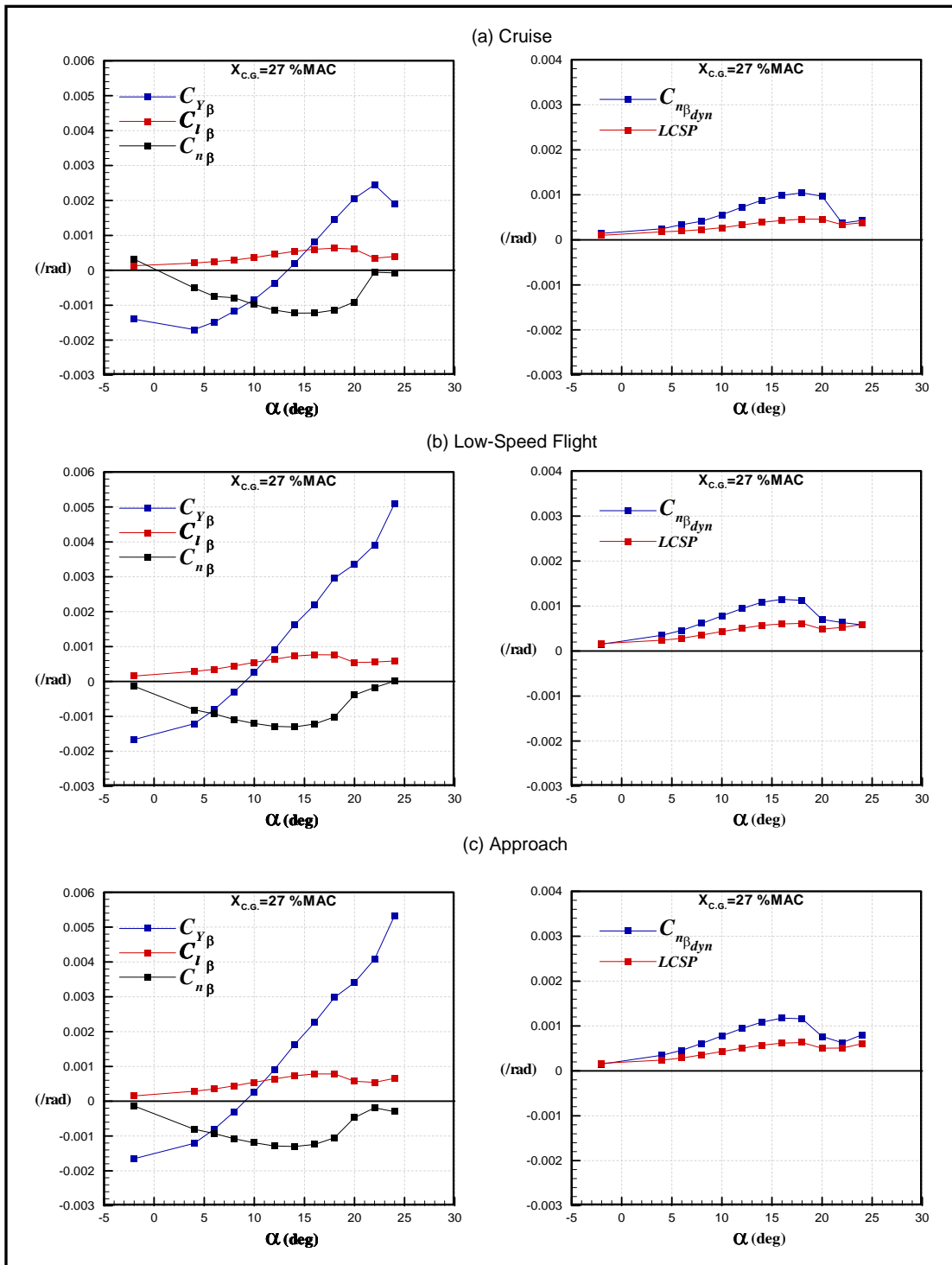


Figure 5.20: Lateral Directional Static Stability as a function of angle of attack for Cruise, Low-speed Flight and Approach

The static directional stability derivatives $C_{n\beta}$, $C_{l\beta}$ remain stable for all angles of attack and mission segments presented but are relatively low, this will present a problem for lateral/directional dynamics stability stiffness as explained in the dynamic stability section of this analysis. The spin resistance and roll reversal parameters remain positive and stable for the mission segments shown.

LONGITUDINAL DYNAMIC STABILITY

While relaxed longitudinal static stability improves performance effects like trimmed aerodynamics and maneuverability, dynamic stability is reduced and can require artificially stiffening and damping of the stability modes. For this study the resulting YB-49 longitudinal dynamic stability modes are compared to the Mil-Spec requirements for a Normal mission segments (Category B flight phases) and Terminal mission segments (Category C flight phases)³², summarized in Table 5.15 and Figure 5.21.

Table 5.15 Mil-Spec Longitudinal Dynamic Stability Requirements³²

<i>Mode</i>	<i>Level 1</i>		<i>Level 2</i>		<i>Level 3</i>	
	Damping	Stiffness	Damping	Stiffness	Damping	Stiffness
<i>Phugoid</i>	$\zeta > 0.04$	-	$\zeta > 0.00$	-	$T_2 > 55s$	
<i>Short Period</i>	$0.35 < \zeta < 1.30$	Fig. 5.19	$0.25 < \zeta < 2.00$	Fig. 5.19	$\zeta > 0.15$	Fig. 5.19

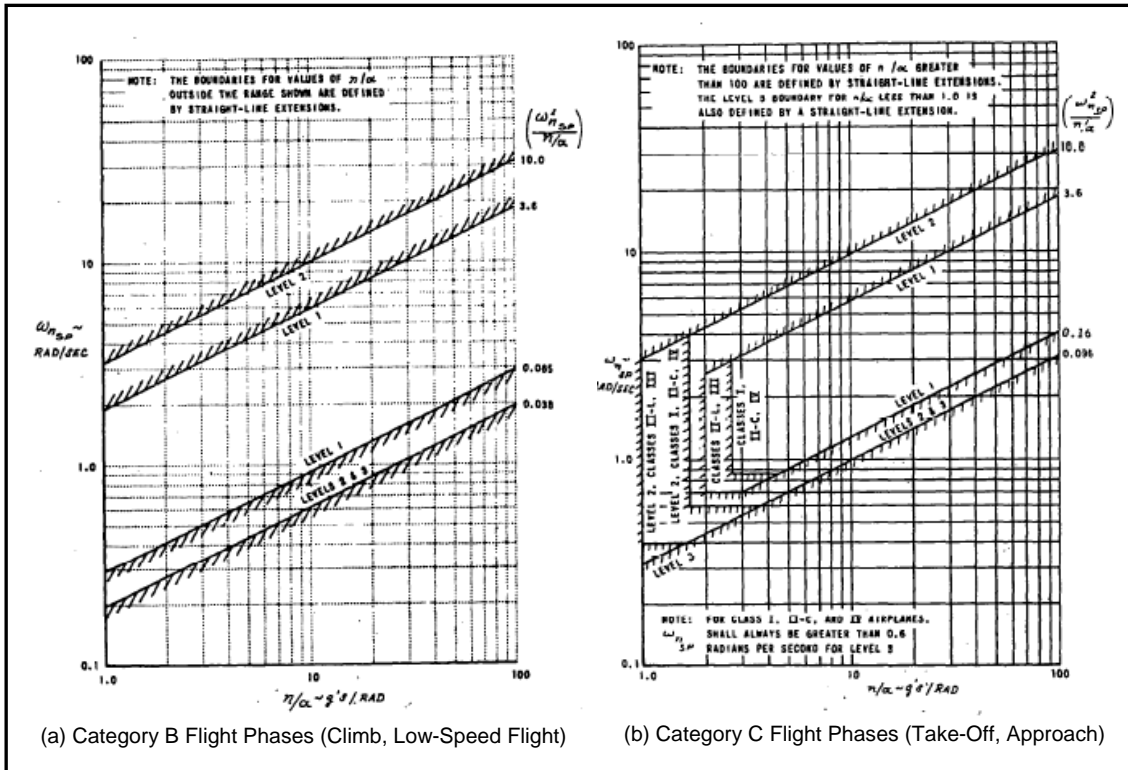


Figure 5.21: Mil-Spec short-period frequency requirements for Category B and C flight Phases³²

While the YB-49 was initially designed to meet these specific requirements, the Mil-Specs³² give a good guideline to estimate the required SAS gains to provide adequate longitudinal flying qualities with relaxed static stability.

The actuator model used in this analysis is a second order lag model from Abzug²³ for a typical hydraulic actuator ($\omega_n = 12.0$, $\zeta = 0.707$).

Figure 5.22 shows the AeroMech results for effects of relaxed static stability on the longitudinal stability modes with the required SAS gains to meet level 1 dynamic stability requirements from Mil-Specs³².

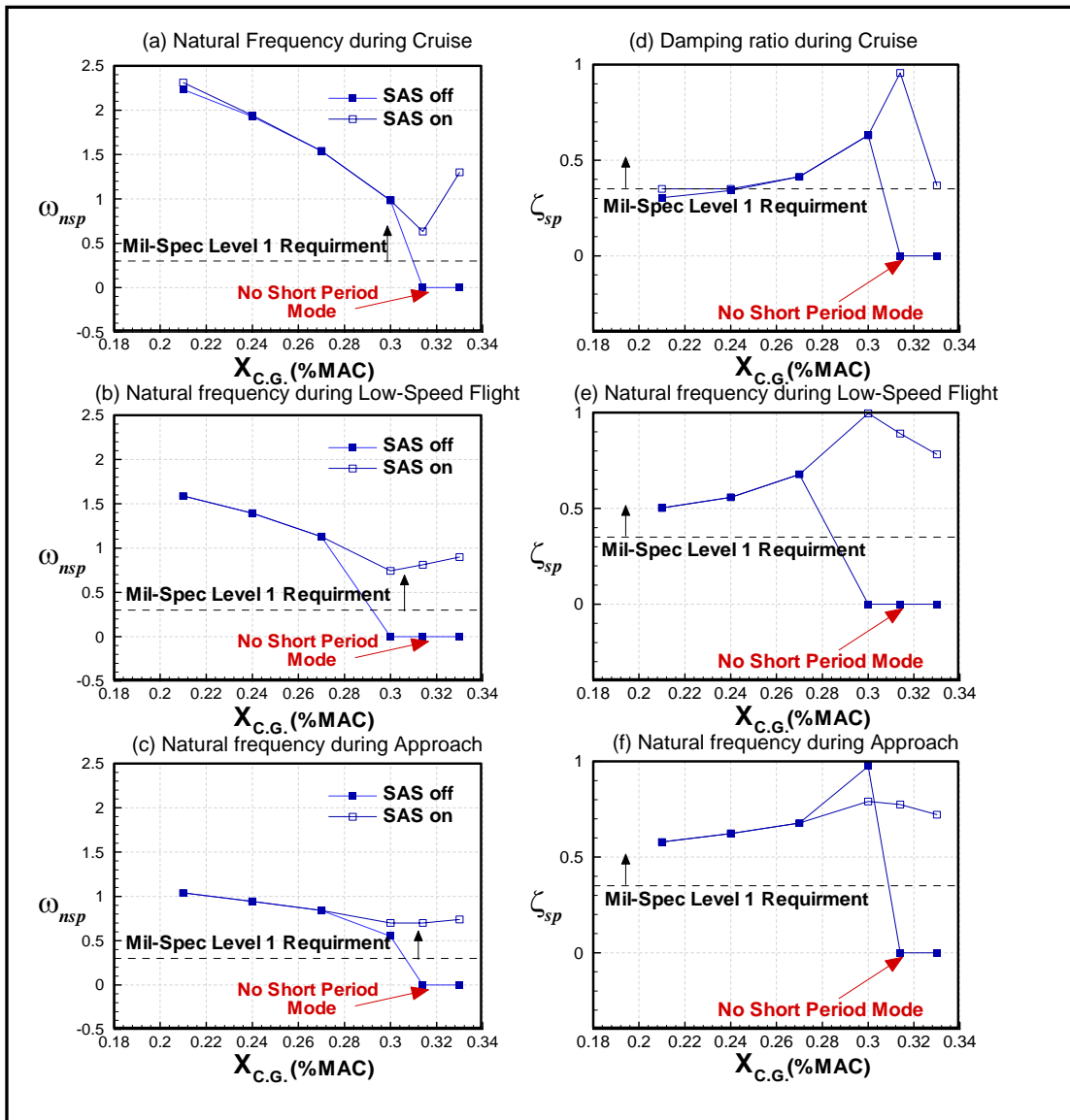


Figure 5.22: Longitudinal Short Period Mode with stability augmentation for Cruise, Low-speed Flight and Approach

Relaxed static stability decrease the stiffness (i.e. natural frequency) of the short period mode until the aircraft is dynamically unstable. At which point the phugoid and short period modes combine to form the third oscillatory mode, as shown in Figure 5.22. To re-stabilize the statically unstable configurations angle of attack feed-back is utilized to separate the third oscillatory mode into the classic short period and phugoid

modes. With the level of angle of attack feed-back required to form the short-period and phugoid modes for the statically unstable configurations the dynamic stability requirements were met, thus no pitch rate feed-back was required.

The forward c.g. location (21% MAC) during Cruise required some pitch rate feed-back to increase the short-period damping ratio slightly, however, during Low-speed flight and Approach no stability augmentation was required for the statically stable configurations. The gain setting to meet the level 1 dynamic stability requirements are shown in Figure 5.23.

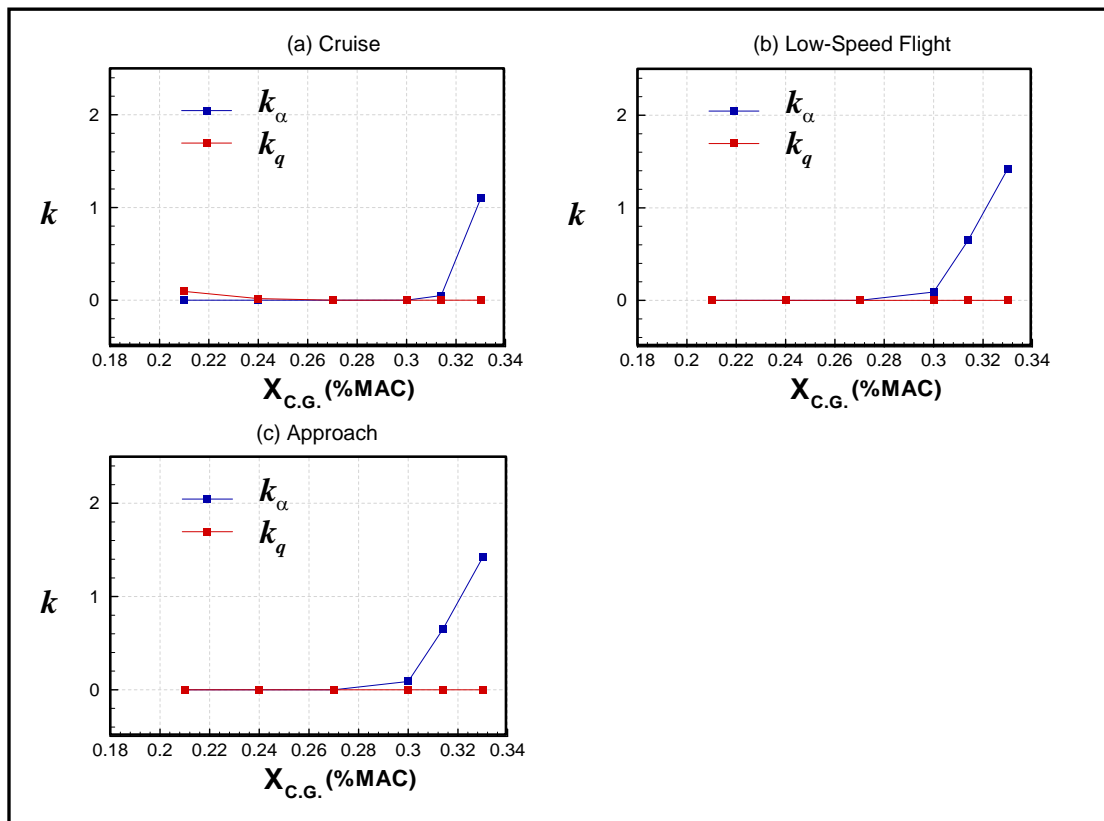


Figure 5.23: Longitudinal Short Period Mode with stability augmentation for Cruise, Low-speed Flight and Approach

These gain settings are required for stabilizing the short-period mode and have the following effects on the phugoid mode (Figure 5.24).

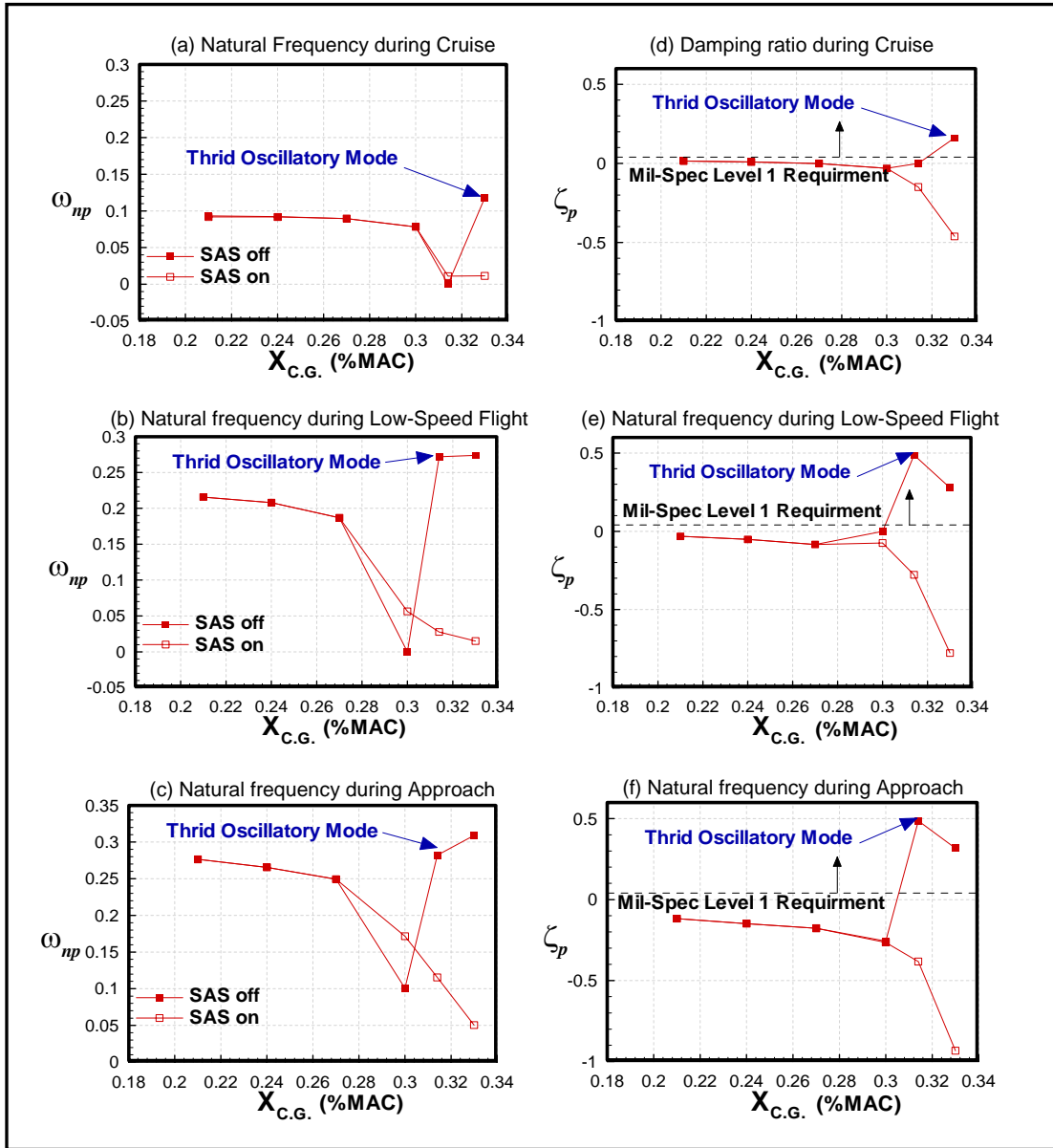


Figure 5.24: Longitudinal Phugoid Mode with stability augmentation for Cruise, Low-speed Flight and Approach

The Phugoid mode does not meet the Mil-Spec requirements for the mission segments analyzed. While the angle of attack feedback separates the short-period and

phugoid motions for the unstable configurations additional autopilot gains (altitude or velocity feed-back) are required to stabilize the phugoid mode. No effort has been made to compute these required gains for the current analysis.

Overall, the longitudinal dynamic stability of the YB-49 is adequate for the short-period mode with stability augmentation and enough control power exists provide the artificial short-period stability. The phugoid mode will require additional flight controller feedback to increase the phugoid damping ratio.

LATERAL / DIRECTIONAL DYNAMIC STABILITY

While relaxed longitudinal static stability directly reduces the longitudinal dynamic stability, the lateral / directional dynamic stability is largely unaffected. However, the lateral / directional dynamic stability of the YB-49 is low due to lack of a large vertical surface providing directional damping and stiffness. To explore the lateral / directional dynamic stability, YB-49 results are compared to the lateral / directional Mil-Spec³² dynamic stability modes requirements for large transport aircraft (Class III airplanes) for Normal mission segments (Category B flight phases) and Terminal mission segments (Category C flight phases)³², summarized in Table 5.16.

Table 5.16 Mil-Spec Minimum and Maximum Lateral / Directional Dynamic Stability Requirements³²

Mode	Flight Phase Category	Level 1	Level 2	Level 3
<i>Dutch Roll</i>				
ζ_{\min}	B and C	0.08	0.02	0.00
ω_{\min}	B and C	0.4	0.4	0.4
$\zeta\omega_{\min}$	B	0.15	0.05	-
	C	0.10	0.05	-
<i>Roll</i>				
τ_{\max}	B and C	1.4	3.0	10.0
<i>Spiral</i>				
$T_{2\min}$	B	20	8	4
	C	12	8	4

While the YB-49 was initially designed to meet these specific requirements, the Mil-Specs³² give a good guideline to estimate the required SAS gains to provide adequate lateral / directional flying qualities with relaxed static stability.

Using the same actuator model as explained for the longitudinal dynamic stability the lateral / directional dynamic stability modes were calculated for Cruise, Low-speed flight and Approach, see Figure 5.25. In Figure 5.25 the open and closed loop dynamic stability modes are shown across the three mission segments through the Mach number corresponding to each mission segment (Cruise Mach = 0.48, Low-speed flight Mach = 0.17 and Approach Mach = 0.12).

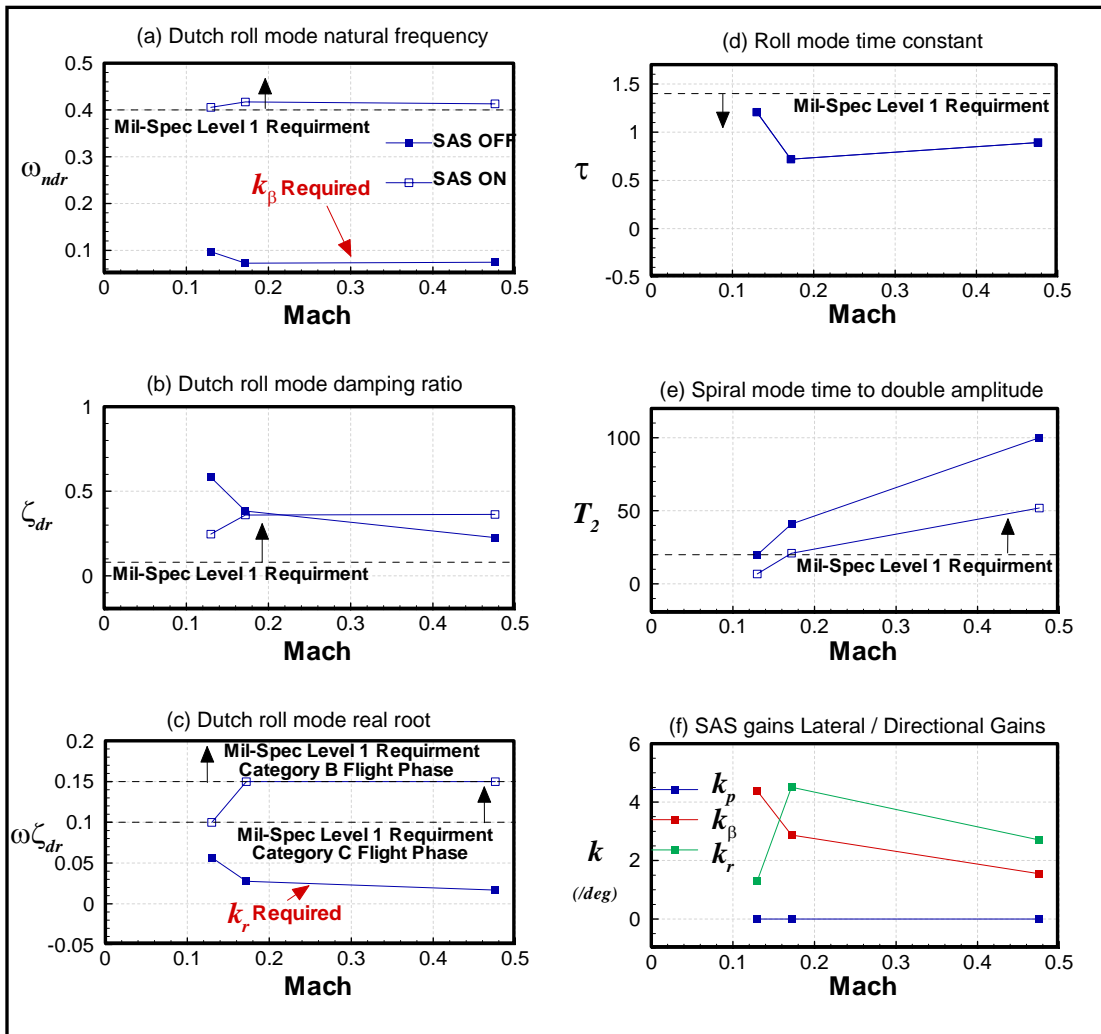


Figure 5.25: Lateral / Directional dynamic stability mode with and without SAS for Cruise, Low-speed Flight and Approach

As shown in Figure 5.25a the Dutch roll natural frequency was low for each mission segment and thus side-slip angle feed-back is utilized to provide to meet the Mil-Spec level 1 requirements. Figure 5.25c demonstrates the $\omega\zeta_{dr}$ term is unacceptable and yaw rate feed-back was implemented to increase the damping ratio and thus increase $\omega\zeta_{dr}$. These findings are similar flight tests which found that “directional

stability is marginal...yaw oscillations seemed to decrease, but did not dampen out completely²⁰,

For cruise and low-speed flight and approach sufficient control power exists for stability augmentation. Recall that the DiCE showed limited side-slip capability during trim with the SAS on. Thus, the DiCE does not possess adequate control power for both side-slip control and stability augmentation

The roll mode for the YB-49 met the Mil-spec level 1 requirements, thus no roll rate feed back is required. The spiral mode however does not comply with the level 1 requirements and an outer auto-pilot loop is required.

Overall, the Dutch roll mode and spiral mode require stability augmentation to meet the level 1 requirements for all mission segments analyzed here. While the DiCE has adequate control power for stability augmentation with zero side-slip, it possesses limited control power for both side-slip trim and stability augmentation.

5.2.5. Summary of Results

The results for DCFC are summarized Table 5.17 for the YB-49 during Take-off, Cruise, Low-speed flight and Approach.

Table 5.17 YB-49 DCFC Summary of Results

DCFC	Mission Segment	Results
Control Effector Sizing		
<i>LOCE Sizing</i>		
1-g Trimmed Flight (SAS on and off)	Cruise, Low-speed flight, Approach	Sufficient control power across all mission segments
Rotation Capability	Take-off	Sufficient control power across all mission segments
Pull-up / Push-over Load Factor Capability	Cruise, Low-speed flight, Approach	Sufficient control power across all mission segments, Stall occurred at high load factors
<i>DiCE Sizing</i>		
1-g Trimmed side-slip (SAS on and off)	Cruise, Low-speed flight, Approach	Insufficient control power for SAS and side-slip during Low-speed flight and Approach
Turn Coordination (Adverse Yaw)	Cruise, Low-speed flight, Approach	Sufficient control power across all mission segments
Horizontal Turn Load Factor Capability	Cruise, Low-speed flight, Approach	Aircraft could not maintain coordinated Turns during Low-speed flight and Approach
<i>LaCE Sizing</i>		
1-g Trimmed side-slip (SAS on and off)	Cruise, Low-speed flight, Approach	Sufficient control power across all mission segments
Maximum Roll Rate	Cruise, Low-speed flight, Approach	Sufficient control power across all mission segments
Time to Bank	Cruise, Low-speed flight, Approach	Sufficient control power across all mission segments
Trimmed Aerodynamics		
1-g Trimmed Flight	Cruise, Low-speed flight, Approach	Maximum L/D during all mission segments around 27% MAC due to zero LoCE deflection
Static and Dynamic Stability		
<i>Longitudinal</i>		
1-g Trimmed side-slip (SAS on and off)	Cruise, Low-speed flight, Approach	Sufficient Control power to provide Mil-Spec Level 1 short-period mode. Autopilot feed-back required for phugoid mode. Problem with pitch break during stall
<i>Lateral / Directional</i>		
1-g Trimmed side-slip (SAS on and off)	Cruise, Low-speed flight, Approach	Sufficient control power for SAS with zero side-slip.

The following conclusions can be drawn from the results shown in Table 5.12 in regards to YB-49.

1. *The YB-49's Aerodynamic efficiency can benefit from relaxed static longitudinal stability* to increase flight performance throughout all mission segments discussed.
2. *The maximum aerodynamic performance does not occur with a c.g. value at the neutral point or when the aircraft is unstable.* The maximum *L/D* occurs

with zero trim flap deflections which occur when the center of gravity is at the center of pressure, which is forward of the neutral point due to negative 4 deg twist at the wing tip which acts like a nose down deflected tail plane. With this twist distribution, the overall aerodynamic performance can be maximized with a c.g. location of 27% MAC during cruise and during low-speed flight.

3. ***The maneuverability of the YB-49 is limited during low-speed flight mainly coordinated turns.*** In a follow-on study, it is recommended that the maneuver stability of the YB-49 be explored.
4. ***The Dutch roll mode stability of the YB-49 is poor for all c.g. locations during all mission segments analyzed.*** This is due to the low inherent static directional stability of the flying wing, a fact confirmed by original flight test results and through calculations obtained by *AeroMech*.

The following recommendations aim to improve the 1950s era YB-49 in its current configuration. Overall objective is to increase aerodynamic efficiency, dynamic stability, and maneuver stability.

5. ***The aerodynamic performance of the YB-49 could be further increased if the wing twist angle is reduced and a SAS is utilized to provide artificial stability at a further aft c.g. location.*** Most aircraft have twist or wash-out at the tip to improve better stall performance, but a flying wing would require excessive wing twist to provide a positive pitch break. The solution to this was found during the B-2 development, the FCS simply does not allow the aircraft to enter stall. Thus, little or no wing twist and camber can be adjusted for obtaining an

elliptic lift distribution and not for stability purposes. The effects of the wing slot have been so far neglected in the current analysis. If a flight control system law is utilized to prevent entering stall the wing slots would not be necessary.

6. ***The DiCE (Drag rudder) must be enlarged.*** The DiCE was found in this study to be inadequate for strait side-slips, turn-coordination and stability augmentation. Both the chord and span of this surface could be expanded to accomplish this.

7. ***A more complex FCS system must be added then presented in this study.*** Including an auto-pilot system to stabilize the phugoid and spiral modes over all mission segments and to provide flight safety during coordinated turns and stall. The additional development costs and system complexity must be evaluated to make the flying wing a practical aircraft.

This case study has also demonstrated the application and accuracy of the *AeroMech* system and it has revealed future areas of growth, such as maneuvering stability analysis. This study has shown that *AeroMech*'s predictions show correctness and even have adequate accuracy for the conceptual design phase. Clearly, *AeroMech*'s numerical results compare very well with flight test results available. Overall, the investigation has uncovered, analyzed, and interpreted several deficiencies of the original YB-49 as confirmed by YB-49 test pilots numerical flight test data available. This YB-49 *AeroMech* study has proven to be a very useful and robust tool, capable of uncovering potential stability and control problems of conventional but as well unconventional aircraft configurations early in the design process. Such unique

capability allows the conceptual designer to quantify, thus consistently compare conventional design solutions with novel or unconventional solution proposals.

CHAPTER 6

CONTRIBUTIONS SUMMARY AND RECOMMENDATIONS

6.1 Contributions Summary

The development of the design tool and software *AeroMech* consists of (1) the development of the overall methodology and mathematical models, (2) the development of the stand-alone *AeroMech* software for validation and demonstration purposes, and (3) the integration of *AeroMech* into the multi-disciplinary design synthesis environment *AVDS PrADO*.

The goals of the present research investigation have been completely achieved, overall consisting of the development, validation, and application of the stand-alone software *AeroMech*. The following specific tasks have been undertaken to meet these objectives.

1. ***Revisiting the aerodynamic integration and steady-state trim solution method developed in Reference 6 and expand the Aerodynamic prediction methods.***

VORSTAB and Digital DATCOM have been modified to automate the building of the un-trimmed aerodynamic look-up table for each DCFC. The trim algorithm has been modified to solve the trim equations of motion with a Newton-Rhapson method for non-linear systems of equations utilizing a cubic-spline interpolation routine to obtain the required trimmed aerodynamic data from the untrimmed aerodynamic look-up table.

2. ***Research, select and integrate a pre-existing aircraft dynamics stability analysis package capable of both open and closed loop dynamic behavior analysis.*** Abzug's ILOCUS.f90 was selected along with an iterative classical controller design methodology to predict the open and closed loop dynamic behavior. Due to time constraints, the coupled 6-DOF small perturbation originally conceived in Reference 1 have not been implemented.
3. ***Research and develop the output file organization and visualization.*** The output files generated by *AeroMech* consist of specific DCFC and maneuver output files along with summary files for exploration static and dynamic stability and control across the entire flight envelope. Using the stability and control map as guidance, the most commonly used figures for deliverables communication are preformatted and organized using TecPlot data files and layout files. This allows for rapid assessment and documentation of stability and control data and their interpretation for the purposes of design decision making.
4. ***Validate AeroMech through case studies of historic aircraft.*** Using the Northrop YB-49 flying wing configuration as the primary design case study for demonstrating the physical correctness of the algorithm and for validation purposes, *AeroMech* is demonstrating its unique capability to bridge the flight dynamicist world with the conceptual designer world. Interestingly, *AeroMech* has been providing additional insight into the YB-49 flying characteristics, information that even may not have been available during the development and flight testing of the original YB-49s in the 1950s.
5. ***Develop an organized and transparent approach to stability and control during the conceptual design phase through the use of AeroMech.*** With the development of the stability and control map as a systematic guide showing how

to logically execute *AeroMech*, the YB-49 has been thoroughly evaluated throughout its flight envelope, thereby exposing the flight vehicle's known and unknown stability and control deficiencies.

AeroMech provides the vital middle ground between the typical reduced order model stability and control methods and full flight simulation on the other extreme of the product development spectrum. This providing an appropriate level of information for (1) sizing the primary and secondary control surfaces, (2) arriving at trimmed aerodynamic performance, and (3) to reliably assess static and dynamic stability in all aircraft axes. With this tool at hand, the conceptual designer is in a far better position to evaluate and compare novel and traditional aircraft configurations, overall uniquely aiding the decision makers to identify the solution space with the least amount of risk associated.

6.2 Recommendations for Future Work

Having completed the development and initial validation of the stand-alone *AeroMech* prototype software, the next logical step is the implementation of *AeroMech* into the flight vehicle synthesis environment AVDS PrADO. The synthesis methodology AVDS PrADO is organized through a database management system, allowing the designer to select the most appropriate disciplinary methods for the design problem at hand from the disciplinary methods library. Consequently, each functional component of *AeroMech* must interface with this database system such as to read and modify the stability and control information stored accordingly. Future research is required to develop interfaces thus enabling robust communication of the stability and control information generated with the overall aircraft system. This integration step is

vital to efficiently apply stability and control during the conceptual design phase. This ultimately will enable us to explore issues like relaxed static stability and their effect on overall vehicle sizing in a truly multi-disciplinary context. Then, AVDS PrADO is in the position to demonstrate multi-disciplinary control-configured vehicle (CCV) synthesis.

While the next logic step is the integration of *AeroMech* into AVDS PrADO, there are several disciplinary *AeroMech* improvements that should be accomplished once integrated. The following improvements are recommended:

1. ***The current control allocation logic*** can be improved by integrating the LOTS methodology into the trim algorithm to solve for minimum trim drag of a three surface aircraft or a two surface aircraft with thrust vectoring. Currently, LOTS computes the aerodynamic effects internally using a quadratic drag model. The algorithm may be able to fit directly into the trim algorithm as an additional constraining equation for redundant control surfaces. Similarly, another constraint equation could be derived to solve for minimum control surface deflections. Further research into control allocation schemes is required.
2. ***The trim and maneuver algorithms*** can be adapted to allow for other types of control effectors, such as thrust vectoring. This modification opens *AeroMech* to fighter design as well as space access vehicle (SAV) design. Furthermore, a separate algorithm can be developed, allowing the user to specify the variables and constants in the trim equations of motion. This allows the advanced designer to assess non-typical stability and control problem of interest.

3. *The dynamic stability and control algorithm* needs expansion to include the coupled 6-DOF small perturbation equations of motion analysis to allow analysis of asymmetric aircraft. In conjunction, more robust controller design techniques are required beyond the classical stability augmentation sizing techniques, to allow for the analysis of asymmetric aircraft inherently requiring more complex controllers. Actuator rate requirements must also be included for closed loop dynamic stability analysis.
4. *Aeroelastic effects* are addressed in the context of AVDS PrADO. Having integrated AeroMech into AVDS PrADO enables the designer to assess the available control power for stability and maneuver assessment for the realistically flexible high-speed flight vehicle.
5. *The effects of inertia coupling* on the flight vehicle's stability and control characteristics need to be modeled and included in the output deliverables map for high-speed fighter and SAV designs.

As the *AeroMech* system grows in complexity and capability, it is important to emphasize on physical design transparency and overall conceptual design relevance. While there are many topics in flight mechanics that can be incorporated into *AeroMech*, they must, at the same time, provide the designer with relevant information related to vehicle sizing or overall configuration selection. Clearly, *AeroMech* does not intend to replace the flight dynamicist, but instead enables the designer to successively incorporate performance-optimal stability and control solutions early into the design.

APPENDIX A

AEROMECH USER'S GUIDE

PREFACE

This document provides a guide for the use and application of the stand-alone *AeroMech* prototype computer code through the following sections:

- Tools Capability – An Introduction
- Execution of *AeroMech* (Input – Analysis – Output)

The aim of this document is give a new user a direction on how to routinely execute the program from start to finish. For a more systematic description of capabilities and limitation, please see Chapters 3 and 5.

INTRODUCTION

The stand-alone *AeroMech* prototype software is a generic stability and control tool capable of providing the following conceptual design relevant information:

1. assessment of Control power,
2. assessment of trimmed aerodynamics,
3. assessment of static and dynamic stability, for both open and close loop aircraft.

This information is generated through combining aerodynamic prediction with a generic trim, maneuver, static and dynamic stability analysis. These modules are described in detail in Chapter 3. Currently, *AeroMech* is capable of analyzing both symmetric and asymmetric aircraft for symmetric and asymmetric flight conditions providing trim, maneuver, and static stability information. The dynamic stability module assumes a plane of symmetry in order to decouple the longitudinal and lateral directional modes. Thus, the dynamic stability module is not yet applicable asymmetric

aircraft and asymmetric flight conditions. The dynamic stability module will be adapted in later versions for asymmetric aircraft and flight conditions.

In order to utilize *AeroMech*, aerodynamic prediction is required. This can be handled through any aerodynamic prediction tool as long as the data is formatted properly. The procedure for building the aerodynamic models and formatting the data for VORSTAB and Digital DATCOM are presented in Appendices B and C. For a detailed description of the *AeroMech* input files, see Appendix D.

HOW TO EXECUTE AEROMECH, INPUT-ANALYSIS-OUTPUT

The following procedure is recommended for setting up and running *AeroMech*, organized by input, analysis, and output.

INPUT

1. Identify which flight conditions and maneuvers are applicable for the aircraft. See, Chapter 2 or Reference 1 for guidance. Specifically, determine the appropriate velocities, altitudes, angle of attack range, and side-slip angle range required for each a) mission segment, b) DCFC, c) aircraft setting, and d) maneuver. Input data into DCFC.INP, the input file. An example of DCFC.INP is provided in Figure A.1.

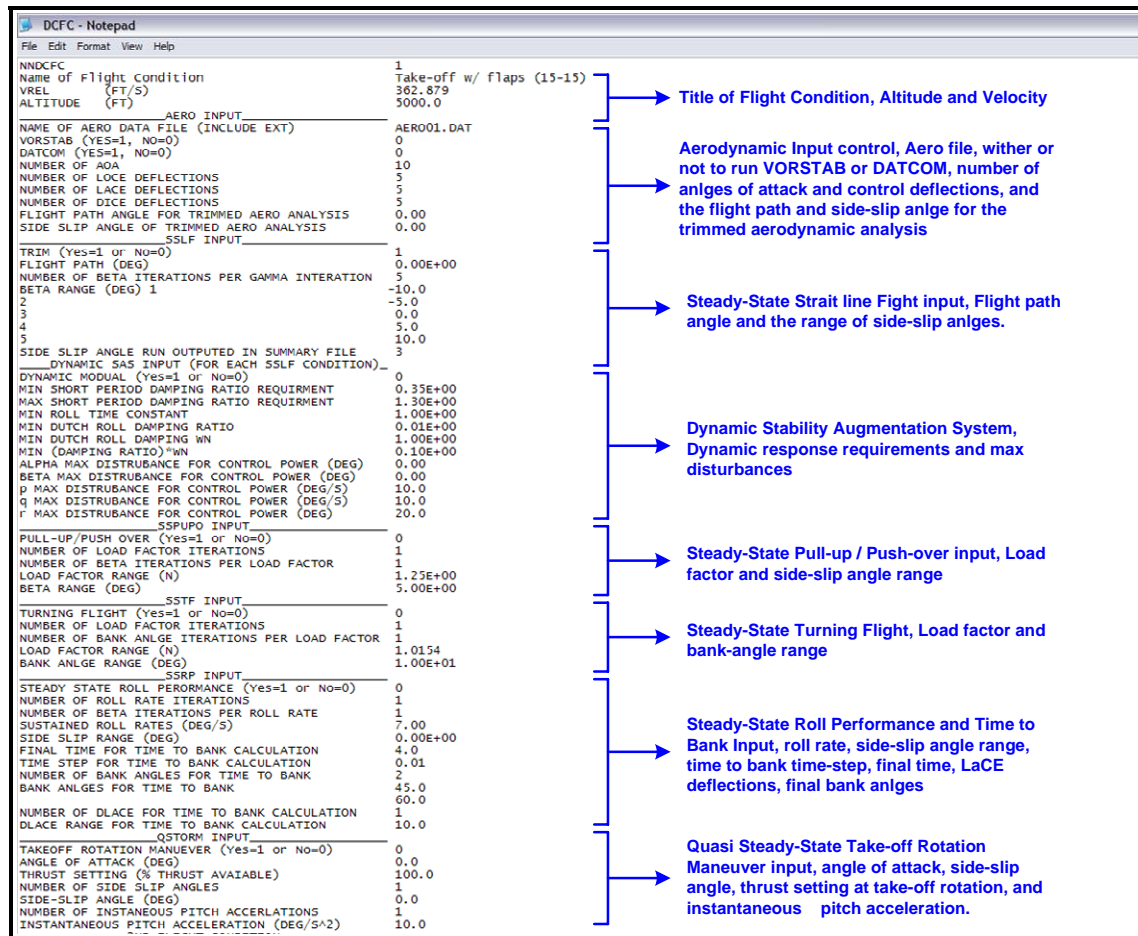


Figure A.1: DCFC Input File Example and Brief Description

- Obtain the required geometry, propulsion, weight and balance data for each, a) mission segment, b) DCFC, c) aircraft setting, and d) maneuver. This data is input into GWP.INP. An example of GWP.INP is shown in Figure A.2.

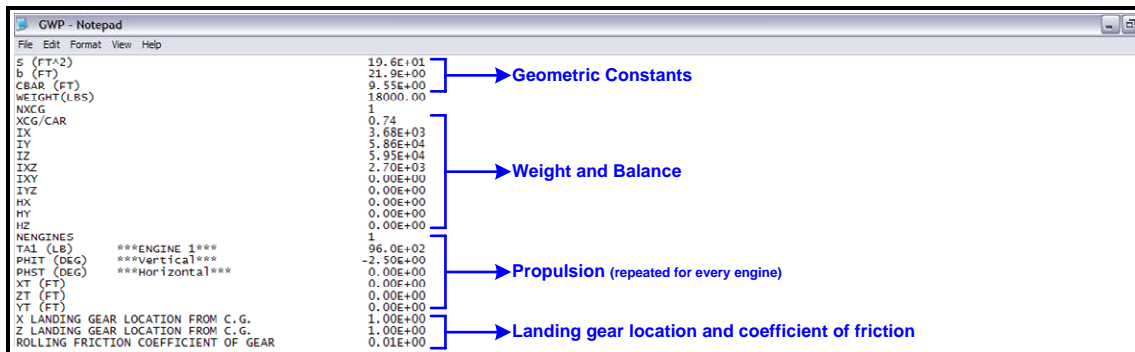


Figure A.2: GWP Input File Example and Brief Description

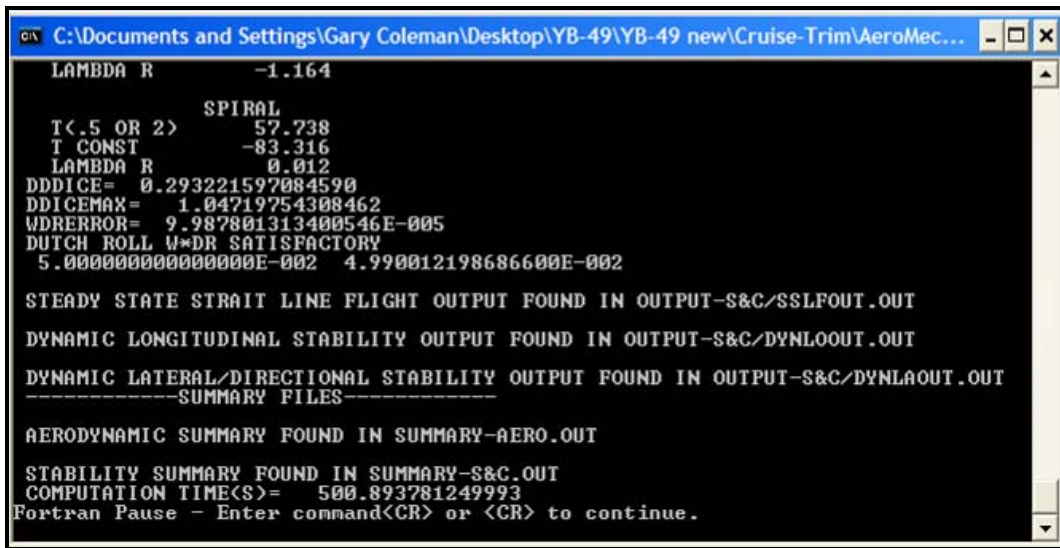
3. Build an aerodynamic look-up table for each individual flight condition. Follow the procedures outline in Appendices B and C for utilizing RUNVORSTAB.exe and RUNDATCOM.exe to respectively automate this task. An example aerodynamic look-up table is shown in Figure A.3.

Figure A.3: Aerodynamic Look-up Table Example

ANALYSIS

4. Make sure that the executable AeroMechGXX.exe (XX refers to the version) and the following input files are all in the same folder:

- DCFC.INP – contains the flight condition data and code control information;
 - GWP.INP – contains the geometric, propulsion, weight and balance data;
 - aerodynamic input file – this file name is specified in DCFC; currently the file names, Aero01.DAT, Aero02.DAT, Aero03.DAT, etc., are used by the author, where the numbering indicates which DCFC the data pertains to.
5. Double click AeroMechXX.exe. The program will output some results as the program runs for a quick inspection of the output data. Executable time can range anywhere from 30 seconds to 10 minutes. Long run times are typical when the dynamics module is operating.
 6. When finished, *AeroMech* will provide a list of the output files along with their location (Figure A.4.) In the example show, the steady-state straight-line flight DCFC and dynamic modules have been run. Thus, a separate output file is created for each module detailing the analysis at each DCFC along with two summary output files summarizing the aerodynamic and stability and control results across all DCFC's.

A screenshot of a Windows command prompt window titled "C:\Documents and Settings\Gary Coleman\Desktop\YB-49\YB-49 new\Cruise-Trim\AeroMech...". The window displays the output of an AeroMech execution. The output includes several lines of numerical data and status messages. At the end, it reports the computation time and provides instructions for the Fortran Pause.

```
LAMBDA R      -1.164
              SPIRAL
T<.5 OR 2>     57.738
T CONST       -83.316
LAMBDA R      0.012
DDICE=        0.293221597084590
DDICEMAX=     1.04719754308462
WDRERROR=     9.987801313400546E-005
DUTCH ROLL W*DR SATISFACTORY
5.000000000000000E-002  4.990012198686600E-002

STEADY STATE STRAIT LINE FLIGHT OUTPUT FOUND IN OUTPUT-S&C/SSLFOUT.OUT
DYNAMIC LONGITUDINAL STABILITY OUTPUT FOUND IN OUTPUT-S&C/DYNLOOUT.OUT
DYNAMIC LATERAL/DIRECTIONAL STABILITY OUTPUT FOUND IN OUTPUT-S&C/DYNLAOUT.OUT
-----SUMMARY FILES-----
AERODYNAMIC SUMMARY FOUND IN SUMMARY-AERO.OUT
STABILITY SUMMARY FOUND IN SUMMARY-S&C.OUT
COMPUTATION TIME(S)= 500.893781249993
Fortran Pause - Enter command<CR> or <CR> to continue.
```

Figure A.4: Example of AeroMech execution Completion

Also note the computational time is presented at the end of the run.

OUTPUT

7. Check the summary output files. The summary output files are located in the main directory called **SUMMARY-AERO.xls** and **SUMMARY-S&C.xls**. An example of **SUMMARY-S&C.xls** is shown in Figure A.5. To open, simply double click on the file.

	A	B	C	D	E	F	G
1	SUMMARY OF STATIC AND DYNAMIC STABILITY ACROSS DCFC						
2	(ALL DERIVATIVES AND ANGLES IN RAD)						
3							
4	FLIGHT CONDITIONS						
5	ALT (FT) =	30000	30000	30000	30000	30000	30000
6	VREL (FT/S) =	472.58	472.58	472.58	472.58	472.58	472.58
7	MACH =	0.475663	0.475663	0.475663	0.475663	0.475663	0.475663
8	QBAR (SLUG/FT ²)=	99.46572	99.46572	99.46572	99.46572	99.46572	99.46572
9	RHO (SLUG/FT ³)=	0.000891	0.000891	0.000891	0.000891	0.000891	0.000891
10	XCG/CBAR =	0.21	0.24	0.27	0.3	0.314	0.33
11							
12	TRIMMED AERODYNAMIC COEFFICIENTS						
13	CL =	0.375264	0.375459	0.375581	0.375637	0.375644	0.375636
14	CD =	0.014896	0.013743	0.013175	0.013185	0.013384	0.013765
15	LD =	25.19195	27.3206	28.5061	28.4889	28.06579	27.28939
16	AOA (deg) =	6.700824	6.455043	6.208619	5.96259	5.847761	5.716864
17							
18	LONGITUDINAL TRIM CONTROL ALLOCATION						
19	DSOCE (DEG) =	0	0	0	0	0	0
20							
21	LONGITUDINAL TRIM						
22	DLOCE (DEG) =	5.88424	2.50167	0.903421	4.339979	5.963889	7.836196
23	GKA =	0	0	0	0	0.341307	1.1
24	GKQ =	0.0945	0.017699	0	0	0	0
25	DDLCE(DEG) =	0.945005	0.176988	0	0	1.706533	5.5
26							
27	LATERAL/DIRECTIONAL						
28	DLACE (DEG) =	0	0	0	0	0	0
29	DDICE (DEG) =	0	0	0	0	0	0
30	GKP =	0	0	0	0	0	0
31	GKB =	1.546991	1.548477	1.549132	0	1.552157	1.552886
32	GKR =	0.809271	0.831326	0.853795	0	0.889957	0.903693
33	DDLACE(DEG) =	0	0	0	0	0	0
34	DDDICE(DEG) =	15.82767	16.05564	16.28361	0	16.66036	16.80036
35							
36	STATIC STABILITY						
37	LONGITUDINAL						
38	CMA =	-0.41413	-0.30122	-0.182	-0.05664	0.003091	0.07232
39	XNP/CBAR =	0.304975	0.306259	0.310852	0.312624	0.313313	0.313971
40	STATIC MARGIN =	0.094975	0.086259	0.040852	0.012624	-0.00069	-0.01603
41	XMP/CBAR =	0.323034	0.324584	0.325611	0.325986	0.326082	0.326107
42	MANUEVER MARGIN =	0.113034	0.084584	0.055611	0.025986	0.012082	-0.00369
43							
44	LATERAL						
45	CYB =	-0.00137	-0.00141	-0.00145	-0.00149	-0.0015	-0.00152
46	CLB =	-0.00077	-0.00077	-0.00076	-0.00075	-0.00074	-0.00073
47	CNB =	0.000263	0.000251	0.000245	0.000229	0.000226	0.000222
48							
49	DYNAMIC STABILITY						

Figure A.4: Example of SUMMAR-S&C.xls

- Check the detailed output files. These output files are located in the OUTPUT-Aero and OUTPUT-S&C folders. To open these files with a text editor like Notepad, simply double click the file to open. To open the files in Excel, **right click the file**, click **open with**, and **Excel** (Figure A.5).

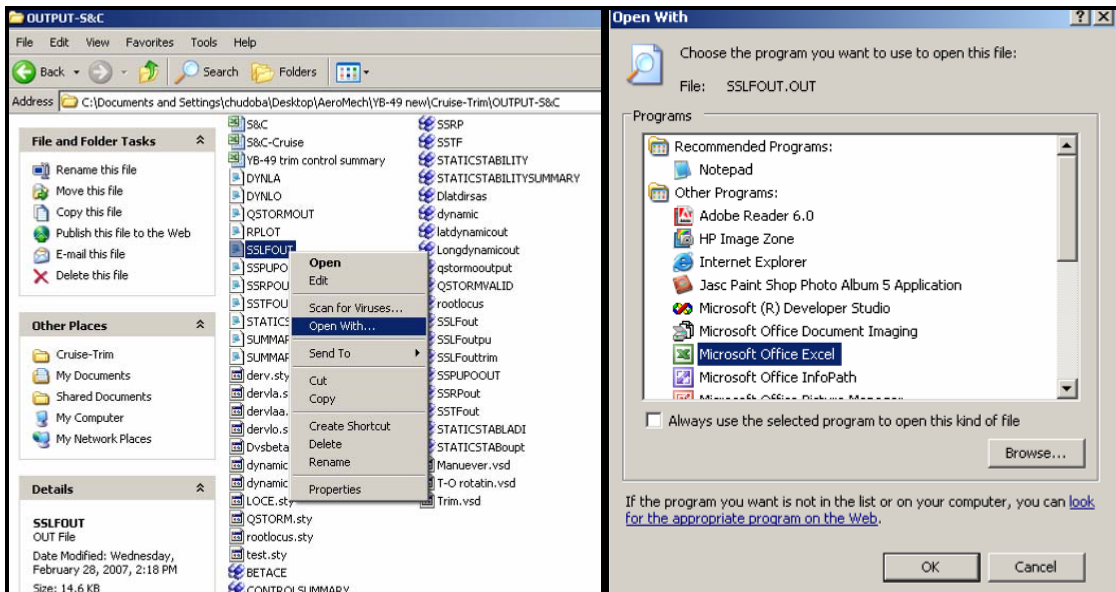


Figure A.5: Opening Text Based Output Files in Excel

The text output files are described in Table A.1.

Table A.1 AeroMech Text Output files Organized by Output Folder

Output File	Description
OUTPUT-Aero	
LINAERO.OUT	Contains all of the linear derivatives calculated for each flight condition.
TRIMAERO.OUT	Contains both the trimmed and untrimmed aerodynamic data set for plotting.
OUTPUT-S&C	
DYNLA.OUT	Contains both the open and closed loop static stability roots, dynamics properties, gain settings and additional control power for the lateral/directional analysis.
DYNLO.OUT	Contains both the open and closed loop static stability roots, dynamics properties, gain settings and additional control power for the longitudinal analysis.
QSTORMOUT.OUT	Contains the take-off rotation velocity, horizontal acceleration, weight on the main landing gear, LaCE deflections and DiCE deflections as a function of the instantaneous pitch acceleration and side-slip angles. The results are repeated for each DCFC.
RPLOT.OUT	Contains the open-loop root locus plot data for all flight conditions.
SSLFOUT.OUT	Contains the angle of attack, bank angle, thrust setting, LaCE deflection, LoCE deflection, and DiCE deflection as a function of flight path angle, and side-slip angle. Results are repeated for each DCFC.
SSPUPOOUT.OUT	Contains the angle of attack, bank angle, thrust setting, LaCE deflection, LoCE deflection, and DiCE deflection as a function of load factor, and side-slip angle. Results are repeated for each DCFC.
SSRPOUT.OUT	Contains the angle of attack, bank angle, thrust setting, LaCE deflection, LoCE deflection, and DiCE deflection as a function of roll rate, and side-slip angle. Also contains the results from the time to bank calculations. Results are repeated for each DCFC.
SSTFOUT.OUT	Contains the angle of attack, side-slip angle, thrust setting, LaCE deflection, LoCE deflection, and DiCE deflection as a function of load factor, and bank angle. Results are repeated for each DCFC.
STATICSTAB.OUT	Contains both the longitudinal and lateral/directional stability derivatives as a function of angle of attack for each DCFC.

9. Each of these output files are also transferred into *Tecplot* input file format. To open, simply double click the appropriate *Tecplot* file. See *Tecplot 10 User's Manual* for more information on formatting and operating the *Tecplot* files. These files are summarized in Table A.2.

Table A.1 AeroMech Text Output files Organized by Output Folder

Output File	Description
OUTPUT-Aero	
AEROSUMMARY.pt	Contains the same information as in SUMMARY-AERO.xls.

TRIMAERO.plt	Contains the same information as TRIMAERO.OUT.
OUTPUT-S&C	
CONTROLSUMMARY.plt	Contains the same control information as found in SUMMARY-S&C.xls.
DYNAMICSTABILITYSUMMARY.plt	Contains the dynamic stability information as found in SUMMARY-S&C.xls.
QSTORM.plt	Contains the same information as QSTORMOUT.OUT.
SSLF.plt	Contains the same information of SSLFOUT.OUT.
SSPUPO.plt	Contains the same information as SSPUPOOUT.OUT.
SSRP.plt	Contains the same information as SSRPOUT.OUT.
STATICSTABILITY.plt	Contains the same information as STATICSTAB.OUT.
STATICSTABILITYSUMMARY.plt	Contains the same static stability information as found in SUMMARY-S&C.xls.

Since *AeroMech* is under constant development and certain aspects may change from version to version, therefore, some of this information presented here may not relate to the version of *AeroMech* you have. If this occurs, contact the AVD Lab at the University of Texas at Arlington for the most up-to-date user's guide. For more information, please see the following sources,

- For more information about the theory and application of *AeroMech* see Chapters 3 and 5.
- For more information related to the input file structure, please see Appendix D.
- For more information on developing the untrimmed aerodynamic input file, see Appendices B and C.

- For more information on the source code, see Appendix E.

APPENDIX B

DIGITAL DATCOM USER'S GUIDE

PREFACE

This document provides a quick tour of the use of Digital DATCOM including:

- Introduction to the Tools Capability
- How to Execute Digital DATCOM, Input – Analysis – Output
- How to Build a Model and Visualize the Geometry
- How to Automate Digital DATCOM with RUNDATCOM.exe

The aim of this document is give a new user a feel of how to routinely execute the program from start to finish. For a more systematic description of capabilities, limitations, variable details, and further guidance, please see *The USAF Stability and Control DATCOM Volume I User's Manual*⁷, and for details on the methods used, please see *USAF Stability and Control DATCOM* by R. D. Finck.

INTRODUCTION

Digital DATCOM is an executable collection of the semi-empirical hand book methods and procedures contained in the *USAF Stability and Control DATCOM* series for the rapid calculation of aerodynamic and control derivatives. This tool is not a true stability and control tool because it does not address issues such as maneuverability, dynamic stability, etc. It is rather an aerodynamic tool for calculating aerodynamic contributions of aircraft components and control surfaces.

This code contains methods for tail-aft configurations (TAC), tail first configurations (TFC), flying wing configurations (FWC), lifting bodies, and other such configurations. For more information on the complete applicability of the tool see *USAF Stability and Control DATCOM Volume I User's Manual*⁷.

HOW TO EXECUTE THE CODE

The following steps should be followed in executing Digital DATCOM; the steps follow the input, analysis, and output pattern.

INPUT

1. Open the Digital DATCOM folder and make sure that your input file is in the same folder as the executable.
2. The input file is in a text format and can be edited with any text editor. The easiest way to get started is to open one of the example input files and adapt it to your problem.

The input file contains a series of control cards. The basic control cards are BUILD, CASE ID, SAVE, and NEXT CASE. With these control cards, multiple configurations can be run and analyzed. The BUILD control card is where all of the aircraft input data is entered. An example of this card is shown in Figure B.1.

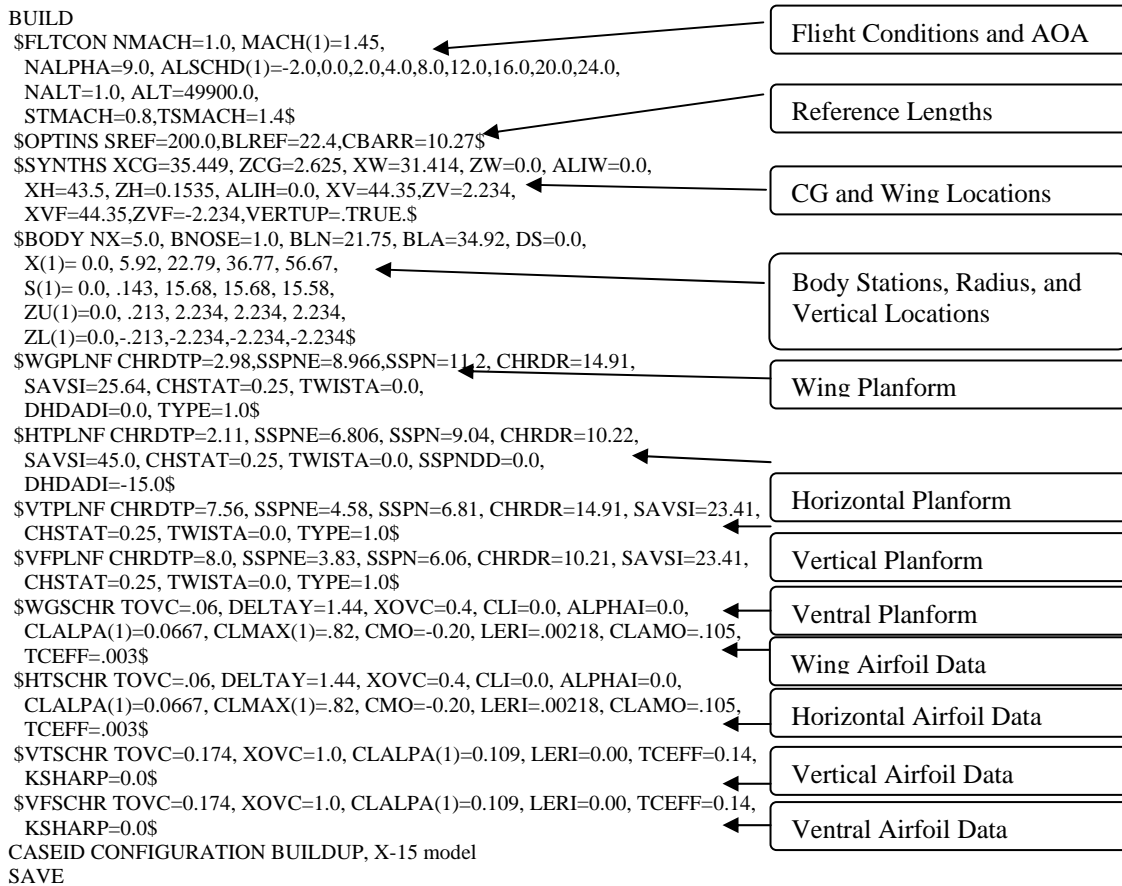


Figure B.1: Digital DATCOM input file structure.

As shown here, the BUILD control card is broken up into flight conditions, reference lengths, c.g. and wing locations, body geometry, wing planforms, and airfoil data.

- Multiple cases can be run with Digital DATCOM in the same input file and the output is print below each preceding case. This is done by adding the NEXT CASE, CASE ID, and SAVE control cards into the input file.

An example input file of this is shown in Figure B.2. The figure shows the input file for the constant area wing trade study. In this study a variety of wing planforms

have been compared for aerodynamic performance. To simplify the tasks at hand, each wing was run as a separate case in one input file.

```

BUILD
$FLTCON NMACH=1.0, VINFL(1)=324.0533,
  ALT=0.0,
  NALPHA=17.0, ALSCHD(1)=-4.0,-2.0,0.0,2.0,4.0,6.0,8.0,10.0,12.0,14.0,16.0,18.0,
  20.0,25.0,30.0,35.0,40.0$
$OPTINS SREF=245.0,BLREF=12.40,CBARR=23.35$
$SYNTHS XCG=16.832, ZCG=4.80, XW=0.0, ZW=0.0, ALIW=0.0$
$WGPLNF CHRDT=0.0,SSPNE=4.73,SSPN=7.29, CHRDR=34.30,
  SAVSI=78.0, CHSTAT=0.0, DHDADI=0.0, TYPE=1.0$
$WGSCHR TOVC=.06, DELTAY=2.11, XOVC=0.39891, CLI=0.1, ALPHAI=0.0,
  CLALPA(1)=0.12, CLMAX(1)=1.15, CMO=-0.0375, LERI=.00256,
  CLAMO=.11, CLMAXL=1.0$
CASEID CONFIGURATION BUILDUP, Wing tradeoff case 1 OUXP 78degree
NEXT CASE
SAVE
BUILD
$FLTCON NMACH=1.0, VINFL(1)=324.0533,
  ALT=0.0,
  NALPHA=17.0, ALSCHD(1)=-4.0,-2.0,0.0,2.0,4.0,6.0,8.0,10.0,12.0,14.0,16.0,18.0,
  20.0,25.0,30.0,35.0,40.0$
$OPTINS SREF=245.0,BLREF=18.544,CBARR=14.839$
$SYNTHS XCG=10.113, ZCG=0.0, XW=0.0, ZW=0.0, ALIW=0.0$
$WGPLNF CHRDT=5.182,SSPNE=9.272,SSPN=9.272, CHRDR=21.24,
  SAVSI=60.0, CHSTAT=0.0, DHDADI=0.0, TYPE=1.0$
$WGSCHR TOVC=.06, DELTAY=2.11, XOVC=0.39891, CLI=0.1, ALPHAI=0.0,
  CLALPA(1)=0.12, CLMAX(1)=1.15, CMO=-0.0375, LERI=.00256,
  CLAMO=.11, CLMAXL=1.0$
CASEID CONFIGURATION BUILDUP, Wing tradeoff case 2 60degree
SAVE

```

Figure B.2: Example of Multiple Cases for Digital DATCOM

After each case input section, there is a text line that allows a title to be entered describing the run case. This title will be displayed in the output file above individual case datasets.

For further examples and detailed explanations of the input variables, see the *USAF Stability and Control DATCOM, Volume 1, User's Manual*⁷.

ANALYSIS/EXECUTION

- Next save the file (example: **X15.inp**) and double click the **DATCOM.exe**. The following Screen will be displayed (Figure B.3).

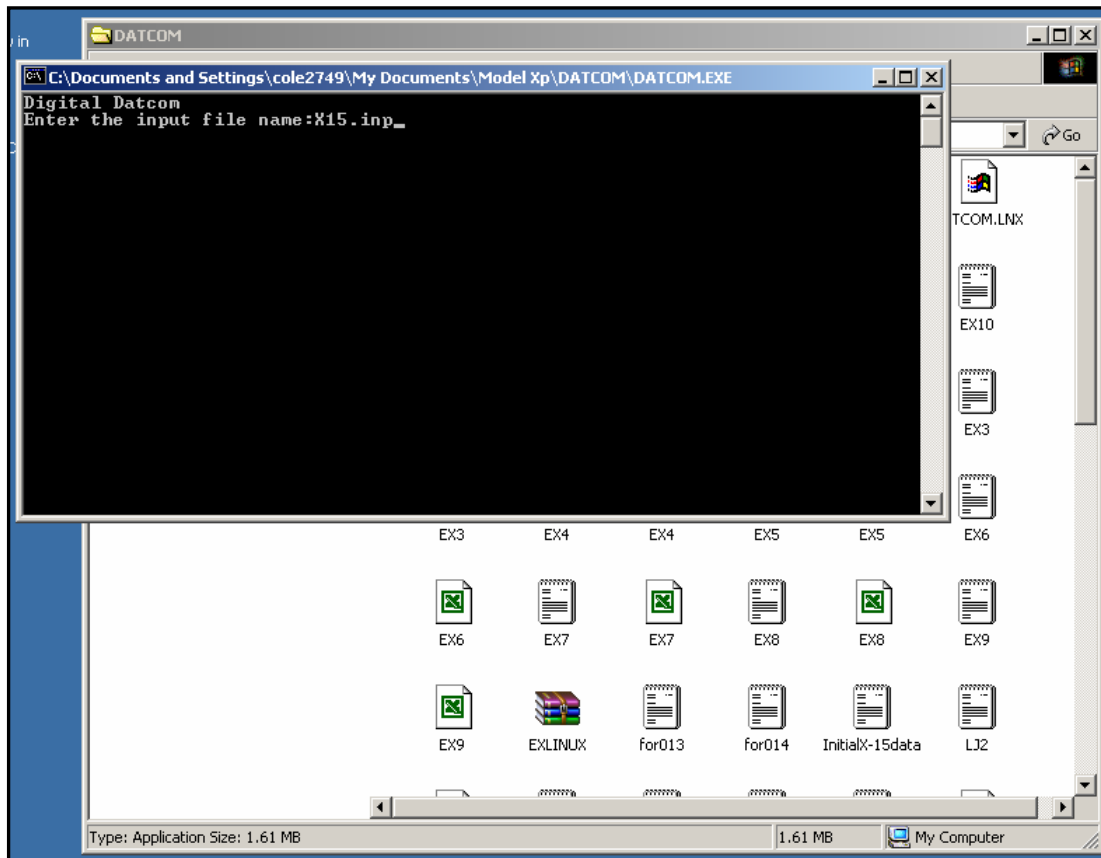


Figure B.3: Input File Name Prompt for Digital DATCOM

Type in the name of the input file and hit ENTER.

- Wait approximately 3 seconds and open **datcom.out**. This is the name of the output file and any old data in it will be over written.

OUTPUT

- The output file is organized in the following manner. First, a short disclaimer and description, then a debug routine that searches the input file for errors and display's them as follows (Figure B.4).

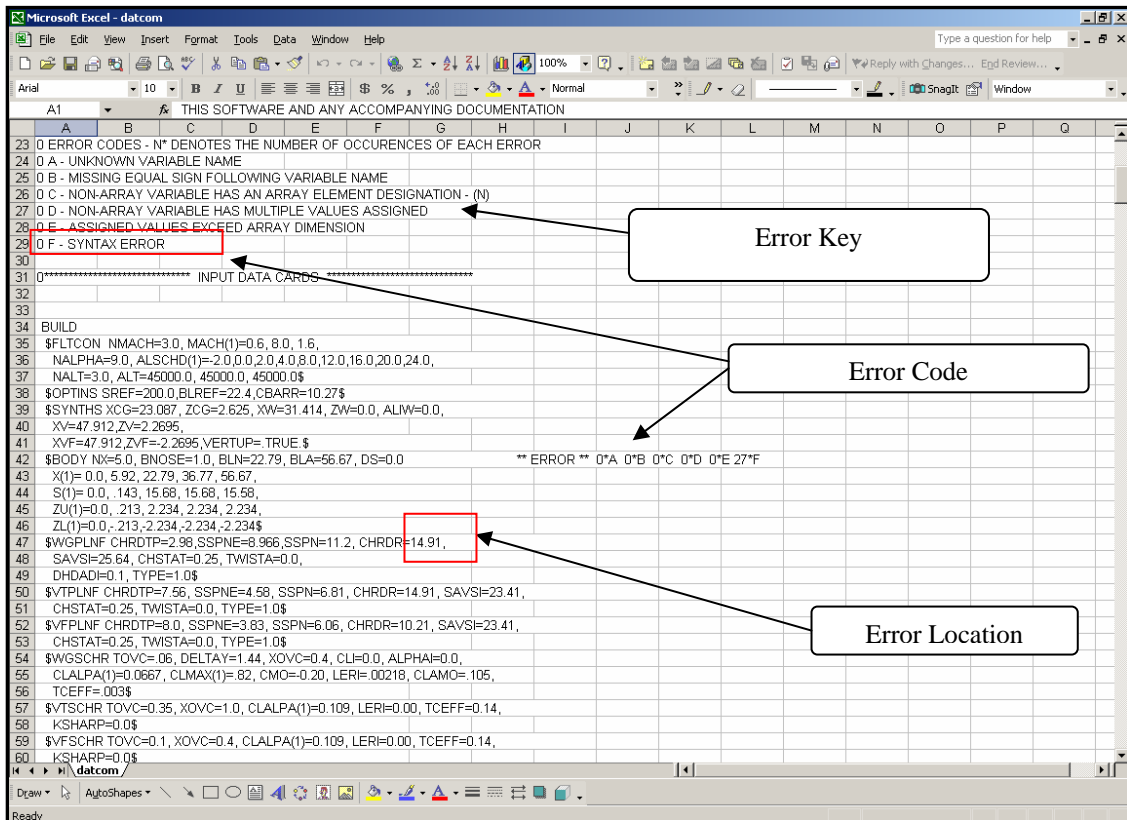


Figure B.4: Output File Error Code for Digital DATCOM

In this case, a comma is missing in row 42 leading to a number of syntax errors indicated. A large number of syntax errors are associated with a missed place comma because the program cannot determine the start of the next variable.

7. The output for each case run is organized as follows:

- input for the specific case;
- output for each component;
- output for each combination of components.

An example output section is presented below for the wing-body, horizontal tail, vertical fin, and ventral fin case of the X-15 model.

The screenshot shows a Microsoft Excel spreadsheet with the following data:

```

327 1 AUTOMATED STABILITY AND CONTROL METHODS PER APRIL 1976 VERSION OF DATCOM
328 CHARACTERISTICS AT ANGLE OF ATTACK AND IN SIDESLIP
329 WING-BODY-HORIZONTAL TAIL-VERTICAL TAIL-VENTRAL FIN CONFIGURATION
330
331 ----- FLIGHT CONDITIONS ----- REFERENCE DIMENSIONS -----
332 MACH ALTITUDE VELOCITY PRESSURE TEMPERATURE REYNOLDS REF. REFERENCE LENGTH MOMENT REF. CENTER
333 NUMBER NUMBER AREA LONG. LAT. HORIZ VERT
334 FT FT/SEC LB/FT**2 DEG R 1/FT FT**2 FT FT FT FT
335 0 1.430 60700.00 1384.19 1.4605E+02 389.970 1.0126E+06 200.000 10.270 22.400 38.315 2.625
336 0 -----DERIVATIVE (PER DEGREE)-----
337 0 ALPHA CD CL CM CN CA XCP CLA CMA CYB CNB CLB
338 0
339 -2.0 0.036 -0.125 0.0298 -0.127 0.032 -0.235 6.209E-02 -1.488E-02 -2.318E-02 8.465E-03 -3.642E-03
340 0.0 0.033 0.000 0.0000 0.000 0.033 ***** 6.250E-02 -1.487E-02 -3.340E-03
341 2.0 0.036 0.126 -0.0290 0.128 0.032 -0.227 6.265E-02 -1.448E-02 -3.033E-03
342 4.0 0.045 0.257 -0.0564 0.259 0.027 -0.218 6.284E-02 -1.410E-02 -2.724E-03
343 8.0 0.080 0.521 -0.1065 0.527 0.007 -0.202 6.334E-02 -1.331E-02 -2.096E-03
344 0NOTE - CANARD CONFIGURATION EFFECTIVE EPSOLN AND D(EPSOLN)/D(ALPHA) ARE AVAILABLE AS PARTIAL OUTPUT AND IN THE FACT ARRAY
345 0ANALYSIS TERMINATED AT ALPHA= 8.0 BECAUSE LEADING EDGE SHOCK IS DETACHED.
346 Return to main program from M57071
347 1 END OF JOB.
348
349
350
351
352
353
354
355
356
357
358
359
360
361
362
363
364

```

Figure B.5: Example Output for Digital DATCOM

The raw output is in text format and must be exported into individual columns using the *Text to Columns* command under the Data menu. From this data, plots of the aerodynamic and stability derivatives can be produced. Automation of

output formatting is also accomplished using the program **RUNDATCOM.exe** and *AeroMech*. RUNDATCOM is explained in a later section.

8. To use the more advanced features of Digital DATCOM, additional control cards are required and these are specified in the user's manual⁷.

How to Build a Model and Input Files

The easiest way to begin to build a model in Digital DATCOM is to modify a pre-existing example input file component by component. The following procedure is recommended for building a new Digital DATCOM Model.

1. Identify the flight conditions you wish to analyze. For example, a commercial transport may require the investigation of the following mission segments: take-off, climb, cruise, descent, and approach. Identify the Mach number, altitude, and angle of attack range for each flight condition.
2. Identify the input variables required for each component. In the *USAF Stability and Control, Volume I, User's Manual*, a detailed list of all variables is given for each component (wing, fuselage, etc.).
3. Build one flight condition with the aircraft geometry and execute.
4. Check the output file for error codes and visually inspect the output data. Sometimes no input errors are found but Digital DATCOM may not have a method for the geometry and/or flight condition you have entered (Figure B.6).

1
RETURN TO MAIN PROGRAM FROM W21000

AUTOMATED STABILITY AND CONTROL METHODS PER APRIL 1976 VERSION OF DATCOM
CHARACTERISTICS AT ANGLE OF ATTACK AND IN SIDESLIP
WING ALONE CONFIGURATION
CONFIGURATION BUILDUP, YB-49, Case 1

MACH NUMBER	FLIGHT CONDITIONS		TEMPERATURE	REYNOLDS NUMBER	REFERENCE DIMENSIONS				MOMENT REF. CENTER VERT				
	ALTITUDE	VELOCITY			REF. AREA	REFERENCE LONG.	REFERENCE LENGTH LAT.	HORIZ					
	FT	FT/SEC	DEG R	1/FT	FT**2	FT	FT	FT	FT				
0.747	40000.00	723.07	389.970	1.4237E+06	4000.000	26.131	172.000	24.790	0.000				
0	ALPHA	CD	CL	CM	CN	CA	XCP	CLA	CMA	DERIVATIVE (PER DEGREE)	CYB	CNB	CLB
-4.0	0.024	NDM	NDM	NDM	NDM	-NaN	-NaN	-NaN	NDM	NDM	NDM	NDM	NDM
-2.0													
0.0													
2.0													
4.0													
6.0													
8.0													
10.0													
12.0													

0*** NDM PRINTED WHEN NO DATCOM METHODS EXIST

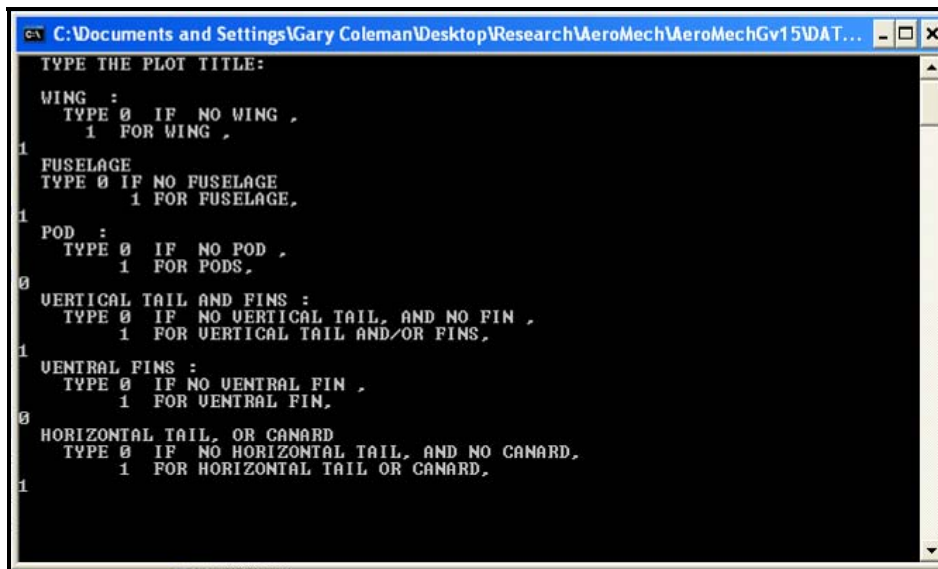
No DATCOM Method (NDM)

Figure B.6: Example of No DATCOM Method Error for Digital DATCOM

In this example, the Mach number was set to the transonic regime which DATCOM cannot calculate without having entered additional experimental data externally. If you encounter this problem, check the user's manual for applicability.

5. Once the input file is executing without errors and it has been checked that the methods apply, check the geometry has been entered properly with **DATCOM PLOT.exe**:

- first save the input file as **for005.dat**;
- double click DATCOM PLOT.exe;
- DATCOM PLOT will prompt you to name the plot (not required), and prompt you to enter a 1 or 0 if the aircraft has the specified feature (Figure B.7).



```
C:\Documents and Settings\Gary Coleman\Desktop\Research\AeroMech\AeroMechGv15\DAT...
TYPE THE PLOT TITLE:
WING :
  TYPE 0 IF NO WING ,
  1 FOR WING ,
1
FUSELAGE
  TYPE 0 IF NO FUSELAGE
  1 FOR FUSELAGE,
1
POD :
  TYPE 0 IF NO POD ,
  1 FOR PODS,
0
VERTICAL TAIL AND FINS :
  TYPE 0 IF NO VERTICAL TAIL, AND NO FIN ,
  1 FOR VERTICAL TAIL AND/OR FINS,
1
VENTRAL FINS :
  TYPE 0 IF NO VENTRAL FIN ,
  1 FOR VENTRAL FIN,
0
HORIZONTAL TAIL, OR CANARD
  TYPE 0 IF NO HORIZONTAL TAIL, AND NO CANARD,
  1 FOR HORIZONTAL TAIL OR CANARD,
1
```

Figure B.7: Example of DATCOM PLOT.exe input Commands

- open fort.file with *Tecplot* Loader (Figure B.9);

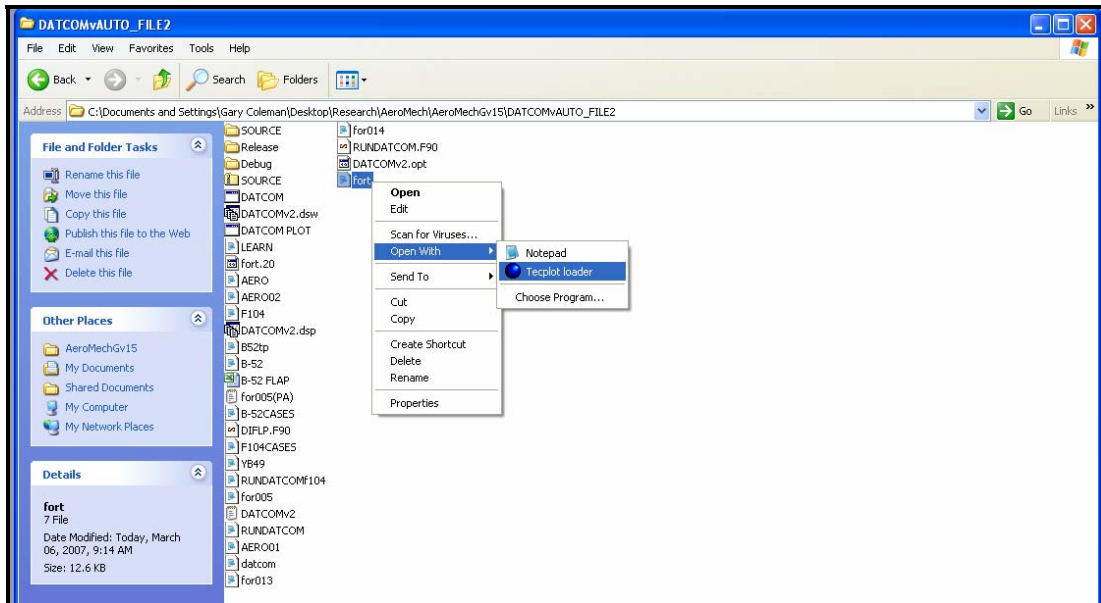


Figure B.9: Demonstration of opening *Tecplot* Visualization from DATCM PLOT.exe

- check the geometry for visual errors; sometimes surfaces can be placed incorrectly or typos in the input file can occur; be sure to inspect all 2d and 3d views before proceeding (Figure B.10).

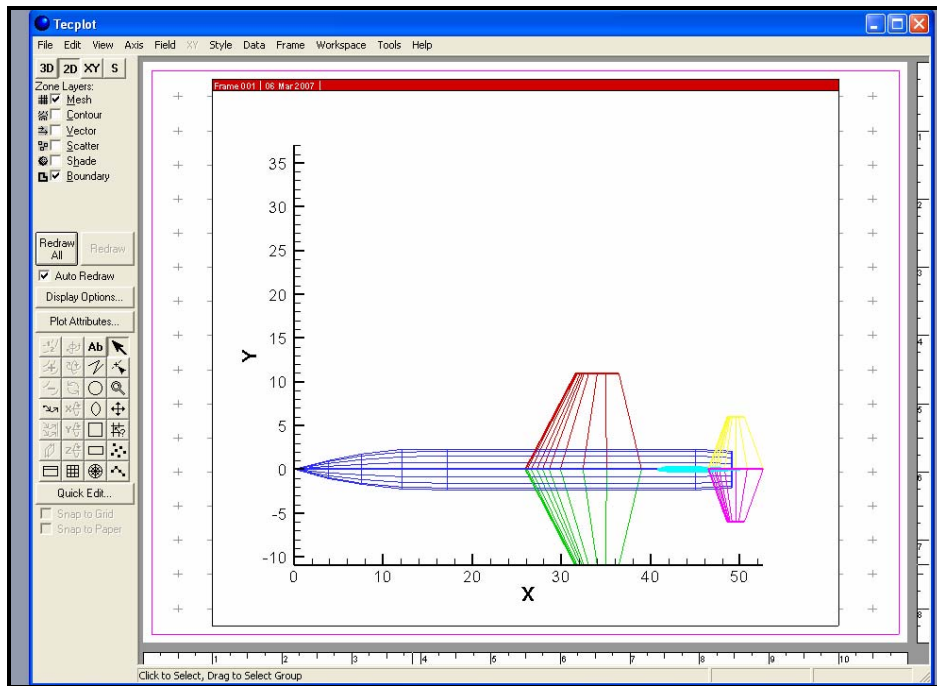


Figure B.10: Example of DATCOM PLOT Visualization in TECPLOT

6. with the aircraft geometry correctly entered, check the flight condition data for plausibility by using your own engineering judgment and by comparing the results to any reference data or hand calculations, if available;
7. now you are ready to run the remainder of the flight conditions; be sure to check for No DATCOM Method (NDM) error in each flight condition. DATCOM methods are typically bounded by speed regimes.

Now you are ready to begin the glorious journey that is Digital DATCOM. If you have any problems take it up with the complaint department or see the *USAF Stability and Control, Volume I, User's Manual* for further information.

HOW TO AUTOMATE DIGITAL DATCOM WITH RUNDATCOM.EXE

Digital DATCOM is structured to run a single control effector in one case. In order to build the aerodynamic lookup table for *AeroMech*, it is required to execute multiple cases. To automate this sweep, RUNDATCOM.exe has been developed to automate the following.

1. ***Running a digital DATCOM case for each LoCE, LaCE, and DiCE.*** Due to the fact that Digital DATCOM is only capable of handling one control effector at a time, several execution runs are required to generate the clean aerodynamics dataset including complete control force and moment increments.

2. ***Running several cases for an all-moveable horizontal tail cases for the LoCE.*** In Digital DATCOM, if an all-movable horizontal surface is required, then the incidence of the surface must be varied requiring a separate execution run for each incidence angle of interest.

INPUT

1. Build the input in the file RUNDATCOM.INP according to the same format as the *AeroMech* DCFC.IN and GWP.IN files, which contains the variables described in Table B.1.

Table B.1 Required VOROP.INP input for RUNVORSTAB

AeroMech Input File	Units	Description
NAME OF AERO FILE	-	Number of DCFC's to be run.
TOTAL NUMBER OF CASES	-	Total number of cases that are in the digital DATCOM input file for007.dat.
CONFIGURATION CODE	-	This number identifies the aircraft configuration type. In Digital DATCOM the configurations are stored according to the code found in Table B.2.
CASE NUMBER OF LOCE RUN	-	The case number of the case that contains the LoCE definition.
ALL MOVEABLE HORIZONTAL TAIL	-	If an all-moveable horizontal tail is required, then set to 1, otherwise 0.
1ST AMHT CASE	-	The case number which has the first all-moveable horizontal tail deflection. Set to any none zero value if not used.
LAST AMHT	-	The case number which has the last all-moveable horizontal tail deflection. Set to any none zero value if not used.
NUMBER OF LOCE DEFLECTIONS		The numerical value of the new control surface. If there are 5 control surfaces on the wing and the new one is the outer most surfaces, than its value is 5. Conversely, if the surface is the inner most surface the value is 1.
LOCE DEFLECTIONS		Number of LoCE deflection in VORSTAB.
CASE NUMBER OF LACE RUN		List the numerical values of the LoCE deflections; one on each line.
NUMBER OF LACE DEFLECTIONS		Number of LaCE deflection in VORSTAB.
LACE DEFLECTIONS		List the numerical values of the LaCE deflections; one on each line.
NUMBER OF DICE DEFLECTIONS		Number of DiCE deflections in VORSTAB.
ZV		List the numerical values of the DiCE deflections; one on each line.
YZ		Drag increment due to landing gear.
DICE DEFLECTIONS		Pitching moment increment due to landing gear.

For example, Figure B.12 shows these options for the F-104 RUNDATCOM.INP file.

```

RUNDATCOM104 - Notepad
File Edit Format View Help
NAME OF AERO OUTPUT FILE      AERO01.DAT
TOTAL NUMBER OF CASES        6
CASE NUMBER OF CLEAN CONFIGURATION 4
CONFIGURATION CODE (B=1, W=2, ..., BWHV=11) 11
CASE NUMBER OF LOCE RUN (NOT USED IF AMHT=1) 1
ALL MOVEABLE HORIZONTAL TAIL (YES=1, NO=0) 1
1ST AMHT CASE                 1
LAST AMHT CASE                 4
NUMBER OF LOCE DEFLECTIONS     4
LOCE DEFLECTIONS               -15.0
                              -10.0
                              -5.0
                              0.0
CASE NUMBER OF LACE RUN        5
NUMBER OF LACE DEFLECTIONS     -10.0
LACE DEFLECTIONS              -5.0
                              0.0
                              5.0
                              10.0
NUMBER OF DICE DEFLECTIONS     5
ZV (Z DISTANCE FROM XCG TO A.C. OF VT IN FT) 5.27
LV (Z DISTANCE FROM XCG TO A.C. OF VT IN FT) 16.6
DICE DEFLECTIONS              -10.0
                              -5.0
                              0.0
                              5.0
                              10.0
Ln 1, Col 1

```

Figure B.12: RUNDATCOM.INP for the F-104 Example

The configuration code is utilized internally by digital DATCOM to store the specific aerodynamic data for each component and all combinations of components.

Table B.2 defines this code.

Table B.2 Required VOROP.INP input for RUNVORSTAB

Configuration Code Number	Acronym	Description
1	B	Body only
2	W	Wing only
3	H	Horizontal only
4	VT	Vertical only
5	VF	Ventricle only
6	BW	Body and Wing
7	BH	Body and Horizontal tail
8	BV	Body and Vertical tail
9	BWH	Body, Wing and Horizontal tail
10	BWV	Body, Wing and Vertical tail
11	BWHV	Body, Wing, Horizontal tail and Vertical tail

- Input the Digital DATCOM cases into the for005.dat input file according to the procedure outlined in *How to build a Digital DATCOM Model*. An example is shown in Figure B.13 for the F-104 for005.dat file.

```

for005 - Notepad
File Edit Format View Help
$FLTCON NMACH=1.0, NALT=1.0, MACH=0.35, ALT=4000.0,
NALPHA=0.0, ALSCHD(1)=-4.0, -2.0, 0.0, 2.0, 4.0, 6.0, 8.0, 10.0, 12.0, 14.0,
STMACH=0.885
$OPTINS SREF=4000.0, BLREF=-172.0, CBARR=-26.1315
$SYNTHS XCG=23.48, ZCG=0.0, XW=0.0, ZW=0.0, ALIW=0.05
$WGPLNF CHRDTF=0.0, SSPNE=86.0, SSPN=86.0, CHRDR=37.33,
$AVSI=29.933, CHSTAT=0.0, DHDAI=.88, TWISTA=-4.0, TYPE=1.05
$WGSCHR TOVC=.18, DELTAY=0.82, XOVC=0.4, CLI=0.00, ALPHAI=-.10,
CLALPA(1)=0.100, CLMAX(1)=1.37, CMO=0.00, LERI=.0196,
CLMAXL=1.3, CAMBER=.TRUE,
$SYNPLP FTTYPE=1.0, NDELTA=5.0,
DELTA=-10.0, -10.0, 0.0, 10.0, 20.0,
PHETE=0.05261,
PHETEP=0.0445,
CHRDFI=5.006,
CHRDFO=4.993,
SPANFI=36.03,
SPANFO=67.1345
DAMP
CASEID CONFIGURATION BUILDUP, YB-49, Case 1
SAVE
NEXT CASE
$FLTCON NMACH=1.0, NALT=1.0, MACH=0.35, ALT=4000.0,
NALPHA=0.0, ALSCHD(1)=-4.0, -2.0, 0.0, 2.0, 4.0, 6.0, 8.0, 10.0, 12.0, 14.0,
STMACH=0.885
$OPTINS SREF=4000.0, BLREF=-172.0, CBARR=-26.1315
$SYNTHS XCG=23.48, ZCG=0.0, XW=0.0, ZW=0.0, ALIW=0.05
$WGPLNF CHRDTF=0.0, SSPNE=86.0, SSPN=86.0, CHRDR=37.33,
$AVSI=29.933, CHSTAT=0.0, DHDAI=.88, TWISTA=-4.0, TYPE=1.05
$WGSCHR TOVC=.18, DELTAY=0.82, XOVC=0.4, CLI=0.00, ALPHAI=-.10,
CLALPA(1)=0.100, CLMAX(1)=1.37, CMO=0.00, LERI=.0196,
CLMAXL=1.3, CAMBER=.TRUE,
$SYNPLP STYPE=.0, NDELTA=5.0,
DELTA=-10.0, -5.0, 0.0, 5.0, 10.0,
DELTAR=10.0, 5.0, 0.0, -5.0, -10.0,
CHRDFI=5.006,

```

Figure B.12: RUNDATCOM.INP for the F-104 Example

ANALYSIS/EXECUTION

- Make sure that the executable RUNDATCOM.EXE, RUNDATCOM.INP and for005.dat are all in the same folder.
- Double click RUNDATCOM.exe.

OUTPUT

- The output file specified will appear in the directory. In the example shown in Figure B.5, the output file name was Aero01.dat.

APPENDIX C

VORSTAB USER'S GUIDE

PREFACE

This document provides a quick tour of the use of the non-linear vortex lattice method VORSTAB. This includes:

- introduction to the tool capability;
- how to execute VORSTAB, Input – Analysis – Output;
- how to build a VORSTAB model and visualize the geometry;
- how to Automate VORSTAB with RUNVORSTAB.exe.

The aim of this section is give a new user a feel of how to routinely execute the program from start to finish. For a more detailed description of its capabilities, limitations, variable details, and further guidance, please see *User's Manual for VORSTAB Code (Version 3.2)*⁵ by Dr. C. Edward Lan.

INTRODUCTION

VORSTAB is a non-linear vortex lattice method (VLM) capable of analyzing symmetric flight vehicle configurations consisting of 6 surfaces and 1 fuselage, or 1 asymmetric wing for subsonic and supersonic flow. VORSTAB has a variety of options that allow the user to model different geometries and aerodynamic phenomena. These options are listed below.

- vortex lift;
- rounded leading edges for vortex lift calculations;
- vortex beak down effect of vortex lift calculations;
- augmented vortex lift;
- nonlinear, 2d airfoil section data input;

- in-ground effects;
- camber and thickness distribution.

The application of these non-linear additional features depends upon the aerodynamic phenomena you wish to model. Initial guidelines for when to use these options are presented in the *How to Build a Model* section.

HOW TO EXECUTE VORSTAB, INPUT-ANALYSIS-OUTPUT

Executing VORSTAB includes building the input file, running the VORSTAB executable and reviewing the output. The following procedure is recommended for executing VORSTAB.

INPUT

1. Make sure that the VORSTAB executables and the input file are located in the same folder. The VORSTAB executables are:
 - **vorstab.exe** – main executable responsible for all calculations;
 - **fcontec.exe** – Post processing executable for *Tecplot* geometry visualizations and some aerodynamic data visualization;
 - **vor3.exe** – an interactive executable for building input files, not recommended.

The input file is named input (this file has no extension; make sure not to add one when saving). The VORSTAB input file is organizing all input data and code control commands by groups which are detailed in the *User's Manual for VORSTAB Code (Version 3.2)*⁵. An example of groups 1 through 8 is shown in

Figure C.1. The Group numbers and their purpose is summarized in Table C.1 which summarizes the *User's Manual for VORSTAB Code (Version 3.2)*⁵.

Figure C.1: Example of VORSTAB Input File

Table C.1 Group Break Summary for the VORSTAB Input File

Group Numbers	Purpose
2 and 3	Group 1 is not labeled and is considered the title (see Figure C.1). Groups 2 and 3 are case commands and VORSTAB option switches. These groups tell VORSTAB what to run.
4 through 43	Contain all the inputs for a single lifting surface. The first surface must be the main wing and these groups are repeated one after another for all additional lifting surfaces (i.e. horizontal tail, vertical tail, etc.). Data such as geometry and 2d airfoil characteristics are input here.
44 and 46	Contain the flight condition variables (Mach and Reynolds number), reference lengths and areas, c.g. locations and angles of attack.
47	Contains input variables for augmented vortex lift.
48	Contains input for ground effect.
49	Contains lateral directional parameters such as side-slip angle, maximum roll helical angle, as well as turbulence input.
50 through 73	Fuselage inputs for geometry description, and forebody vortices input description.
74 through 83	Information for the simu output file. Whether or not the vortex lift output is used and the range of angles of attack and control surface deflections required. For consistency, input the same angels of attack as in group 46.

For a more detailed description of the input file see the *User's Manual for VORSTAB Code (Version 3.2)*⁵.

ANALYSIS

2. To run the code, first double click **vorstab.exe**, a blank window will appear. When the code finishes execution, the window will disappear. This can take anywhere from 30 sec. to 10 minutes. If the window appears and immediately disappears then most likely something is wrong with the input file. Some troubleshooting tips are given in the *How to Build a VORSTAB Model* section.
3. Once the VORSTAB execution is complete, double click **fcontec.exe**. This will create the Tecplot visualization files for geometry visualization. This executable should run very quickly, approximately 1 sec.
4. The execution of these two executables has been automated with the runvor.bat file but this file is not required for operation.

OUTPUT

5. VORSTAB creates the following output files with vorstab.exe and fcontec.exe:
 - fplot. – geometry and some aerodynamic data; this file is created by VORSTAB and is utilized by fcontec.exe to build
 - fshape.DAT – created by fcontec.exe for Tecplot; open with the *Tecplot* loader (shown below).

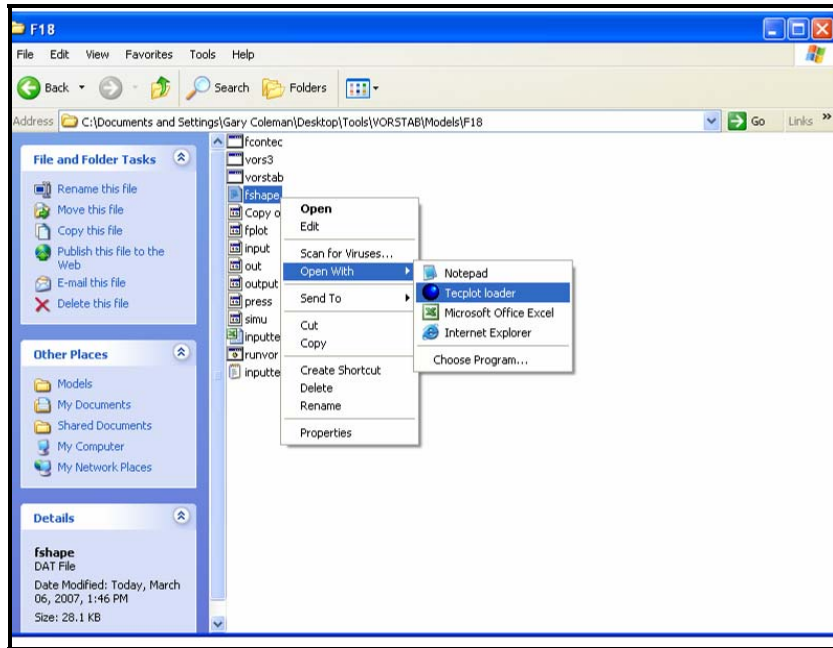


Figure C.2: Demonstration of opening *Tecplot* Visualization from *fcontec.exe*

- **output.** – created by *vorstab.exe* and contains a reprint of the input file and details the analysis results for each angle of attack; includes pressure distribution;
 - **simu.** – created by *vorstab.exe* and provides the aerodynamic and control forces, moments, and dynamic derivatives.
6. The **simu** file tabulates the following aerodynamic coefficients and derivatives. This file is most useful when aircraft and control surface aerodynamic data is required. For more details on the analysis or the pressure distributions, see file call **output.**
- Clean C_L , C_D , C_M , C_{Lq} , C_{Dq} , C_{mq} , $C_{Y\beta}$, $C_{l\beta}$, $C_{n\beta}$, C_{Yp} , C_{lp} , C_{np} , C_{Yr} , C_{lr} , C_{nr} as a function of angle of attack.

- For the elevator or all-movable tail, VORSTAB tabulates the total C_L , C_D , C_M as a function of angle of attack and elevator deflection.
- For the aileron or differentially deflected tail, VORSTAB tabulates the total C_Y , C_b , C_n as a function of angle of attack and aileron deflection.
- For the rudder, VORSTAB tabulates the total C_Y , C_b , C_n as a function of angle of attack and rudder deflection.

HOW TO BUILD A VORSTAB MODEL AND VISUALIZE GEOMETRY

The easiest way to begin to build a model in VORSTAB is to modify a pre-existing example file component by component. The following procedure is recommended for building a new VORSTAB Model.

1. Identify the flight conditions you wish to analyze. For example, a commercial transport may require to investigate the following mission segments: take-off, climb, cruise, descent, and approach conditions. Identify the Mach number, altitude, and angle of attack range for each flight condition.
2. Obtain all necessary geometry and center of gravity data. This includes wing locations, wing dimensions, fuselage cross-sections, control surface geometry, 2d airfoil section data, geometry, etc.
3. Normalize all geometry data to the maximum fuselage radius. VORSTAB requires that the fuselage radius must be less than or equal to 1. Thus, divide all geometry measurements, reference lengths, and reference areas accordingly. (Note: reference area must be divided by the square of the fuselage radius).

Steps 2 and 3 have been mechanized by the author through the use a spread sheet. Here, the basic geometry is input for each surface, it then converts the data into the format required for VORSTAB which requires all of the geometry to be in a Cartesian coordinate system reference from the nose of the aircraft. An example for the wing of the F-104 Starfighter is shown in Figure C.3.

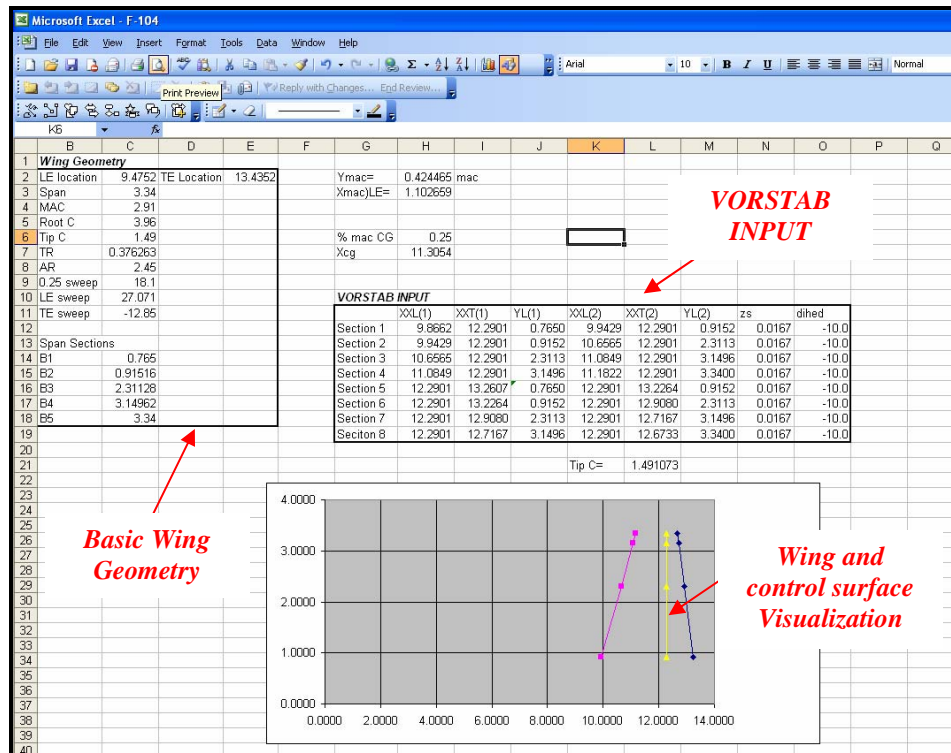


Figure C.3: Example of Converting from conventional wing design variables to VORSTAB coordinates

4. Modify the main lifting surface (wing) of the starting example to the new aircraft wing and remove the remaining surface definitions. Turn off any of the additional options such as 2d airfoil sections or augmented vortex lift.
5. Execute VORSTAB according to the procedure described in *How to execute VORSTAB*.
6. If an error occurs in reading the input file, then VORSTAB will stop almost immediately. This means that something has been formatted improperly in the input file. To debug this, open **output.file** and notice where it stops reproducing the input file. Typically, the error can be found somewhere on the line above where the file stops.

7. Once VORSTAB is running properly, Check the geometry by opening the **fshape.DAT** file with the *Tecplot* loader and inspect the geometry (Figure C.4).

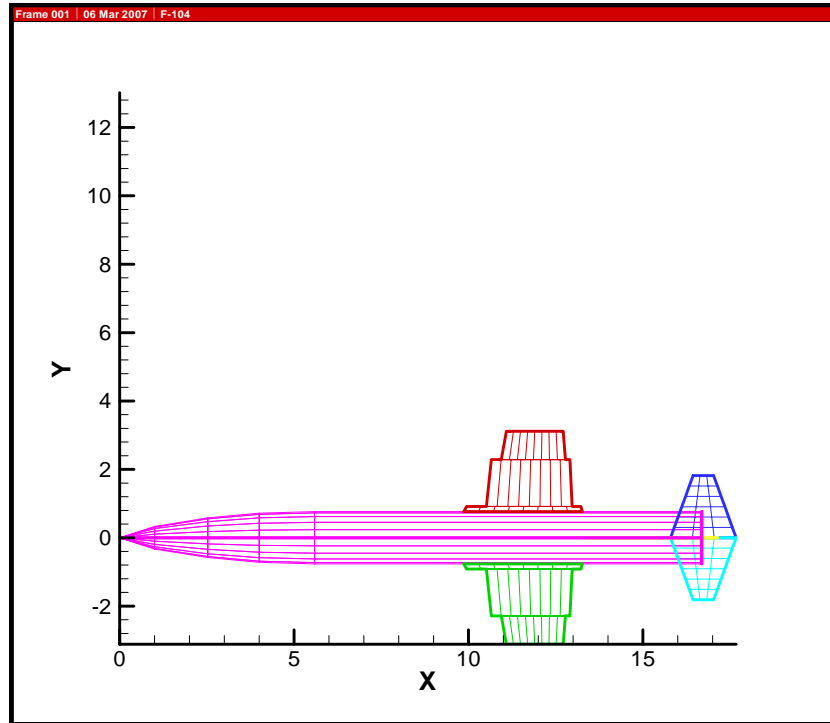


Figure C.4: Example *Tecplot* Visualization of Geometry from VORSTAB with an input error

The error in the wing geometry shown in Figure C.4 was caused by a typo in the wing definition

8. Fix any errors in the geometry input dataset.
9. Check the **simu** file for any gross errors in the aerodynamic data. If a numerical instability has occurred, some coefficients may be very large ($C_L > 1000$) or dramatic sign changes may occur in the derivatives. In this case, increase the number of control points along the wing or revisit the geometry description.
10. Repeat steps 5 through 8 until the remainder of the new lifting surfaces and fuselage have been included.

11. With the geometry specified properly, the results can now be tune utilizing additional options available. Table C.2 outlines the possible uses for the above mentioned options. This table is assembled from personal communications with Dr. Lan³⁹. and personal experiences made by the researcher.

Table C.2 Additional VORSTAB Options, Summarized from Reference 39

VORSTAB Option	Applicability
Vortex Lift	Utilize for aircraft with high sweep angles where the vortex structure above the wing is the primary lift generating mechanism or a strake is present and augmented vortex lift is used.
Rounded Leading Edges for Vortex Lift Calculation	If a highly swept wing has a round leading edge (subsonic LE), then this can decrease the amount of vortex lift generated.
Vortex Breakdown Effect for Vortex Lift Calculation	The 'stall' of highly swept delta wings occurs when the vortex structure begins to break down. Use this option to include this effect.
Nonlinear, 2d Airfoil Section Data Input	Incorporates the 2d lift, drag and pitching moment from the airfoil sections. Applicable to any aircraft for improved drag and stall prediction. Can also be used to correct for transonic effects on the lifting surfaces.
Augmented Vortex Lift	If a strake is used, then the augmented vortex lift option allows for its effects on the wing to be modeled.
Camber Distribution	Input camber whenever camber is present in the wing.
Thickness Distribution	Wing thickness is needed whenever vortex lift is utilized. Partial leading edge suction will remain that reduces drag.
Forebody Vortices	Choose the appropriate method based on the <i>User's Manual for VORSTAB Code (Version 3.2)</i> ³⁹ .

From the experience of the author it is recommended to implement each of these options one at time to (1) quickly find any input errors and (2) to learn how each of these options effects the final solution. Essentially, since more physics is added, it becomes the problem to judge how the correctness and accuracy of the model behaves.

12. With the geometry specified and the additional analysis options implemented for a single flight condition, execute VORSTAB for the remainder of the flight conditions. Be sure to check that the 2d airfoil data and other options are still applicable for the new flight conditions.

Other analysis options are available to the user in VORSTAB such as steady-state aeroelastic effects. For more information on these features and additional modeling information and tips see the *User's Guide for VORSTAB Code (Version 3.2)*⁵. While the above procedure will get you started with VORSTAB, there is much more to learn to efficiently and effectively utilize this tool; and this only comes with experience.

HOW TO AUTOMATE VORSTAB WITH RUNVORSTAB.EXE

The executable RUNVORSTAB.exe was created to format the VORSTAB output into the *AeroMech* compatible aerodynamic lookup table and to automate several different runs which may be required for different configurations. The automations are to model:

1. ***Elevons*** – VORSTAB considers one LoCE, LaCE and DiCE in a single run. To model an elevon, the first run of RUNVORSTAB runs first the LoCE, then renames the surface to a LaCE in the input file and then reruns the input file. Both the data generated for the LoCE and LaCE are stored internally and fed to the *AeroMech* aerodynamic look-up table.
2. ***Secondary Longitudinal Control Effector*** – For control allocation purposes, *AeroMech* can currently utilize one LoCE for trim and one LoCE for maneuvering. This option runs VORSTAB with the first LoCE and then

modifies the input file to activate the second LoCE for the second surface, then reruns VORSTAB. Both are stored internally and the results are transferred to the *AeroMech* aerodynamic look-up table.

3. ***Landing Gear Drag and Pitching Moment Effects*** – This option allows for the incorporation of landing gear effects by simply adding the ΔC_m and ΔC_D to the clean aerodynamics dataset.
4. ***Incorporation of Flap Effects*** – Due to the fact that VORSTAB only allows one LoCE per lifting surface the flying wing model could not incorporate both, the landing flap deflection and control surface deflection at the same run. Consequently, two separate input files are used, **input.file** and **inputf.file**. The second file is used to calculate the clean aerodynamic characteristics with both flap deflection and taking appropriate 2d aerodynamic characteristics into account while the first file calculates the control force and moment increments from the LoCE. The data is stored internally between runs and is transferred to the *AeroMech* aerodynamic look-up table.

INPUT

6. Build the input in the file VOROP.INP according to the same format as the *AeroMech* DCFC.IN and GWP.IN files; the input file contains the variables described in Table C.3.

Table C.3 Required VOROP.INP input for RUNVORSTAB

AeroMech Input File	Units	Description
NAME OF AERO FILE	-	Number of DCFC's to be run.
NUMBER OF ANGLES OF ATTACK	-	Any name for the flight condition, up to 50 characters.
SIDE-SLIP ANGLES	ft/2	Relative velocity
NLOCE SCE	ft	<i>AeroMech</i> contains a borrowed standard atmosphere subroutine.
GROUP 5 MARK (FOR SCE)	-	The group 5 comment line defining the LoCE. For renaming the LoCE as the second control surface.
NUMBER OF VARIABLES ON LINE		The number of variables on the line; or modification purposes.
NUMERICAL LOCATION IN INPUT FILE		The numerical order of the input file line where the definition must be changed.
NUMERICAL VALUE OF SCE		The numerical value of the new control surface. If there are 5 control surfaces on the wing and the new one is the outer most surfaces, than its value is 5. Conversely, if the surface is the inner most surface the value is one.
NLOCE		Number of LoCE deflection in VORSTAB.
LOCE		List the numerical values of the LoCE deflections; one on each line.
NLACE		Number of LaCE deflection in VORSTAB.
LACE		List the numerical values of the LaCE deflections; one on each line.
NDICE		Number of DiCE deflection in VORSTAB.
DICE		List the numerical values of the DiCE deflections; one on each line.
DRAGE DUE TO LANDING GEAR		Drag increment due to landing gear.
PITCH MOMENT DUE TO LANDING GEAR		Pitching moment increment due to landing gear.
SECOND INPUT FILE?		If the second input file is used, then set to one, otherwise zero.
ELEVON?		If an elevon is used then set to one; otherwise zero.
GROUP 5 MARK (FOR ELEVON)		The group 5 comment line is positioned above the definition for the elevon. The last variable in this group identifies the surface as a LoCE or LaCE.
NUMBER OF VARIABLES ON LINE		The number of variables on this line. For changing the value LoCE definition to LaCE.
NUMERICAL VALUE OF ELEVONS		For example, if there are five surfaces but only two are specified as control surfaces. In case the first is the LaCE, then the parameter is set to one.

For example, Figure C.5 shows these options for the YB-49 VOROP.INP

file.

```

VOROP - Notepad
File Edit Format View Help
NAME OF AERO FILE                AERO06.DAT
NUMBER OF ANLGES OF ATTACK        12
NUMBER OF SIDE SLIP ANLGES        3
SIDE SLIP ANLGES                  -10.0
                                   0.0
                                   10.0
NLOCE (NUMBER OF LOCE'S, FOC CA, 1 OR 2) 2
GROUP 5 MARK (FOR SCE)            GROUP 5  NFP, [NJW(I),I=1,NFP], NVRTX,MVRTX,NLEF,IV,NAL (wing)
NUMBER OF VARIABLES ON LINE        7
NUMERICAL LOCATION IN INPUT FILE  2
NUMERICAL VALUE OF SCE             5
NLOCE (NUMBER OF LONGITUDINAL DEFLECTIONS) 5
LOCE (1)                           -30.0
(2)                                  -15.0
(3)                                   0.0
(4)                                  15.0
(5)                                   30.0
NLACE (NUMBER OF LATERAL DEFLECTIONS) 5
LACE (1)                             -20.0
(2)                                  -10.0
(3)                                   0.0
(4)                                   10.0
(5)                                   20.0
NDICE (NUMBER OF DIRECTIONAL DEFLECTIONS) 5
DICE (1)                              -20.0
(2)                                   -10.0
(3)                                   0.0
(4)                                   10.0
(5)                                   20.0
DRAG DUE TO LANDING GEAR           0.00
PITCH MOMENT DUE TO LANDING GEAR   0.00
SECOND INPUT FILE? (YES=1, NO=0)   1
ELEVON (YES=1, NO=0)               1
GROUP 5 MARK (FOR ELEVON)          GROUP 5  NFP, [NJW(I),I=1,NFP], NVRTX,MVRTX,NLEF,IV,NAL (wing)
NUMBER OF VARIABLES ON LINE        7
NUMERICAL VALUE OF ELEVONS         1
Ln 32, Col 33

```

Figure C.5: VOROP.INP for the YB-49 Example

ANALYSIS/EXECUTION

7. Make sure that the VORSTAB executables and the input file are located in the same folder.
8. Double click RUNVORSTAB.exe.

OUTPUT

9. The output file specified will appear in the directory. In the example shown in Figure C.5 the output file name is Aero06.dat.

APPENDIX D

AEROMECH INPUT FILE DESCRIPTION

The input variables and description for the *AeroMech* DCFC.INP and GWP.INP input files are contained in Tables D.1 and D.2 respectively.

Table D.1 Required DCFC Input for *AeroMech*

AeroMech Input File	Units	Description
NDCFC	-	Number of DCFC's to execute.
NAME OF FLIGHT CONDITON	-	Any name for the flight condition, up to 50 characters.
VREL	ft/2	Relative velocity.
ALTITUDE	ft	<i>AeroMech</i> contains a standard atmosphere subroutine, borrowed from Reference 3, to calculate air density, Mach number, and dynamic pressure from altitude and velocity.
<u>AERO INPUT</u>		
NAME OF AERO DAT FILE	-	Name of the aerodynamic look-up table file including extension.
VORSTAB (YEST=1, NO=0)	-	Old <i>AeroMech</i> option, leave as zero.
DATCOM (YES=1, NO=0)	-	Old <i>AeroMech</i> option, leave as zero.
NUMBER OF AOA	-	Number of angles of attack in the aerodynamic look-up table.
NUMBER OF SIDE-SLIP ANLGES	-	Choose the appropriate method based on the <i>User's Manual for VORSTAB Code (Version 3.2)</i> ⁵ .
NUMBER OF LOCE DEFLECTIONS	-	Number of longitudinal control effector deflections in aerodynamic lookup table file.
NUMBER OF LACE DEFLECTIONS	-	Number of lateral control effector deflections in aerodynamic lookup table file.
NUMBER OF DICE DEFLECTIONS	-	Number of directional control effector deflections in aerodynamic lookup table file.
FLIGHT PATH ANGLE FOR TRIMMED AERO ANALYSIS	deg	For an older version of <i>AeroMech</i> , set to same value as specified in SSLF input.
SIDE SLIP ANGLE OF TRIMMED AERO ANALYSIS	deg	The side-slip angle can be varied with the SSLF module, specify the side-slip angle desired for trimmed aerodynamic analysis.
<u>CONTROL ALLOCATION INPUT</u>		
NUMBER OF SOCE DEFLECTIONS	-	Number of secondary control effector deflections in the aerodynamic lookup table, set to zero if no secondary control effector is necessary.
SECONDARY CONTROL FOR TIRM WITH SSLF?	-	If the secondary control effector is to trim to 1-g flight, set to 1. otherwise 0.
SECONDARY CONTROL EFFECTOR DEFLECTION (MANUAL)	deg	If a secondary control effector is required and is not to trim to 1-g flight, then manually set the deflection here. If the SOCE is to trim to 1-g flight, set this value to 0.0.
<u>SSLF INPUT</u>		
TRIM (YES=1, NO=0)	-	If the SSLF module is desired set to 1, otherwise 0. Must with the dynamic stability module.
FLIGHT PATH (DEG)	deg	Flight path angle required for trim.

NUMBER OF BETA ITERATIONS PER GAMMA	-	Number of side-slip angles for analysis.
BETA RANGE	deg	Numerical value of each side-slip angle, repeat for each side-slip angle specified.
SIDE SLIP ANGLE RUN OUTPUTED IN SUMMARY FILE	-	The numerical order of the side-slip angle analysis run which will be summarized in the summary stability and control output file.
<u>DYNAMIC SAS INPUT</u>		
DYNAMIC MODUAL (YES=1, NO=0)	-	If this dynamic stability module is desired set to 1, otherwise 0.
MIN SHORT PERIOD DAMPING RATION REQUIRMENT	-	The minimum short period mode damping ratio from design requirements.
MAX SHORT PERIOD DAMPING RATIO REQUIRMENT	-	The maximum short period mode damping ratio from design requirements.
MIN SHORT PERIOD NATURAL FREQUENCY REQUIREMENT	-	The minimum short period mode natural frequency from design requirements.
MAX ROLL TIME CONSTANT	-	The maximum roll mode time constant from design requirements.
MIN DUTCH ROLL DAMPING RATIO	-	The minimum Dutch roll mode damping ratio from design requirements.
MIN DUTCH ROLL WN	-	The minimum Dutch roll mode natural frequency from design requirements.
MIN (DAMPING RATIO)*WN	-	The minimum Dutch roll mode product of the damping ratio and natural frequency from design requirements. Can also be interpreted as the minimum Dutch roll real root.
ALPHA MAX DISTRUBANCE FOR CONTROL POWER	deg	The maximum angle of attack disturbance for additional control power calculation. <i>If no angle of attack feed back is desired, set to 0.0.</i>
BETA MAX DISTRUBANCE FOR CONTROL POWER	Deg	The maximum side-slip angle disturbance for additional control power calculation. <i>If no side-slip angle feed back is desired, set to 0.0.</i>
p MAX DISTRUBANCE FOR CONTROL POWER	Deg/s	The maximum roll rate disturbance for additional control power calculation. <i>If no roll rate feed back is desired, set to 0.0.</i>
q MAX DISTRUBANCE FOR CONTROL POWER	Deg/s	The maximum pitch rate disturbance for additional control power calculation. <i>If no pitch rate feed back is desired, set to 0.0.</i>
r MAX DISTRUBANCE FOR CONTROL POWER	Deg/s	The maximum yaw rate disturbance for additional control power calculation. <i>If no yaw rate feed back is desired, set to 0.0.</i>
<u>SSPUPO INPUT</u>		
PULL-UP/PUSH-OVER (YES=1, NO=0)	-	If push-up/push-over analysis is desired set to 1, otherwise 0.
NUMBER OF LOAD FACTOR ITERATIONS	-	Number of load factors to be analyzed.
NUMBER OF BETA ITERATIONS PER LOAD FACTOR	-	Number of side-slip angle for each load factor to be analyzed.
LOAD FACTOR RANGE	g	Numerical value of each load factor, repeat for the number of load factors specified.
BETA RANGE	deg	Numerical value of each side-slip angle, repeat for the number of side-slip angles specified.
<u>SSTF INPUT</u>		
TURNING FLIGHT (YES=1, NO=0)	-	If horizontal turning analysis is required, then set to 1, otherwise 0.

NUMBER OF LOAD FACTOR ITERATIONS	-	Number of load factors to be analyzed.
NUMBER OF BANK ANGLE ITERATIONS	-	Number of bank angles to be analyzed, one per load factor.
LOAD FACTOR RANGE	deg	Numerical value of each load factor, repeat for the number of load factors specified.
BETA RANGE	deg	Numerical value of each bank angle, repeat for the number of bank angles specified.
<u>SSRP INPUT</u>		
STEADY STATE ROLL PERFORMANCE (YES=1, NO=0)	-	If steady-state roll performance analysis is desired, set to 1, otherwise 0.
NUMBER OF ROLL RATE ITERATIONS	-	Number of roll rates to be analyzed.
NUMBER OF BETA ITERATIONS PER ROLL RATE	-	Number of side-slip angles per roll rate, typically 0.0.
SUSTAINED ROLL RATES	deg/s	Numerical value of each roll rate, repeat for the number of roll rates specified.
SIDE SLIP RANGE	deg	Numerical value of each side-slip angle, repeat for the number of side-slip angles specified.
FINAL TIME FOR TIME TO BANK CALCULATION	S	The final time for the time to bank calculation.
TIME STEP FOR TIME TO BANK CALCULATION	S	The time step for the time to bank calculation.
NUMBER OF BANK ANGLES FOR TIME TO BANK	-	The number of target bank angles for the time to bank calculation.
BANK ANGLES FOR TIME TO BANK CALCULATION	deg	Numerical value of the target bank angles for the time to bank calculation, repeat for the number of bank angles specified.
NUMBER OF DLACE FOR TIME TO BANK CALCULATION	-	Number of lateral control surface deflection settings for the time to bank calculation.
DLACE RANGE FOR TIME TO BANK CALCULATION	deg	Numerical value of the lateral control surface deflections for the time to bank calculation, repeat for the number of deflections specified.
<u>QSTROM INPUT</u>		
TAKEOFF ROTATION MAUNEUVUER (YES=1, NO=0)	-	If quasi-steady state take-off rotation analysis is desired set to 1, otherwise set to 0.
ANGLE OF ATTACK	deg	Angle of attack while the aircraft is on the runway.
THRUST SETTING	% thrust	Thrust setting for take-off.
DLoCE	deg	The longitudinal control surface deflection commanded for take-off rotation.
NUMBER OF SIDE SLIP ANGLES	-	Number of side-slip angles during take-off rotation analysis.
SIDE-SLIP ANGLE	deg	Numerical value of side-slip angles, repeat for the number of side-slip angles specified.
NUMBER OF INSTANTANEOUS PITCH ACCERLATIONS	-	Number of instantaneous pitch accelerations required for take-off rotation.
INSTATANEOUS PITCH ACCERLATIONS	deg/s ²	Numerical value of instantaneous pitch accelerations, repeat for the number of instantaneous pitch accelerations specified.

Table D.2 Required GWP.INP Input for *AeroMech*

AeroMech Input File	Units	Description
S	ft ²	reference area
b	ft	reference span
CBAR	ft	reference chord
WEIGHT	lbs	aircraft weight
NXCG	-	for older versions of <i>AeroMech</i> , set to 1
XCG	-	distance from the reference chord's leading edge to aircraft c.g. divided by reference chord
IX	slug/ft ³	x-moment of inertia
IY	slug/ft ³	y-moment of inertia
IZ	slug/ft ³	z-moment of inertia
IXZ	slug/ft ³	xz-product moment of inertia
IXY	slug/ft ³	xy-product moment of inertia
IYZ	slug/ft ³	yz-product moment of inertia
HX	slug/ft ³	x-rotational inertia from spinning rotors
HY	slug/ft ³	x-rotational inertia from spinning rotors
HZ	slug/ft ³	z-rotational inertia from spinning rotors
NENGINES	-	Number of engines, TA, PHIT, PHST, XT, ZT, and YT must be repeated NENGINE times
TA1	lbs	thrust from 1 engine
PHIT	deg	vertical thrust angle
PHST	deg	lateral thrust angle
XT	ft	x-distance from engine to aircraft c.g.
ZT	ft	z-distance from engine to aircraft c.g.
YT	ft	y-distance from engine to aircraft c.g.
X LANDING GEAR LOCATION FROM C.G.	ft	x-distance from main landing gear reaction point to c.g.
Z LANDING GEAR LOCATION FROM C.G.	ft	y-distance from main landing gear reaction point to c.g.
ROLLING FRICTION COEFFICIENT OF LANDING GEAR	-	rolling friction coefficient between landing gear and runway
MAX LOCE DEFLECTION	deg	maximum longitudinal control effector deflection

MAX LACE DEFLECTION	deg	maximum lateral control effector deflection
MAX DICE DEFLECTION	deg	maximum directional control effector deflection
WR NATURAL FREQ. (LACE)	-	natural frequency of the lateral control surface actuator
WP NATURAL FREQ. (LOCE)	-	natural frequency of the longitudinal control surface actuator
WY NATURAL FREQ. (DICE)	-	natural frequency of the directional control surface actuator
ZR DAMPING RATIO (LOCE)	-	damping ratio of the lateral control surface actuator
ZP DAMPING RATIO (LACE)	-	damping ratio of the longitudinal control surface actuator
ZY DAMPING RATIO (DICE)	-	damping ratio of the directional control surface actuator

APPENDIX E

DERIVATION OF STEADY-STATE EQUATIONS OF MOTION

The steady-state equations of motion are embedded in the trim and maneuvering analysis algorithms. In these algorithms, these generic equations are solved for the control surface deflections at certain attitude variables (such as angle of attack or side-slip angles) to maintain the prescribed maneuver. The derivations of this set of equations are presented here in two parts.

1. Restating the *steady-steady force and moment equations* which are explained in Chapter 3. These equations are initially derived by Chudoba¹ from the Euler equations of motion. The form chosen for this set of equations in the present context differs from the form selected by Chudoba¹ in that the pitch rate (q), roll rate (p) and yaw rate (r) are not expanded out for each individual maneuver.
2. Derivation of the appropriate pitch, roll, and yaw rates from the *kinematic equations of motion* for each maneuver. These calculated first and then inserted into the steady-state equations of motion.

STEADY-STATE FORCE AND MOMENT EQUATIONS

The steady-state force and moment equations have been derived by Chudoba¹ with the following assumptions, see Table A.1.

Table A.1 Steady-State Equations of Motion Assumptions

Assumptions	
1	The Earth is treated as flat and stationary in inertia space.
2	Equations are valid for any orthogonal axis system fixed at the c.g. of the aircraft.
3	Aircraft is a rigid body having any number of rigid spinning rotors.
4	Spinning rotors have a constant angular velocity relative to the body axis.
5	Wind velocity is zero.
6	Steady state flight, no acceleration.
7	No plane of symmetry, i.e. full moment of inertia matrix I_{xy} and I_{zy} are included.
8	Aerodynamic cross coupling included.

With these assumptions the force, moment, and kinematic equations of motion

become (Equations E.1 to E.16)

$$X_A + X_T - mg \sin \theta = m(qw - rv) \quad \text{Eq. E.1}$$

$$Y_A + Y_T + mg \cos \theta \sin \phi = m(ru - pw) \quad \text{Eq. E.2}$$

$$Z_A + Z_T + mg \cos \theta \cos \phi = m(pv - qu) \quad \text{Eq. E.3}$$

$$L_A + L_T = I_x \dot{p} - I_{yz}(q^2 - r^2) - I_{zx}pq - I_{xy}rp - (I_y - I_z)qr + qh'_z - rh'_y \quad \text{Eq. E.4}$$

$$M_A + M_T = I_y \dot{q} - I_{zx}(r^2 - p^2) - I_{xy}qr - I_{yz}pq - (I_z - I_x)rp + rh'_x - ph'_z \quad \text{Eq. E.5}$$

$$N_A + N_T = I_z \dot{r} - I_{zx}(p^2 - q^2) - I_{yz}rp - I_{xy}qr - (I_x - I_y)pq + ph'_y - qh'_x \quad \text{Eq. E.6}$$

$$p = \dot{\phi} - \dot{\psi} \sin \theta \quad \text{Eq. E.7}$$

$$q = \dot{\theta} \cos \phi + \dot{\psi} \sin \phi \cos \theta \quad \text{Eq. E.8}$$

$$r = -\dot{\theta} \sin \phi + \dot{\psi} \cos \phi \cos \theta \quad \text{Eq. E.9}$$

$$\dot{\phi} = p + (q \sin \phi + r \cos \phi) \tan \theta \quad \text{Eq. E.10}$$

$$\dot{\theta} = q \cos \phi - r \sin \phi \quad \text{Eq. E.11}$$

$$\dot{\psi} = (q \sin \phi + r \cos \phi) \sec \theta \quad \text{Eq. E.12}$$

$$\dot{x}^E = u^E \cos \theta \cos \psi + v^E (\sin \phi \sin \theta \cos \psi - \cos \phi \sin \psi) + w^E (\cos \phi \sin \theta \cos \psi + \sin \phi \sin \psi) \quad \text{Eq. E.13}$$

$$\dot{y}^E = u^E \cos \theta \sin \psi + v^E (\sin \phi \sin \theta \sin \psi + \cos \phi \cos \psi) + w^E (\cos \phi \sin \theta \sin \psi - \sin \phi \cos \psi) \quad \text{Eq. E.14}$$

$$\dot{z}^E = -u^E \sin \theta + v^E \sin \phi \cos \theta + w^E \cos \phi \cos \theta \quad \text{Eq. E.15}$$

When including the aerodynamic and thrust components to the force and moment equations (Equations E.2 – E.7), we obtain the following generic trim equations written in the stability axis (Equations E.17 – E.22).

$$\left(-C_{T_D} \tau + C_D(\alpha, \beta) + C_{D_q}(\alpha, \beta) \frac{q\bar{c}}{2V} + \Delta C_{D_{LoCE}}(\alpha, \delta_{LoCE}) + \Delta C_{D_{LaCE}}(\alpha, \delta_{LaCE}) + \Delta C_{D_{DiCE}}(\alpha, \delta_{DiCE}) \right) \bar{q} S_{ref} - \text{Eq. E.16}$$

$$- mg \sin \gamma - mrV \sin \beta = 0$$

$$\left(C_{T_Y} \tau + C_Y(\alpha, \beta) + C_{Y_r}(\alpha, \beta) \frac{rb}{2V} + C_{Y_p}(\alpha, \beta) \frac{pb}{2V} + \Delta C_{Y_{LoCE}}(\alpha, \delta_{LoCE}) + \Delta C_{Y_{LaCE}}(\alpha, \delta_{LaCE}) + \Delta C_{Y_{DiCE}}(\alpha, \delta_{DiCE}) \right) \bar{q} S_{ref} -$$

$$- mg \cos \gamma \sin \phi - mrV = 0$$

Eq. E.17

$$- \left(-C_{T_L} \tau + C_L(\alpha, \beta) + C_{L_q}(\alpha, \beta) \frac{q\bar{c}}{2V} + \Delta C_{L_{LoCE}}(\alpha, \delta_{LoCE}) + \Delta C_{L_{LaCE}}(\alpha, \delta_{LaCE}) + \Delta C_{L_{DiCE}}(\alpha, \delta_{DiCE}) \right) \bar{q} S_{ref} - \text{Eq. E.18}$$

$$- mg \cos \gamma \cos \phi + mqV - mpV \sin \beta = 0$$

$$\left(C_{T_I} \tau + C_I(\alpha, \beta) + C_{I_r}(\alpha, \beta) \frac{rb}{2V} + C_{I_p}(\alpha, \beta) \frac{pb}{2V} + \Delta C_{I_{LoCE}}(\alpha, \delta_{LoCE}) + \Delta C_{I_{LaCE}}(\alpha, \delta_{LaCE}) + \Delta C_{I_{DiCE}}(\alpha, \delta_{DiCE}) \right) \bar{q} S_{ref} b +$$

$$+ I_{yz}(q^2 - r^2) + I_{zx}pq - I_{xy}rp + (I_y - I_z)qr - qh'_z + rh'_y = 0$$

Eq. E.19

$$\left(C_{T_m} \tau + C_m(\alpha, \beta) + C_{m_q}(\alpha, \beta) \frac{q\bar{c}}{2V} + \Delta C_{m_{LoCE}}(\alpha, \delta_{LoCE}) + \Delta C_{m_{LaCE}}(\alpha, \delta_{LaCE}) + \Delta C_{m_{DiCE}}(\alpha, \delta_{DiCE}) \right) \bar{q} S_{ref} \bar{c} + \text{Eq. E.20}$$

$$+ I_{zx}(r^2 - p^2) + I_{xy}qr - I_{yz}pq + (I_z - I_x)rp - rh'_x + ph'_z = 0$$

$$\left(C_{T_n} \tau + C_n(\alpha, \beta) + C_{n_r}(\alpha, \beta) \frac{rb}{2V} + C_{n_p}(\alpha, \beta) \frac{pb}{2V} + \Delta C_{n_{LoCE}}(\alpha, \delta_{LoCE}) + \Delta C_{n_{LaCE}}(\alpha, \delta_{LaCE}) + \Delta C_{n_{DiCE}}(\alpha, \delta_{DiCE}) \right) \bar{q} S_{ref} b +$$

$$+ I_{zx}(p^2 - q^2) + I_{yz}rp - I_{xy}qr + (I_x - I_y)pq - ph'_y + qh'_x = 0$$

Eq. E.21

Derivation of Thrust Coefficients

The thrust coefficients in equations 17 through 22 represent the force and moment components from the propulsion system defined by the dynamic pressure and reference area (including reference length for the moment components). The thrust vector is defined in the body axis by the x, y, and z distances from the aircraft's c.g. and vertical (ϕ_{Ti}) and horizontal angles (ψ_{Ti}) as shown in Figure A.1.

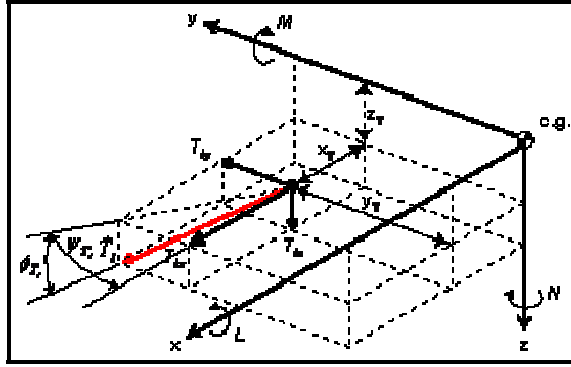


Figure A.1: Thrust and Force Component Break-Down

The following derivation is repeated here from Reference 1. for convenience.

The thrust vector is defined as,

$$\vec{T}_i = [T_{i_x} + T_{i_y} + T_{i_z}]^T \quad \text{Eq. E.22}$$

Written in the body axis

$$T_{i_{xb}} = T_i \cos \phi_{T_i} \cos \psi_{T_i} \quad \text{Eq. E.23}$$

$$T_{i_{yb}} = T_i \cos \phi_{T_i} \sin \psi_{T_i} \quad \text{Eq. E.24}$$

$$T_{i_{zb}} = T_i \sin \phi_{T_i} \quad \text{Eq. E.25}$$

Transforming from the body axis to the stability axis,

$$\begin{pmatrix} T_{i_{xs}} \\ T_{i_{ys}} \\ T_{i_{zs}} \end{pmatrix} = \begin{pmatrix} \cos \alpha & 0 & \sin \alpha \\ 0 & 1 & 0 \\ -\sin \alpha & 0 & \cos \alpha \end{pmatrix} \begin{pmatrix} T_{i_{xb}} \\ T_{i_{yb}} \\ T_{i_{zb}} \end{pmatrix} \quad \text{Eq. E.26}$$

Yields,

$$T_{i_{xs}} = T_i (\cos \phi_{T_i} \cos \psi_{T_i} \cos \alpha + \sin \phi_{T_i} \sin \alpha) \quad \text{Eq. E.27}$$

$$T_{i_{xs}} = T_i \cos \phi_{T_i} \sin \psi_{T_i} \quad \text{Eq. E.28}$$

$$T_{i_{zs}} = T_i (-\cos \phi_{T_i} \cos \psi_{T_i} \sin \alpha + \sin \phi_{T_i} \cos \alpha) \quad \text{Eq. E.29}$$

To calculate the moments around the c.g. first the distance x_T , z_T and y_T from Figure A.1 must be converted to the stability. With this transformation, the following roll, pitch, and yaw moments about the c.g. can be calculated in stability axis.

$$L_s = T_i \cos \alpha (-\cos \phi_{T_i} \sin \psi_{T_i} z_T + \sin \phi_{T_i} y_T) + T_i \sin \alpha (\cos \phi_{T_i} \sin \psi_{T_i} x_T - \cos \phi_{T_i} \cos \psi_{T_i} y_T) \quad \text{Eq. E.30}$$

$$M_s = T_i \cos \alpha (\cos \phi_{T_i} \cos \psi_{T_i} z_T - \sin \phi_{T_i} x_T) \quad \text{Eq. E.31}$$

$$N_s = T_i \sin \alpha (\cos \phi_{T_i} \sin \psi_{T_i} z_T - \sin \phi_{T_i} y_T) + T_i \cos \alpha (\cos \phi_{T_i} \sin \psi_{T_i} x_T - \cos \phi_{T_i} \cos \psi_{T_i} y_T) \quad \text{Eq. E.32}$$

Collecting these terms and dividing by the dynamic pressure, and appropriate reference areas and lengths produces the final form of the thrust coefficients. These coefficients sum the individual contributions of engines $i=1, 2, \dots, n$.

$$C_{T_D} = \frac{1}{\bar{q}S} \sum_{i=1}^n T_i (\cos \phi_{T_i} \cos \psi_{T_i} \cos \alpha + \sin \phi_{T_i} \sin \alpha) \quad \text{Eq. E.33}$$

$$C_{T_y} = \frac{1}{\bar{q}S} \sum_{i=1}^n T_i \cos \phi_{T_i} \sin \psi_{T_i} \quad \text{Eq. E.34}$$

$$C_{T_L} = \frac{1}{\bar{q}S} \sum_{i=1}^n T_i (-\cos \phi_{T_i} \cos \psi_{T_i} \sin \alpha + \sin \phi_{T_i} \cos \alpha) \quad \text{Eq. E.35}$$

$$C_{T_i} = \frac{1}{\bar{q}Sb} \sum_{i=1}^n T_i \cos \alpha (-\cos \phi_{T_i} \sin \psi_{T_i} z_T + \sin \phi_{T_i} y_T) + T_i \sin \alpha (\cos \phi_{T_i} \sin \psi_{T_i} x_T - \cos \phi_{T_i} \cos \psi_{T_i} y_T) \quad \text{Eq. E.36}$$

$$C_{T_M} = \frac{1}{\bar{q}S\bar{c}} \sum_{i=1}^n T_i \cos \alpha (\cos \phi_{T_i} \cos \psi_{T_i} z_T - \sin \phi_{T_i} x_T) \quad \text{Eq. E.37}$$

$$C_{T_N} = \frac{1}{\bar{q}Sb} \sum_{i=1}^n T_i \sin \alpha (\cos \phi_{T_i} \sin \psi_{T_i} z_T - \sin \phi_{T_i} y_T) + T_i \cos \alpha (\cos \phi_{T_i} \sin \psi_{T_i} x_T - \cos \phi_{T_i} \cos \psi_{T_i} y_T)$$

Eq. E.38

DERIVATION OF THE PITCH, ROLL AND YAW RATES FOR SPECIFIC DCFCs

The steady-state straight-line flight (SSLF), steady-state pull-up/push-over (SSPUPO), steady-state turning flight (SSTF), and steady-state roll performance (SSRP) analysis solve the above force and moment equations for specific pitch, roll and yaw rates which are defined through the kinematic equations of motion. These are derived below. The quasi steady-state take-off rotation (QSTORM) is explained in Chapter 4. For this maneuver, the pitch, roll, and yaw rates are set to zero.

STEADY-STATE STRAIGHT-LINE FLIGHT (SSLF)

SSLF is characterized by both zero acceleration and zero rotational velocity (Figure A.2).

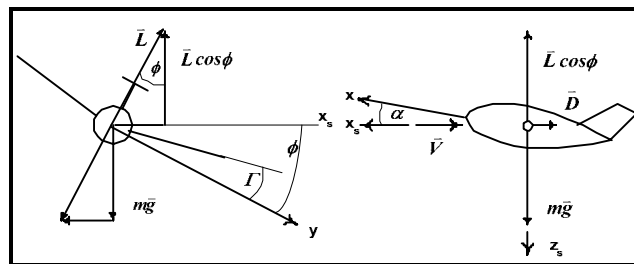


Figure A.2: Steady-State Straight-Line Flight¹

Thus,

$$p = 0, q = 0, r = 0$$

STEADY-STATE PULL-UP/PUSH-OVER (SSPUPO)

SSPUPO is characterized by a constant upward pitching motion tangent to the horizontal plane at both the top and bottom of the curve of rotation (see Figure A.2). This maneuver approximates the load factor capability of the aircraft during the pull-up/push-over load maneuvers. Figure A.3 from Reference 1 illustrates this motion.

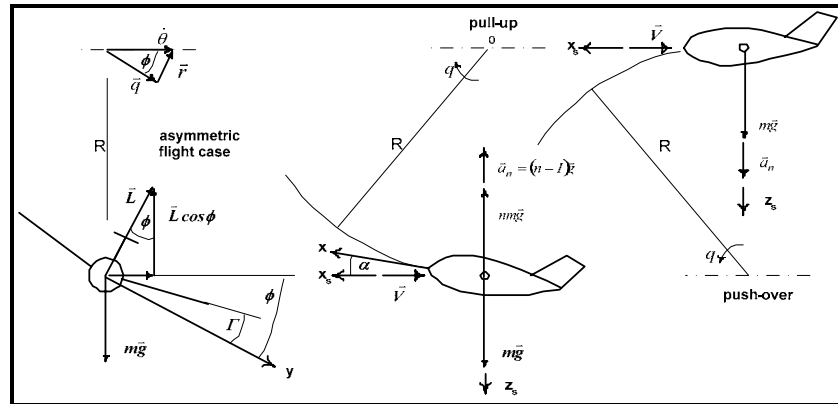


Figure A.3: Steady-State Pull-up / Push-over Flight¹

To derive this motion in terms of the rotation rates p , q , and r , the following steps are required.

1. **Derive the lift required as a function of load factor.** The load factor is defined as the resultant force required divided by the mass. For the cause of the pull-up/push over maneuver, the aircraft's lift is the resultant force.

$$n = \frac{L}{mg} \quad \text{Eq. E.39}$$

Rearranging

$$L = nmg \quad \text{Eq. E.40}$$

2. **Derive the pitch rate as a function of velocity and radius.** Using the relationship between translational and rotation velocity, $v = \omega r$

$$\dot{\theta} = \frac{V}{R} \quad \text{Eq. E.41}$$

3. **Derive pitch rate as a function of lift.** For this condition the aircraft is rotating about the center of the arc and at the top and bottom of this arc the total lift required can be written as,

$$L = mg + m\dot{\theta}^2 R \quad \text{Eq. E.42}$$

Expanding with relationship 2 yields,

$$L = m \left(g + \frac{V^2}{R^2} R \right) \quad \text{Eq. E.43}$$

$$\frac{L}{m} = g + \frac{V^2}{R} \quad \text{Eq. E.44}$$

Thus,

$$\frac{V}{R} = \frac{L}{mV} - \frac{g}{V} \quad \text{Eq. E.45}$$

4. **Combine relationships 1, 2, and 3 with the pitch rate kinematic equation.**

Assuming a constant heading the pitch rate kinematic equation becomes

$$q = \dot{\theta} \cos \phi \quad \text{Eq. E.46}$$

Inserting relationship 2 for the pitch angular velocity yields,

$$q = \frac{V}{R} \cos \phi \quad \text{Eq. E.47}$$

Utilizing relationship 3 the equation becomes

$$q = \left(\frac{L}{mV} - \frac{g}{V} \right) \cos \phi \quad \text{Eq. E.48}$$

Utilizing relationship 1 the and rearranging the final form becomes,

$$q = \left(\frac{gn}{V} - \frac{g}{V} \right) \cos \phi = \frac{g}{V} (n-1) \cos \phi \quad \text{Eq. E.49}$$

5. Combine relationships 1, 2, and 3 with the yaw rate kinematic equation.

Assuming a constant heading the yaw rate kinematic equation becomes,

$$r = -\dot{\theta} \sin \phi \quad \text{Eq. E.50}$$

Inserting relationship 2 for the pitch angular velocity yields,

$$r = -\frac{V}{R} \sin \phi \quad \text{Eq. E.51}$$

Utilizing relationship 3 the equation becomes

$$q = -\left(\frac{L}{mV} - \frac{g}{V} \right) \sin \phi \quad \text{Eq. E.52}$$

Utilizing relationship 1 the and rearranging the final form becomes,

$$q = -\left(\frac{gn}{V} - \frac{g}{V}\right)\sin\phi = -\frac{g}{V}(n-1)\sin\phi \quad \text{Eq. E.53}$$

This maneuver describes a motion in the vertical plane, but the aircraft can encounter side-slip, thus the bank angle can be set to a *constant* value to maintain the motion in the vertical plane. Therefore, no angular roll velocity is allowed.

The final roll, pitch, and yaw rates for the pull-up/push-over maneuver are shown below.

$$p = 0 \quad \text{Eq. E.54}$$

$$q = \frac{g}{V}(n-1)\cos\phi \quad \text{Eq. E.55}$$

$$r = -\frac{g}{V}(n-1)\sin\phi \quad \text{Eq. E.56}$$

STEADY-STATE TURNING FLIGHT (SSTF)

SSTF is characterized by a constant rate turn only. This implies no change in altitude and a constant bank angle (Figure A.2). This maneuver approximates the load factor capability of the aircraft to maintain this a constant rate turn at various bank angles . Figure A.4 from Reference 1 illustrates this motion.

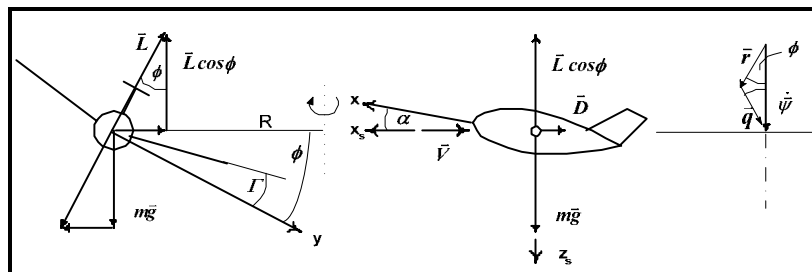


Figure A.4: Steady-State Turning Flight¹

To derive this motion in terms of the rotational rates p , q , and r , the following steps are required.

1. **Horizontal and vertical force equilibrium.** For this condition both the horizontal and vertical equilibrium must be satisfied to maintain the circular flight path.

Horizontal balance of the centrifugal force F_{CF} with the lift vector

$$F_{CF} = m\omega^2 R = m\dot{\psi}^2 R = L \sin \phi \quad \text{Eq. E.57}$$

Vertical balance of the a/c weight with the lift vector

$$mg = L \cos \phi \quad \text{Eq. E.58}$$

2. **The Constant turn rate as function of velocity and radius.** According to the kinematics relationship, $v = \omega R$, the turn rate (which is defined as the angular rate about center of the horizontal arc) can be defined as

$$\dot{\psi} = \frac{u}{R} \quad \text{Eq. E.59}$$

3. **Combine relationships in steps 1 and 2 to obtain the turn radius.** Substituting the turn rate definition in relationship 2 into the horizontal turn equilibrium equation yields,

$$m\dot{\psi}^2 R = m \frac{u^2}{R^2} R = L \sin \phi \quad \text{Eq. E.60}$$

Solving for R ,

$$R = \frac{mu^2}{L \sin \phi} \quad \text{Eq. E.61}$$

Solving the vertical equilibrium equation for m and substituting into the above relationship for R,

$$m = \frac{L \cos \phi}{g} \quad \text{Eq. E.62}$$

$$R = \frac{L \cos \phi u^2}{gL \sin \phi} = \frac{u^2}{g} \frac{1}{\tan \phi} \quad \text{Eq. E.63}$$

4. ***The turn rate corresponding to this radius can be found through utilizing relationship 2.*** Substituting the turn rate definition in relationship 2 into the turn radius expression above yields,

$$u = \psi \frac{u^2}{g} \frac{1}{\tan \phi} \quad \text{Eq. E.64}$$

$$\psi = \frac{g}{u} \tan \phi \quad \text{Eq. E.65}$$

5. ***Determine the load factor as a function of bank angle.*** The relationship between the load factor and lift is,

$$L = nmg \quad \text{Eq. E.66}$$

Substituting the rearranged vertical equilibrium equations from relationship 3 yields

$$L = n \frac{L \cos \phi}{g} g \quad \text{Eq. E.67}$$

$$n = \frac{1}{\cos \phi} \quad \text{Eq. E.68}$$

6. *Substitute relationships 4 and 5 into the kinematic equations.* The pitch rate kinematic equation with zero pitching velocity is,

$$q = \dot{\psi} \sin \phi \quad \text{Eq. E.69}$$

Substituting relationship 4 for the turn rate gives,

$$q = \frac{g}{u} \tan \phi \sin \phi = \frac{g \sin \phi}{u \cos \phi} \sin \phi \quad \text{Eq. E.70}$$

Substituting relationship 5 for the load factor gives,

$$q = \frac{g}{u} n \sin^2 \phi \quad \text{Eq. E.71}$$

The yaw rate kinematic equation with zero pitching velocity is,

$$r = \dot{\psi} \cos \phi \quad \text{Eq. E.72}$$

Substituting relationship 4 for the turn rate gives,

$$r = \frac{g}{u} \tan \phi \cos \phi \quad \text{Eq. E.73}$$

Substituting relationship 5 for the load factor gives,

$$r = \frac{g}{u} \tan \phi \frac{1}{n} \quad \text{Eq. E.74}$$

No rolling motion is present during this maneuver to the constant altitude horizontal turn,

$$p = 0 \quad \text{Eq. E.75}$$

To summarize, the following definitions for the roll, pitch, and yaw rates are chosen to define steady-state turning flight:

$$p = 0 \quad \text{Eq. E.76}$$

$$q = \frac{g}{u} n \sin^2 \phi \quad \text{Eq. E.77}$$

$$r = \frac{g}{u} \tan \phi \frac{1}{n} \quad \text{Eq. E.78}$$

STEADY-STATE ROLL PERFORMANCE (SSRP)

SSRP is characterized by a constant roll rate about the stability axis. This maneuver approximates the control surface deflections to maintain a required roll rate and can also be used approximate initial turn coordination. Figure A.5 from Reference 1 illustrates this motion.

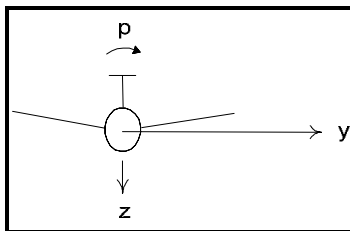


Figure A.5: Steady-state roll performance¹.

For this condition no translational or angular accelerations are allowed and all rotation rates are set to zero except for the roll rate which is a constant value. Thus,

$$p = \dot{\phi} \quad \text{Eq. E.79}$$

$$q = 0 \quad \text{Eq. E.80}$$

$$r = 0 \quad \text{Eq. E.81}$$

This maneuver is also described by a single degree of freedom time to bank approximation given by Equation E.82.

$$L_A = I_x \dot{p} \quad \text{Eq. E.82}$$

$$\left[C_{l_0} + C_{l_p} \frac{pb}{2V} + C_{l_{LaCE}}(\alpha, \delta_{LaCE}) \right] qSb = I_x \dot{p} \quad \text{Eq. E.83}$$

Solving for the rotation acceleration,

$$\dot{p} = \left[C_{l_0} + C_{l_p} \frac{pb}{2V} + C_{l_{LaCE}}(\alpha, \delta_{LaCE}) \right] \frac{qSb}{I_x} \quad \text{Eq. E.84}$$

The solution to this ordinary differential equation is given with

$$p = \dot{\phi}(t) = -\frac{2V}{b} \frac{C_{l_{LaCE}}(\alpha, \delta_{LaCE})}{C_{l_p}} (1 - e^{L_p t}) \quad \text{Eq. E.85}$$

where,

$$L_p = \frac{qSb^2}{2VI_x} C_{l_p} \quad \text{Eq. E.86}$$

Integrating again gives the bank angle as a function of time for a given LaCE deflection.

$$\int p = \phi(t) = -\frac{2V}{b} \frac{C_{l_{LaCE}}(\alpha, \delta_{LaCE})}{C_{l_p}} \left(t + \frac{1}{L_p} (1 - e^{-L_p t}) \right) \quad \text{Eq. E.87}$$

In *AeroMech*, the time-to-bank is solved by specifying an initial time, final time, and time step. An internal storage array stores the bank angle corresponding to the time step. The cubic spline interpolation routine, which is originally used for the aerodynamic lookup table, is used to determine the time-to-bank to the specified bank angle.

APPENDIX F

STABILITY AND CONTROL MAP BIBLIOGRAPHY

1. Chudoba, B., “*Stability and Control of Conventional and Unconventional Aircraft Configurations, A Generic Approach,*” Cranfield University, BoD – Books on Demand, 2001.
2. Corning, G., “*Supersonic and Subsonic Airplane Design,*” 2nd Edition, Edwards Brothers, Inc., Michigan, 1953
3. Abzug, M., “*Computational Flight Dynamics,*” AIAA Education Series, American Institute of Aeronautics and Astronautics, Inc., Virginia, 1998.
4. Nguyen, V., “*Flight Mechanics of High-Performance Aircraft,*” Cambridge University Press, Cambridge, England, 1995
5. Press, W., Teukolsky, S., Vetterling, W., Flannery, B., “*Numerical Recipes in FORTRAN,*” 2nd Edition, Cambridge University Press, Cambridge, England, 1992
6. Nelson, R., “*Flight Stability and Automatic Control,*” 2nd Edition, McGraw Hill, Boston, 1998.
7. Roskam, J., “*Airplane Flight Dynamics and Automatic Flight Controls*” Part I and II, DARcorporation, Kansas, 1995.
8. Roskam, J., “*Airplane Design, Part VII: Determination of Stability, Control and Performance Characteristics: FAR and Military Requirements,*” DARcorporation, Kansas, 2002.
9. Torenbeek, E., “*Synthesis of Subsonic Airplane Design,*” Delft University Press, Dordrecht, The Netherlands, 1996.
10. Stevens, B., Lewis, F., “*Aircraft Control and Simulation,*” 2nd Edition, John Wiley and Sons, Inc., New Jersey, 2003

11. Raymer, Daniel, "*Aircraft Design: A Conceptual Approach*," 3rd Edition, AIAA Education Series, American Institute of Aeronautics and Astronautics, Inc. Virginia, 1999.
12. Blausey, J., Personal Communication, 24 Feb 2006
13. Lee, H.P., Change, M., Kaiser, M.K., "*Flight Dynamics and Stability and Control Characteristics of the X-33 Technology Demonstrator Vehicle*," AIAA-98-4410, 1998 [S&C in Design]
14. Mavris, D., DeLaurentis, Soban, D., "*Probabilistic Assessment of Handling Qualities Characteristics in Preliminary Aircraft Design*," AIAA 98-0492, 1998 [S&C in Design]
15. Lamar, W., Neighbor, T., "*Handling Qualities Criteria and Requirements*," AGARD-CP-119, [S&C in Design]
16. Goran, M., "*Method For The Evaluation Vertical Tail Surfaces of a Light Aircraft Based on Lateral Flying Qualities*," ICAS-96-7.9.3, 1996[S&C in Design]
17. Ransom, S., "*Configuration Development of a Research Aircraft with Post-Stall Maneuverability*," JoA, Vol. 20, No. 7, July 1983[S&C in Design]
18. Roskam, J., "*Evolution of Airplane Stability and Control: A Designer's Viewpoint*," J. Guidance, Vol. 14, No. 3, May 1991. [S&C in Design]
19. Ericsson, L.E., "*A Summary of AGARD FDP Meeting on Dynamic Stability Parameters*," AGARD C-260, 1978 [S&C in Design]
20. Lee, G.H., "*The Aeroplane Designer's Approach to Stability and Control*," North Atlantic Treaty Organization, Report 334, 1961 [S&C in Design]

21. Murphy, P.C., Davidson, J.B., “*A Control Law and Design Method Facilitating Control Power, Robustness, Agility and Flying Qualities Tradeoffs: CRAFT,*” NASA TP-1998-208563, 1998 [S&C in Design]
22. Mangold, P., Wunnenberg, H., “*Possibilities for the Valuation of Different Combat Aircraft Configurations with Respect to Flight Mechanics,*” ICAS-80-2.2, [S&C in Design]
23. Pinsker, W.J.G., “*The Lateral Motion of Aircraft, and in particular of Inertially Slender Configurations,*” Ministry of Aviation, R & M No. 3334, 1961[S&C in Design]
24. Pinsker, W.J.G., “*The Dynamics of Aircraft Rotation and Lift-off and its Implication for Tail Clearance Requirements, Especially with large Aircraft,*” Ministry of Aviation, R & M No. 3569, 1967[S&C in Design]
25. Goldsmith, H.A., “*Stability and Control of Supersonic Aircraft at Low Speeds,*” Forth Congress – Aeronautical Sciences,
26. McRuer, D., Graham, D., “*Eighty Years of Flight Control: Triumphs and Pitfalls of the Systems Approach,*” J. Guidance and Control, Vol. 4, NO. 4, July-August 1981. [S&C in Design]
27. Roskam, J, Anemaat, W., “*An Easy Way to Analyze Longitudinal And Lateral-Directional Trim Problems with AEO or OEI,*” SAE 941143, Aerospace Atlantic Conference and Exposition, Dayton, Ohio, 1994. [S&C in Design]
28. Pinsker, W.J.G, “*Directional Stability in Flight with Bank Angle Constraints As a Condition Defining A Minimum Acceptable Value of n_v ,*” Royal Aircraft Establishment Technical Report 67127, 1967[S&C in Design]
29. Wright, I.E., “*Flight on Asymmetric Engine Power,*” Aircraft Engineering, 1950. [S&C in Design]

30. Woodcock, R. J., “*Estimation of Flying Qualities of Piloted Airplanes,*” AFFDL-TR-65-218, Air Force Flight Dynamics Laboratory, Wright-Patterson Air force Base, Ohio, 1966. [S&C in Design]
31. Paulson, J.W., Martin, M., T., “*Dynamic Lateral Behavior of High-Performance Aircraft,*” NACA RM L58E16, 1958. [S&C in Design]
32. Ogburn, M., E., “*Preliminary Study of Relationships Between Stability and Control Characteristics and Affordability for High-Performance Aircraft,*” AIAA-98-4265, 1998. [S&C in Design]
33. Byrnes, A.L., Hensleigh, W. E., Tolve, L. A., “*Effect of Horizontal Stabilizer Vertical Location on the Design of Large Transport Aircraft,*” JoA, Vol. 3, No. 2, March-April 1966. [S&C in Design]
34. Root, L. E., “*Dynamic Longitudinal Stability Charts for Design Use,*” J. AE. S., May 1935. [S&C in Design]
35. Wimpenny, J. C., “*Stability and Control in Aircraft Design,*” Journal of the Royal Aeronautical Society, Vol. 58, May 1954. [S&C in Design]
36. Anonymous, “*Choice and Sizing of Longitudinal Stabilizer and Control,*” Cranfield Institute of Technology, Aircraft design lecture notes, Feb. 1995.
37. Durham, W. C., Bordignon, K. A., “*Multiple Control Effector Rate Limiting,*” AIAA-95-3208, 1995. [S&C in Design]
38. Bordignon, K. A., Durham, W. C., “*Null-Space Augmented Solutions to Constrained Control Allocation Problems,*” AIAA-95-3209, 1995.
39. Durham, W.C., “*Constrained Control Allocation,*” Journal of Guidance, Control and Dynamics, Vol. 16, No.4, July-August 1993. [S&C in Design]
40. Young, A.D., “*The Aerodynamics of Controls,*” AGARD CP-384, Oct 1984. [Aero of Controls]

41. Thomas, H.H.B.H., "*The Aerodynamics of Aircraft Control*," AGARD R-711, March 1983. [Aero of Controls]
42. Korner, H., "*Mathematical Modeling and Theoretical Methods for the Aerodynamics Behavior of Control Devices*," AGARD R-711[Aero of Controls]
43. Skow, A.M., "*Control of Advanced Fighter Aircraft*," AGARD-R-711, March 1983. [Aero of Controls]
44. Jenny, R.B., Krachmalnick, F.M., "*Air Superiority with Controlled Configured Fighters*," AIAA 71-764, AIAA 3rd Aircraft Design and Operations Meeting, 1971. [CCV]
45. Graeber, U.P., "*Realization of Relaxed Static Stability on a Commercial Transport*," AGARD CP-384, 1984.[CCV]
46. Sliwa, S.M., "*Impact of Longitudinal Flying Qualities Upon The Design of A Transport with Active Controls*," AIAA 80-1570, 1980. [CCV]
47. Beh, H.B., Korte, U., Lobert, G., "*Stability and Control Aspects of The CCV-F104G*," AGARD CP-260, 1978. [CCV]
48. Anderson, M.R., "*An MDO Approach to Control-Configured-Vehicle Design*," AIAA-96-4058-CP, 1996.
49. Schweikhard, W., "*F-104B Category II Performance and Stability Evaluation*," AFFTC-TR-59-32, Air Force Flight Test Center, Edwards Air Force Base, California, 1959.
50. Klung, H.A., "*F-5B Category II Stability and Control Test*," FTC-TR-65-8, Air Force Flight Test Center, Edwards Air Force Base, California, 1965.
51. Adolph, C.E., "*B-52 Category II Performance and Stability Tests*," FTC-TDR-63-16, Air Force Flight Test Center, Edwards Air Force Base, California, 1963.

52. Anonymous, “*US Navy Flight Test School Flight Test Manual , Fixed Wing Stability and Control Theory and Flight Test Techniques,*” Naval Air Warfare Center Aircraft Division, Patuxent River, Maryland, 1997.
53. Blausey, G., Personal Communication with Dr. Bernd Chudoba, 1998.
54. Morris, J., “*DARPA Taps Northrop Grumman For Oblique Flying Wing Program,*” AviationNow.com,
http://www.aviationnow.com/avnow/news/channel_aerospacedaily.jsp?id=news/OFW0246.xml, 2006
55. Mason, W.H., “*Control and Stability in Aircraft Conceptual Design,*” Class Presentation, Aerospace and Ocean Engineering, Virginia Tech, Sept. 1999.
56. Major Flick, Nelson D. USAF, “*AFFTC Stability and Control Techniques,*” United States Air Force Air Research and Development Command, Air Force Flight Test Center, Edwards Air Force Base, Edwards, California, 1959.

REFERENCES

1. Chudoba, B., “*Stability and Control of Conventional and Unconventional Aircraft Configurations, A Generic Approach*,” Cranfield University, BoD – Books on Demand, 2001.
2. Moore, W.F., “*A Model for the Configuration Integration Process*,” AIAA Paper 95-3905, 1995
3. Dr. Chudoba’s communication with Gerald Blausey
4. Mason, W.H., “*Applied Computation Aerodynamics*,” Class Notes for AOE 4114, Dept. of Aerospace and Ocean Engineering, Virginia Polytechnic Institute and State University, 1995
5. Lan, E., “*User’s Manual for VORSTAB Code (Version 3.2)*,” Department of Aerospace Engineering, The University of Kansas, Kansas, 1999.
6. Pippalapalli, K., “*AeroMech – A Conceptual Design Stability and Control Analysis Tool*,” Masters of Science Thesis, University of Oklahoma, Oklahoma, 2004
7. Ammoniums, “*The USAF Stability and Control DATCOM, Volume I, User’s Manual*,” Public Domain Aeronautical Software, California, 1999.
8. Kay, J., Mason, W.H., Durham, F. Lutze, and A. Benoliel, “*Control Authority Issues in Aircraft Conceptual Design: Critical Conditions, Estimation Methodology, Spreadsheet Assessment, Trim and Bibliography*”, VPO-Aero-200, Department of Aerospace and Ocean Engineering, Virginal Polytechnic Institute and State University, Virginia, 1993.

9. Heinze, W., "*Ein Beitrag zur quantitativen Analyse der technischen und wirtschaftlichen Auslegungsgrenzen verschiedenster Flugzeugkonzepte für den Transport großer Nutzlasten,*" Ph.D. Thesis, Technische Universität Braunschweig, Institut für Flugzeugbau und Leichtbau, ZLR-Forschungsbericht 94-01, Februar 1994
10. Roskam, J., "*Airplane Design, Part VII: Determination of Stability, Control and Performance Characteristics: FAR and Military Requirements,*"
11. Pohl, T., "*Improvement and Extension of Tail Sizing Procedures for Preliminary Design Purposes,*" M.Eng. Thesis, Imperial College of Science, Technology and Medicine, Department of Aeronautics, June 1997
12. Lee, H.P., Change, M., Kaiser, M.K., "*Flight Dynamics and Stability and Control Characteristics of the X-33 Technology Demonstrator Vehicle,*" AIAA-98-4410, 1998 [S&C in Design]
13. Nicolai, L.M., "*Fundamentals of Aircraft Design,*" METS, Inc., San Jose, California, 1984
14. Jeffery, J., "*The Benefits of Using Virtual Environments Throughout an Aircraft's Design and Development Process,*" SAE International, General Aviation Technology Conference and Exhibition, 2006
15. Takahashi, T.T., Fanciullo, T., and Ridgely, D.B., "*Incorporation of Flight Control Design Tools into the Multidisciplinary Conceptual Design Process,*" 45th AIAA Aerospace Sciences Meeting and Exhibit, Reno, Nevada, AIAA 2007-656, 2007
16. Goodrich, K. H., Sliwa, S.M. and Lallman, F.J., "*A Closed-Form Trim Solution Yielding Mimimum Trim Drag For Airplanes with Multiple Longitudinal Control Effectors,*" NASA TP 2907, Langley Research Center, Virginia, 1989.

17. Nicolai, L.M. and Carty, A., “*Role of the Aerodynamicist in a Concurrent Multidisciplinary Design Purpose,*” Paper Presented at the Symposium of the RTO (Research and Technology Organization) Applied Vehicle Technology Panel (AVT) held in Ottawa, Canada, 1999
18. Miranda, L., Elliot, D., “*A Generalized Vortex Lattice Method for Subsonic and Supersonic Flow Applications,*” NASA CR-2865, 1977.
19. Lane, W. H., “*Stability and Control Flight Test of the YB-49 Airplane, USAF No. 42-1012367,*” Memorandum Report No. MCRFT-2280, Wright-Paterson Air Force Base, Ohio, 1950.
20. Capt. Amann, J., “*Phase II Test of the YB-49 Airplane USAF No. 42-102368,*” Memorandum Report No. MCRFT-2156, Wright-Paterson Air Force Base, Ohio, 1948.
21. Ashkenas, I., and Kyde, H., “*Tailless Aircraft Performance Improvements with Relaxed Static Stability,*” NASA CR 181806, Hampton, Virginia, 1989.
22. Stevens, B., Lewis, F., “*Aircraft Control and Simulation,*” 2nd Edition, John Wiley and Sons, Inc., New Jersey, 2003
23. Abzug, M., “*Computational Flight Dynamics,*” AIAA Education Series, American Institute of Aeronautics and Astronautics, Inc., Virginia, 1998.
24. Michael A. Jackson, “*Principles of Program Design,*” Academic Press, London, 1975
25. Nassi, I., and Schniederman, B., “*Flowchart Techniques for Structured Programming,*” SIGPLAN Notices, Department of Computer Science, State University of New York, New York,
<http://geocities.siliconValley/way/4747/nsd.html>, 1973
26. Dogan, A., Personal Communication, Feb 2006

27. Press, W., Teukolsky, S., Vetterling, W., Flannery, B., "*Numerical Recipes in FORTRAN*," 2nd Edition, Cambridge University Press, Cambridge, England, 1992
28. Torenbeek, E., "*Synthesis of Subsonic Airplane Design*," Delft University Press Kluwer Academic Publishers, Boston, 1982
29. Loftin, L.K., "*Subsonic Aircraft: Evolution and Matching of Size to Performance*," NASA Reference Publication 1060, Virginia, 1980
30. Blausey, J., Personal Communication, Feb 2006
31. Nicolai, L.M., "*Fundamentals of Aircraft Design*," METS, Inc., San Jose, California, 1984
32. Anonymous, "*Military Specification Flying Qualities of Piloted Airplanes*," MIL-F-8785, 1980.
33. Cooper, G.E., Harper, R.P., "*The Use of Pilot Rating in the Evaluation of Aircraft Handling Qualities*," NASA TN D-5153, Washington, D.C., 1969
34. Major Flick, Nelson D. USAF, "*AFFTC Stability and Control Techniques*," United States Air force Air Research and Development Command, Air Force Flight Test Center, Edwards Air Force Base, Edwards, California, 1959.
35. Roskam, J., "*Airplane Flight Dynamics and Automatic Flight Controls*" Part I and II, DARcorporation, Kansas, 1995.
36. Roskam, J., "*Airplane Design, Part VII: Determination of Stability, Control and Performance Characteristics: FAR and Military Requirements*,"
37. Pape, G.R., Campbell, J.M., "*Northrop Flying Wings, A History of Jack Northrop's Visionary Aircraft*," Schiffer Publishing Ltd., Pennsylvania, 1995.
38. Anonymous, "*Pilot's Handbook for Model YB-49 Airplane*," AN 01-15EAB-1, Army Air Forces, Prepared by Northrop Aircraft, Inc., California, 1948

39. Lan, E., Personal Communication, March 2007

BIOGRAPHICAL INFORMATION

Gary Coleman's began his master research at the tender age of 24 with the Aerospace Vehicle Design Lab (AVD) at the University of Oklahoma. He was a strapping young lad with a heart full of dreams and mind for aircraft design. His involvement with the AVD Lab began (from day one) with a conceptual design study for a space tourism launch vehicle, modified from a LearJet 23, under contract from RocketPlane LTD.

At the conclusion of the RocketPlane contract he began with master's research into the developing of the *AeroMech* Prototype source code. During this research the AVD Lab relocated to the University of Texas at Arlington where he earned his Master of Science in Aerospace Engineering.

In addition to his Master's research he also (1) work on the AVD Lab team, under contract with Spritwing Aviation, on a Supersonic Business Jet conceptual design, (2) has produced 2 AIAA conference papers and has been a coauthor on 5 additional conference papers, (3) presented 3 papers at the AIAA Aerospace Science Meeting and Exhibit in Reno, Nevada, and (4) has worked as an mentor and teaching assistant for the Senior Design class at both the University of Oklahoman and the University of Texas at Arlington.

His future plans include continuing with the AVD Lab at the University of Texas at Arlington for his PhD. in aircraft design synthesis, marrying his fiancée Jessica, have kids and become a “*bestest aircraft designer in the world!*”